9950-532

(NASA-CR-164316) ADVANCED SOLAR CONCENTRATOR: PRELIMINARY AND DETAILED DESIGN Final Report (Acurex Corp., Mountain View, Calif.) 252 p HC A12/MF A01 CSCL 10A

N81-23623

Unclas
G3/44 42383

ACUREX FINAL REPORT FR-80-16/AE

ADVANCED SOLAR CONCENTRATOR: PRELIMINARY AND DETAILED DESIGN

March 1981

Acurex Project 7740
Contract 955477
DRL 014
DRD SE002

For

California Institute of Technology
Jet Propulsion Laboratory
4800 Oak Grove Drive
Pasadena, California 91103

By

D. M. Bell, R. A. Maraschin, M. T. Matsushita,
D. Erskine, R. Carlton, A. Jakovcevic, and A. K. Yasuda
Acurex Corporation
Alternate Energy Division
485 Clyde Avenue
Mountain View, California 94042

Acurex Final Report FR-80-16/AE

ADVANCED SOLAR CONCENTRATOR: PRELIMINARY AND DETAILED DESIGN

March 1981

Acurex Project 7740
Contract 955477
DRL 014
DRD SE002

For

California Institute of Technology
Jet Propulsion Laboratory
4800 Oak Grove Drive
Pasadena, California 91103

By

D. M. Bell, R. A. Maraschin, M. T. Matsushita,
D. Erskine, R. Carlton, A. Jakovcevic, and A. K. Yasuda
Acurex Corporation
Alternate Energy Division
485 Clyde Avenue
Mountain View, California 94042

This work was perf ormed for the Jet Propulsion Laboratory, California Institute of Technology, sponsored by the National Aeronautics and Space Administration under Contract NAS7-100.

This report contains information prepared by Acurex Corporation under JPL subcontract. Its content is not necessarily endorsed by the Jet Propulsion Laboratory, California Institute of Technology, or the National Aeronautics and Space Administration.

ABSTRACT

This report presents the results of a 9-month technical study effort performed by Acurex Corporation for the Jet Propulsion Laboratory (JPL). The purpose of the study was to perform a preliminary design of the JPL concept for an advanced point-focusing solar concentrator and to carry the design of the outer reflective element (gore) through the detailed design level.

The Advanced Solar Concentrator is a single reflection point-focusing two-axis tracking paraboloidal dish with a reflector aperture diameter of approximately 11 m. The reflective surface is made up of 64 independent, optical quality gores. Each gore is a composite of a thin backsilvered mirror glass face sheet continuously bonded to a contoured substrate of lightweight, rigid cellular glass. The use of largely self-supporting gores allows a significant reduction in the weight of the steel support structure as compared to alternate design concepts.

The results of the study are (1) a preliminary design package for a low-cost, low-weight, mass producible concentrator in which primary emphasis was placed on the design of the higher cost subsystems, and (2) a sufficiently detailed design of the outer gore element to allow fabrication of prototype gores.

TABLE OF CONTENTS

TABLE OF CONTENTS (Concluded)

LIST OF ILLUSTRATIONS

LIST OF ILLUSTRATIONS (Concluded)

LIST OF TABLES

SECTION 1

INTRODUCTION AND SUMMARY

This report presents the results of a 9-month technical study carried out by Acurex Corporation for JPL under contract number 955477 entitled, "An Advanced Solar Concentrator Design." The effort reported herein includes the preliminary design (Task 1) of JPL's concept for an advanced point-focusing solar concentrator, and the detailed design (Task 2) of one of the reflective elements comprising the paraboloidal reflective surface.

A conceptual sketch of the Advanced Solar Concentrator is shown in Figure 1-1. It consists of an articulated space frame structure supporting a paraboloidal mirror glass reflector. The structure is driven in azimuth and elevation by electric actuators to align the reflector with the incoming solar radiation to obtain an optical focus and maintain proper image placement in the receiver. When coupled with a receiver/engine/generator package mounted at the focus of the paraboloid, the unit is capable of generating electricity for remote applications or as a supplement to a utility grid system.

The key feature of the Advanced Solar Concentrator is the low-cost, lightweight, self-supporting gores making up the paraboloidal reflective surface. Each element, or gore, is made of a sandwiched construction with a thin backsilvered sheet glass front skin, a lightweight cellular glass

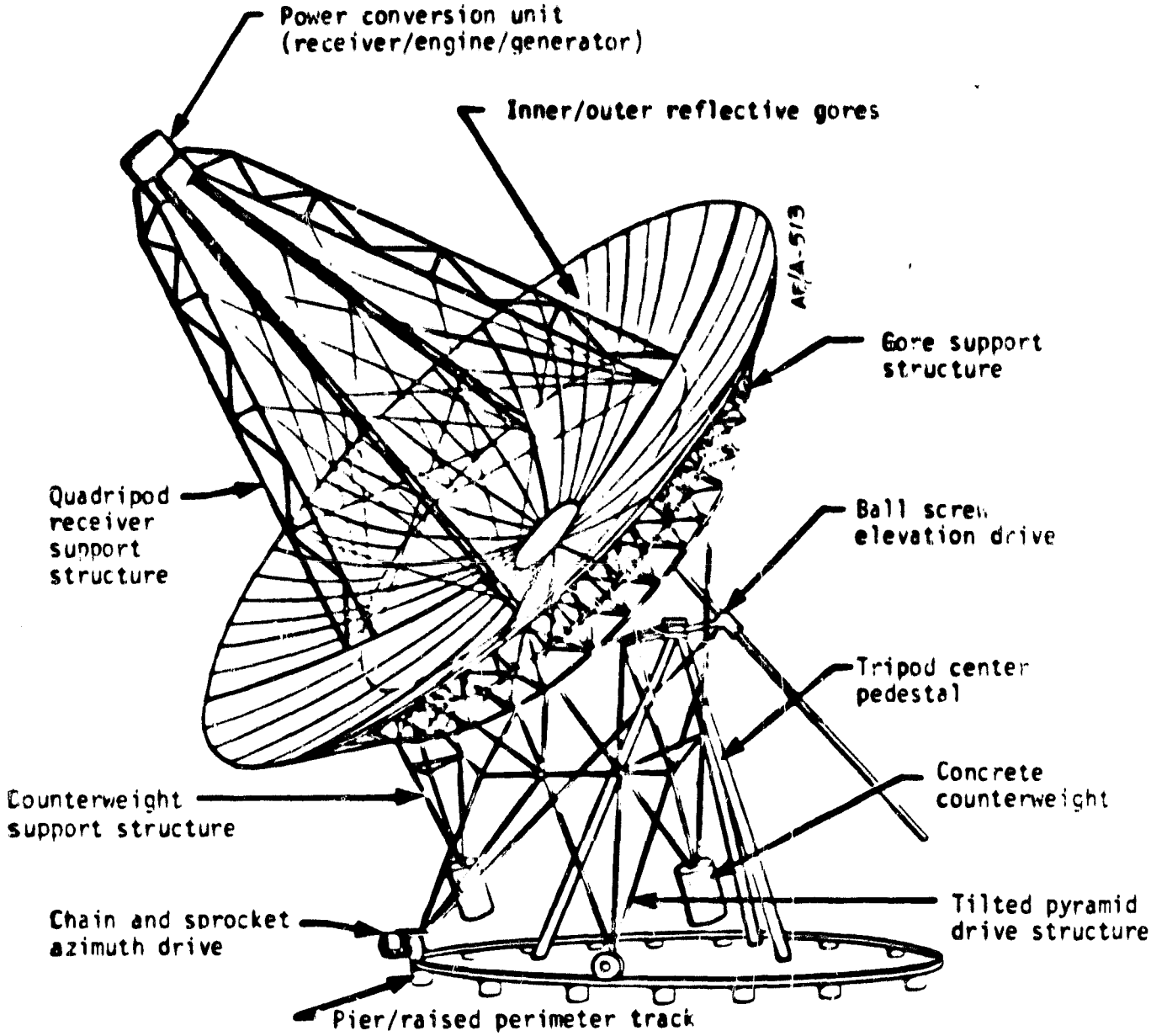

Figure 1-1. Advanced Solar Concentrator

contoured core, and a thin unsilvered sheet glass backing strip. These lightweight, structurally efficient gores allow a significant reduction in the mass of the structure, thereby reducing structure cost in mass production.

The primary emphasis of Acurex's effort was directed at refining and detailing the design of the critical gore element and optimizing the strength and rigidity of the structure as traded against the installed cost and performance of the concentrator.

1.1 PROJECT OBJECTIVES AND APPROACH

The objective of the preliminary design task was a low-cost, mass producible concentrator design capable of meeting the performance and functional requirements of the design specification.

The major constraints on this effort were:

- The concentrator was to embody the general configuration of the JPL concept
- The reflective surface was to be made of largely self-supporting gores
- The gores were to be made of a thin backsilvered mirror glass reflector bonded to a contoured substrate of cellular glass

The objective of the detailed design task was to carry the design of only the outer gore element to a level of detail sufficient to allow the fabrication of prototype hardware.

Throughout preliminary design, a systems approach was emphasized to ensure a balanced design with potential for low cost in mass production. Design emphasis was placed in those areas of significant cost where cost benefits could be achieved through analysis and design refinement. Preliminary estimates indicated that the primary factory cost centers

were the reflective panels, the structure, and the drives. The electrical and control costs were estimated to be relatively small in magnitude and insensitive to the level of preliminary design effort. The level of detail in the preliminary design, therefore, reflects this emphasis.

The results of the preliminary design were fed directly into the detailed design task. The analysis of the outer gore was refined based on JPL updated material properties, and preproduction prototype layout drawings were developed.

1.2 REPORT ORGANIZATION

This report has been organized to follow the division of work between Task 1 and Task 2 to the greatest practical extent. The preliminary design is discussed fully in Section 2, while Section 3 presents the results of the detailed design effort.

To aid the reader, the Advanced Solar Concentrator design as it stood at the completion of the preliminary design effort is described in detail in Section 2.1. Pertinent subsystem characteristics are summarized in this section. The balance of Section 2 then presents the discussion of the trade-off and analysis leading to this design.

Several appendices have been provided. They include:

- Appendix A — "Design Requirements, Specification, and Definition for a Point-Focusing Advanced Solar Concentrator" (Exhibit I of JPL contract 955477)
- Appendix B — "Preliminary Design Basis and Requirements for an Advanced Point-Focusing Solar Concentrator" (Acurex specification number S-7740-01, Revision A)
- Appendix C — "Preliminary Hazards Analysis (PHA) for the Advanced Point-Focusing Solar Concentrator"

- Appendix D — "JPL Advanced Concentrator Preliminary Drawing Package"
- Appendix E — "JPL Advanced Concentrator Outer Gore Detailed Drawing Package"
- Appendix F — "Prototype Fabrication Specification for a Reflective Element (Gore) of an Advanced Point-Focusing Solar Concentrator" (Acurex specification number S-7740-02)
- Appendix G — "Cellular Glass Gore Test Plan"

SECTION 2

PRELIMINARY DESIGN

The preliminary design of the Advanced Solar Concentrator was based on the conceptual design developed by JPL and the specified design requirements (Appendix A). Acurex's efforts on this program refined the design requirements and the JPL design concept to attain a minimum weight design amenable to high-volume mass production. This section presents the discussion of the preliminary design effort. It is organized into three major subsections: Section 2.1 presents a description of the Advanced Solar Concentrator at the preliminary design level, Section 2.2 discusses the analysis and trade-offs behind the subsystem design decisions, and Section 2.3 presents the methodology and results of the preliminary performance analysis.

2.1 DESIGN DESCRIPTION

The Advanced Solar Concentrator (Figure 1-1) is a single reflection point-focusing, two-axis tracking parabolic dish with an aperture diameter of approximately 11 m. The highly accurate unit is capable of achieving an average solar flux concentration in excess of 1,740 suns while operating in design winds of 50 km/hr (31 mph).

The concentrator is defined as consisting of the following five subsystems:

- Reflective surface
- Support structures
- Drive subsystem
- Foundations
- Electrical and control

A summary subsystem mass statement is provided in Table 2-1. Each of these subsystems is described in the following sections.

Table 2-1. Subsystem Mass Statement

Reflective surface	1,460 kg	(3,220 lb)
Support structures	1,965 kg	(4,327 lb)
Drive subsystem	4,995 kg*	(11,000 lb)[a]
Foundations	11,445 kg	(25,200 lb)
Electrical and control	225 kg	(500 lb)

[a]Includes 4,540 kg (10,000 lb) of reinforced concrete counterweights

2.1.1 Reflective Surface

The reflective surface of the concentrator consists of two concentric rings of independent, optical quality reflective elements forming a complete, but physically discontinuous paraboloidal surface with a common focal point. As noted in Figure 1-1, two types of reflective elements, designated as inner and outer gores, are used to make up the reflective surface.

Each gore is installed on a ring-like gore support structure with statically determinant three-point attachments. These attachments have sufficient degrees of freedom to allow fine tuning of the composite surface geometry and to accommodate differential thermal expansion between the gores and the structure.

During preliminary design, 20 inner and 40 outer gores were selected for the structure/reflector interface. As will be discussed in Section 3, a breakdown of 24 inner gores and 40 outer gores was selected during the detailed design effort as the best interface configuration. Since only the design of the outer gore was carried through detailed design, all discussions relative to the balance of the concentrator (structure, drives, foundations, etc.) are based on the preliminary 20/40 gore interface.

The preliminary analysis and design of the gores resulted in a lightweight, structurally rigid reflective element that is largely self-supporting. Over 35 percent of the outer gore area is overhung beyond its outermost support point.

As shown in Figure 2-1, each gore is fabricated from a composite of 1.0 mm (0.040 in.) Corning Glass Works 7809 borosilicate glass and a Pittsburgh Corning Foamsil® 75 cellular glass core. The Foamsil® 75 has been specially formulated to match the thermal expansion characteristics of the 7809 sheet glass. A single sheet of backsilvered thin glass is continuously bonded to a contoured substrate of the cellular glass material. A narrow strip of unsilvered thin glass is bonded to the outer face of the cellular glass spar running longitudinally along the backside of the gore. The face sheets and the cellular glass core form a composite structure in which the mirror glass and the spar cap carry a significant portion of the aerodynamic and gravitationally induced bending loads.

Near-term fabrication techniques will require an initial bonding of standard sized cellular glass blocks to form a large slab which will subsequently be machined to form the desired contour. The mirrored and unsilvered glass sheets will then be bonded to the core along with the

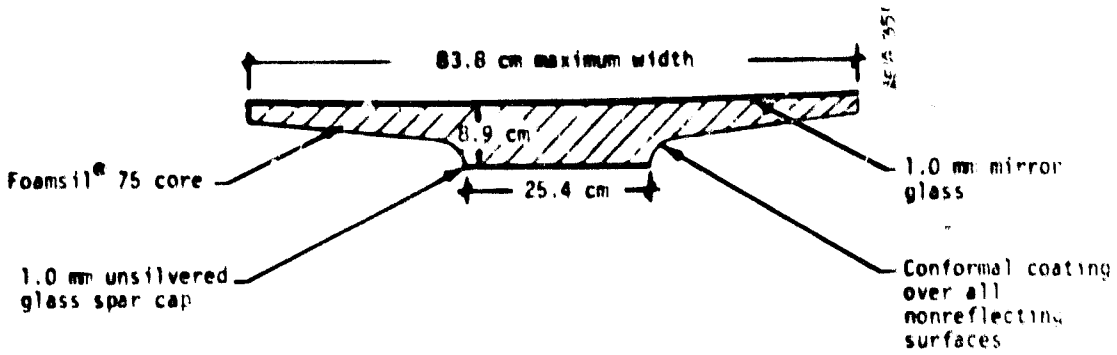

Figure 2-1. Reflective Element Cross Section

attachment hardware, and all nonreflective surfaces coated with a weatherproof conformal coating.

The key physical properties of the gore design at the preliminary design level are summarized in Table 2-2.

2.1.2 Support Structures

The concentrator support structure serves three functions: (1) interfacing between the receiver/engine/generator package, or power conversion module (PCM), the drive subsystem, the reflective surface, and the foundations; (2) providing a rigid support of the required subsystems; and (3) providing an articulated two-axis tracking capability. To provide the required rigidity while meeting the low-weight design goal, structurally efficient steel space frame structures were designed. The structure subsystem is comprised of the following subassemblies:

- Gore support ring structure
- Drive structure
- Counterweight structure
- Receiver/engine support structure
- Pedestal

Each of these subassemblies is described in the following paragraphs.

Table 2-2. Preliminary Gore Design Summary

	Outer Gore	Inner Gore
Length, cm (in.)	229 (90)	269 (106)
Maximum width, cm (in.)	84 (33)	99 (39)
Number required/concentrator	40	20
Mass (bare gore), kg (lb)	23 (51)	17 (38)
Mass (with attachment pads), kg (lb)	26 (58)	20 (45)
Sizing criteria	Stress limit	Slope error limit
Sizing wind speed, km/hr (mph)	110 (68)	50 (31)
Accumulated exposure in 30 yr	1 min	--
Maximum deflection slope error, mrad[a]	0.22	0.38
Approximate rms deflection slope error, mrad[a]	0.17	0.24[b]
Maximum deflection, cm (in.)[a]	0.0127 (0.005)	0.0305 (0.012)

[a]50 km/hr (31 mph) wind speed, uniform pressure, $C_p = 3.3$
[b]Used for preliminary performance calculations

Gore Support Structure

The gore support structure is a steel space frame ring supporting the 60 gore elements and interfaces with the receiver support structure, the elevation drive mechanism and bearings, and the counterweight support structures. Gore support ring deflections translate directly into lower concentrator performance due to the reduction in optical concentration ratio resulting from the rigid body rotation of the gores. The support ring design has therefore been optimized to provide the best balance between stiffness and structure weight.

The gore support structure consists of a truss-like ring with tetrahedron "outriggers" (see Drawing 7740-002, Appendix D). Each gore is supported at the tip of an outrigger and at two points near the central ring. The gore support structure has been carefully designed to minimize midspan loading of members thereby maximizing structural efficiency.

Drive Structure

The drive structure (see Drawing 7740-004, Appendix D) serves as an intermediate structure between the reflector assembly, the center pivot pedestal, and the azimuth drive. It also makes use of the space frame concept to maximize structural efficiency. The drive structure is pivoted about the azimuth axis at the top of the pedestal. Loads are transmitted to the pedestal through the azimuth bearing and to the track through the azimuth drive unit and idler wheels located at the lower corners of the drive support structure.

The drive structure geometry was carefully analyzed to select a configuration providing a good balance between actuator loads, structural weight, and concentrator motion limits.

Counterweight Structure

The counterweight structure (see Drawing 7740-005, Appendix D) is a simple tubular steel space frame providing a structural interface between the precast concrete counterweights and the gore support ring. Two counterweight structures are required per concentrator.

Receiver/Engine Support Structure

The receiver/engine support structure (Drawing 7740-003, Appendix D) is a guyed, truss-leg quadripod designed to provide the required strength and rigidity while minimizing optical losses due to shadowing and blockage. The receiver mounting flange and sleeve located at the quadripod apex do not make use of the receiver housing as a load-carrying member.

Pedestal

The center pivot pedestal (Drawing 7740-006, Appendix D) is a simple tubular steel tripod. The pedestal supports the azimuth bearing and provides the structural load path to react the loads transmitted through the bearing. Since no significant moments can be transmitted through the azimuth bearing, the simple tripod design provides the most efficient structural configuration.

The analysis and design trade-offs leading to each of the structural subassemblies and the structural subsystem as a whole are described in detail in Section 2.2.2. The mass of each structural subassembly is summarized in Table 2-3.

Table 2-3. Structural Design Summary

Description of Structure	Refer to Drawing Number	Mass of Structure kg (lb)
Gore support ring	7740-002	658 (1,450)
Drive structure	7740-004	590 (1,300)
Counterweight structure	7740-005	154 (340)[a]
Receiver/engine support structure	7740-003	253 (557)
Pedestal	7740-006	154 (340)

[a]Each structure (two required per concentrator)

2.1.3 Drive Subsystem

The drive subsystem provides power and activation for solar tracking and for emergency stow and desteer. An elevation over azimuth two-axis tracking drive scheme was a basic feature of the JPL design concept. As discussed in Section 2.2.4, the drive design options were carefully evaluated to select the most cost-effective means of providing the required azimuth/elevation motions.

Both hydraulic and electric actuators were considered. An all-electric approach was selected primarily due to the backup emergency stow requirement in the event of a grid power failure. The required power is provided by a gasoline motor-generator set.

The selected elevation drive incorporates an electrically driven ball screw actuator with an automatic motor brake to prevent unpowered backdriving of the unit. The actuator uses a fixed screw with a driven nut. The motor, reduction unit, and drive nut are mounted in a support yoke at the top rear end of the drive support structure. Accordian boots

provide environmental protection of the screw to minimize maintenance requirements.

The azimuth drive consists of an electrically driven chain and sprocket unit. The motor, gear reduction unit, and drive sprocket are mounted to one of the drive structure support legs with the chain being anchored to the elevated track. The chain is housed in a steel channel with flexible rubber closures to minimize environmental contamination. Due to the mechanical advantage afforded by the perimeter drive scheme, very low azimuth backlash can be achieved with relatively low chain tensioning requirements. The high longitudinal stiffness to lateral flexibility ratio of a chain makes it the preferred choice when compared to similar perimeter drive schemes employing cables. Azimuth drive maintenance costs will be minimized through the use of the environmental enclosures and the relatively slow rate at which the unit will be operated.

The trade-off and analysis of the drive subsystem are described in Section 2.2.3. The key features of the drive subsystem components are summarized in Table 2-4 and shown on Drawing 7740-001 of Appendix D.

2.1.4 Foundations

The concentrator foundation subsystem includes the three reinforced concrete piers supporting the center pivot pedestal structure, the 12 reinforced concrete piers supporting the raised steel perimeter track, and the track itself. Given that a perimeter track is required (it is basic to the JPL concept), the raised steel/concrete pier configuration provides the lowest life-cycle cost and the greatest flexibility for varied terrain and soil conditions.

The trade-offs and analysis of the foundation subsystem is presented along with the pedestal structure design in Section 2.2.4. The

Table 2-4. Drive Component Summary

• Elevation drive		
--	Ball screw	90 kN (10-ton capacity) 5.72 cm (2.25 in.) diameter screw 6.1 m (20 ft) stroke
--	Gear box	18:1 ratio 5.65 N-m (800 in.-oz) output
--	Motor	1750 rpm 0.75 kW (1 hp) Permanent split capacitor
• Azimuth drive		
--	Chain	2.54 cm (1 in.) pitch No. 80 roller
--	Drive sprocket	30 cm (12 in.) pitch diameter
--	Gear box	100:1 ratio 1,500 N-m (1,100 ft-lb) output
--	Motor	72 rpm 0.12 kW (1/6 hp) Permanent magnet stepper
• Emergency power unit		
--	Generator	6.5 kW, 208V, three-phase, 60-cycle, gasoline-powered
--	Transfer switch	30A, 480V, three-phase, four-wire

key features of the foundation components are summarized in Table 2-5 and Drawing 7740-006 of Appendix D.

2.1.5 Electrical and Control

The electrical subsystem consists of off-the-shelf components for power distribution, overload protection, and lightning protection. A separate utility fed circuit is provided for the tracker control unit and the drive subsystem. Fused disconnects protect all circuitry with separate motor starters for the azimuth and elevation drive motors.

The receiver support structure legs were sized to serve the combined function of electrical conduits in addition to their structural roles. Flexible weatherproof cabling is provided for the power circuits at the azimuth and elevation bearings.

Table 2-5. Foundation Design Summary

Track	Full circle divided into six arc segments 17.8 x 7.62 x 0.48 cm wall (7 x 3 x 3/16 in.) structural steel tubing 4.1 m (13 ft, 4-1/2 in.) inside diameter
Track piers	12 piers required Reinforced concrete 0.3 m (1 ft) diameter 3.0 m (10 ft) deep
Pedestal piers	Three piers required Reinforced concrete 0.3 m (1 ft) diameter 4.1 m (13 ft 4 in.) deep

A conventional lightning protection system employing structure mounted lightning arrestors and a dedicated grounding path is provided for incorporation in lightning susceptible areas.

The major electrical subsystem components are summarized in Table 2-6.

Table 2-6. Electrical Subsystem Component Summary

Quantity	
1	100-amp disconnect switch
1	100-amp fused disconnect switch
1	30-amp fused disconnect switch with motor starter
1	30-amp fused disconnect switch
1	Single pole starter size 00
2	Lightning arrestors
2	Ground rods and accessories

The tracker/control subsystem is a microprocessor-based hybrid unit incorporating synthetic (ephemeris) and active (optical) tracking schemes. Each concentrator will be furnished with a self-contained tracker/control unit. Ephemeris tracking, provided by the microprocessor in conjunction with precision positional feedback potentiometers, maintains gross concentrator alignment and incorporates safe desteer and sun acquisition schemes. An image sensing optical sensor provides fine tuning override signals to maintain an accurate focus during high insolation periods.

The tracker control unit accepts external receiver malfunction desteer commands and high wind stow commands overriding the normal tracking functions.

The key features of the tracker/control subsystem are summarized in Table 2-7. The rationale for selection of the image sensing hybrid control system is discussed in Section 2.2.5.

2.2 SUBSYSTEM ANALYSIS AND TRADE-OFFS

The fundamental objective of the preliminary design effort was to refine the JPL design concept through analysis and trade-offs to attain a minimum cost concentrator capable of meeting the specified performance goals. To maximize the cost-effectiveness of the design effort, those areas with the highest percentage cost and those with the greatest potential for cost reduction through design were first identified. The preliminary design effort was then structured to balance the effort expended on each subsystem area with the potential benefit to be achieved.

Prior to initiating the subsystem design activities, the design requirements specified in the contract (Appendix A) were closely reviewed to ensure consistency, clarity, and the appropriateness of the requirement

Table 2-7. Control Subsystem Component Summary

Tracker computer	Two-axis hybrid system -- microcomputer-based with built-in clock and battery backup
Tracker photodetector	Multielement photobalancing apparatus located to monitor reflected flux on receiver
Positional feedback transducers	Absolute digital shaft encoders or potentiometers for azimuth and elevation angular position information
Interconnection hardware	Cabling, conduit, connection boxes, etc.
Control interfacing equipment	Supplied with computer for control/data acquisition

with respect to the low-cost goals of the program. Acurex worked closely with JPL throughout preliminary design to refine and update the requirements.

A separate design specification entitled "Preliminary Design Basis and Requirements for an Advanced Point-Focusing Solar Concentrator" was generated by Acurex and reviewed and approved by the JPL technical team. This specification, included as Appendix B, expands upon and supersedes the JPL document.

To ensure that all necessary safety considerations were properly accounted for, a preliminary hazards analysis was performed at the outset of the preliminary design effort. The hazards analysis performed by the Acurex safety engineer in conjunction with the design team is included for reference as Appendix C.

The methodology and results of the design analysis and trade-offs leading to the preliminary design described in Section 2.1 is presented in this section. For clarity, it has been subdivided into five subsections.

Section 2.2.1 presents the discussion of the preliminary gore design; Section 2.2.2 presents the structural design trade-offs; and Sections 2.2.3 through 2.2.5 present the drives, foundations, and electrical and control subsystem discussions, respectively.

2.2.1 Preliminary Gore Design

The design of the reflective gore elements is the key to the Advanced Solar Concentrator. The configuration and weight of the gores are significant factors in the design of the balance of the concentrator. The gore design effort was complicated by the static fatigue susceptibility of the sheet and cellular glass materials and the relative lack of statistical design data for these materials.

Initial concept selection was based on conservative fatigue limit allowable stress values for the sheet glass and JPL's preliminary estimates of material property data for the Foamsil® 75 cellular glass. Updated design values for the cellular glass and static fatigue data for sheet glass were provided by JPL near the end of the preliminary design effort. These values were used in the final gore sizing analysis.

2.2.1.1 Material Characterization

The failure characteristics of static fatigue-susceptible materials are expressed by Weibel curves which plot failure probability as a function of stress level for a given loading rate. A series of these curves can be used to generate a curve showing the stress level associated with a given failure probability as a function of exposure time to that stress level. Since failure stresses are associated with the probability of having a flaw in the material under stress, the resulting design curve is volume sensitive. Design stress levels must therefore be corrected for the difference between the actual stressed volume and that of the test

samples used to generate the data. In glass materials static fatigue is caused by slow crack growth when the material is subjected to a tensile stress. Since tensile loading, simple bending, and uniform bending result in different volumes of material experiencing peak tensile stresses, allowable design stress levels are also dependent on the type of loading causing the stress.

A curve of the design stress level associated with a 5-percent failure probability was produced from failure data generated for cellular glass by JPL and Pittsburgh Corning Corporation and reported by JPL in Reference 1. The data was gathered from test bars 10.16 cm (4 in.) wide, 4.45 cm (1.75 in.) thick, and 45.72 cm (18 in.) long subjected to uniform (4-point) bending. Design stress values used for the gore design were therefore modified from the test bar values to account for the larger volume of the gore, and for the decreased percentage of that volume experiencing peak stresses in simple bending. The resulting design curve as well as the test bar curve is presented in Figure 2-2.

It should be noted that the test bar data was based on fast fracture strengths determined at loading rates of 12.7 cm (5 in.) per sec. JPL has continued work on the characterization of cellular glass since the aforementioned data was furnished, and has since achieved loading rates in excess of 5 in. per sec. As loading rates increase, the true fast fracture strength of the material, upon which the static fatigue curves are based, is more closely approached. One should expect to see a slight improvement in the cellular glass properties in forthcoming publications.

Sheet glass as a structural material must be treated in a similar manner to cellular glass. A recently published JPL report (Reference 2),

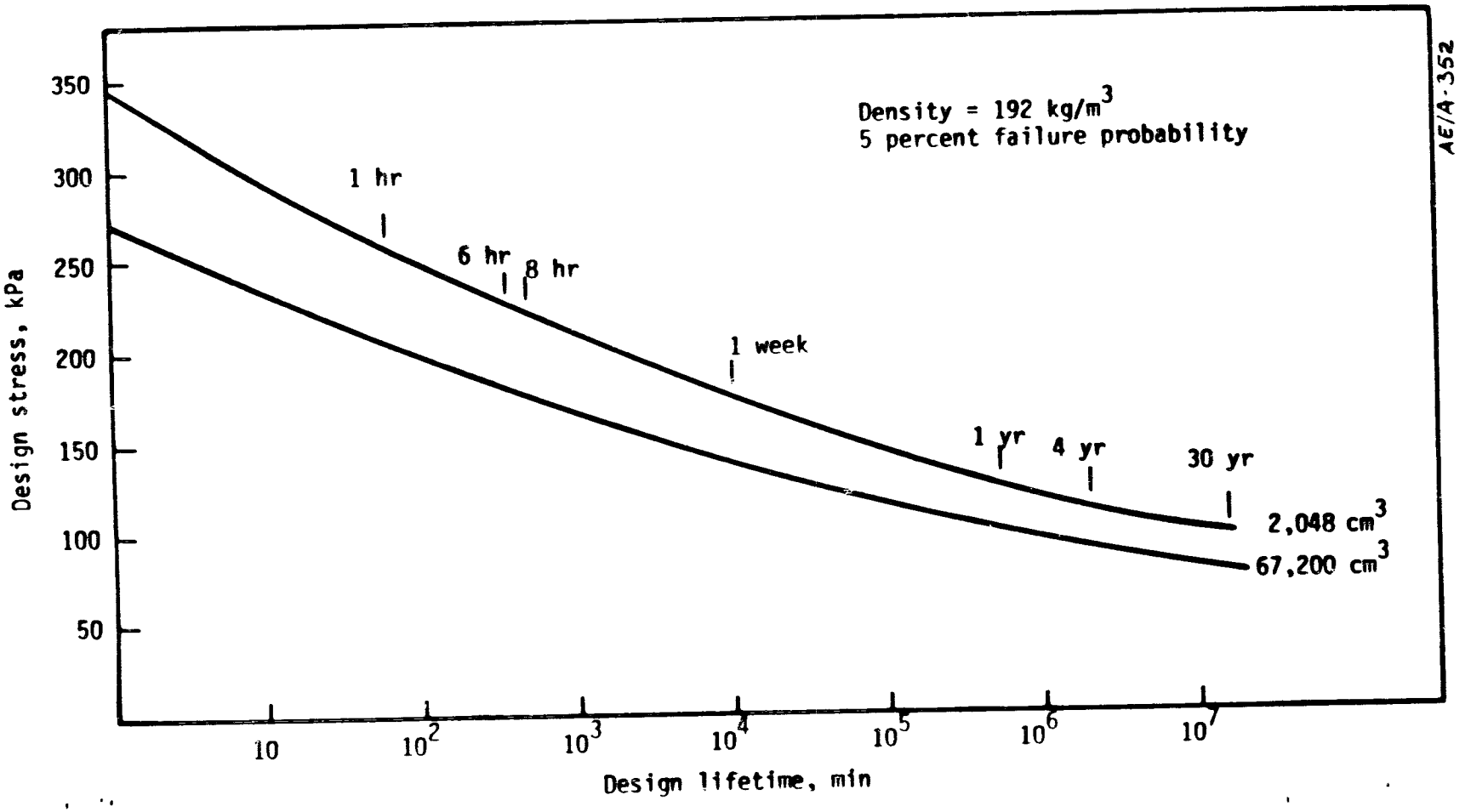

Figure 2-2. Foamsil® 75 Design Stress Versus Lifetime

received late in this program, provided the design data for sheet glass. The failure probability of sheet glass is sensitive to surface flaws and to edge flaws. The data provided for a 1-ft square panel of glass was therefore corrected to account for the actual gore surface area. The design curves for the sheet glass are presented in Figure 2-3 for mirror panels sized to cover full and one-half gore widths.

2.2.1.2 Applied Loads

The complex nature of sheet glass and cellular glass as design materials requires a comparison of each load and its accumulated duration with an allowable design stress specific to that duration. Because of the large variation of allowable stress with accumulated exposure, the largest load may not govern the design. To minimize unnecessary conservatism in the gore design, Acurex reevaluated the gore design loads as originally specified by JPL (Appendix A).

In lieu of the specified pressure distributions of Appendix A, operating and survival wind speeds were specified (Appendix B) and combined with wind tunnel pressure coefficients (References 3 and 4) and statistical wind data (Reference 5) to determine appropriate gore loads and their respective durations.

To establish a reasonably accurate schedule of loads and accumulated exposure times, the following design ground rules were established by JPL:

- The concentrator will initiate driving to the stow position at a wind speed of 50 km/hr, whether operating or in the retire position
- Stow position will be the zenith pointing position, with the concentrator close to the ground

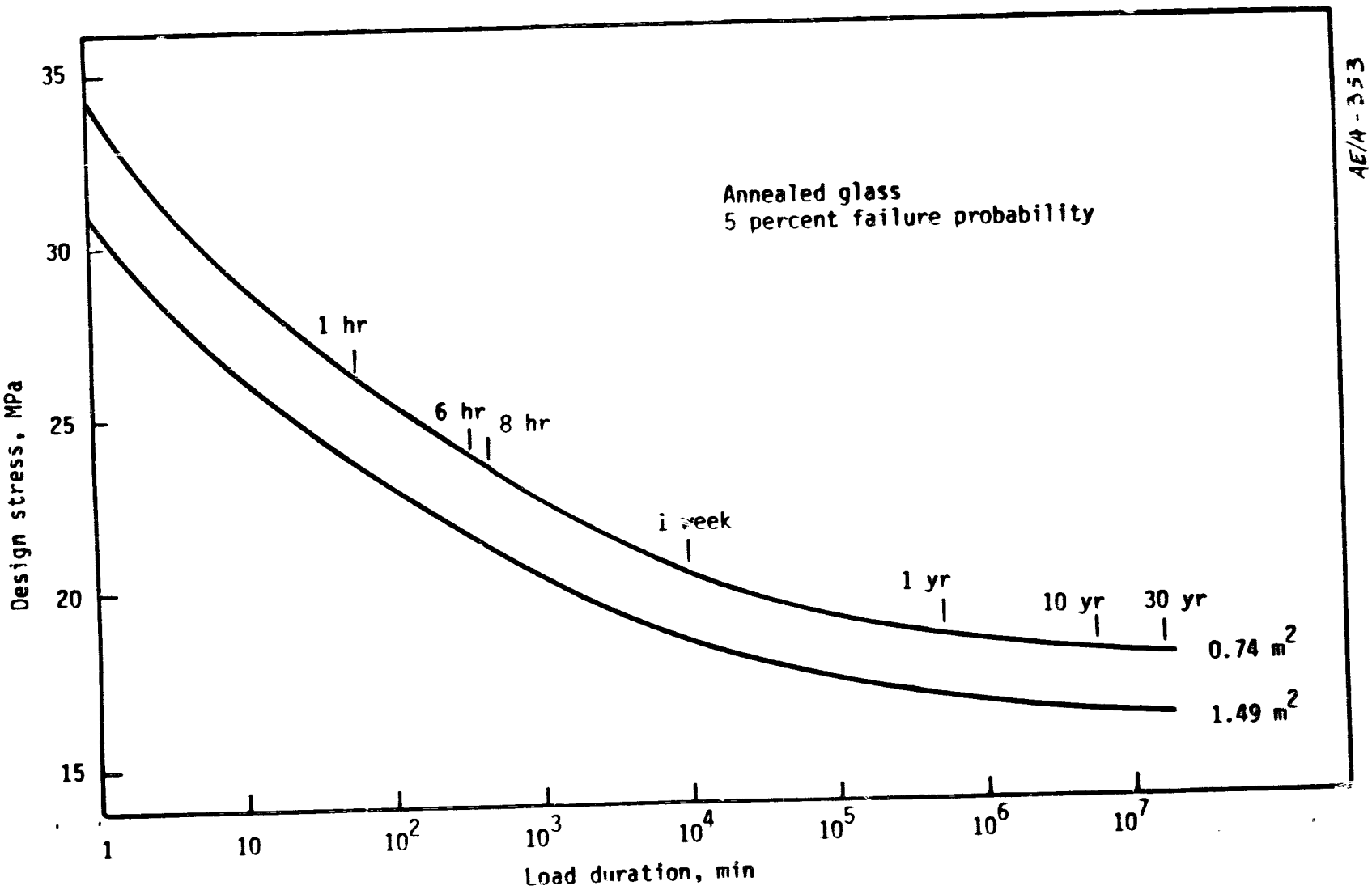

Figure 2-3. Sheet Glass Design Stress Versus Lifetime

- The maximum time required to complete the stow operation will be 17 min
- The concentrator will be capable of withstanding the following wind loads for accumulated exposure times consistent with a 30-yr operating life:
  - 50 km/hr winds -- operating
  - 60 km/hr wind gusts -- operating
  - 80 km/hr winds -- driving to stow
  - 110 km/hr winds -- a single "short" exposure
  - 120 km/hr winds -- stowed

To establish accumulated exposure times to these wind speeds over a 30-yr period, a table of annual frequency of occurrence versus wind speed for the United States was consulted. The two locations experiencing the most severe wind conditions were conservatively chosen as the geographical areas modeling the design conditions. These areas were Cold Bay, Alaska and Great Falls, Montana. From the wind frequency data for these two locations, frequency curves were generated and used to determine the frequency of occurrence pertaining to each wind speed cited above.

The aerodynamic wind loads on the individual gores are dependent not only on the wind speed, but also on the angle of attack of the wind relative to the paraboloidal dish and the location of that gore within the paraboloid. Based on JPL-furnished wind tunnel data (References 3 and 4), pressure coefficient maps were generated for the concentrator at several attitudes. These attitudes, expressed as the pitch angle of the concentrator relative to the wind direction, were 0^{0} (facing into wind), 60^{0}, 90^{0}, 120^{0}, and 180^{0} (backside wind). From these maps the attitude resulting in the most severe gore loading was chosen and the

loads on the critical gore were computed. The attitude producing the highest gore loading was a 60^{o} angle between the wind direction and the axis of the concentrator. Figure 2-4 shows the isobaric map for the concentrator at a 60^{o} pitch angle relative to the wind direction. Isobars are indexed with the combined pressure coefficient for concave and convex sides of the paraboloid ($C_{p_{concave}} - C_{p_{convex}}$). Indicated on the map are the inner and outer gore positions where maximum bending loads are experienced, as well as the outer gore receiving the maximum torsional loading. The loading conditions used to size the gores were derived from the pressure profiles on these key gores at a 60^{o} angle to the wind.

The most probable accumulated residence time in the critical attitudes (60^{o} pitch, $\pm 60^{o}$ yaw, and pitch and yaw combinations producing a 60^{o} resultant angle with the wind) were combined with the annual frequency of occurrence data for the design locations, and probable exposure times to these maximum loads were determined. Also computed were probable exposure times to 120 km/hr survival loads in the stowed position. The resulting design load requirements are presented in Table 2-8, along with the uniform pressure distribution producing the same maximum bending moment as the actual aerodynamic pressure distribution.

A 30-yr accumulated exposure time of 1 min at the worst case angle of attack was assumed for the 110-km/hr "single short exposure" requirement. Since the concentrator begins driving to stow at the onset of a 50 km/hr wind and takes a maximum of 17 min to reach the low drag zenith stow position, it is extremely unlikely that the concentrator will be subjected to a 110-km/hr wind at the worst case angle of attack. Furthermore, should such conditions be encountered, a 1-min duration is more than ample time for an individual gore to pass through the critical

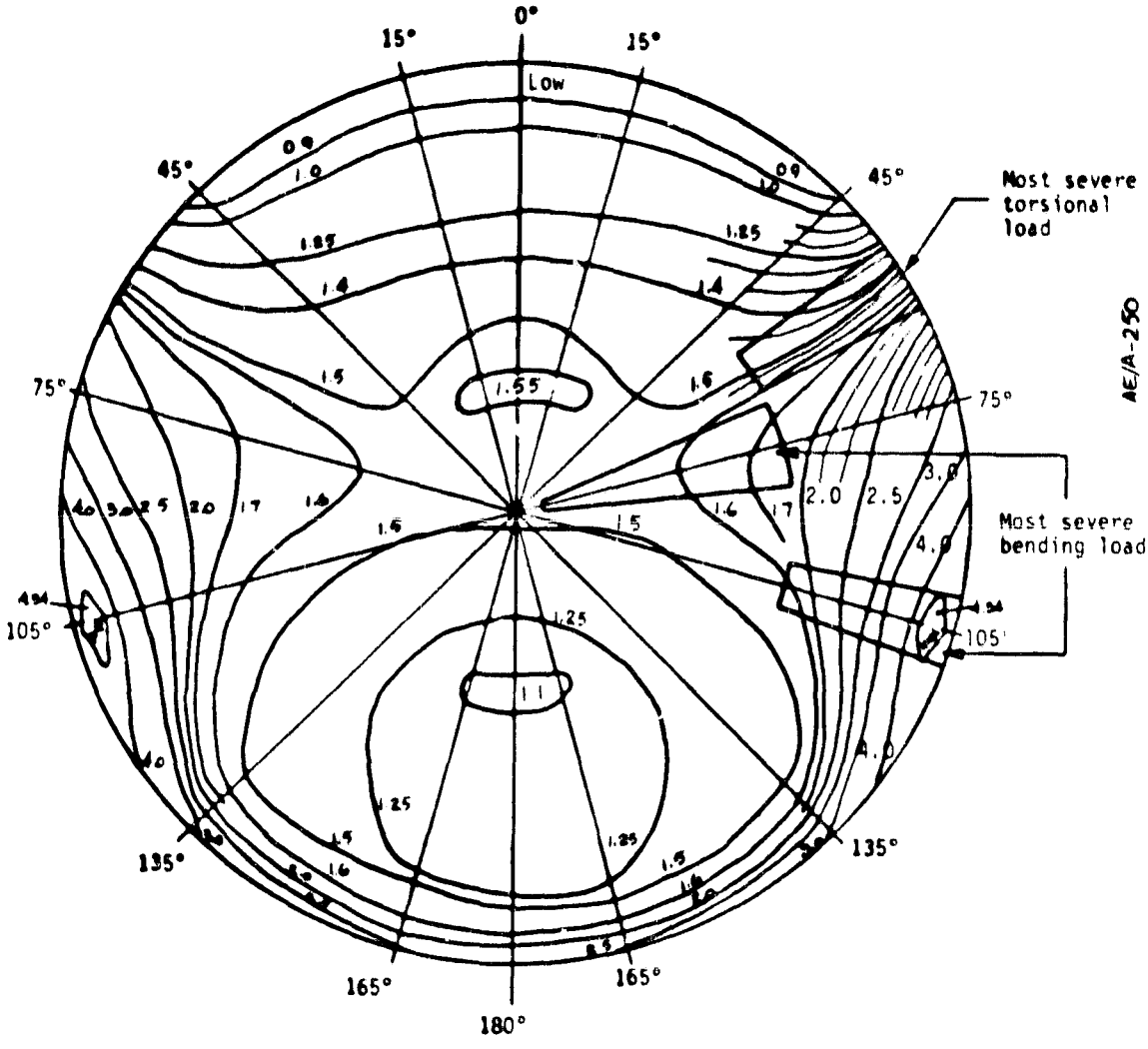

Figure 2-4. Combined Pressure Coefficient (60^{o} Angle of Attack)

Table 2-8. Load Summary -- 30-Year Operational Life

Condition	Wind Speed (km/hr)	C_p	$P_{effective}$ kPa (psi)	Accumulated Exposure
Operating (steady-state)	50	Most severe aerodynamic distribution	0.3234 (0.0469)	1 yr
Operating (20 percent gusts)	60	Most severe aerodynamic distribution	0.4916 (0.0713)	4 mo
Drive to stow	80	Most severe aerodynamic distribution	1.0887 (0.1579)	8.2 hr
Survival in stow	120	1.1 (uniform)	0.7447 (0.1080)	6 hr
Survival unstowed (instantaneous)	110	Most severe aerodynamic distribution	2.1340 (0.3095)	1 min
Survival unstowed (most severe to torsional load)	110	Most severe aerodynamic distribution	18.4 N-m (163 in.-lb) at gore root	1 min

alignment position. These are therefore felt to be very conservative assumptions.

2.2.1.3 Governing Load Determination

The determination of the governing design load was made by combining the probabilistic allowable stress curves for the sheet and cellular glass materials (Figures 2-2 and 2-3) with the accumulated load exposures of Table 2-8. Since, for a given design, the maximum bending stresses are proportional to the maximum bending moments, relative stress levels can be directly determined by comparing the effective pressure

values from Table 2-8. By proportionally plotting each load value with its appropriate exposure on the material design curves, as in Figures 2-5 and 2-6, the governing load can be determined.

A stress level below the design curve indicates a longer than specified exposure for 5-percent failure probability, or a less than 5-percent failure probability for the indicated exposure time. Loads not appearing on the curve for annealed glass fall below the minimum ordinate value depicted.

As can be seen from Figures 2-5 and 2-6, the 110-km/hr "single short exposure" requirement is the governing design load for both the sheet and cellular glass material. Due to the arbitrary nature of this requirement, its impact on the final gore design was evaluated at the end of the preliminary design effort.

2.2.1.4 Configuration Selection

Due to the relatively short duration of the preliminary design task and the significant impact of the gore design on the balance of the concentrator, an early selection and freeze of the gore configuration was necessary. The JPL design concept was based on 20 inner and 40 outer gores, each fabricated with a mirror glass face sheet bonded to a contoured, low-density (192 kg/m^3 or 12 pcf) Foamsil® 75 substrate with a single high density (320 kg/m^3 or 20 pcf) Foamsil® 75 full-length longitudinal spar.

The mirror glass face sheet sees steady-state curvature stresses in addition to the aerodynamic wind loads and gravitational loads. The curvature stresses are a combination of membrane and bending stresses with the membrane stresses being dependent on the panel width and radius of curvature of the gore. Lacking the detailed sheet glass design data, an

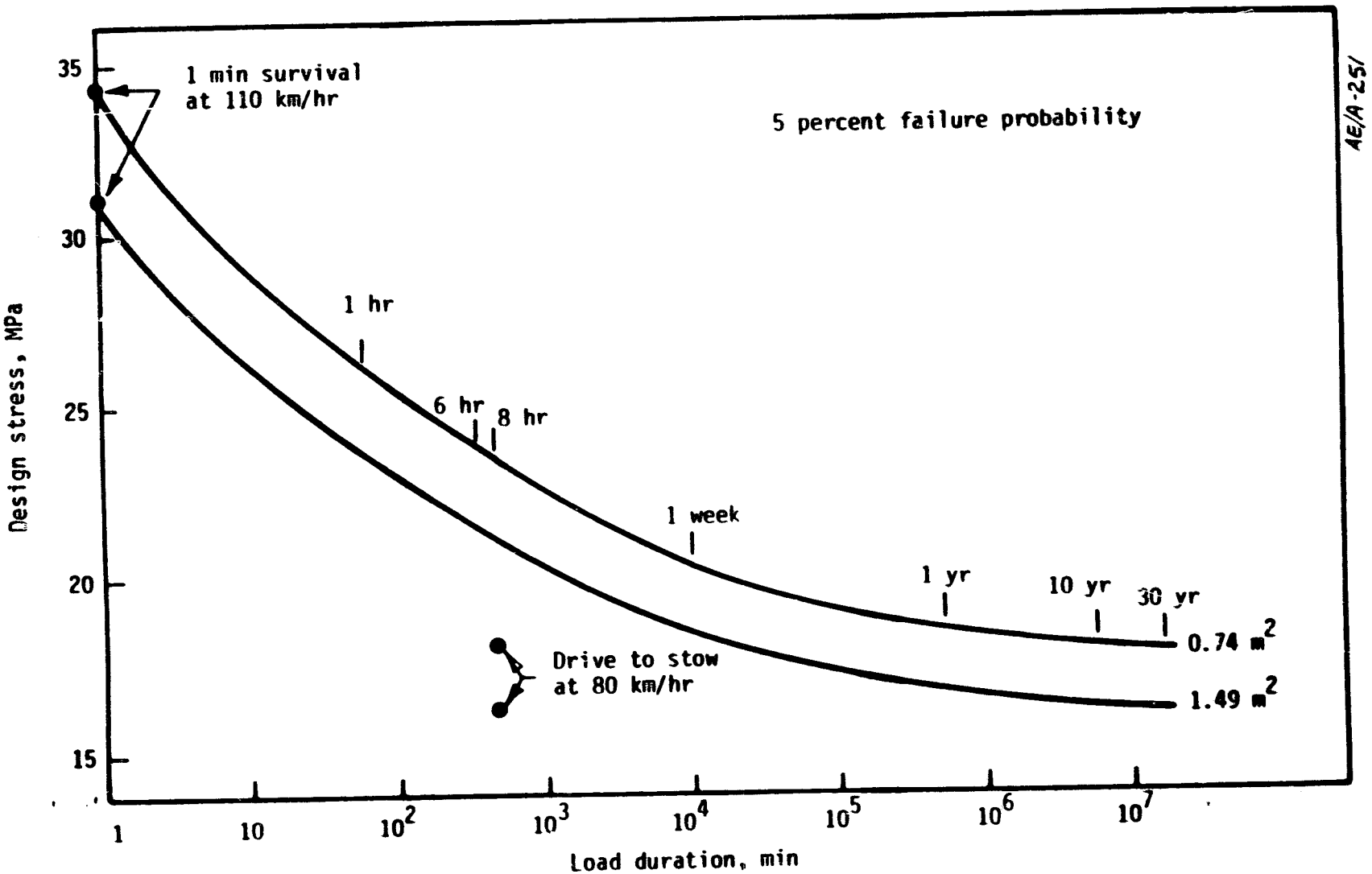

Figure 2-5. Governing Design Stress -- Annealed Glass

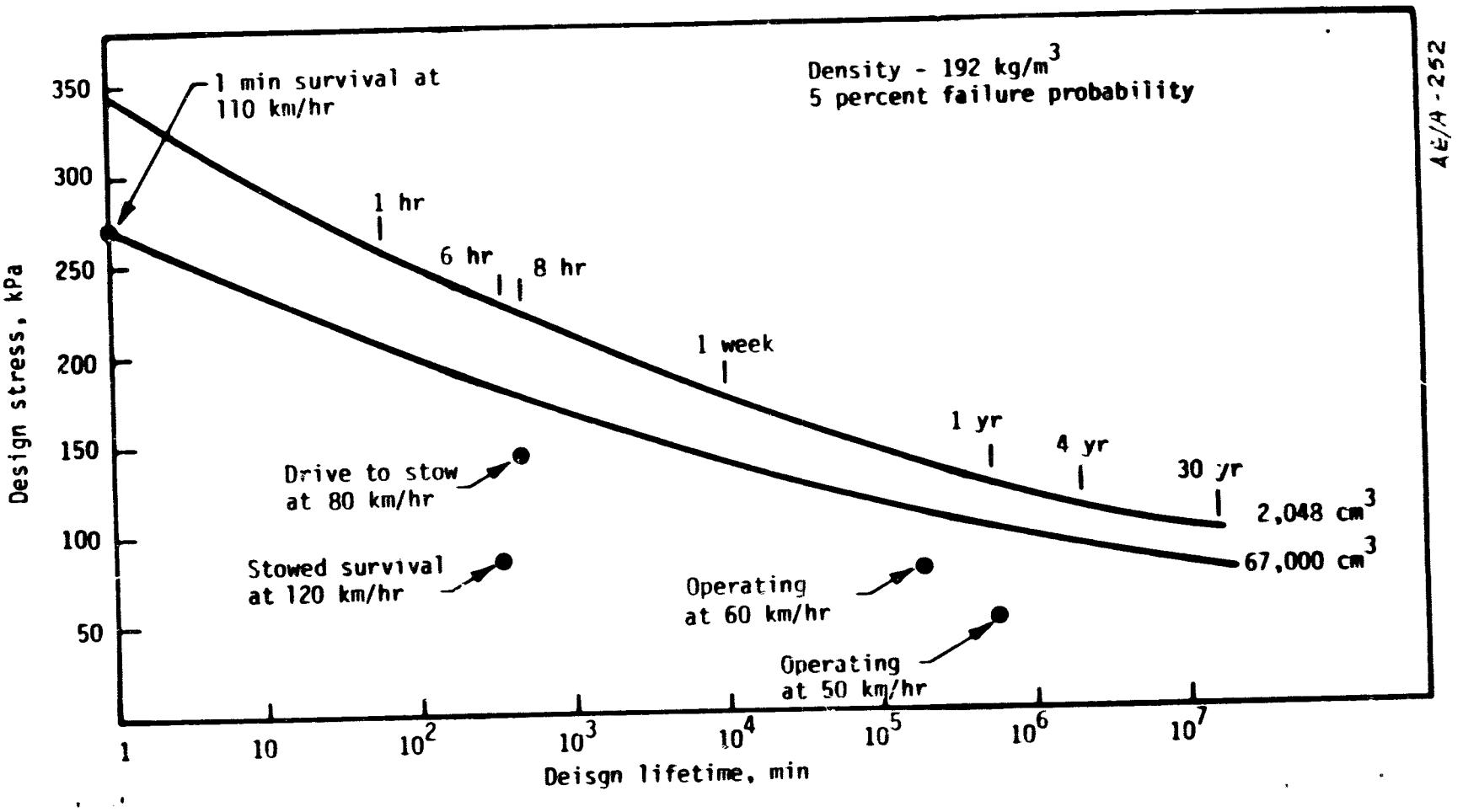

Figure 2-6. Governing Design Stress -- Foamsil® 75

evaluation of the optimum number of gores was not feasible. The 20 inner gore/40 outer gore arrangement was therefore retained for preliminary design.

In an attempt to minimize the weight of the reflective panels, three basic gore concepts (including the JPL baseline) were evaluated. As shown in Figure 2-7, these included:

- A thin mirrored glass face sheet bonded to a contoured sheet of cellular glass with a waffle or isogrid stiffened rear surface (Figure 2-7(a))
- A thin mirrored glass face sheet bonded to a contoured sheet of cellular glass stiffened by longitudinal spars on the rear surface (Figure 2-7(b)) (JPL baseline concept)
- A sandwich-type panel employing thin glass face sheets on a contoured cellular glass core (Figure 2-7(c))

The first concept was rejected because a complex, structurally efficient stiffening network such as an isogrid is not currently feasible in cellular glass. An optimum isogrid structure requires thin deep ribs in a closely spaced network that could only be produced by casting or by an elaborate coring procedure. Casting of cellular glass in such a structure is not presently feasible, and the high cost of coring, coupled with the minimum allowable thickness of 2.54 cm (1 in.), would result in a heavy and excessively costly panel.

The second approach considered is a viable one. Cellular glass spars can be easily and inexpensively formed by any of several techniques, such as sawing and bonding to the face sheet, or routing out of a single slab.

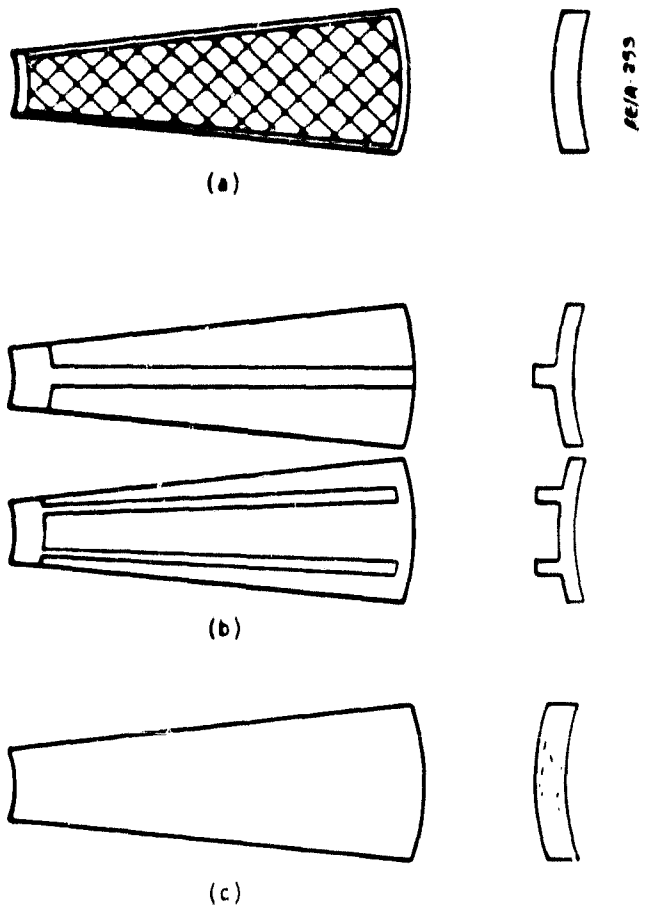

Figure 2-7. Gore Concepts Considered

The sandwich-type panel is also a viable approach offering good strength and stiffness to weight ratios. It allows the higher load bearing capacity of glass to be used to improve the structural efficiency of the panel. However, applied to the gore design, it has some disadvantages. The compound-curved front surface of the gore requires a compound-curved rear surface for maximum structural efficiency. If the gore is contoured from a flat slab by some machining process, this increases the cost of manufacturing. Since sagging, pressing, and foaming to contour have been ruled out by the projected state of the art for 1985,

this must be taken as a disadvantage. A simply curved rear surface would add weight to the gore in a parasitic fashion by producing excessively thick edges where stresses are low, and a thin midsection where maximum bending strength is needed.

Due to practical considerations of gore manufacturability and the potential for lower gore weight, the JPL baseline spar configuration was retained. The single spar design was shown to be superior to the double spar concept due to its increased torsional rigidity. An investigation of the effects of variations in spar density (see Figure 2-8) led to the incorporation of a simply curved sheet glass cap running the full length of the spar. The high load bearing capability of the sheet glass was thus incorporated in the predominant load direction (longitudinal bending) without suffering the parasitic weight effects of a full sandwiched configuration.

2.2.1.5 Design Analysis

The objective of the preliminary gore design effort was to develop a minimum weight design capable of being mass produced with near-term technology. Having selected the overall configuration, the design was refined to provide a minimum weight unit capable of meeting the strength and deflection specifications.

The major variables in the optimization of the gore design were:

- Mirror glass thickness
- Cellular glass substrate thickness (depth)
- Cellular glass substrate density
- Cellular glass spar width
- Cellular glass spar thickness (depth)

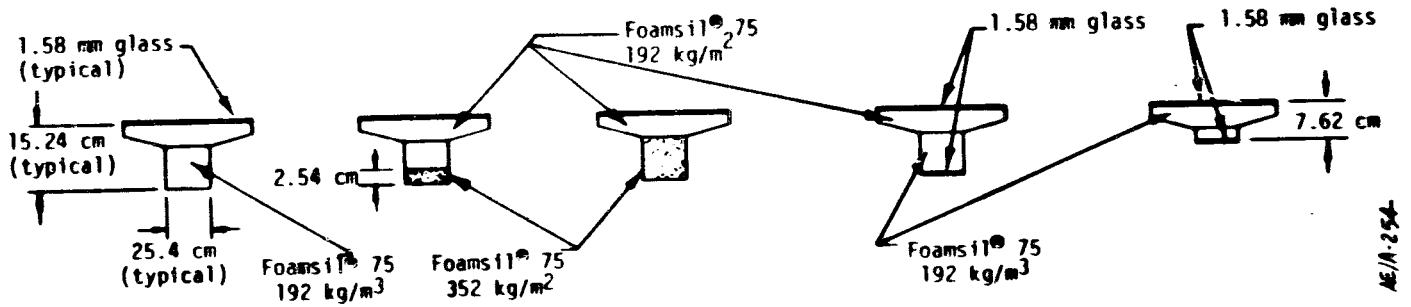

Configuration:	Baseline	Modification 1	Modification 2	Modification 3	Modification 4
Stiffness:	1.00	1.41	1.80	2.11	0.65
Capacity:	1.00	2.02	4.25	2.48	1.17
Weight:	1.00	1.08	1.31	1.07	0.73
Limitation:	Stress in Foamsil®	Stress in Foamsil®	Stress in Foamsil®	Stress in Foamsil®	Stress in Foamsil®
Section height:	1.00	1.00	1.00	1.00	0.50

Figure 2-8. Evolution of Gore Shape -- Spar Concept

- Cellular glass spar density
- Sheet glass spar cap thickness

Based on the simplified configuration trade-off analysis (Figure 2-8), a 25.4-cm (10-in.) wide cellular glass spar was selected to meet the torsional rigidity requirements. The 192 kg/m^3 (12 pcf) density Foamsil® 75 material was selected as the cellular glass material for both the substrate and spar, since the additional strength of the higher density material (320 kg/m^3 or 20 pcf) was more than offset by its increased weight. To simplify gore fabrication, the thickness of the sheet glass for the mirrored face sheet and the spar cap were assumed to be identical.

A matrix of gore designs combining the remaining variables was analyzed. The ranges for each variable were:

- Sheet glass thickness -- 0.50 to 1.58 mm (0.020 to 0.062 in.)
- Cellular glass substrate thickness -- 5.08 to 7.62 cm (2 to 3 in.)
- Cellular glass spar thickness -- 0 to 22.86 cm (0 to 9 in.)

A 5.08-cm (2-in.) minimum substrate thickness was assumed based on recommendations from Pittsburgh Corning Corporation. A 2.54-cm (1-in.) minimum edge thickness for the substrate was also assumed as a practical limit for material handling. A preliminary investigation of the matrix indicated that the minimum substrate thickness was preferred.

Detailed plots of worst case cellular glass core stress, mirror glass face sheet stress, and spar cap stress as a function of overall gore thickness (substrate plus spar) were developed for three sheet glass thicknesses at two wind speeds. Sheet glass thicknesses of 0.50 mm (0.020 in.), 1.0 mm (0.040 in.), and 1.58 mm (0.062 in.) were

investigated. The 80-km/hr load condition with an accumulated exposure of 8.2 hr was investigated in addition to the governing load of 110 km/hr for 1 min. This allowed a determination of the sensitivity of the final gore weight to the governing load condition.

Figure 2-9 is a representative plot showing the state of stress for each of the gore components for an outer gore at the point of maximum bending stress for the governing design load. Since the mirror glass and spar cap are stressed components, the state of stress is dependent on glass thickness as well as core thickness. The figure is for the 1.0-mm (0.040-in.) mirror glass and spar cap thickness. Similar curves were developed for the 0.50-mm (0.020-in.) and 1.58-mm (0.062-in.) glasses. The ordinate depicts bending stress due to wind load, while the scales running along the mirror and cap curves indicate combined stress level resulting from gore bending, plus the curvature and membrane stresses associated with the gore contour. Since membrane stress is dependent upon the size of the mirror sheet, curves for full and half gore width sheets were developed. The scale above the mirror curve is for a gore comprised of two mirror sheets, situated side by side on the face of the gore, with a parting line running down the centerline of the gore. The scale below the mirror curve is for a gore having a single full-width mirrored face sheet. The abscissa is the total gore thickness (less glass), the sum of the 2-in. substrate and the spar. From the allowable stress curves presented in Section 2.2.2.1, limiting stress levels appropriate to the accumulated load durations were chosen. As the thickness of the gore is decreased, the maximum allowable stress level is reached in the cellular glass core before the mirror or spar cap. The deflection limit calculated for the 50-km/hr load condition is also shown. The outer gores are

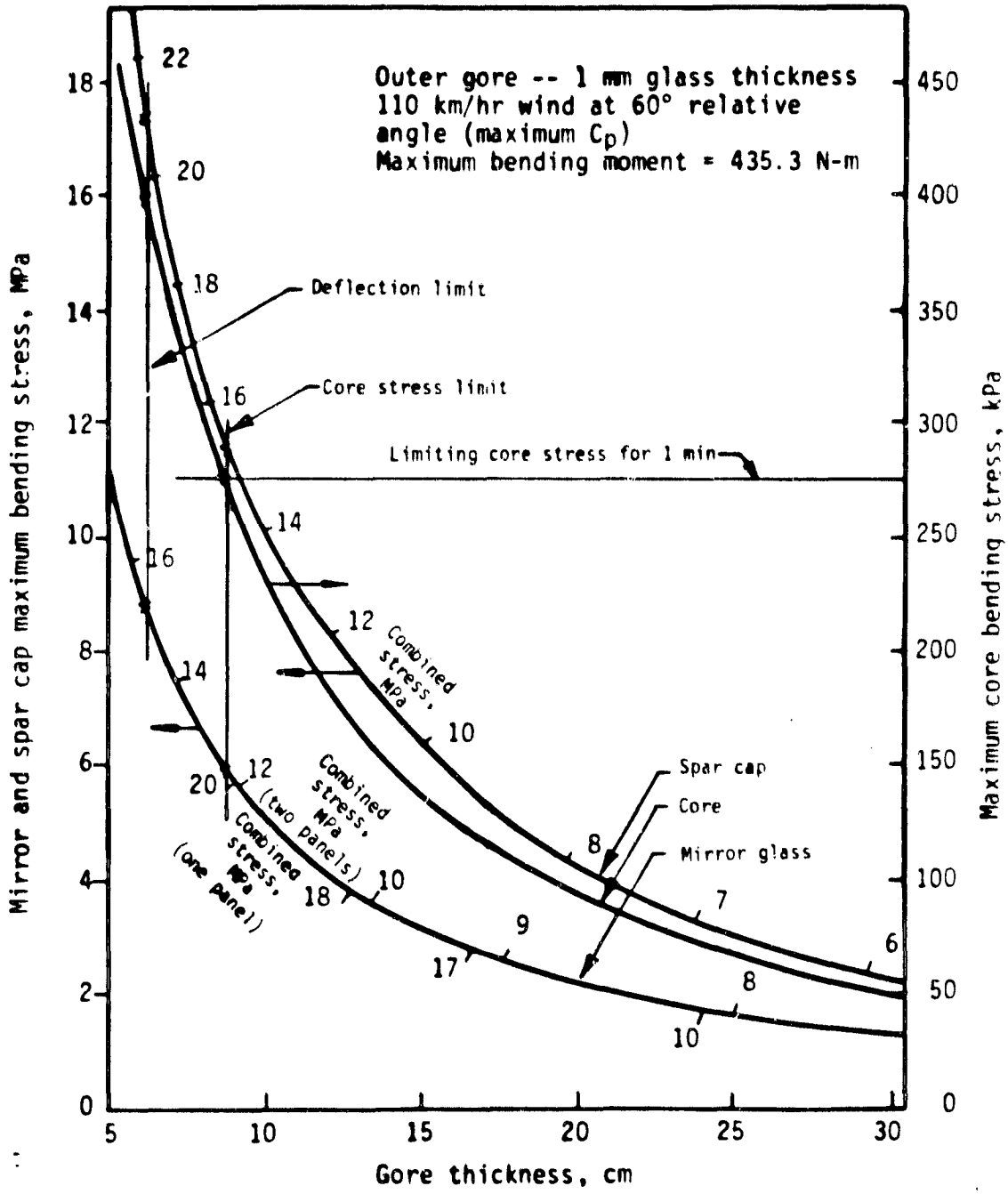

Figure 2-9. Outer Gore Design Curves

stress-limited by the cellular glass core. Due to a very conservative assumption for the operating C_p for the gores (C_p = 3.0), the inner gores proved to be deflection limited, however.

As indicated in Figure 2-9, the minimum outer gore thickness for the 1.0-mm (0.040-in.) thick full face sheet configuration is 8.89 cm (3.5 in.). Similar curves were developed for the 0.50-mm (0.020-in.) and 1.58-mm (0.062-in.) glass sheets and for the inner gore. For a given sheet glass thickness and overall gore thickness, the gore mass can be directly determined. Cross plots of gore mass versus glass thickness were developed to allow selection of the minimum mass inner and outer gore designs. Figure 2-10 is the plot for the outer gore at the governing design load condition.

The mirror stress level is composed of a short duration bending stress superimposed on a long-term curvature/membrane stress level. It must therefore be examined in light of two limiting stress levels, one for combined stress with a relatively short accumulated duration, one for a curvature associated stress for a duration of 30 yr. The design lifetime for the mirror glass with a 5-percent failure probablity for the long-term stress is listed at the upper end of each curve. The steady-state curvature stresses for the full face sheet 1.58 mm (0.062 in.) mirror glass are too great to meet the 30-yr, 5-percent failure criteria. While both the 1.0- and 0.5-mm (0.040- and 0.020-in.) glass sheets can easily meet this requirement, the increased load carrying capability of the 1.0-mm (0.040-in.) mirror allows a thinner gore with lower overall weight than does the 0.50-mm (0.020-in.) material. In addition, the use of the thicker sheet material avoids the requirements for advancements in the state of the art for production by the fusion process and for techniques

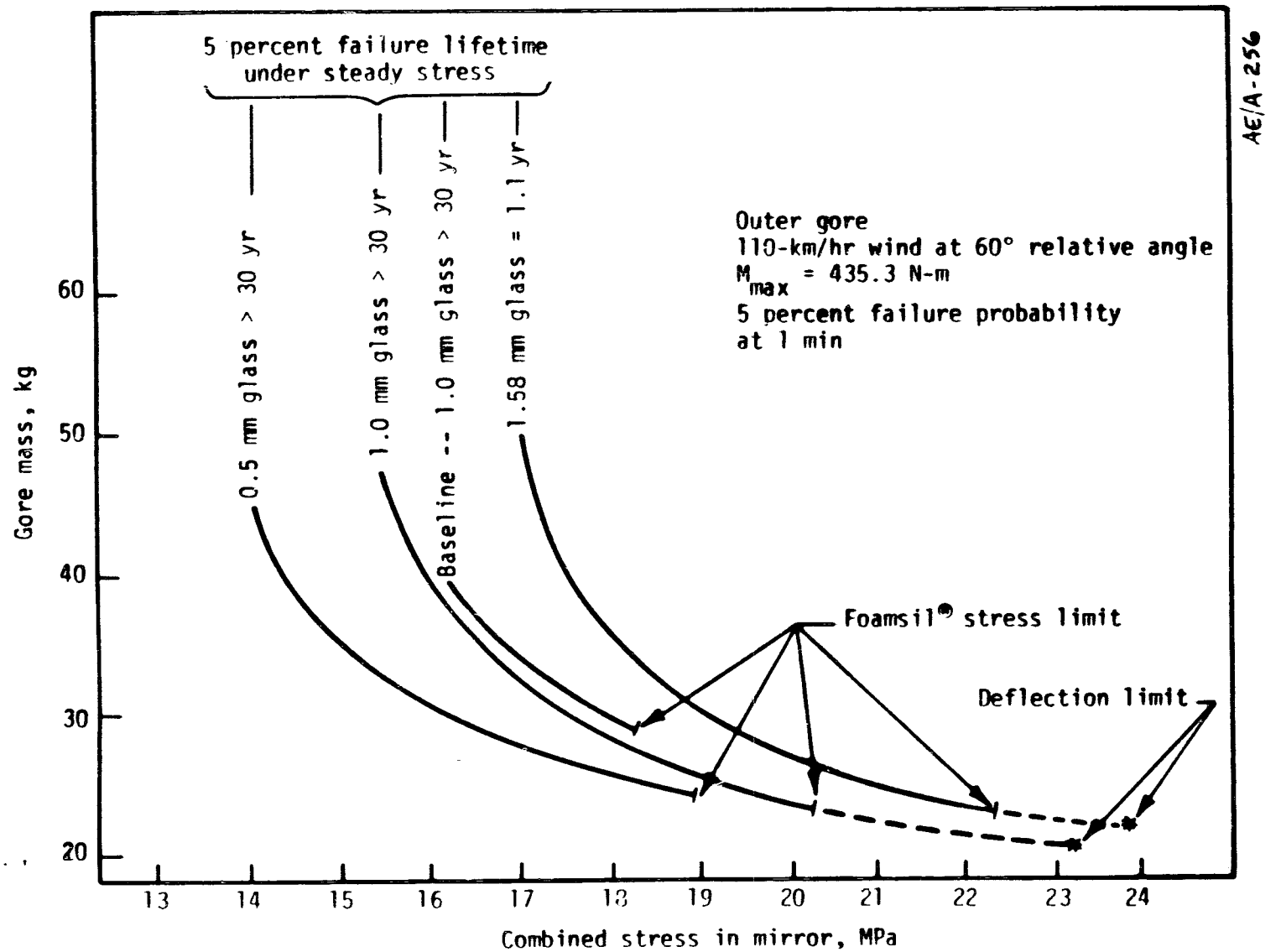

Figure 2-10. Outer Gore Sheet Glass Thickness Trade-Off

of handling the large sheets of glass required for the present gore design. Also depicted in Figure 2-10 is a curve for the uncapped baseline design updated to use 1.0-mm (0.040-in.) mirror glass. It is apparent that the addition of the glass cap to the reinforcing spar allows a 23-percent reduction in the weight of the gores.

The larger width of the inner gore precludes the use of a single mirror panel. A two-panel inner gore design using 1.0-mm (0.040-in.) mirror glass was therefore selected. Again the limiting stress is in the cellular glass core. The minimum weight inner gore design has an overall (substrate plus spar) depth of 6.35 cm (2-1/2 in.) and a mass of 17.2 kg (38 lb).

Figure 2-11 shows the impact of the dominant load choice upon gore mass. For the 31.7-MPa (4,600-psi) allowable 1-min glass stress, the choice of a 110 km/hr wind exposure for 1 min can be seen to have only a minor effect upon gore mass, amounting to a penalty of 0.9 to 1.4 kg (2 to 3 lb) per gore. As can be seen in the figure, a lower allowable glass stress could have a pronounced effect upon the sensitivity of gore mass to the wind specification (i.e., a 7.25 kg (16 lb) difference in outer gore mass at 17.2 MPa (2,500 psi) allowable). While the importance of this load should still be considered for future design work, deletion of this load will have no major effects on the present design.

2.2.1.6 Analysis of a Two Mirror Panel Inner Gore

Since the curvature associated stress forces the 99-cm (39-in.) wide inner gore to be fabricated with two mirrored face sheets, the effects of an interruption in the load bearing mirror sheet were investigated. The junction line between mirror sheets is oriented along

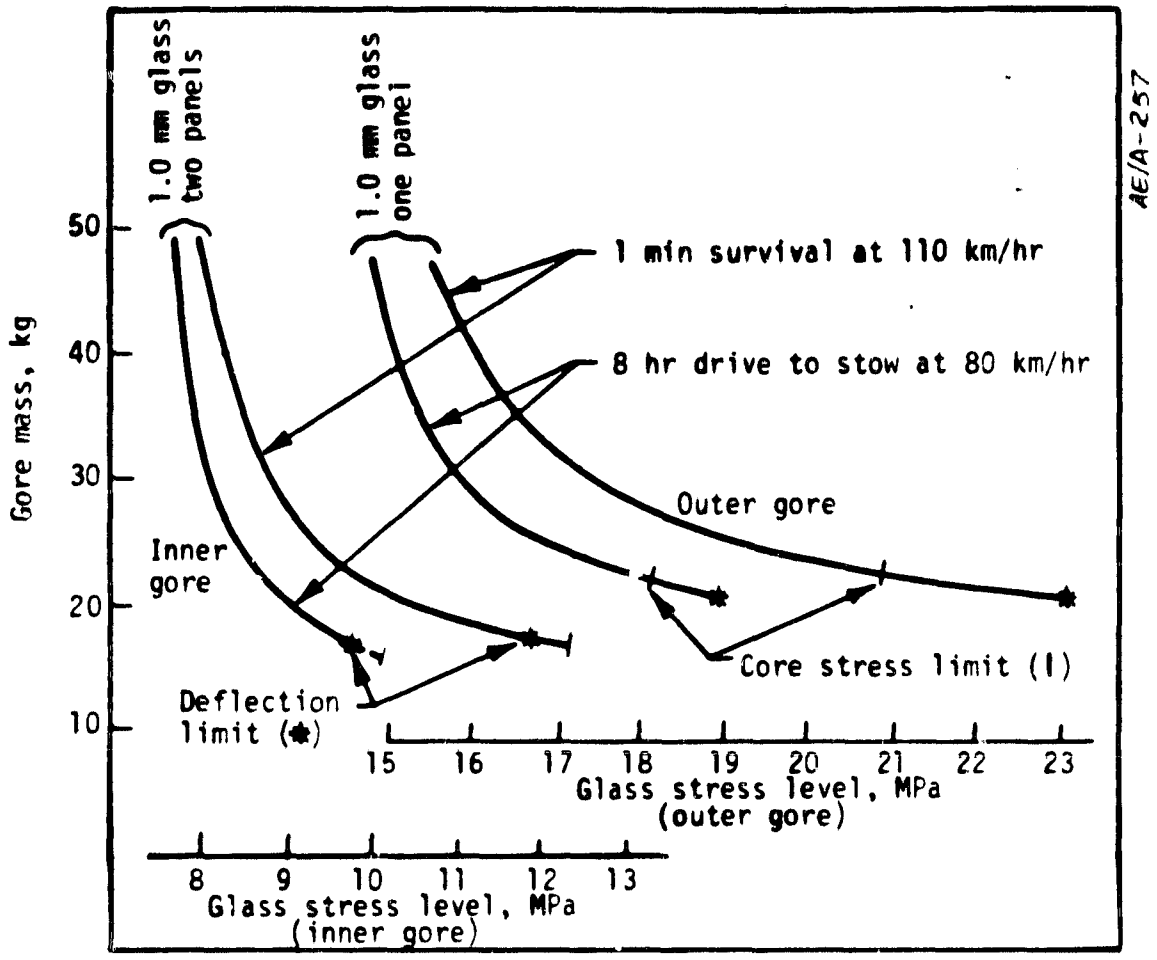

Figure 2-11. Effect of Dominant Load Upon Gore Mass

the longitudinal axis of the gore (Figure 2-12) to allow major (axial) bending loads to be carried in a continuous face sheet, but lateral bending also exists in the gore. Since the main gore support is located at a single point along the gore centerline, the gore bends laterally about this point in a manner resembling two cantilever beams joined at the root. The location of maximum bending stress therefore coincides with the split line between mirror sheets. The rib size could apparently be increased to provide ample strength in this area, but a stress concentration exists at the point of discontinuity between mirror sheets.

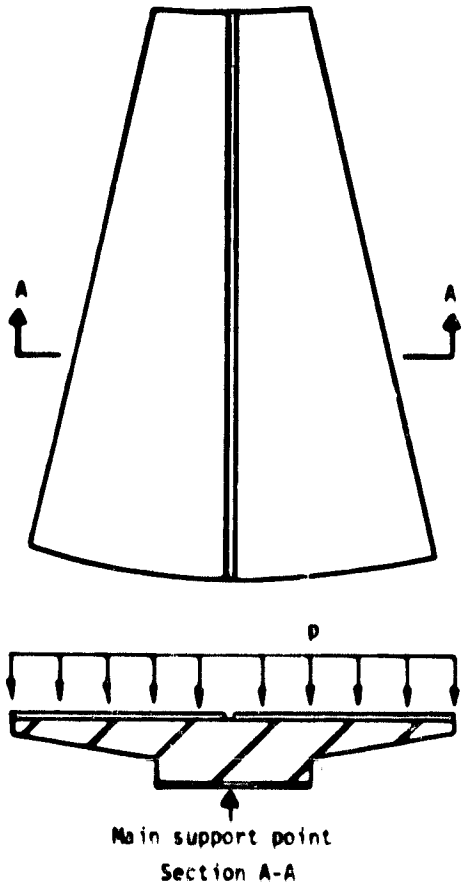

Figure 2-12. Two Mirror Panel Inner Gore

A computer model of the gore was set up using the ANSYS finite element computer program.

The results of the computer analysis revealed the existence of a peak tensile stress of much higher level than anticipated, located at the center of the notch between mirror panels. The effective stress concentration factor, K_t, associated with the peak stress value was 47.2. The ANSYS model was used to explore the possibility of reducing the stress concentration factor to a region between 1.0 and 1.3 by changes in notch geometry and/or load-bridging to prevent the tensile load carried by the mirror glass from being locally transferred to the cellular glass core.

Figure 2-13 summarizes the results of the exploratory survey. Geometric modifications of the notch were capable of reducing the K_t values from 47.2 to 14.4. Various bridging techniques resulted in K_t values ranging from 10.8 down to 1.1. When considering the sensitivity of the gore design to the stress level in the core, the choice of a double-shear type bridge of titanium with its associated K_t of 1.1 was made. Titanium was chosen as the bridge material because its coefficient of thermal expansion is a reasonably close match to the chosen mirror glass. This represents a viable solution to the problem, but unfortunately involves an increase in the manufacturing cost of the gore both due to the cost of titanium and the extra labor required to groove the core and bond the bridge to the glass after the glass has been flexed

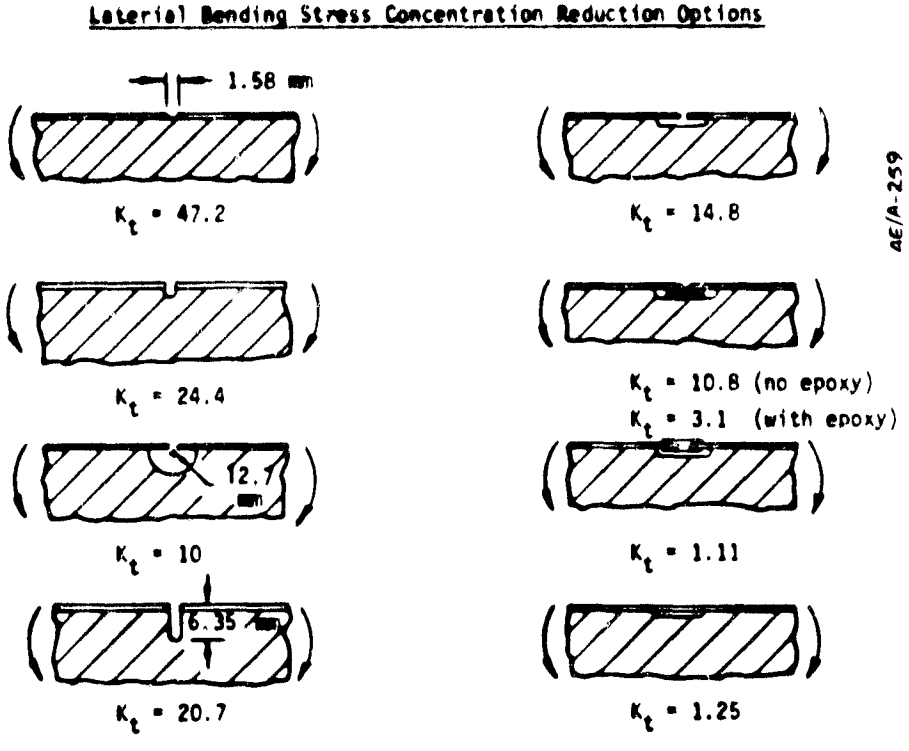

Figure 2-13. Lateral Bending Stress Concentration Reduction Options

into place. A more efficient solution to the stress buildup problem that avoids the added cost and complexity of the titanium load bridge was sought in the detailed design task and is discussed in Section 3.

2.2.2 Structures Design

The preliminary design of the Advanced Solar Concentrator produced a minimum weight structure with the necessary strength and deflection characteristics to meet the overall performance goals. The design was based on high-volume mass production technology allowing the use of nonstandard structural sizes for optimum weight/strength/deflection characteristics.

The structural subsystem must provide an articulated two-axis tracking capability in addition to interfacing with and rigidly supporting the reflective panel, the power conversion module, and the drive subsystem. The kinematics of the structure were therefore an important consideration in all subassembly designs.

This section presents a brief discussion of the structural design approach and the results of the trade-offs and analysis for the following structural subsystem components:

- Gore support ring structure
- Receiver/engine support structure
- Counterweight structure
- Drive structure

The design of the center pedestal is discussed in Section 2.2.4 along with the foundation design.

2.2.2.1 Approach

The design of each structural subassembly included four main efforts:

- Functional requirements definition
- Load definition
- Configuration selection
- Analysis and weight optimization

The approach to each of these operations is briefly described in the following paragraphs.

Functional Requirements

The functional requirements of each structural subassembly were identified and summarized. Included were the interface requirements, deflection limits, and kinematic requirements. This functional requirements statement then served as the basis for configuration selection and design/performance analysis.

Load Definition

The applied loads, both static and dynamic, were identified and summarized for each structural subassembly. Due to the cascading load path from one structural subassembly to another, the order of analysis is important.

The aerodynamic wind loads were analyzed at two levels of detail. Since the gore ring serves to define the paraboloidal shape through rigidly and accurately supporting the individual gores, the individual gore loads and their distribution around the ring were very important. The torsional windup or racking of the ring translates directly into distortions of the focal plane image. Worst case loadings based on the contour maps described in Section 2.2.1 were therefore used to analyze the gore support ring. Gross body force and moment coefficients (Reference 3), however, were sufficient for determining the aerodynamic loads which must be reacted by the drive structure.

Due to the redundant load paths inherent in the complex multimember frame structures, different loading conditions may govern the design of various elements of the structure. Several orientations with their corresponding worst case wind velocities were therefore analyzed for each subassembly. The load cases analyzed are summarized in Table 2-9. The dominant load case, that which governed the design of the majority of the elements for the subassembly, is also noted.

Due to the short schedule for the preliminary design task, the design and analysis of several of the structural subassemblies had to proceed in parallel. Assumed values for the mass of several elements of the concentrator were therefore used to estimate dead loads. The assumed values are summarized in Table 2-10 along with the actual values resulting from the analysis. As can be seen from the table, all assumed values were conservative, leading to a slightly overdesigned structure. It is estimated that an iterative analysis with the actual weights could lead to a 9- to 10-percent reduction in overall concentrator structural weight.

Configuration Selection

Based on the interface constraints, the kinematic requirements, and the ground rules of the JPL baseline concept, several geometric configurations were developed for each of the structural subassemblies. Joint loaded space frame designs were emphasized to maximize structural efficiency and minimize material costs. Where possible, configuration options were screened based on preliminary calculations to minimize detailed analysis efforts.

Analysis and Weight Optimization

Detailed analysis of each subassembly was performed with the aid of computerized finite element modeling to allow accurate design of the

Table 2-9. Load Case Summary

Structure Analyzed	Case Number	Elevation (0° Horizon)	Wind			Lateral Seismic	Comments
			Speed		Direction		
			km/hr	mph			
Gore support ring	I	90° (stow)	120	75	Front	--	• ΔC_p distribution used to generate loads • Receiver/engine and counterweight structures in model
	II[a]	55°-60°	80	50	Front	--	
	III	0°	80	50	Back	--	
	IV	55°-60°	50	31	Front	--	
Drive structure	I[a]	90°	120	75	Front	--	• Loads determined by estimated gimbaled weights and gross body force and moment coefficients
	II	-25°	80	50	Back	--	
	III	0°	80	50	Front	--	
	IV	0°	80	50	Back	--	
	V	90°	120	75	Side	--	
Receiver/ engine support structure	I	-25°	80	50	Side	0.25g	• Lateral seismic and side wind loads act in concert
	II[a]	0°	80	50	Side	0.25g	
	III	45°	80	50	Side	0.25g	
	IV	90°	120	75	Side	0.25g	
Counterweight structures	I	90°	120	75	±Side	±0.25g	• Lateral seismic and side wind loads act in concert • ± → two directions, each case
	II	-25°	80	50	±Side	±0.25g	

[a]Dominant load case

Table 2-10. Estimated Mass of Structure Subassemblies

Description	Estimated		Actual	
	kg	(lb)	kg	(lb)
Receiver/engine (R/E)	1,350	(3,000)	1,350	(3,000)
R/E support structure	910	(2,000)	253	(557)
Gores	3,330	(7,320)	1,460	(3,220)
Counterweight	455	(10,000)	455	(10,000)
Gimbaled mass	10,830	(23,820)	8,630	(18,984)
Maximum hinge moment[a] N-m (ft-lb)	116,630	(86,000)	70,073	(51,670)
Minimum hinge moment[a] N-m (ft-lb)	-219,698	(-162,000)	-145,231	(-107,090)

[a]Hinge moments do not include counterweight system weight

multimember space frame structures. Each assembly was first sized to meet all loading conditions at its minimum weight design by assuring that each member was near its stress limit under at least one of the loading conditions. The structure was then selectively stiffened as required to achieve the required deflection characteristics.

It should be noted that all detailed analysis was performed for a nominal concentrator aperture diameter of 11 m. Final concentrator sizing to achieve the required performance at minimum cost was based on weight and deflection values scaled from the 11-m design (see Section 2.3).

2.2.2.2 Gore Support Ring (Refer to Drawing 7740-002)

The basic concept of the JPL Advanced Solar Concentrator is to use large inherently stiff reflective elements with a minimum of supporting structure. The panels (gores) are attached to the gore support ring, a ring truss with a diameter less than that of the reflective panel assembly (dish). The panel elements overhang the ring truss thereby allowing a smaller, less distributed and therefore lighter panel support structure. This low weight design not only results in a low-cost panel support structure, but also cascades down to the structures supporting the panel and gore support ring assembly.

The gore support ring serves to maintain the individual gores in their respective spatial positions forming the paraboloidal reflective surface. The receiver/engine support structure and the counterweight structures attach to the ring to form a subassembly hinging about a horizontal elevation axis. The location of the elevation axis on the ring and the point at which the elevation drive jack screw attaches to the ring were carefully chosen to achieve the desired elevation travel limits while minimizing the stow height in the zenith orientation. The location of these points strongly impacts the drive structure configuration and the elevation drive kinematics and load conditions.

Functional Requirements

The gore support ring must:

- Interface with and support 40 outer and 20 inner gores with three point attachments
- Limit panel rotations under worst case operating winds to meet performance specifications
- Interface with receiver/engine support structure

- Interface with counterweight structure
- Interface with drive structure
- Interface with elevation drive actuator
- Allow elevation motion limits of -25^{o} (below horizon) to 90^{o} (zenith position)
- Survive all specified loading conditions

Configuration Selection

In addition to the ring truss configuration, a radially cross-tied, front-braced structure and a radially cross-tied, rear-braced structure were considered. The ring truss was quickly shown to be torsionally more efficient and was therefore evaluated in detail. Three alternative ring truss structure configurations were analyzed. While all are triangular cross section toroidal ring trusses, the details of the internal bracing differentiate one from the others. The ring trusses are shown in plan view in Figure 2-14 and are designated as (1) 18^{o} Modified Warren, (2) 9^{o} Modified Warren, and (3) Hybrid. Each gore is supported by two points near the apex of the triangular ring truss and at a third point by an "outrigger" structure. The outrigger is formed by either three or four strut-type members rigidly attached to the ring truss.

Since space frame structures derive their high strength/low-weight characteristics through the efficient use of members in only tension/compression service, it is important to minimize the introduction of side loads through midspan member loading. Both the 9^{o} Modified Warren and the Hybrid configurations were carefully laid out to eliminate all midspan loadings. The 18^{o} and 9^{o} designations refer to the arc subtended by the internal diagonal braces and are determined by the number of gores and their arrangement. The "Modified Warren" designation refers

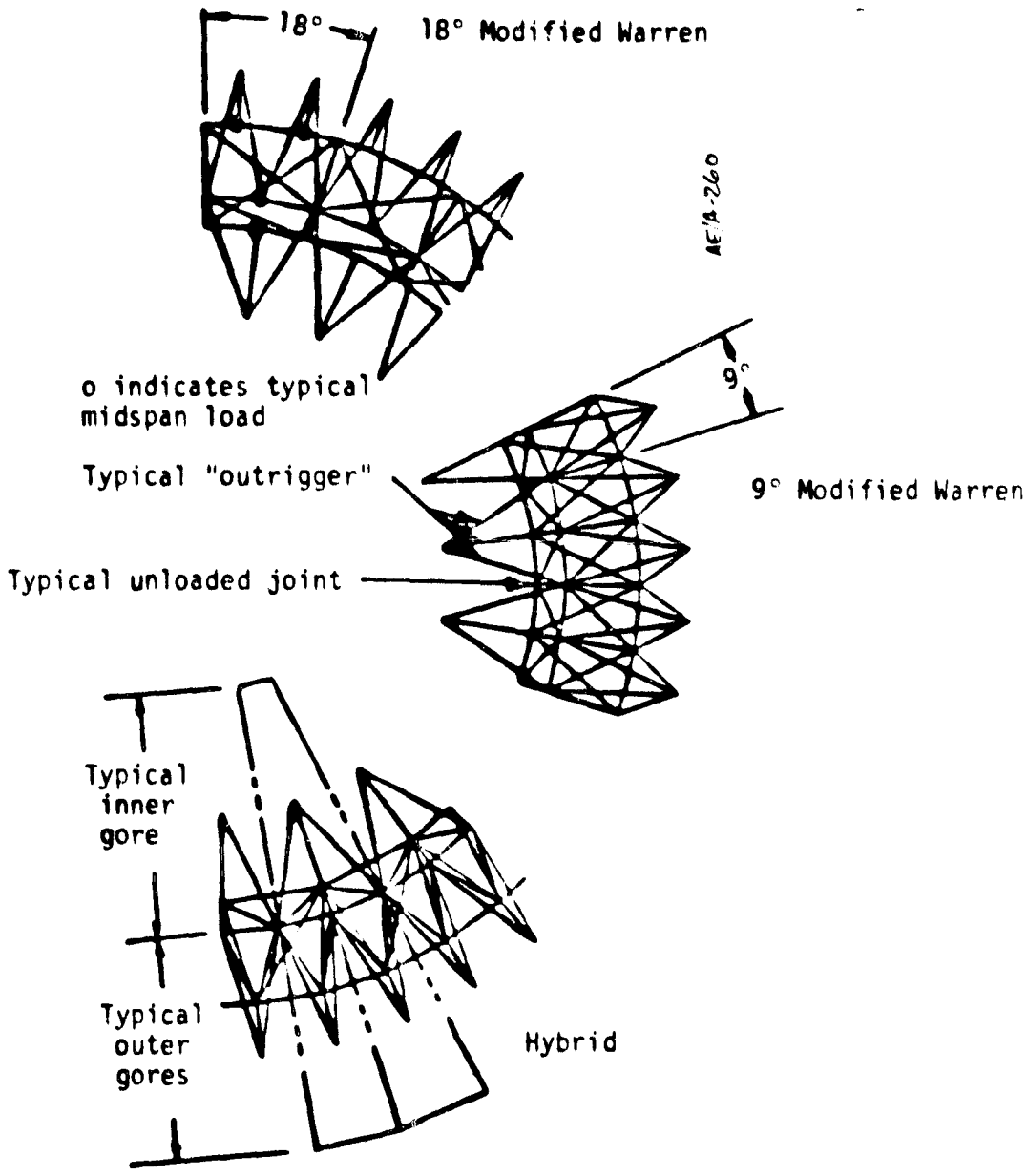

Figure 2-14. Alternate Ring Truss Concepts

to the relative positions of adjacent diagonals forming a Warren truss modified by the addition of struts which lie in radial planes and connect the three primary rings at the apices of the triangular cross section.

The 18^{o} Modified Warren configuration has a large number of midspan loading points occurring where the gore-supporting outriggers attach to the ring between joints. These midspan loads induce bending stresses in the structural members which is an inefficient method of carrying loads. The 9^{o} Modified Warren configuration eliminates all midspan loads by using a four-member outrigger for the outer gores. Several unloaded joints exist, however. The Hybrid configuration eliminates all midspan loads and nonloaded joints while using three-member outriggers for both inner and outer gores.

Each of the previously described concepts was modeled for computer analysis using the ANSYS structural analysis code. All members were initially sized to be stress-limited under the worst case loading condition. This resulted in the minimum weight design of each configuration that could meet all survival requirements. The area weighted rms panel rotation for each configuration was then calculated for the worst case operating wind load. As shown in Table 2-11 with all weights normalized to the Hybrid configuration, the 9^{o} Modified Warren design is clearly the most structurally efficient from a stress standpoint. However, due to the high optical concentration ratio required for the Advanced Solar Concentrator, structural stiffness is a primary concern. At its stress-limited design point, the Hybrid configuration is clearly the most rigid structure. To determine which structural configuration is the lightest weight design under deflection limited conditions, both the 18^{o} and 9^{o} Modified Warren configurations were

systematically stiffened to provide comparable rigidity to the hybrid configuration. As can be seen from Table 2-11, the 9° Modified Warren and the Hybrid configuration are of comparable weight at deflection parity.

A preliminary performance analysis indicated that with a 3-mrad rms gore slope error, the gore support ring would be deflection limited. With the 9° Modified Warren and the Hybrid designs being essentially equivalent in weight under deflection limited conditions, secondary cost considerations of fabrication complexity became important. Based on the fact that the Hybrid design had 15 percent fewer members and 9 percent fewer joints, it was considered less costly to manufacture and was therefore selected.

Analysis and Optimization

The final sizing of the Hybrid gore support ring members was performed using a finite element structural model incorporating the receiver/engine support structure and the counterweight structure in an

Table 2-11. Gore Ring Trade-Off Matrix

Concept	Primary Considerations			Secondary Considerations	
	Relative Weight at Stress Parity	rms Deflection at Stress Limit (mrad)	Relative Weight at Deflection Parity	Number of Joints	Number of Element
18° Warren (mod)	1.3	2.16	1.8	200	440
9° Warren (mod)	0.76	1.98	0.96	180	580
Hybrid	1.0	1.57	1.0	164	492

integrated assembly. This allowed the stiffening effects of the receiver support quadripod to be accounted for along with the eccentric loading due to the counterweights. Both the receiver support and counterweight structural subassemblies were individually optimized prior to incorporation in the integrated model.

Final structural analysis resulted in a gore support ring with a mass/deflection relationship as shown in Table 2-12.

Table 2-12. Gore Support Ring
(11-m nominal dish diameter)

Mass kg (lb)	Area Weighted rms Deflection, σ_d (mrad)
657 (1447)	1.90[a]
739 (1627)	1.68
966 (2127)	1.28
1193 (2627)	1.04

[a]Stress limited design

The final trade-off of gore support ring stiffness and mass is discussed in the performance analysis section (see Section 2.3).

2.2.2.3 Receiver/Engine Support Structure (Refer to Drawing 7740-003)

In addition to supporting the receiver/engine/generator package, the structural subassembly also serves to stiffen the gore support ring. Due to its statically indeterminant four-legged configuration, the receiver/engine support structure provides a very deep section which significantly adds to the rigidity of the ring truss.

Functional Requirements

The functional requirements of the receiver/engine support structure are:

- Interface with, support, and provide alignment capabilities for the receiver/engine/generator package
- Minimize translation of the receiver aperture relative to the optical centerline of the paraboloid under all orientations
- Provide a minimum of shading of the reflector surface and blockage of reflected rays
- Provide a protected cabling of minimum specified dimensions for instrumentation and power cable routing
- Interface with the gore support structure
- Survive all specified loading conditions

Configuration Selection

In addition to the baseline quadripod concept, a tripod structure was also considered. Several factors led to the selection of the quadripod structure, including:

- The quadripod provides greater stiffening of the gore support ring
- The quadripod allows a slightly lower concentrator stow height (based on the constraint that the elevation hinge line be coincident with the receiver support structure/gore ring interface)
- Based on the same constraint, the quadripod allows a smaller drive structure

Lateral bracing accomplished by opposing guy wires at three points along each leg is required to obtain adequate column buckling stability.

Guy wires between the receiver mounting flange and the uppermost point of bracing on the legs is omitted to provide clear transit of the fireball for initial sun acquisition and for emergency desteer conditions.

Analysis and Optimization

The structural analysis and sizing of the receiver/engine support structure was performed using an ANSYS finite element structural model. All loading conditions summarized in Table 2-8 were analyzed with the 0^{o} (horizon pointing) orientation being dominant. The structure was analyzed in detail for the specified 1,350-kg (2,970-lb) receiver/engine/generator package. The resulting structure mass was 253 kg (557 lb).

Receiver aperture centerline deflections were determined through an analysis of the complete gimbaled structure including the gore support ring and the counterweights. At 60^{o} elevation in a 50-km/hr (31-mph) front wind (0^{o} yaw) the centerline of the receiver aperture at the focal plane is laterally displaced 5.74 mm (0.226 in.). Simultaneously, the receiver/engine package longitudinal axis undergoes a negative pitch of -1.25 mrad increasing the net displacement of the aperture centerline resulting in a total of 6.50 mm (0.256 in.) lateral displacement. Much of this deflection is due to the gore ring being pulled down by the counterweights while coincidently experiencing the highest differential pressure coefficient in this orientation.

This receiver displacement can be considered as a pointing error and corresponds to an angular displacement of approximately 1 mrad (0.057^{o}). If uncompensated by the control system, this displacement could be additive to the tracker/drive pointing error, thereby reducing the error budget for those subsystems. This fact was instrumental in

selecting the image sensing control scheme which automatically compensates for receiver displacement.

2.2.2.4 Counterweight Structures (Refer to Drawing 7740-005)

The purpose of counterweighting is to reduce elevation drive actuator loads and parasitic power requirements. ments about the elevation axis are due to the weight of the gimbaled subassembly plus wind-induced forces and moments. A properly located counterweight can totally negate the overhung weight-induced moment leaving only the variable wind-induced moment. Since the uncounterweighted weight moments at the extremes of the elevation travel are much greater than the wind moments, the maximum elevation mechanism drive push/pull requirements can be significantly reduced, thereby reducing drive mechanism sizing and parasitic power consumption. To prevent cascading structural failures, the elevation drive components should be structurally sized to statically withstand the extremes of both wind and weight moments in the event of total loss of the counterweight system. Though counterweighting unfavorably impacts the drive structure and foundation designs, the additional deadweight is beneficial in counteracting wheel uplifting caused by high winds.

Functional Requirements

The counterweight structure must:

- Interface with and support the counterweights
- Interface with the gore support ring
- Survive all specified loading conditions
- Clear the drive structure in all orientations
- Have sufficient stiffness to avoid dynamic instabilities

Configuration Selection

As an alternate to a counterweight system, a torsion spring counterbalance system was considered. Two springs, one on each side of the central drive structure member, coiled about a structural member along the elevation axis were sized. To generate the desired torque at the extremes of elevation travel, springs with a mass of about 308 kg (680 lb) each were required. Cost trade-offs between the two counterbalancing systems clearly favor the counterweight system over the torsion spring by a factor of over 3 to 1.

It was determined that a 70-percent counterbalancing system was most favorable to the elevation drive mechanism. Based on the estimated subassembly masses of Table 2-10, two concrete counterweights 2,270 kg (5,000 lb) each were required, one located on each side of the gore ring. The center of gravity of the concrete weights are 3.05 m (10 ft) from the elevation axis directly opposite the center of gravity of the gimbaled subassembly.

Analysis and Optimization

The counterweight support structures are mirror images (left and right sides). Prior to incorporating the counterweight structures into the integrated gore ring/receiver support/counterweight structure model, the counterweight structures were separately analyzed. The extremes of the elevation travel limits (-25^{0} and 90^{0}) proved to be the governing load case orientations. The final mass of the counterweight structures sized to support 2,270-kg (5,000-lb) counterweights for the 11-m nominal dish diameter, are 154 kg (340 lb) per side or 308 kg (680 lb) total.

2.2.2.5 Drive Structure (Refer to Drawing 7740-004)

The primary function of the drive structure is to support the gimbaled subassemblies and provide a platform containing the elevation and azimuth axes bearings and drives. The minimum height of the elevation axis above grade is determined by the reflector diameter, minimum desired gore ground clearance, and elevation travel limits. The "retire" or maintenance orientation of -25^{o} elevation requires that the front face of the structure (defined by the elevation hinges and the wheels) be recessed in the center to provide clearance for the gore ring. The side elevation view reveals the dog-leg nature of the structure. The wheels are located directly beneath the elevation axis hinge. The azimuth pivot and elevation drive mechanism pivot locations constitute the remaining interfaces and together with the wheel and elevation hinge points determine the overall size of the drive structure.

Functional Requirements

The functional requirements of the drive structure can be summarized as:

- Interface with the gore support ring
- Support the receiver/engine/generator package, receiver support structure, gores, gore support ring, counterweight structures, and the counterweights
- Interface with the pedestal through the azimuth bearing
- Interface with and support the elevation drive actuator
- Interface with and support the azimuth drive actuator
- Interface with the azimuth support idler wheels

- Allow elevation motion limits of -25^{o} (below horizon) to 90^{o} (zenith position)
- Clear the counterweights and counterweight structure in all orientations
- Have sufficient stiffness to avoid dynamic instabilities
- Survive all specified loading conditions

Configuration Selection

Three drive structure configurations were considered. These included the JPL baseline configuration (Configuration A, Figure 2-15) with elevation travel limits of -25^{o} to 82^{o}, and two alternate arrangements which allowed the full -25^{o} to 90^{o} elevation travel. These alternate configurations, designed B and C, are shown in Figures 2-16 and 2-17, respectively.

Configuration A was eliminated from further consideration due to its inability to attain a 90^{o} zenith position for high wind stow or low latitude summer tracking. Preliminary sizing of Configurations B and C indicated that Configuration B was 15 percent lighter than Configuration C due to its more compact design. The kinematics of this configuration, however, produce a poor line of action for the elevation actuator thereby requiring a significantly stronger drive system. The final selection of the drive structure configuration was based on a system-level trade-off incorporating the effects of the drive structure and the drive subsystem. The most cost-effective overall system was achieved with Configuration C.

Analysis and Optimization

The final sizing of the drive structure made use of an ANSYS finite element model. The estimated mass of the gimbaled subassemblies from Table 2-10 was used along with the aerodynamic loading conditions and

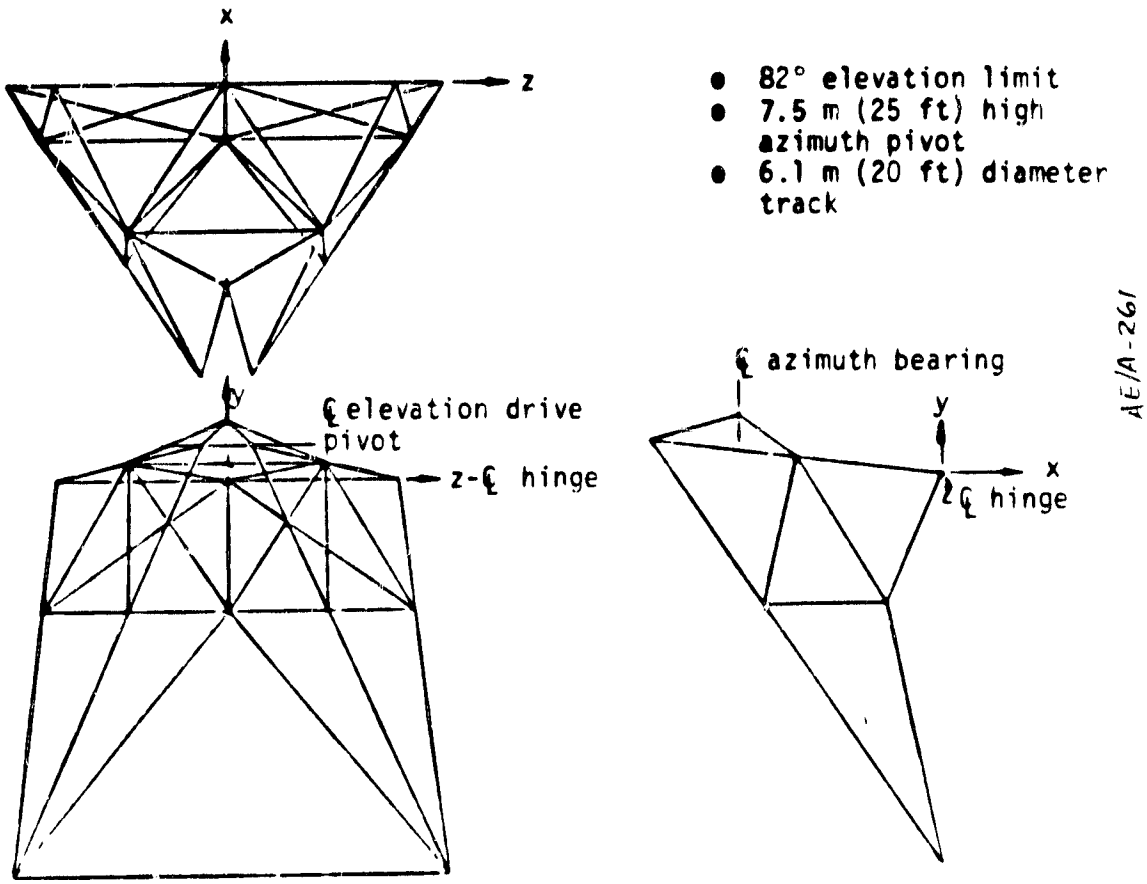

Figure 2-15. Drive Structure -- Configuration A

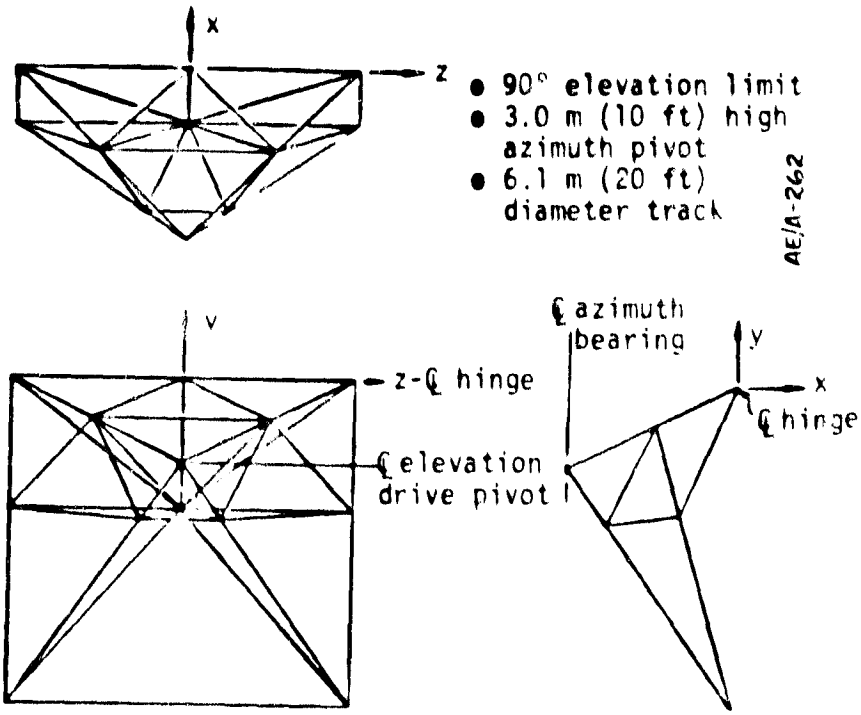

Figure 2-16. Drive Structure -- Configuration B

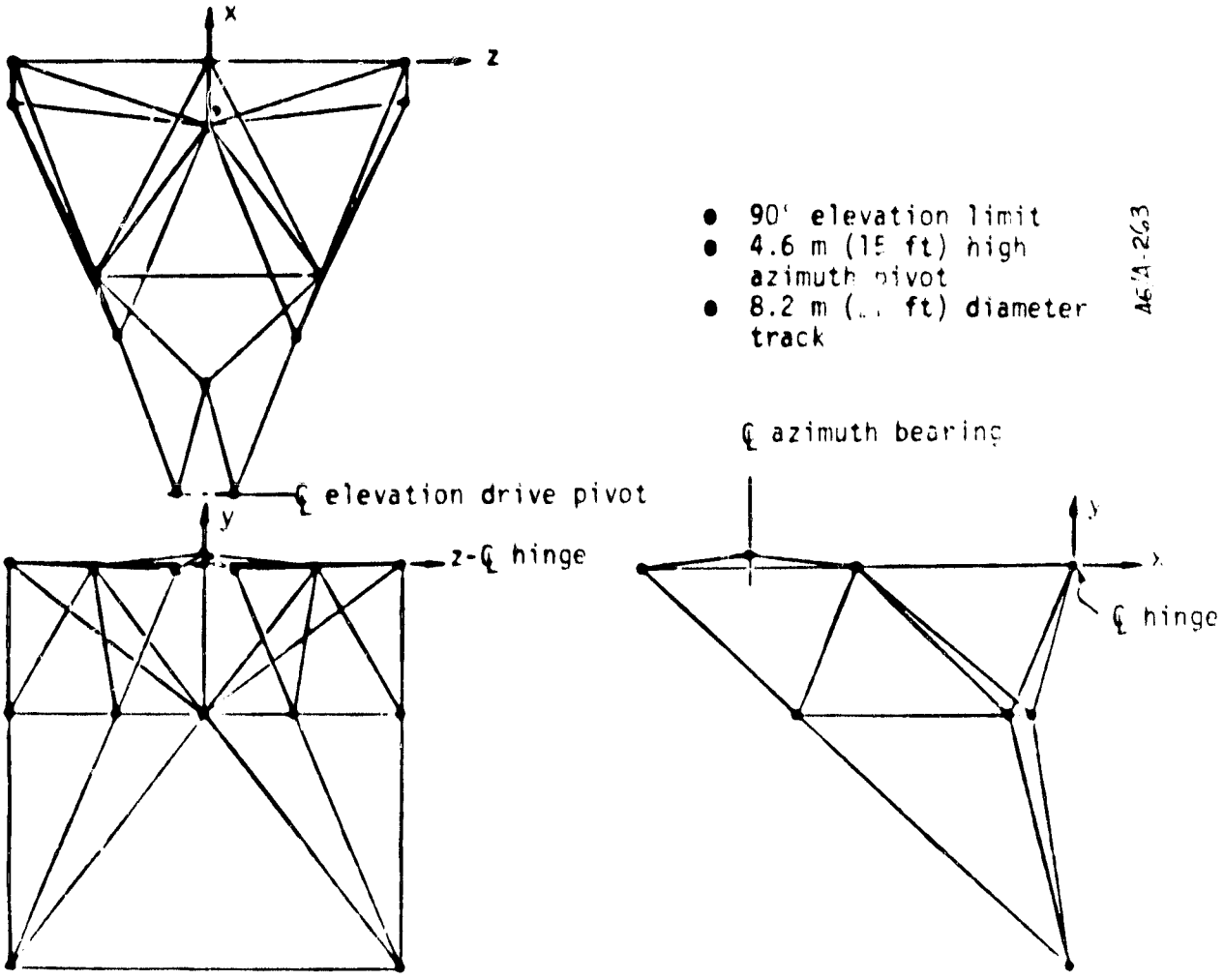

Figure 2-17. Drive Structure -- Configuration C

corresponding weight moments associated with the orientations summarized in Table 2-9. The resulting drive structure for an 11-m nominal dish diameter has a mass of 590 kg (1,300 lb).

2.2.3 Drive Subsystem Design (Refer to Drawings 7740-001 and 7740-006)

The drive subsystem consists of an elevation actuator, an azimuth drive unit, and an auxiliary backup power system. Backup power is required to slew the concentrator to a stow or desteer position in the event of a grid power failure. Several factors influence the design and selection of the drive subsystem components. These can be grouped as functional and cost factors. The functional factors include:

- Kinematic requirements
- Force requirements
- Minimum slew rates
- Positional accuracy (backlash)
- Stiffness requirements
- Backup power requirements

Any candidate drive subsystem must meet the minimum functional requirements. Component and subsystem selection can then be based on minimizing the appropriate cost factors. Since the overall objective of the Advanced Solar Concentrator is to provide a minimum cost of delivered energy, annual maintenance and operating costs must be considered along with first costs when making component decisions.

2.2.3.1 Approach

The preliminary design of the drive subsystem consisted of four main efforts:

- Functional requirements definition
- Load analysis

- Concept selection
- Analysis and final sizing

Each element is summarized in the following paragraphs.

Functional Requirements Definition

The functional requirements effort required the establishment of minimum acceptable levels for each of the functional factors listed previously. The kinematic requirements for each drive component were dictated by the geometry of the structural options and the specified azimuth and elevation travel limits. Force requirements were a function of the geometry and the applied loads as discussed herein. The minimum slew rate requirement was a part of the specification as was the overall minimum pointing accuracy of the concentrator. Drive subsystem positional accuracy, however, is only one element of concentrator pointing error. The sensitivity of the control system was therefore evaluated and the composite backlash in the structure due to the elevation and azimuth bearing tolerances was determined to establish a maximum allowable drive subsystem backlash consistent with the required concentrator pointing accuracy. The resulting backlash limit was 9 mrad (0.5^{o}). While the image sensing control system can correct for steady-state drive system deflections, the stable response time is severely hampered by a "soft" drive system. Therefore, a minimum drive subsystem stiffness of 3.5 mrad (0.2^{o}), expressed as an angular deflection due to a 10-km/hr (6.2-mph) gust, was specified.

Load Analysis

The drive actuator loads are dependent on several factors, including:

- Aerodynamic forces and moments
- Hinged weights and moments
- Counterbalancing scheme
- Structure geometry
- Drive concept

Initial drive concept sizing and trade-off evaluations were based on the estimated structural weights of Table 2-10. At the completion of the structural design effort, the actual structural weights were used for the final analysis and sizing of the selected drive components.

Aerodynamic loads were based on the gross body force and moment coefficients of Reference 3. The governing load condition for both the elevation and azimuth drives proved to be the 80-km/hr (50-mph) slew to stow requirement with the concentrator at a 60^{0} angle of attack to the wind. Separate actuator design loads were developed for each drive concept and structural configuration using this load condition.

While the counterweighting scheme was selected to minimize drive motor requirements and parasitic power consumption, all structural components of the drive subsystem were sized to statically withstand the worst case loading condition without the benefit of the counterweights. This not only prevents cascading structural failures in the event of the loss of a counterweight, but also eliminates the need for any special procedures and tools during installation or service.

Concept Selection

Based on the functional requirements outlined above, a matrix of drive subsystem options was developed. Electric and hydraulic actuators and power systems were evaluated along with central and peripheral azimuth drive schemes and a variety of elevation drive concepts.

Each component was sized to meet the minimum functional requirements and the present worth of its life-cycle cost evaluated. The life-cycle cost included the estimated first cost of the component, annual maintenance and repair costs, periodic replacement costs, and parasitic power costs. The time value of all estimated expenditures was consistently accounted for using the approved life-cycle costing methodology of Reference 5.

To minimize unnecessary effort, separate component-level comparisons of azimuth and elevation drive concepts were performed to narrow the scope of the integrated system evaluation. The final drive subsystem selection, however, was based on the aggregate life-cycle cost of the entire drive subsystem including the auxiliary power system and the cost of the drive structure.

Analysis and Final Sizing

Final sizing of all drive subsystem components was based on a final load analysis employing the actual structural weights as determined in the structural design effort.

2.2.3.2 Azimuth Drive

Table 2-13 lists the concepts developed for the Advanced Solar Concentrator azimuth drives. There are two basic types, peripheral and central drives. Peripheral drives have a traction element (chain, cable, ring gear or traction surface) anchored to the foundation track and a drive element (sprocket, drum, pinion gear or traction wheel) mounted on the drive substructure. The principal advantage of this type of drive is that it uses the track radius for a mechanical advantage. With the large track radius, the forces imposed on the drive unit are small, thereby allowing a small, efficient gear box and motor. Also the pointing error

Table 2-13. Azimuth Drive Concepts

	Drive Type		Power	
Drive Option	Peripheral	Central	Electric	Hydraulic
Cable/drum	X		X	X
Chain/sprocket	X		X	X
Ring gear/pinion	X		X	X
Traction wheel	X		X	X
Rotary actuator		X		X
Gear box		X	X	X

resulting from drive unit backlash and deflection is minimized and resolution is greatly improved.

Central drives are located at the azimuth pivot of the drive substructure. The advantages are that the drive unit is easily enclosed for environmental protection and the track is less expensive.

A component-level evaluation of the azimuth drive options was performed. The trade-off results are shown in Table 2-14. The central gear box concept was eliminated because it could not meet the minimum positional accuracy requirements with standard design practice. The traction wheel concept was eliminated, because it could not maintain traction throughout the range of operating conditions. Of the other concepts, the cable/drum and chain/sprocket combinations are clearly lowest in cost, and within the accuracy of the costing are essentially equivalent. While both concepts meet the minimum stiffness criteria, the inherent additional stiffness of the chain design made it the preferred choice.

Table 2-14. Azimuth Drive Trade-Off Results

Option	Actuator	Criteria		
		Meets Requirements	Relative Total Cost	Relative Rigidity
1	Cable/drum	Yes	1.0	2.5
2	Chain/sprocket	Yes	1.1	1.0
3	Ring gear, electrical	Yes	1.3	1.0
4	Traction wheel	No	--	--
5	Rotary actuator	Yes	2.4	1.0
6	Gear box	No	--	--

The selection between an electric or hydraulic drive motor is dependent upon the choice of auxiliary power schemes and could only be made through a system-level trade-off.

2.2.3.3 Elevation Drive

The elevation drive design is highly dependent upon the degree of counterbalancing and the kinematics of the various concentrator components as determined by the drive structure configuration. The location of the elevation hinge line, the azimuth pivot, and the elevation actuator anchor points were selected to obtain a minimum cost arrangement that would satisfy the specification requirements for travel limits, wind loads, and positional accuracy.

Table 2-15 lists the elevation concepts considered. There are six actuator types. The first three are linear actuators which may be either connected directly between the drive structure and the gore support ring or work through a linkage arrangement. The latter three actuators utilize a sector built onto the backside of the gore support ring and are similar

Table 2-15. Elevation Drive Concepts

Actuator	Type			Drive Structure Configuration		Power	
	Linear	Sector	Linkage	B	C	Electric	Hydraulic
Hydraulic cylinder	X		X	X	X		X
Ball screw jack	X		X	X	X	X	X
Rack/pinion	X		X	X	X	X	X
Ring gear/pinion		X			X	X	X
Chain/sprocket		X			X	X	X
Cable/drum		X			X	X	X

to the peripheral azimuth drives. Due to the impact of drive structure configuration on actuator loads, both alternative Configurations B and C (see Section 2.2.2) were analyzed for each linear actuator concept. Due to geometric constraints, only Structure C was considered for the sector-type drives. Both hydraulic and electric power were considered where applicable.

While the final elevation drive selection could only be made with a system-level analysis, several of the clearly more costly options were eliminated through a component-level trade-off. This analysis considered the interactive effects of the drive structure on actuator load requirements and relative rigidity. The results are presented in Table 2-16, where the relative cost figure is for the elevation actuator only and does not include the cost of a hydraulic power module for Options 1 or 2. The linear actuator/linkage options were eliminated due to the massive structural requirements necessary to meet the drive system positional accuracy and

Table 2-16. Elevation Drive Trade-Off Results

Option	Actuator	Drive Structure Configuration	Criteria		
			Meets Requirements	Relative Total Cost	Relative Rigidity
1	Hydraulic cylinder	B	Yes	1.0	0.5
2	Hydraulic cylinder	C	Yes	1.5	1.0
3	Ball screw	B	Yes	1.4	0.5
4	Ball screw	C	Yes	1.2	1.0
5	Rack/pinion	B	Yes	2.0	0.5
6	Rack/pinion	C	Yes	1.8	1.0
7	Ring gear/pinion	C	Yes	1.7	0.6
8	Chain/sprocket	C	Yes	1.7	0.6
9	Cable/drum	C	Yes	1.5	0.5

rigidity specifications. A ball screw is clearly the best elevation actuator design for incorporation with drive structure Configuration C. It can be driven by either a hydraulic or electric motor thereby effectively eliminating Options 2, 6, 7, 8, and 9 from further consideration. Options 1 and 3, however, had to be carried forward to the system-level comparison since the hydraulic cylinder and ball screw designs were the best hydraulically and electrically driven actuators, respectively, for incorporation with the drive structure Configuration B.

2.2.3.4 Auxiliary Power System

An auxiliary power source is required for desteering and stowing the concentrator in the event of a grid power failure. A desteer capability is required to ensure that the receiver and structural support components are not damaged by the fireball. A stow capability is required to ensure that the concentrator is not vulnerable to wind damage.

Two alternative types of auxiliary power systems were considered, namely:

- A hydraulic accumulator in conjunction with hydraulically actuated drives
- A generator in conjunction with electrically actuated drives

A small volume accumulator is needed as a standard element of the hydraulic power package which must be provided with any of the hydraulic drive options. The hydraulic backup power system then simply consists of a larger capacity pressurized gas hydraulic accumulator and a spring-loaded valve. In a power failure, a solenoid is deenergized and the spring opens the valve allowing the accumulator to discharge powering the drive actuator. Short-term desteer capability can also be incorporated provided the control system is maintained functional with an uninterruptible power supply (UPS).

The electrical auxiliary power system consists of a small diesel or gasoline generator set powering the electric drive motors and control system.

2.2.3.5 Integrated Drive Subsystem Selection

As a result of the component-level analyses and trade-offs, the matrix of azimuth and elevation actuator, drive structure, and auxiliary power system combinations was significantly reduced. A life-cycle cost analysis was performed for each of the remaining options and is summarized in Table 2-17. Due to the complexity of distributing high-pressure hydraulic fluids between adjacent concentrators, it was assumed that a separate hydraulic power package and accumulator would be required for each concentrator. A 6.5-kW auxiliary electric generator can, however, easily service two concentrators through a common field wiring tie-in.

Table 2-17. Integrated Drive Subsystem Trade-Off Results

Option	Elevation Drive	Azimuth Drive	Power Unit	Emergency Power	Drive Structure	Relative Cost	
						With Emergency Power	Without Emergency Power
1	Hydraulic cylinder	Chain, hydraulic	Motor/pump	Accumulator	B	1.00	1.00
3B	Ball screw, electric	Chain, electric	--	Gasoline generator	B	1.35[a]/1.13[b]	0.94
3A	Ball screw, hydraulic	Chain, hydraulic	Motor/pump	Accumulator	B	1.11	1.11
4	Ball screw, electric	Chain, electric	--	Gasoline generator	C	1.28[a]/1.05[b]	0.85

[a]One concentrator per generator
[b]Two concentrators per generator

Relative costs were therefore estimated for the electric drive options with a single backup generator serving one and two concentrators. As can be seen in the table, an all electric system (Option 4) is essentially equivalent to an all hydraulic system (Option 1) if two concentrators are powered by a single backup generator. If the generator size is increased and more units connected to it, the concentrator/backup system cost becomes asymptotic to the cost without backup power. The all hydraulic concentrator cost is constant, however. This indicates that there is a significant cost benefit potential for an electric backup system for multiunit fields. Since most applications are envisioned to incorporate several concentrators per site, the all electric drive system was selected. A detailed trade-off study between backup generator size, number of concentrators served, and the risk of concentrator damage due to a generator failure or a line break within the backup electrical distribution network should be performed to determine the optimum auxiliary generator sizing strategy.

2.2.3.6 Final Sizing

The key parameters of each component of the electrically driven chain and sprocket azimuth drive and ball screw elevation drive are summarized in Table 2-4 and presented in Section 2.1.3 of this report. The final component sizing was based on the final structural weights of Table 2-3 and the aerodynamic loads discussed in Section 2.2.3.1.

2.2.4 Foundation and Pedestal Design (Refer to Drawing 7740-006)

Due to the high degree of interaction between the center pivot pedestal structure design and the design of the foundations, they are jointly discussed in this section. The foundation subsystem is composed of two distinct elements. The first is the center pivot pedestal

foundation and the second is the perimeter track and foundation. The foundation subsystem distributes all weight and wind imposed loads to the soil through bearing and shear effects. Uplifting forces are reacted through the combination of foundation deadweight and soil shear. Due to the site specific nature of foundation design, all trade-off analyses were performed for the "nominal" soil conditions as summarized in Table 2-18 with the sensitivity of the selection checked against the "poor" soil condition values. The objective was to select a flexible, low-cost foundation concept that could easily be tailored to site-specific conditions.

Worst case pedestal and foundation loads were based on the results of the structure design and the drive subsystem load analysis. Due to the random direction of the wind, the pedestal and the foundation subsystem must be capable of adequately reacting and distributing loads from any azimuth orientation.

Table 2-18. Assumed Soil Characteristics

Property	Nominal	Poor
Soil type	Sandy gravel or gravel	Sandy or silty clay
Allowable foundation pressure	95,760 N/m^2 (2,000 lb/ft^2)	47,880 N/m^2 (1,000 lb/ft^2)
Allowable lateral bearing	31,640 $N/m^2/m$ (200 $lb/ft^2/ft$)	15,820 $N/m^2/m$ (100 $lb/ft^2/ft$)
Frost depth	1 m (3 ft)	1 m (3 ft)

2.2.4.1 Pedestal Structure and Foundation Design

Three pedestal/foundation concepts were evaluated:

- Tripod pedestal/pier foundation
- Tripod pedestal/slab foundation
- Single column pedestal/pier foundation

In all cases, the structure above ground was constructed of steel, while reinforced concrete was used for the foundations. The worst case pedestal load occurs with the concentrator in its highest drag position producing the maximum horizontal load at the azimuth bearing interface.

A simple comparison of the slab supported pedestal and the pier supported concept eliminated the slab foundation. To avoid settling during freeze/thaw cycles, any foundation must extend below the frost line. Three feet is a reasonable minimum frost line for much of the continental United States. A 1-m (3-ft) deep slab results in a very inefficient design. Cast in-place piers use the concrete much more efficiently by placing it only at the load bearing locations.

The pier-supported tripod and single column designs were evaluated as shown in Figure 2-18. The total installed cost of the tripod design was estimated as a function of the tripod angle. A zero tripod angle corresponds to the single column pedestal design. The tripod leg angle is restricted to a maximum of 30^{o} by the drive structure geometry. For angles less than 10^{o}, the leg member loads change from predominantly axial to bending, thereby significantly increasing the required size and cost of the pedestal structure.

The tripod design requires three separate piers, designed to separately handle the worst case loads. Consequently, under any particular load orientation, the loads will be unequally distributed with

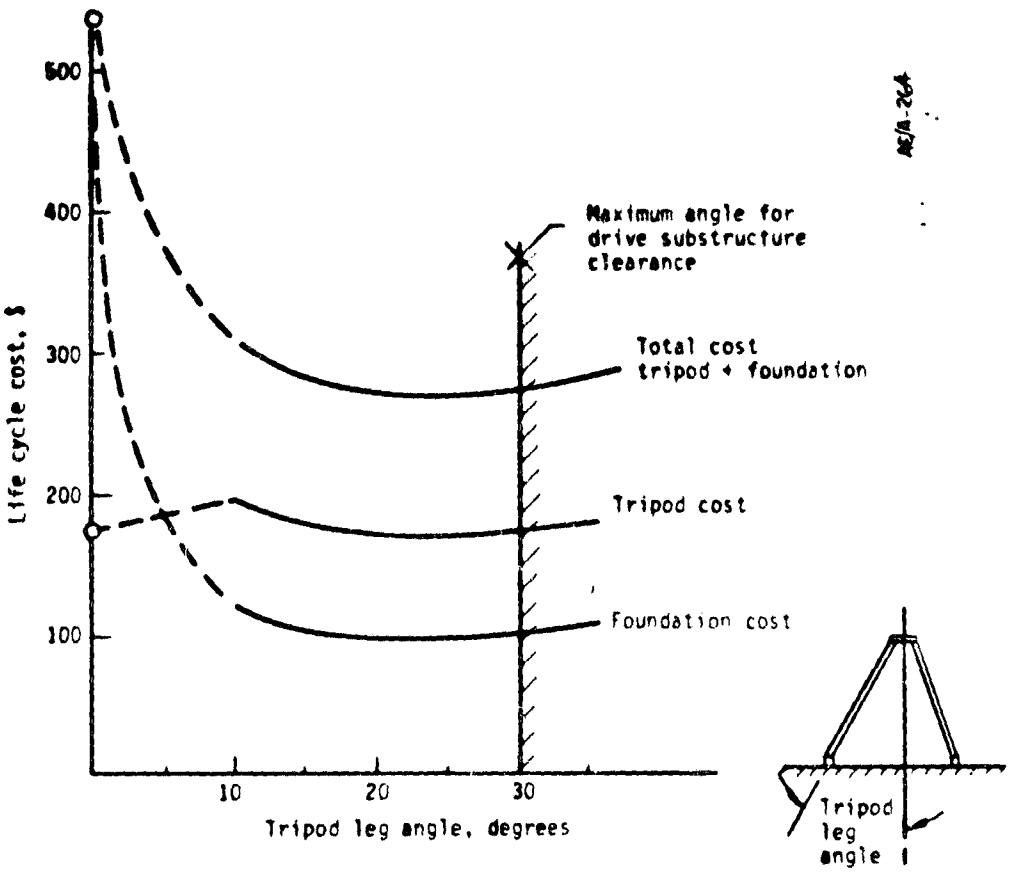

Figure 2-18. Pedestal and Foundation Cost Trade-Off

two piers having excess capacity. This effect becomes significant for tripod leg angles less than 10^{o}. Each pier becomes so large that a single central pier uses less concrete.

The combined steel and concrete cost has a minimum between 20^{o} and 25^{o}. This region is nearly horizontal indicating an insensitivity to leg angle in this region. A leg angle of 25^{o} was therefore chosen.

2.2.4.2 Perimeter Track and Foundation Design

Three track/foundation concepts were evaluated:

- Raised metal track/pier foundations
- Raised metal track/continuous ring foundations
- Continuous concrete track/foundations

Based on the frost line constraints cited here, the raised metal track with pier foundations was shown to be clearly superior.

A trade-off between the number of equally spaced concrete piers and the requirements for the raised metal track was performed to select the minimum cost configuration. Again, due to the random orientation of the wind loads and the variable location of the load bearing azimuth idler wheels, each pier must be capable of supporting the full worst case bearing load. Independent of the number of piers, each pier is therefore identical.

The raised steel track is subjected to a combined bending and torsional load. The large torsional component makes a closed beam section more efficient than an open section. A rectangular steel tube track was therefore selected.

Figure 2-19 shows the track, pier, and combined track/pier installed costs as a function of the number of piers. Since each pier is the same size, the foundation cost increases linearly with increasing number of piers. Twelve piers is a critical point for the torsional stress in the track. With fewer piers, the torsional component increases rapidly requiring large beam sections. The sharply rising beam cost with reducing pier numbers and steeply rising concrete cost with increasing number of piers gives a sharp minimum combined cost for the 12-pier configuration.

2.2.4.3 Final Sizing

The final foundation sizing was based on the optimized structural weights as summarized in Table 2-3, the worst case aerodynamic loads corresponding to the 80 km/hr (50 mph) slew to stow condition with the concentrator at a 60^{0} angle of attack, and the nominal soil conditions

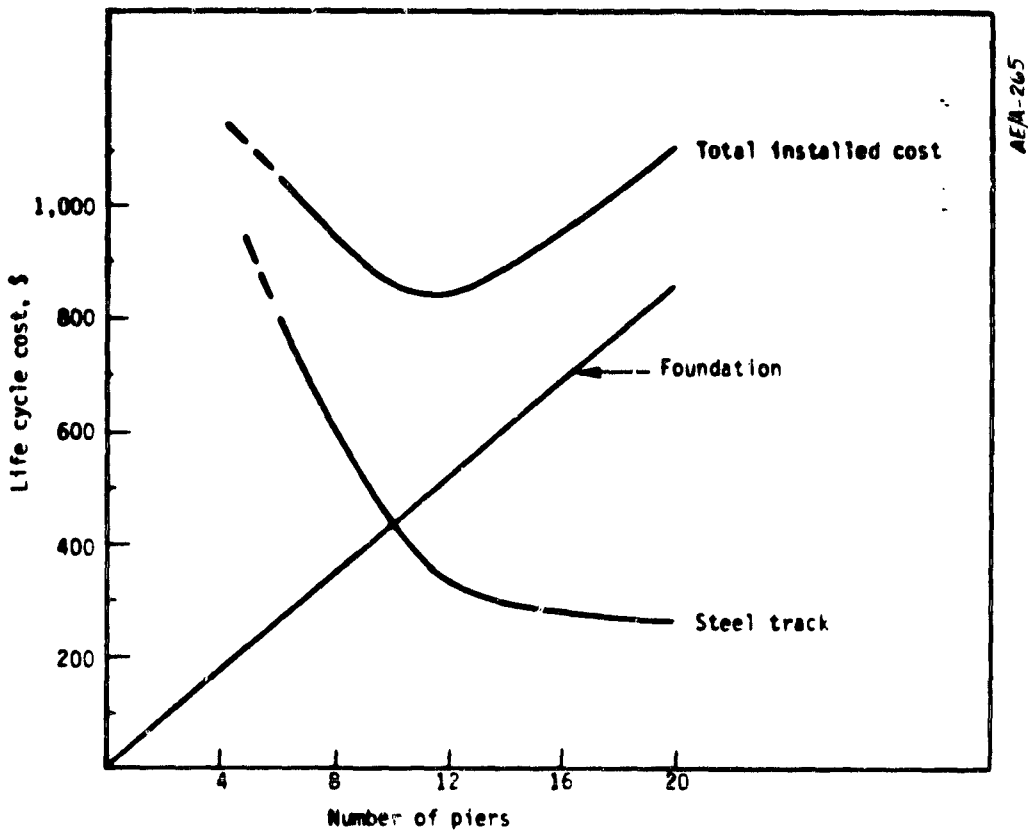

Figure 2-19. Track and Foundation Cost Trade-Off

of Table 2-18. The results are summarized in Section 2.1.4 of this report and Drawing 7740-006 of Appendix D.

2.2.5 Electrical and Control Subsystem Designs

As discussed in Section 1.1, the emphasis of the preliminary design effort was placed on those elements of the concentrator whose cost, as estimated for high-volume production, was a major portion of the total cost and could be significantly impacted by trade-offs and analysis at the preliminary level. The combined cost of the electrical and control systems was estimated to be less than 10 percent of the total manufactured cost of the concentrator. The preliminary design effort in these areas was therefore scoped only to provide general component requirements

information to allow a reasonable assessment of their mass production costs.

While not being a major cost item in high-volume production, the selected tracker/control scheme does impact some of the more dominant cost elements such as the structure and drive designs. The tracker/control approach was therefore evaluated in slightly more detail.

2.2.5.1 Electrical Subsystem Design

The electrical subsystem requirements are straightforward and can be cost-effectively met with standard design practice. No in-depth cost trade-offs were therefore required for the preliminary stages of the electrical subsystem design.

The electrical subsystem must:

- Interface with the power conversion module (PCM) electrical generator
- Provide short circuit protection and cabling for the generated electricity from the PCM interface to the site distribution interface
- Provide grid power to the PCM, the drive subsystem and the tracker/control subsystem
- Provide auxiliary power to the drive subsystem and tracker/control subsystem
- Provide lightning protection for the concentrator

To provide the greatest concentrator operational flexibility, an isolated utility grid powered circuit is required to feed the drive and control subsystems. By decoupling the parasitic operating power requirements from the electrical power generated by the PCM, system startup, shutdown, testing, and service are significantly simplified.

Based on the peak drive subsystem power requirements and estimates of control subsystem needs, circuit loads were estimated and standard cabling, disconnect, and overload components selected. A single line electrical diagram (Figure 2-20) was developed to ensure that all required electrical power distribution components were identified.

Two disconnects are provided on the PCM output circuit. A fused disconnect is located at the generation source to protect all downstream wiring, while a second disconnect is located at ground level to allow easy access for service or emergency conditions.

The standby generator and automatic transfer switch discussed in the previous section can be sized to service any number of concentrators. Commercially available units with the necessary environmental enclosures, automatic periodic exercisors, and proven reliability are readily available above power ratings of 1 kW. As previously discussed, final component sizing is dependent on the number of concentrators to be served.

There are two basic approaches to lightning protection. The most conventional is the use of well-grounded lightning rods to serve as target points for electrostatic discharges. In large concentrator field applications, tall lightning arrestor poles can be strategically located to provide a network of grounded target points. For single unit or small field applications, the use of structure mounted lightning arrestors and a dedicated ground path through the structure itself can prove more cost-effective.

An alternative approach, as marketed by Lightning Elimination Associates of Santa Fe Springs, California, is to prevent the spontaneous discharge of electrostatic energy through an active dissipation array

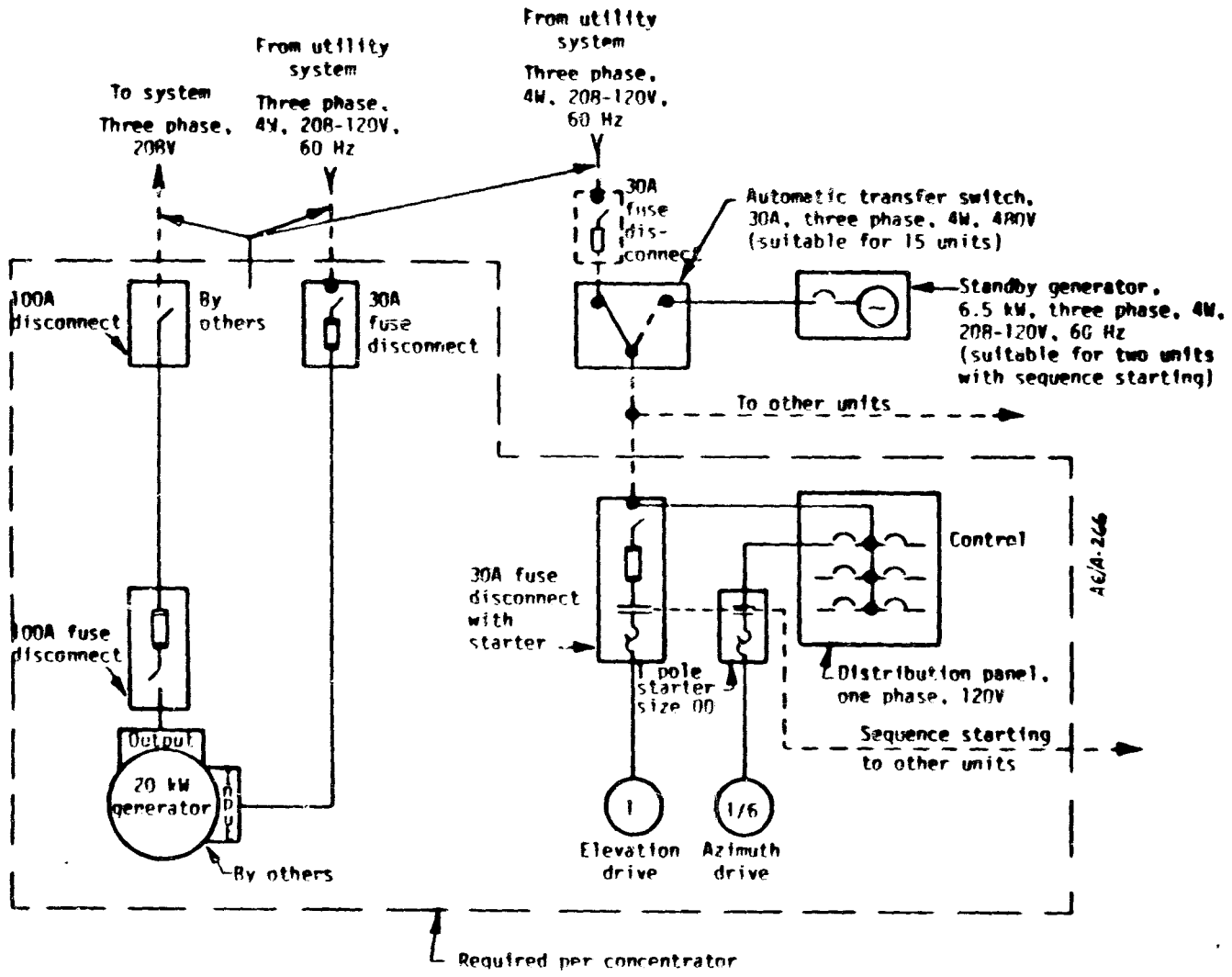

Figure 2-20. Electrical Single Line Diagram

reducing the electrostatic potential between the cloud cells and the area being protected.

For large field installations in areas of frequent lightning activity, such a system may be warranted. For preliminary design purposes, however, the more conventional approach was assumed. Individual structure mounted lightning arrestors were selected with grounding provided through the structure with flexible shunt wires around all bearings and high resistance joints. A local ground rod will be provided at each concentrator.

The key features of the electrical subsystem were summarized in Table 2-6 of Section 2.1.5.

2.2.5.2 Control Subsystem Design

The control subsystem for the Advanced Solar Concentrator must provide several functions. It must:

- Maintain the required pointing accuracy during periods of sufficient insolation for PCM operation
- Maintain sufficiently accurate gross-pointing accuracy during periods of low insolation or obscuration to allow rapid focusing upon an insolation rise
- Employ a sun acquisition scheme preventing the focusing of highly concentrated sunlight on structural support members
- Provide a desteer capability maintaining the fireball in a safe position focused in space adjacent to the receiver
- Provide a stow capability which drives the concentrator to the low drag zenith position yet maintains a oesteer override

- Provide a nighttime retire capability driving the concentrator to the -25° altitude position (below the horizon) to reduce dew formation while maintaining a stow override
- Provide manual overrides for testing and servicing
- Incorporate battery backup power to bridge between loss of grid power and auxiliary power startup

Control Schemes

Two-axis solar tracking can be effected through any of three basic control schemes:

- Programmed or synthetic tracking
- Active or optical tracking
- Combined or hybrid tracking

For an azimuth/elevation drive scheme, synthetic tracking is typically a computer-based (microprocessor or minicomputer) approach positioning the concentrator in response to the calculated position of the sun. Positional feedback devices such as shaft encoders or precision potentiometers are most often employed. While the sun's position can be calculated with great precision, the accuracy of a synthetic control scheme is very sensitive to initial concentrator alignment, feedback device calibration, and subsequent settling of foundations. The extremely close installation tolerances and periodic alignment and/or recalibration make purely synthetic tracking schemes prohibitively expensive.

Active tracking schemes employ an optical sensor which senses the concentrator's misalignment with the sun and issues a corrective action signal. A number of two-axis shadowband-type devices have been developed providing an azimuth and/or elevation signal in response to a nonaxisymmetric alignment with the sun. Such devices have two major

drawbacks. While they can easily be designed with sufficient sensitivity and resolution to achieve the pointing accuracies required, they must be rigidly located on the structure at a point maintaining alignment with the optical centerline of the concentrator throughout all operating conditions. Except for very rigid structures, such a location is most often very difficult to find. The second limitation deals with the rate of reacquisition of focus following a period of obscuration. To prevent hunting and the inadvertent tracking of bright clouds, active sensors must be cut off below a minimum insolation threshold. They cannot therefore maintain a gross alignment during overcast periods and will therefore require a longer reacquisition period following the reemergence of the sun. A significant loss of available energy may therefore be suffered with the use of a purely active control scheme. The incorporation of desteer and safe sun acquisition schemes are more difficult with strictly active control approaches, but they can be provided.

The hybrid control scheme provides the best features of the synthetic and the active approaches with only a slight cost penalty relative to the active system in mass production. With the hybrid approach, gross alignment as well as desteer and safe sun acquisition is provided with a microprocessor-based synthetic input. Due to lesser synthetic accuracy requirements, lower cost precision potentiometers can often be used in lieu of shaft encoders and less exacting installation requirements need be enforced. Highly accurate optical fine tuning is employed to maintain the desired tracking accuracy during high insolation periods. Much narrower fields of view can be employed for the optical sensors thereby allowing greater design flexibility and higher resolution for the optical system.

With the hybrid scheme, an additional option becomes viable for the active fine tuning. Due to the synthetic gross alignment capability, the use of an image sensing optical system can be considered. Such an approach employs optical sensors at the receiver plane to detect any misalignment. It therefore has a very narrow field of view and can only be used in a hybrid mode. Image sensing has several advantages. These include:

- Inherent gravity compensation capability (allows less rigid structural design)
- Direct measurement of controlled media (standard preferred control approach)
- Compensates for structural wind deflections (maximizes output of concentrator)

However, image sensing is also subject to some near-term technical drawbacks. Localized flux concentrations in excess of 10,000 are to be expected for the Advanced Solar Concentrator. An image sensing scheme must therefore employ sensors with suitable filters and isolation elements to allow at least momentary exposure to such fluxes. By locating the sensors in the fringes of the focal plane image, steady-state fluxes can be reduced to an acceptable level. Only during transient sun acquisition or desteer operations will the high intensity levels be seen.

The use of highly filtered fiber-optically coupled sensors in a ring-like arrangement around the receiver aperture is seen as a possible approach to sensor fabrication. A promising alternative approach makes use of sensors mounted on the receiver support structure legs which "look" back at the receiver aperture and cavity. With proper view factor limitations, such sensors could be used to either balance the internal cavity flux or the aperture spillage flux.

While the details of the sensor design will need much development, the advantages of the image sensing concept were felt to outweigh the slight mass production cost penalties. Such an approach was deemed to be within the scope of the advanced technology 1985 time frame appropriate for the Advanced Solar Concentrator and was therefore selected as the preferred tracking approach.

In mass production, each concentrator will be provided with a microprocessor-based tracker control unit which will provide the synthetic tracking capability, desteer, and stow logic and the safe sun acquisition scheme. Precision potentiometers should be sufficient to provide the required synthetic tracking accuracy with one of the image sensing schemes described above being selected for the optical fine tuning input.

Interface Requirements

The tracker control unit will require electrical power to supply the output drivers and to maintain the battery powered electronics. The battery power scheme provides for uninterruptible power for the control logic and clock (required for ephemeris tracking). A simple representation of the signal inputs and outputs is given in Figure 2-21. The emergency override signals include the stow command, assumed to come from a system wind sensor, and the receiver malfunction signal. Both are considered to be external to the tracker/control system. All external input/output signals will be optically coupled to provide the maximum interface flexibility.

2.3 PRELIMINARY PERFORMANCE ANALYSIS

This section presents the optical performance analysis results for the Advanced Solar Concentrator at the preliminary design point. The concentrator aperture diameter and structural stiffness have been

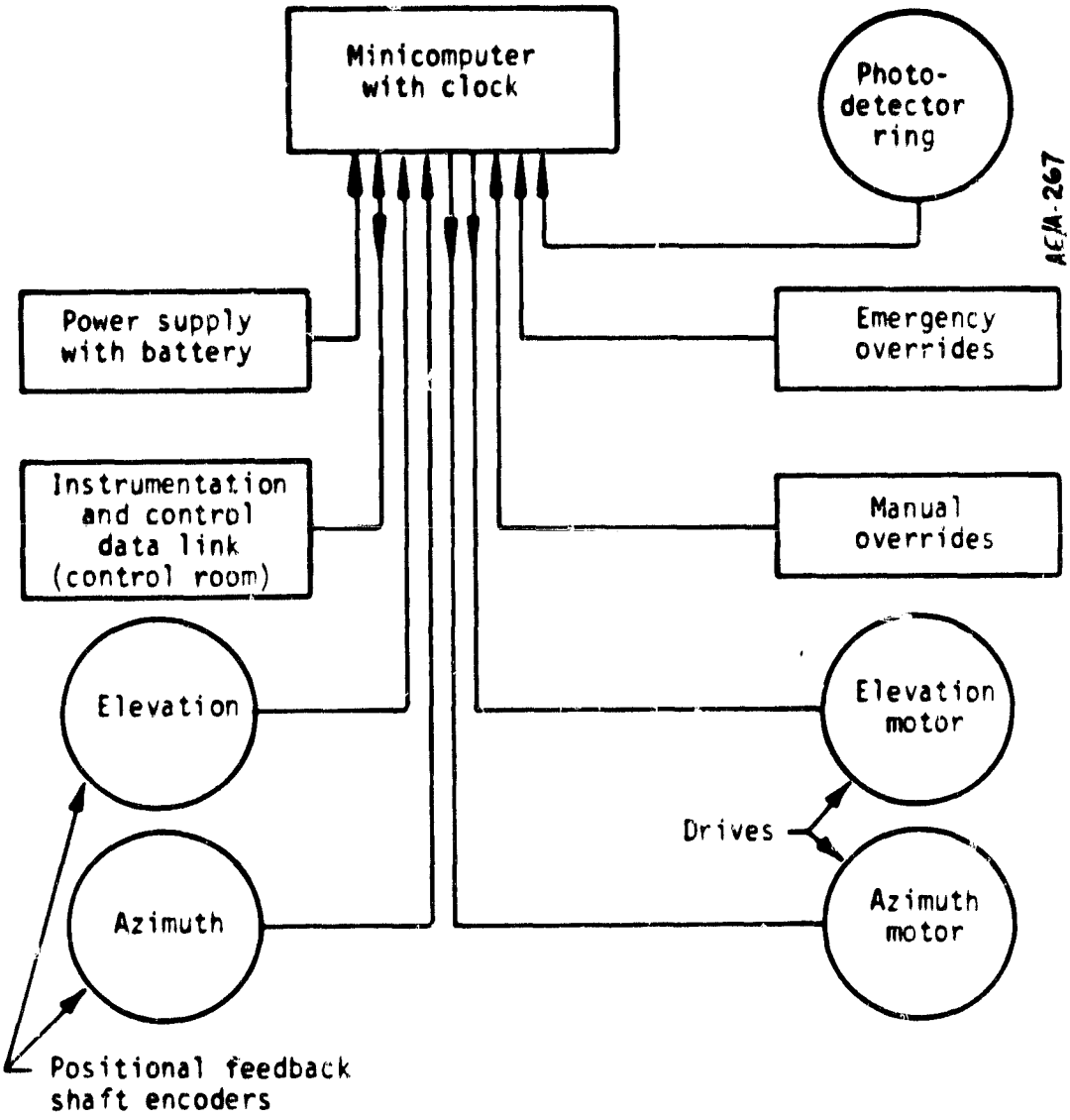

Figure 2-21. Simplified Control Interface Diagram

optimized for minimum concentrator weight given the performance requirement of delivering 56 kW of radiant energy to a 22-cm (8.7-in.) diameter receiver aperture with a direct normal insolation of 845 W/m^2 and an operating wind of 50 km/hr (31 mph).

The methodology for computing optical performance is presented in detail in Section 2.3.1. Section 2.3.2 discusses the optimization approach and results, and Section 2.3.3 summarizes the performance results.

2.3.1 Methodology

The concentrator optical performance is defined as the solar radiation incident upon the receiver aperture. It can be computed from the equation:

$$P = I \times A \times \eta_{conc} \qquad (2\text{-}1)$$

where

P = optical power at receiver aperture (kW)

I = direct normal insolation (kW/m^2)

A = concentrator gross aperture area (m^2)

η_{conc} = concentrator optical efficiency

The concentrator optical efficiency, η_{conc}, characterizes the quality of the concentrator. It is a measure of the percentage of incident energy which will be intercepted by the receiver aperture. It is computed from the equation

$$\eta_{conc} = \rho \times K_G \times K_S \times K_B \times \phi \qquad (2\text{-}2)$$

where

ρ = solar averaged hemispherical reflectance

K_G = gap factor

K_S = shading factor

C - 2

K_B = blockage factor

ϕ = intercept factor

The solar averaged hemispherical reflectance is a property of the mirror glass reflector. A value of 0.94 is the specified reflectance of a clean backsilvered mirror glass reflector. The gore gap loss coefficient is the ratio of the aperture area containing reflective surface to the total aperture area. The gap between gore quadrants to allow penetration of the receiver support legs and the hole in the center of the reflector surface shaded by the receiver are considered gap losses. The gaps between adjacent gores and the edge losses due to mirror edge sealant are also accounted for in this term. The design of the advanced concentrator provides a gore gap loss coefficient of 0.919. The shading coefficient accounts for the radiant energy that does not reach the reflector due to shading. Since the receiver and receiver support legs are located in gap areas, only the support leg guy wires contribute to a shading loss. The shading loss coefficient for the advanced concentrator is 0.998. The radiant energy that is reflected but does not reach the receiver aperture due to blocking is characterized by the blocking factor. The design of the Advanced Solar Concentrator provides a blocking loss coefficient of 0.989. This loss is due to the support legs and guy wires.

The intercept factor represents the fraction of the unblocked reflected radiation that is intercepted by the receiver aperture and represents the cumulative effect of many parameters, namely:

- Sunshape error (σ_{ss})
  - -- Spreading of the solar image begins at the sun itself. Due to limb darkening effects and atmospheric scattering, the solar image cannot be modeled as a disc of uniform intensity. The sunshape used in modeling the Advanced Solar Concentrator

performance analysis was based on empirical data taken by Lawrence Berkeley Laboratory expressing the solar intensity as a function of cone angle (Reference 6). It was also possible to correlate solar width as a function of insolation levels (Reference 7).

- Structural deflection (σ_d)
  - -- Structural deflection will also distort the solar image. A structural analysis code computed the deflections in the gore support structure caused by gravity and wind loads. The resultant angular deviation from the focal point for each reflective gore was then computed, as well as the mean and standard deviation of the distribution of angular deviations. While the deflection of each gore can be deterministically computed for any orientation, the aggregate effect was treated statistically to simplify the optical analysis. Because of the asymmetric wind and gravity loads the mean is not located at the original focal point. Since this can be corrected by the image sensing tracker control system, the image spreading due to structural deflections can be characterized as being solely a function of the standard deviation from the mean.
- Reflective surface quality -- Surface shape error (σ_s), gore deflection (σ_g), and specularity (σ_ω)
  - -- The reflective gores contribute to image spreading in three ways. The major contributor is the surface slope error from the manufacturing process. The design specification required the rms slope error to be less than or equal to 3 mrad. In the

absence of manufacturing data, a conservative approach was taken with an assumed rms slope error of 3 mrad.

The cellular glass gores will deflect relative to their supports when loads are applied. A structural analysis provided the angular deflections at 50 discrete points on a typical gore. To simplify the optical analysis, these errors were also treated statistically. The rms slope error was computed and used in the model.

The specularity of the reflective glass mirror sheet is the final contributor to image spreading. Laboratory measurements have characterized the reflected beam profile for a number of reflective materials (Reference 8). The beam profile is described by a normal distribution with a characteristic standard deviation. As no measurements have been made for Corning 7809 mirror glass, data from a similar product, backsilvered Corning 0317 was used.

- Concentrator geometry -- rim angle and concentration ratio
  - -- The concentrator rim angle (45^{o}) and receiver aperture diameter (22 cm) have been specified. The concentrator aperture diameter and therefore, geometric concentration ratio was variable, however.
- Pointing error (E_p)
  - -- Pointing error is the angular deviation between the center of the reflected solar beam and the center of the receiver aperture. Pointing errors result from errors in the solar tracker and drive mechanism and uncompensated deflections of the receiver support structure. If the receiver aperture is

not centered about the flux distribution, the concentrator performance will degrade. During normal operation, the pointing error will not exceed 0.1^{o} as required in the specification.

The intercept factor is computed in two stages. First, the flux distribution at the focal plane is determined. The shape of the two-dimensional flux distribution is influenced by the concentrator rim angle, the sunshape, and the image spreading effects (σ_s, σ_g, σ_d, and σ_ω). Next, the energy actually intercepted by the receiver aperture is computed. The energy intercepted varies with the ratio of receiver aperture diameter to concentrator diameter and pointing error.

The flux distribution at the focal plane is computed using a well-established cone optics technique for assessing the effects of image spreading errors (Reference 9). This approach treats the image spreading statistically, using a probability density function to describe the distribution of directions for the reflected rays for a specified incoming ray. The probability function used to define the image broadening is a two-dimensional normal distribution. This is illustrated in Figure 2-22.

Assuming the image spreading follows a two-dimensional normal distribution, the individual effects can be combined or convolved into one representative error cone. The following expression is used in the convolution:

$$\sigma^* = \left[\sigma_\omega^2 + (2\sigma_d)^2 + (2\sigma_g)^2 + (2\sigma_s)^2\right]^{1/2} \qquad (2\text{-}3)$$

where σ^* is the convolved standard deviation (mrad). The factor of 2 which appears in Equation (2-3) for σ_d, σ_g, and σ_s is due to the representation

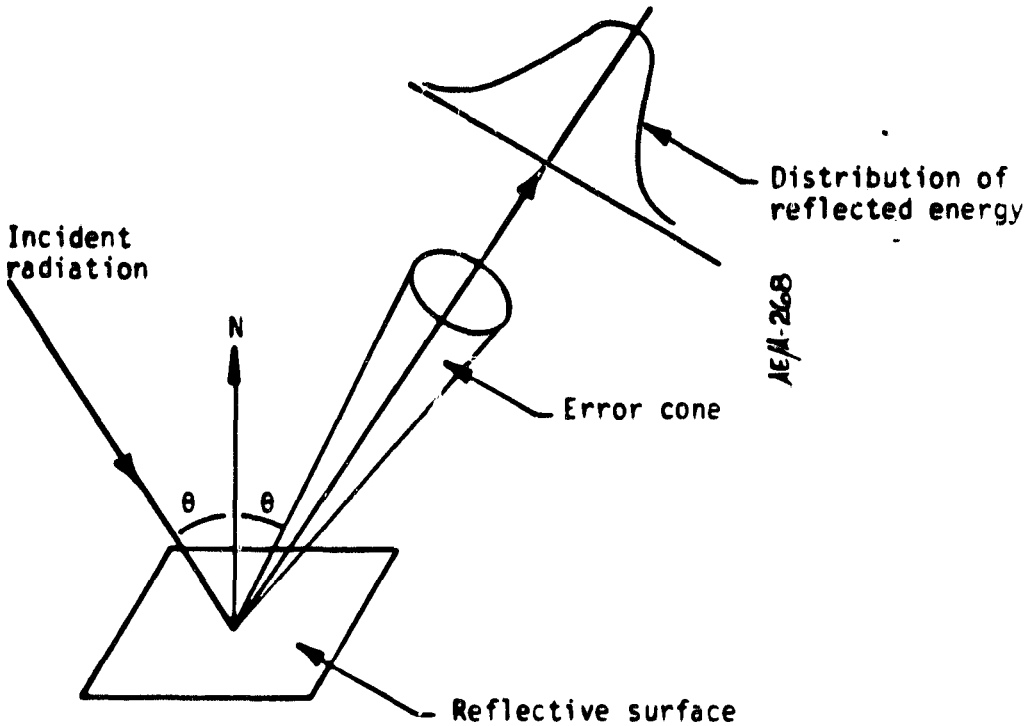

Figure 2-22. Error Cone Methodology

of surface slope errors. For a given slope error of σ, the reflected ray will have an error of 2σ.

The cumulative effect of σ^* and sunshape is an "effective" sunshape combining the distribution of energy across the solar image, and the image spreading effects. If the solar image were modeled as a normal distribution, it too would be included in Equation (2-3). Since an empirically defined sunshape was used, the effects were convolved using a Fourier transform.

The computer code HELIOS (Reference 10) was used to apply the error cone methodology and compute the flux distribution at the focal plane. It was chosen because it offered greater flexibility than other similar codes. Briefly, HELIOS represents the focal plane and the concentrator surface as a matrix of points. For each point at the focal plane, it computes the energy contribution from each segment of the concentrator. In this manner, the flux

distribution at the focal plane is computed. The flux distribution can now be integrated for a given receiver aperture to compute the percentage of incident energy intercepted.

The flux distribution was integrated for different receiver aperture diameters. This was done to represent the intercept factor parametrically as a function of receiver radius divided by concentrator diameter (r/D). Pointing errors were modeled by misaligning the center of the receiver aperture and the flux distribution. Figure 2-23 summarizes the effects of σ^* and pointing error or intercept factor for different values of r/D.

2.3.2 Concentrator Size/Stiffness Optimization

The optimum concentrator, for purposes of this analysis, is a minimum weight concentrator which meets the performance specifications. In mass production, the cost of the concentrator will be proportional to the weight or mass. Therefore, minimizing weight is analogous to minimizing cost.

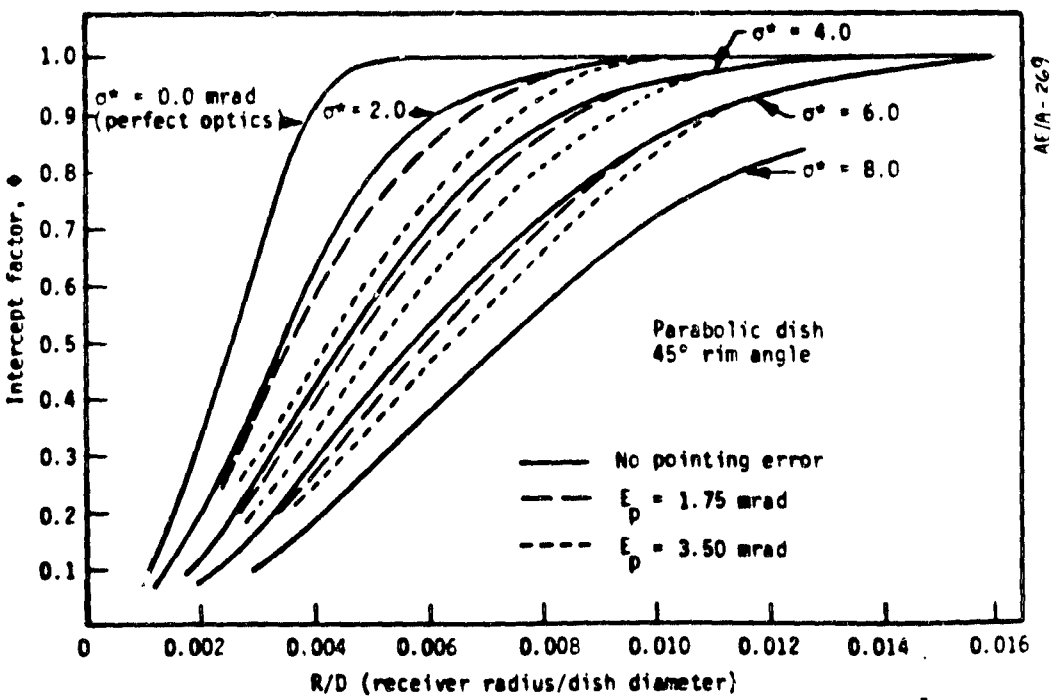

Figure 2-23. Intercept Factor

The given performance requirement is that the concentrator provide 56 kW of optical energy to a 22-cm (8.7-in.) diameter receiver aperture with a direct normal insolation of 845 W/m^2 and an operating wind of 50 km/hr (31 mph).

Design and material selections dictated all variables except for the concentrator aperture diameter and structural deflection. A trade-off between these two variables existed because reducing the concentrator diameter requires a stiffer structure to collect the same amount of energy. Reducing the diameter lowers the weight; however, stiffening the structure increases the weight. The optimization analysis solves for the specific diameter and stiffness that results in minimum concentrator weight.

To execute the parametric study, relationships were developed to describe concentrator structural deflection at the operating wind velocity as a function of weight for different diameters. This was done in three steps. First, the structural deflections were computed for the baseline concentrator design at the worst case orientation under maximum operating wind conditions. The baseline concentrator was a stress-limited design for an 11-m diameter concentrator. Secondly, member sizes in the gore support structure were increased to stiffen the structure. The resultant increase in structural stiffness was found to follow the relationship

$$\sigma_d = \sigma_d'\left(1 + \frac{\Delta w}{w_o}\right)^{-1.01} \qquad (2\text{-}4)$$

where

σ_d = rms structural deflection (mrad)

σ_d' = rms structural deflection for stress-limited design (mrad)

Δw = change in gore support structure weight

w_o = gore support structure weight for stress-limited design

Finally, the structural deflection (σ_d) and structure weight were computed for a 10- and 12-m dish with a stress-limited design. This information was used for computing structural deflection and weight of stress-limited designs at several concentrator diameters. It was assumed that the relationship between deflection and weight expressed in Equation (2-4) is valid at all concentrator diameters. This effort to quantify the relationship between σ_d, concentrator weight, and diameter was based on structural analysis results from the ANSYS computer code.

Once the equations relating structural deflection to concentrator diameter and weight were developed, they were applied to compare weight and performance of various design options. Performance is influenced by concentrator diameter and structural deflection (see Equations (2-1), (2-2), and (2-3)). Concentrator cost varies with diameter and stiffness. Concentrator weight variations occurred primarily in two areas; the reflective gores and the gore support structure.

The results of the concentrator size optimization are presented graphically in Figure 2-24. Concentrator weight variations are shown as a function of structural deflection, diameter, and power output. At any given diameter, concentrator weight and cost decrease as the structure is made more flexible and σ_d increases. There is a limit to the flexibility of the structure. Beyond this limit, denoted by a square, the stresses get too large and the structure can fail. Increasing concentrator diameter will increase structure cost as expected.

Concentrator optical output is a function of both diameter and deflection. To generate 56 kW at the focal plane, the optimum concentrator has a diameter of 10.9m, and a structural deflection with σ_d = 1.26 mrad.

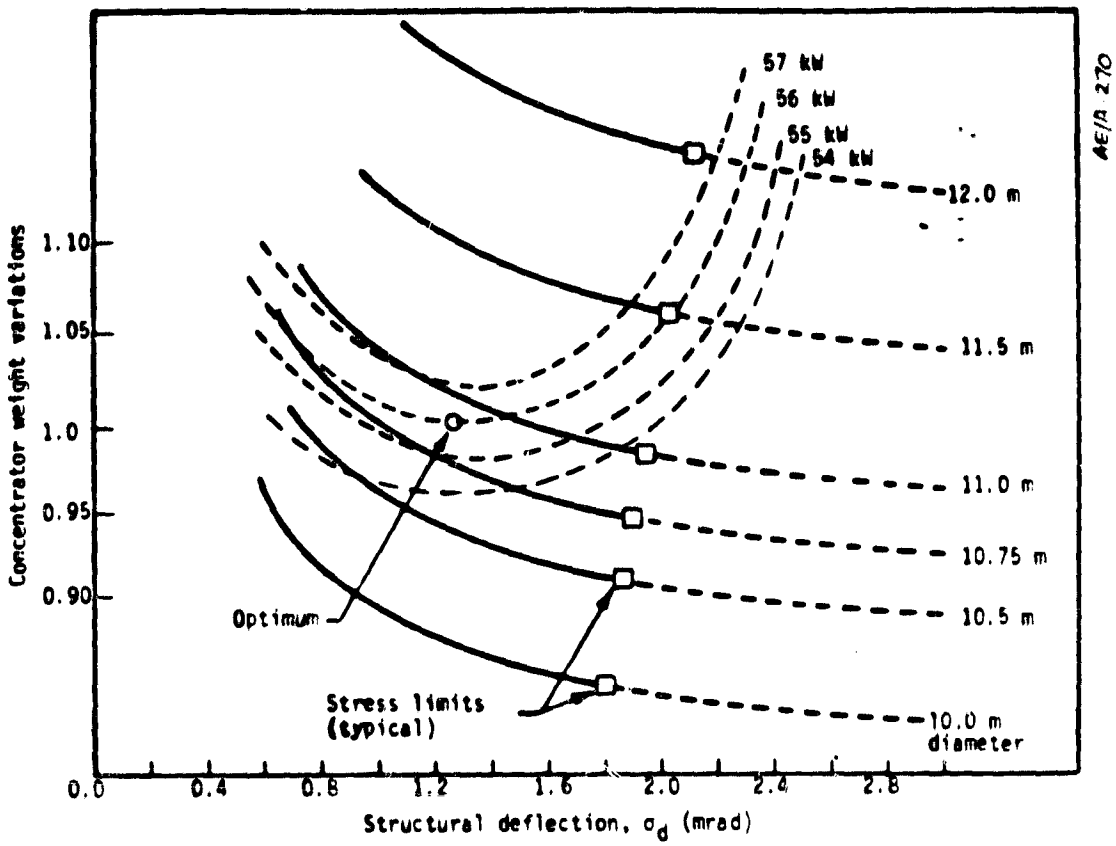

Figure 2-24. Concentrator Cost Versus Structural Deflection and Diameter

An optimum size is reached for several reasons. A stiffer structure will reduce structural deflection. After a certain point, however, the reduction in σ_d has a minor impact on σ^*, and the overall optical performance. As deflections increase, the required concentrator area to maintain a constant power output must also increase. The combination of larger diameters and lower intercept factors more than offset any savings in weight from a lighter structure. There is also the limit on maximum deflection due to stress limitations.

Although these results clearly show an optimum size, the optimum is relatively flat. For 56 kW, the concentrator diameter could vary from 10.75 to 11.45 m with a 5-percent variation in estimated concentrator weight.

2.3.3 Performance Summary

The optimum concentrator design will produce 56 kW of optical energy at the receiver aperture under the design conditions at the lowest cost. Results indicate the optimum diameter to be 10.9 m. The structure will be approximately 50 percent stiffer than the stress-limited design. With an r/D ratio of 0.0101, and σ^* 6.53 mrad, this concentrator will have an intercept factor of $\phi = 0.829$. The design conditions, concentrator parameters, and results at the preliminary design point are presented in Table 2-19.

Table 2-19. Performance Summary

Design Conditions	
Insolation	$I = 0.845$ kW/m^2
Sunshape error	$\sigma_{ss} = 3.07$ mrad
Wind	$W = 50$ km/hr
Collector rim angle	$\theta = 45^o$
Receiver aperture diameter	$D_r = 22$ cm
Concentrator Parameters	
Concentrator diameter	$D_c = 10.9$ m
Convolved error cone	$\sigma^* = 6.53$ mrad
Specularity	$\sigma_w = 0.25$ mrad
Structural deflection	$\sigma_d = 1.26$ mrad
Gore slope error	$\sigma_s = 3.00$ mrad
Gore deflection	$\sigma_g = 0.24$ mrad
Reflectance	$\rho = 0.94$
Gap loss coefficient	$K_G = 0.919$
Shading loss coefficient	$K_S = 0.998$
Blocking loss coefficient	$K_B = 0.989$
Pointing error	$E_p = 1.7$ mrad
Results	
Optical energy at receiver aperture	$E = 56$ kW
r/D	$r/D = 0.0101$
Intercept factor	$\phi = 0.829$

SECTION 3

DETAILED DESIGN

The detailed design task included only the design of the outer reflective gore element and a final evaluation of the concentrator's thermal performance. The resulting gore design was intended to be of sufficient detail to allow fabrication of prototype hardware with limited interaction with the design engineers. Due to the concurrent development work being performed by JPL and other contractors, several aspects of the design could not be finalized during this task. An outline prototype fabrication specification (Appendix F) was therefore developed as part of the detail design effort to provide the framework in which to incorporate the results of these efforts to complete the design.

Two key questions remained unresolved at the completion of preliminary design; namely, the most cost-effective elimination of the stress concentration problem at the inner gore and the most cost-effective gore support scheme. Preliminary conclusions had been drawn in each area, but further study was warranted. As such, this section also reports the results of these additional efforts performed as elements of the detailed design task. Section 3.1 presents the solution to the inner gore stress concentration problem, Section 3.2 presents the gore support system trade-off with its impact on final gore design, Section 3.3 discusses the design of the gore attachment hardware, Section 3.4 reviews several

prototype core grinding options, and Section 3.5 presents a summary of the gore design and the final thermal performance estimate.

3.1 ELIMINATION OF CORE STRESS CONCENTRATION AT MIRROR FACE

The preliminary design task closed with the discovery of a serious stress concentration at the discontinuity between the two half-width glass mirror sheets on the inner gore. Various techniques for mitigating the local stress concentration were investigated and a viable, though complex, load-bridging technique was developed. Since increased complexity usually results in higher costs and a potential for lower reliability, the merits of a simple solution are high. The proposed solution involves a reduction of the inner gore width from 15.4 to 13.0 cm (39 to 33 in.), allowing a single full-width mirror panel to be used. The entire problem of stress concentration is thereby avoided, simplifying the gore design considerably. The new 13-cm (33-in.) wide inner gore results in an increase in the number of inner gores from 20 to 24. The new arrangement as shown in Figure 3-1, will group into quadrants (as did the original) to provide clearance gaps for the quadripod legs. The new inner gore width is identical to that of the outer gore, which may offer some manufacturing benefits in terms of dual purpose tooling or assembly fixtures.

The ring truss, designed for the 20 inner and 40 outer gore arrangement, will be impacted by this design change. The impact of this design change upon cost and performance of the structure is expected to be minor, but since the ring truss provides a member junction at each loading point, the truss must be reconfigured for the 40/24 gore arrangement.

3.2 GORE SUPPORT SYSTEMS EVALUATION

The basic design concept behind the Advanced Solar Concentrator centers about the use of a cellular glass substrate for the silvered glass

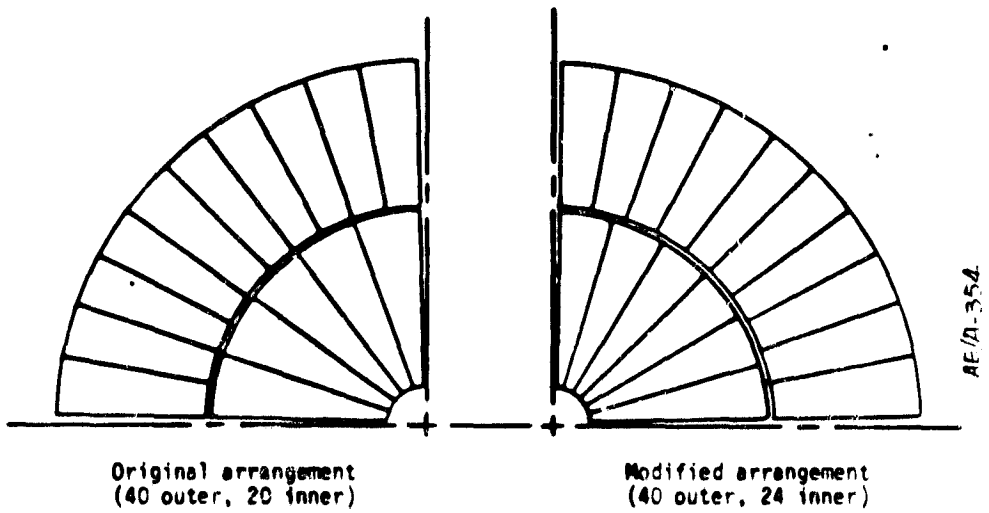

Figure 3-1. Modified Gore Arrangement

reflective panels in such a way that it would replace a substantial portion of the structural steel framework normally used to support the reflective surface of a dish-type concentrator. The basic approach involves the use of a ring-shaped structural truss, from which the reflective gores are supported, and through which the weight and aerodynamic loads are transmitted to ground. The diameter of the ring truss is a substantial fraction (50 to 65 percent) of the dish diameter to allow reflective gores to be supported on both the inward side, toward the center of the dish, and the outward side, toward the rim of the dish. Using these basic conceptual ground rules, the most obvious support would be cantilevered gores radiating outward and inward from the structural ring. However, a cantilever beam suffers two disadvantages in comparison with other types of beams:

- The highest bending moment for a given uniform load
- The greatest deflection and slope error of any support system

The impact of these disadvantages upon the system are:

- Large gore bending moments result in thicker, heavier gores when the gores are stress-limited (as they are)
- For an optical concentrator, performance is very sensitive to local and general deviations in slope of the reflective surface from the design paraboloidal surface

The larger bending moment inherent in the cantilever results in lower performance for a given weight, plus the requirement of a large reacting moment from the ring truss. Small angular deflections in the ring truss supporting members result in rotation of the entire panel from its ideal position.

The addition of a second support point along the length of the gore eliminates the large supporting end moment inherent in the cantilever. Placing the second support at the opposite end of the gore requires the structure to extend across the entire dish surface, which is undesirable. A support location can be found at a point slightly past midspan of the gore, where the maximum value of the slope error is minimized for a given pressure distribution. This location was chosen for the second gore support point. Having chosen the second support point, the load can be removed by a simple strut extending from the truss to the gore (Figure 3-2) or by a rigid extension of the truss (Figure 3-3). These options were examined in detail to determine the most cost-effective method of removing loads from the second support point.

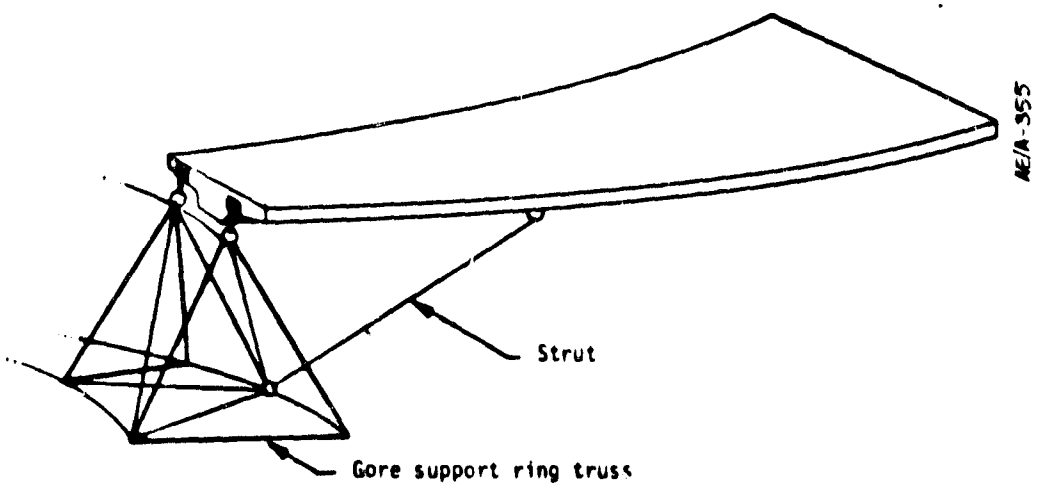

Figure 3-2. Strut Support System

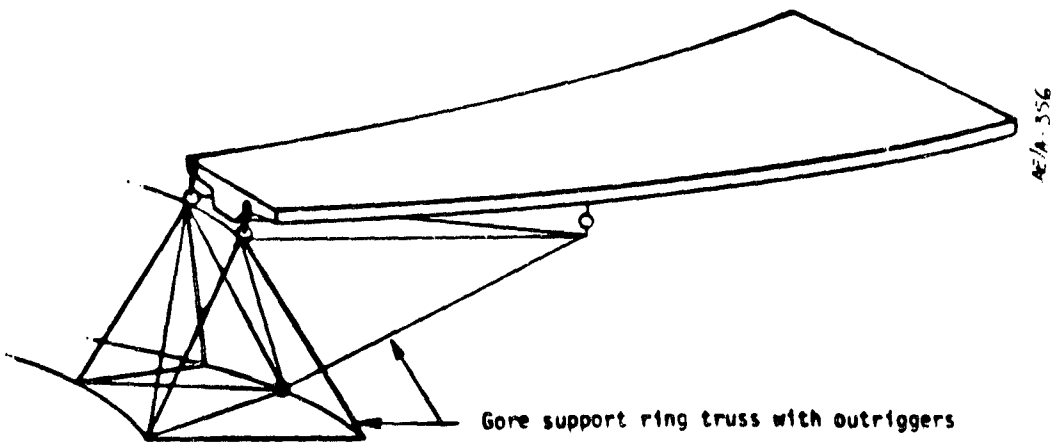

Figure 3-3. Simple Support System

The ring truss design was optimized to use simply supported gores, that is, fixed points on the truss located at the support points of the gores. Using this approach, the exact weight of any structural elements eliminated or modified for a strut-type support system would be known. Figure 3-4 shows the outer gore designed for simple supports along with its bending moment distribution and elastic curve. When the truss section beneath the gore is replaced with a single compression strut, the strut intersects the gore at an angle of 37-1/2° to the plane of the gore. Removal of a large load normal to the gore by an oblique strut results in a large load component in the plane of the gore. The gore must carry this tensile load and it must be removed at the root end of the gore by a horizontal support reaction. The gore geometry and the need to minimize

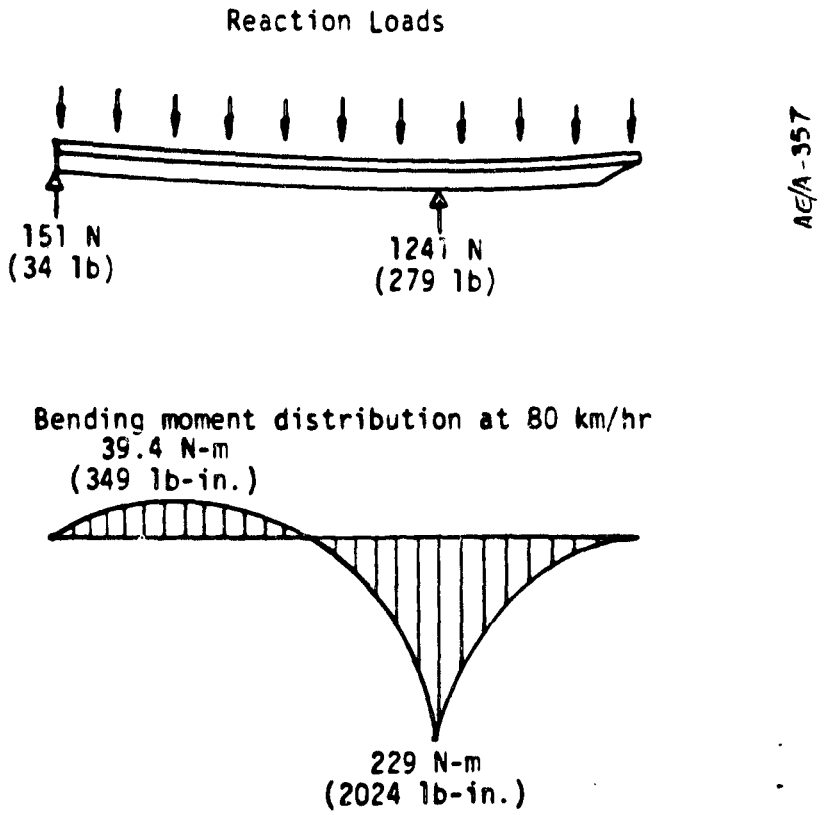

Figure 3-4. Simply Supported Gore Moment Diagram

the gap between gores causes the in-plane load to be removed eccentrically to the neutral axis of the gore. This introduces an end moment into the gore, which in turn must be reacted by an increase in the midspan support reaction. This change in load distribution causes the optimum support location for minimum slope error to move a short distance toward the root of the gore, thereby increasing the length of overhang of the gore tip and the maximum bending moment in the gore. Figure 3-5 shows the outer gore design for strut support along with its bending moment distribution and elastic curve. The resulting gore experiences a 39-percent increase in the maximum bending stress, plus an increase of 43.4 kPa (6.3 psi) (16 percent) in the core tensile stress and of 1,965 kPa (285 psi) in the

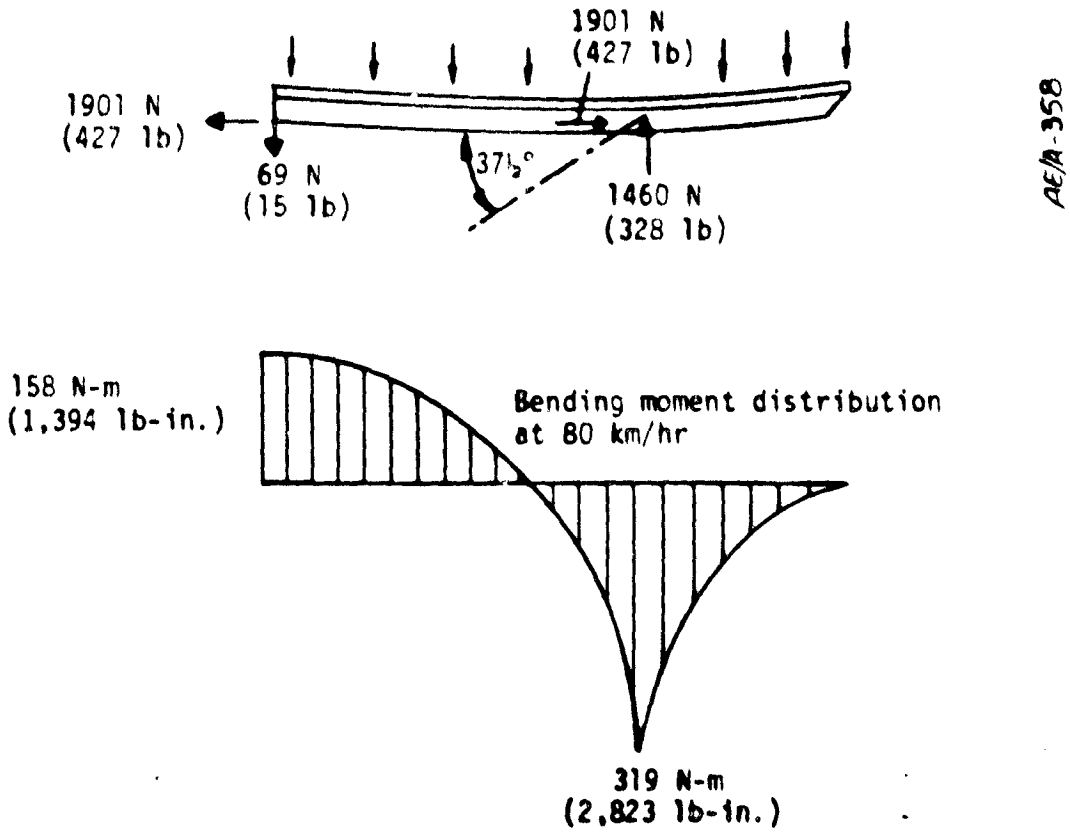

Figure 3-5. Strut Supported Gore Moment Diagram

glass tensile stress. Resizing the gore for these additional loads increases its core thickness by 60 percent, resulting in an increase of 5.5 kg (12.2 lb) per gore. For a 60-gore concentrator, the total increase in gore mass is 331 kg (730 lb). The corresponding savings in the ring truss resulting from elimination of two structural members per gore is only 136 kg (300 lb), however. The cost per unit mass of Foamsil® 75 is approximately equivalent to fabricated steel. The concentrator with strut supported gores is therefore clearly heavier and more costly than with simply supported gores, even without considering the impact of the increased weight on the structure between the ring truss and the ground.

There are other advantages to a simple support system for the gore. The requirements of a kinematic support system allow only one support to fix the x, y, and z coordinate of the gore simultaneously. The others must constrain y and z, and only z, respectively. In a strut supported gore, the main (x, y, z) support cannot be the strut, but must be one of the root supports (Figure 3-6). The strut is forced to be completely compliant in x and y and define the z coordinate only. A consequence of this support geometry is that when the concentrator points near the horizon, the weight of the horizontal gores is totally supported by a reaction couple at the two root supports, which for the outer gores are approximately 30.5 cm (12 in.) apart. The distance between the root end and the center of gravity for the gore, and the short 29.2-cm (11.5-in.) distance between the end supports causes the reaction load at the end support to be approximately four times the weight load. In addition to amplified loads, any compliance in the root end supports is readily translated into a rotational movement of the gore. With the rigid truss point located at the midspan support in the simple support system,

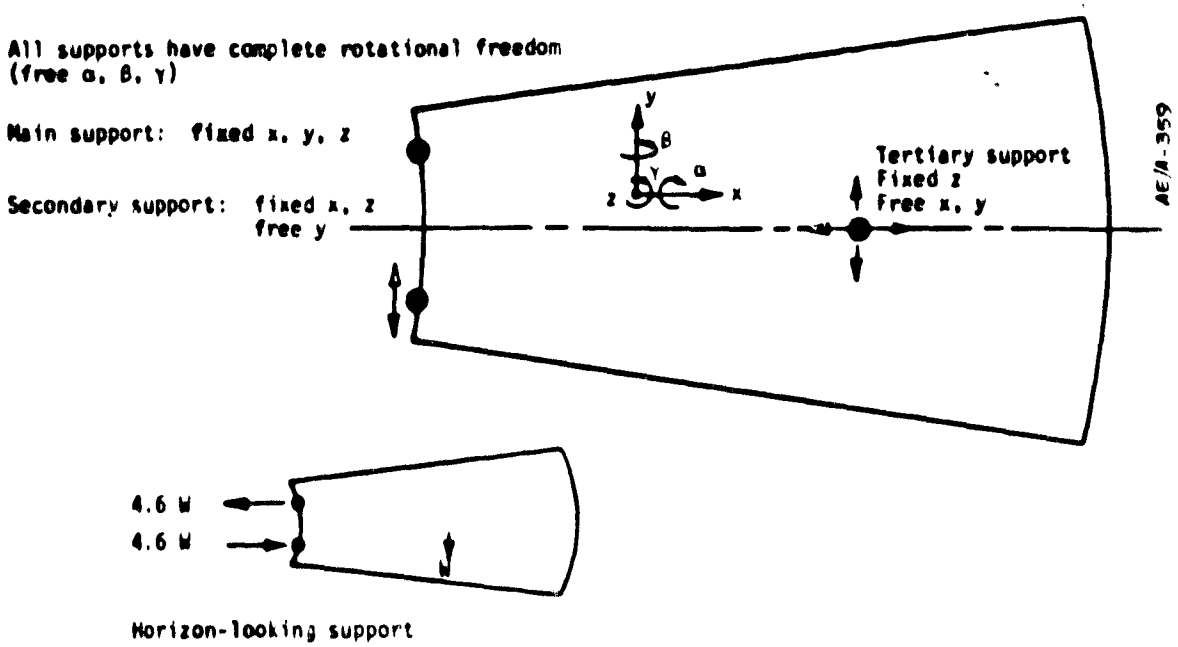

Figure 3-6. Kinematic Support System -- Strut Support

the midspan support can be designed to be the main (x, y, z) support. Being located near the gore center of gravity, it absorbs the majority of the weight load of the gore. Horizon-looking weight loads imposed on the root end supports by this system are minimal, and the large amplification of root end support play is removed. The results of this analysis indicate that the simple support system offers across-the-board advantages over the strut support system.

3.3 GORE ATTACHMENT HARDWARE DESIGN

With the choice of a simple support system made, a central support location was chosen to minimize the maximum value of the slope error of the gore when subjected to a uniform wind pressure. Reaction loads were calculated for each support under the most severe loading conditions for the gore. Table 3-1 summarizes these loads. The most severe loads for each support location were used to design that support structure. The

Table 3-1. Attachment Pad Loads -- Simple Support System

Wind Speed km/hr (mph)	Pressure Distribution	Main Support Load N (lb)	Root Support Load N (lb)
110 (68)	Aerodynamic -- outer gore	2,358 (530)	142 (32)
110 (68)	Aerodynamic -- inner gore	983 (221)	262 (59)
110 (68)	Uniform, $C_p = 1.5$ -- outer gore	1,561 (351)	209 (47)
110 (68)	Uniform, $C_p = 1.5$ -- inner gore	974 (219)	227 (51)
0 (0)	Maximum side force due to weight of 1 vertical gore	245 (55) (lateral)	58 (13) (lateral)

interface between support linkage and the glass gore is accomplished by a ribbed attachment pad of glass fiber reinforced polyester.

The compression molded pad allows a complex yet stiff lightweight structure to be produced at a low production cost. The glass/polyester material can incorporate filler material to allow its coefficient of thermal expansion to approach or match that of the Foamsil® and 7809 glass, while maintaining high structural properties. The gore with attachment pads is shown in Drawing 7740-010 of Appendix E. The root and midspan support pads are respectively detailed in Drawings 7740-012 and 7740-013 of Appendix E.

Both pads can easily absorb the most severe structural loads. The most critical design criterion was the ability of the attachment pad structure to distribute the point reaction load to the glass over the full surface of the pad. Determination of the interface contact pressure was complex, so the attachment pad and gore were modeled for a finite element problem solution, and the solution obtained using ANSYS, a comprehensive

finite-element structural computer code. Figure 3-7 depicts the ANSYS model for the midspan attachment pad. The entire gore was first modeled and subjected to the most severe aerodynamic pressure profile for the 110 km/hr "single short exposure" condition. The ANSYS superelement technique was then used to isolate the attachment pad for detailed study. The resulting pressure distribution indicates that for the most severe face-on wind loading, compressive stresses induced in the glass spar cap and in the Foamsil® core remain within the allowable design limits for tensile loading (compressive limits are considerably higher). The ANSYS analysis also assumed direct contact between the attachment pad and a spar cap without the use of lower modulus bonding agent to aid in the distribution of load over the contact surface. Aerodynamic pressure maps generated for the concentrator during the preliminary design task reveal that, for backside wind loading, maximum wind pressure loading is much lower. This assures that for wind conditions imposing tensile loads at the attachment pad/gore interface, additional conservatism exists in the design.

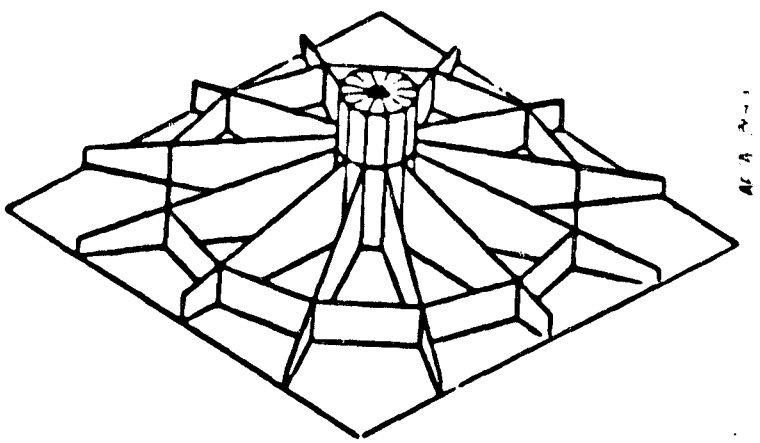

Figure 3-7. ANSYS Model of Main Support Pad

Both the requirements to distribute the reaction load over the pad area and the uncertainty in the degree of expansion match between pad and glass require the use of a compliant bond between the pad and the gore. A 0.81-mm (0.032-in.) sheet of isobutylene isoprene rubber was therefore placed in the interface between the pad and glass cap. This will easily handle the expansion mismatch between standard commercial glass/polyester and 7809 glass as well as distributing the reaction loads. Eventually the function of the sheet of rubber can most likely be assumed by a suitable elastomeric bonding agent.

The main or midspan attachment pad is bonded to the spar cap glass and serves as the fixed point (with free rotation) in the kinematic mounting system. The root attachment pads serve as the secondary and tertiary supports, having 1 and 2 orthogonal degrees of freedom, respectively, to isolate the gore from ring-induced loading. The z-axis is adjustable on all supports to allow proper alignment of the gore on the concentrator. The root attachment pads are bonded to the Foamsil® core and overhang the gore at the root end to place the gore loads directly over the apex member of the triangular ring truss. A preliminary concept of the attachment linkage is depicted in Figures 3-8 and 3-9. The linkage is secured to the attachment pad by means of a stainless steel threaded insert (see Drawing 7740-014, Appendix E), which is intimately locked into the pad during the compression molding process. The main or midspan support linkage is a rigidly mounted ball joint with adjustable height. The height adjustment is accomplished by varying the length of engagement of the threaded stud on the ball joint. The height is then fixed by a jam nut. The secondary support consists of a flexure-type hinge, an adjustable length link, and a ball joint. This support fixes the height

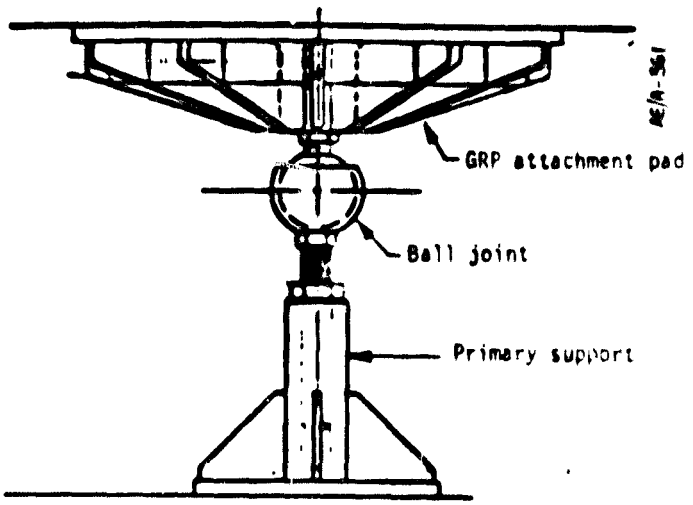

Figure 3-8. Primary Support

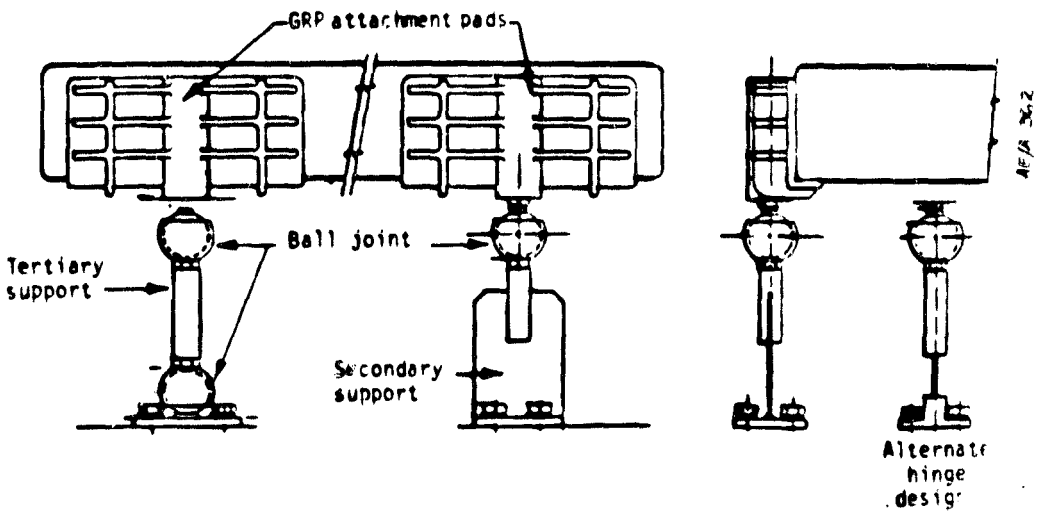

Figure 3-9. Secondary and Tertiary Supports at Gore Root

and restrains movement in the tangential direction (transverse to the hinge axis). The tertiary support uses an adjustable length link between two ball joints to fix the height while allowing freedom of movement in the radial and tangential direction. Since all supports use one or more ball joints, each support allows complete freedom in rotation.

3.4 PROTOTYPE FABRICATION OPTIONS

Present state of the art requires that gores be manufactured from a monolithic or composite slab of cellular glass by a machining process. Cellular glass machines very easily, therefore high feeds and speeds can be employed to generate finished surfaces in two or three passes. Several techniques can be used to generate the paraboloidal contoured surface of the gore. A curve-grinding machine was proposed by Pittsburgh-Corning Corporation. This machine uses a full-length shaped rotating arbor oriented in the radial direction to generate the face contour (Figure 3-10). A separate arbor would be required for the inner and outer gore. A second technique employs a full radius parabolic track carrying a grinding head and tool. The track would rotate about the central axis of the paraboloid and the cutter would move radially along the parabolic-shaped track to generate the surface (Figure 3-11). A third technique would employ a numerically controlled vertical mill to generate the surface with a small spherical cutter using a curve fitting program between a net of supplied surface coordinates. The mill would generate the surface in a series of x and y passes with the table motion controlled by the computer (Figure 3-12).

A fourth technique uses a contoured barrel cutter oriented in the transverse direction to generate an approximation to the paraboloid (Figure 3-13). The cutter is contoured to a radius of curvature whose

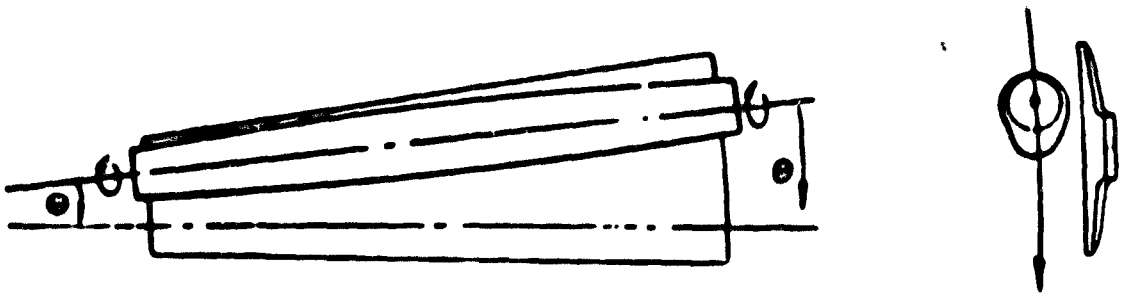

Figure 3-10. Generation of Paraboloidal Contour by Shaped Radial Cutter

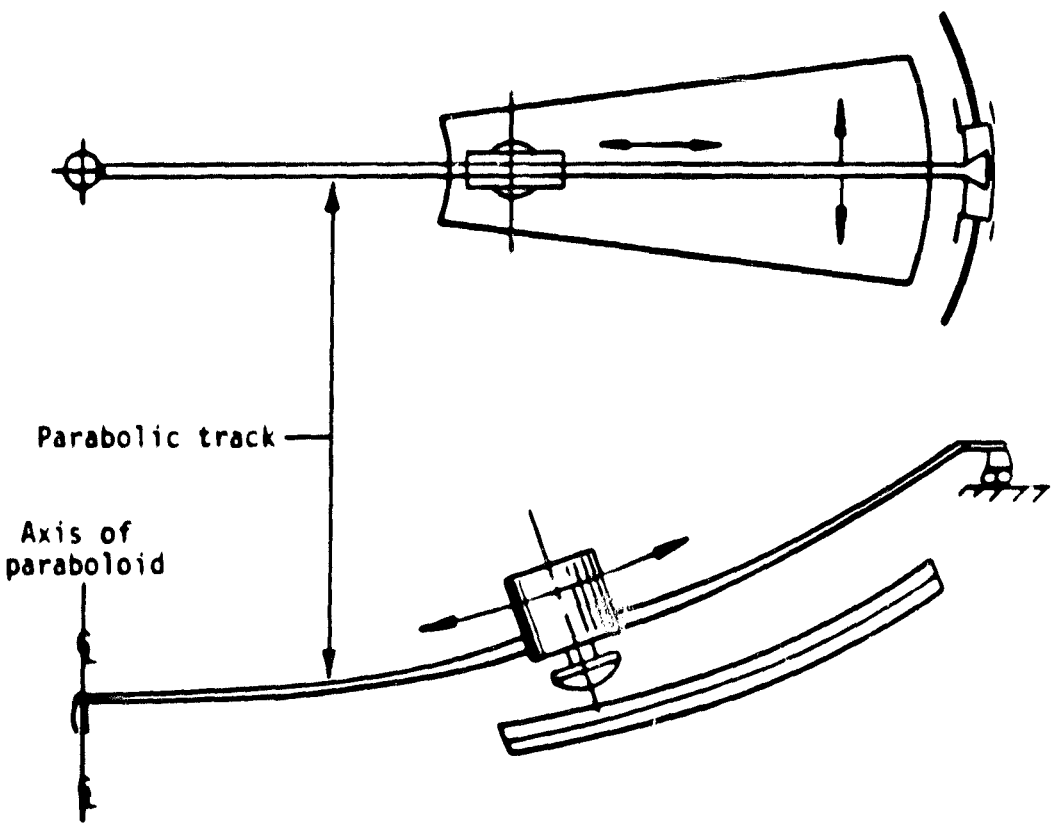

Figure 3-11. Generation of Paraboloidal Contour Using Rotating Parabolic Track and Moving Rotary Cutter

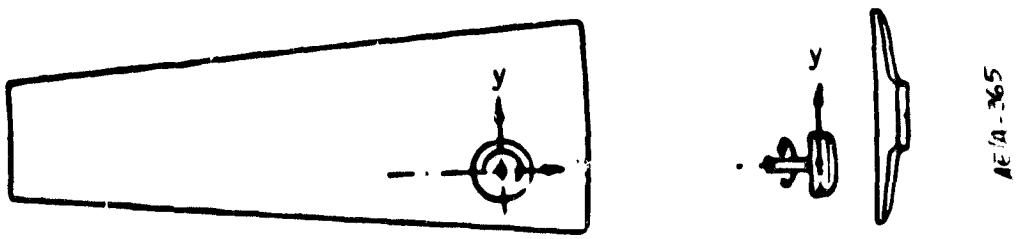

Numerically controlled x-y curve generation

Figure 3-12. Generation of Paraboloidal Contour by Three-Axis Numerical Control of Large Radius Spherical Cutter

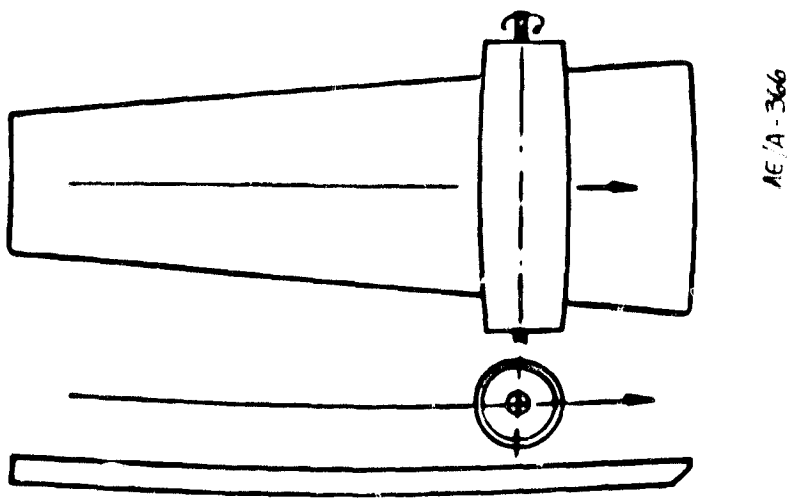

Figure 3-13. Paraboloidal Curve Generation by Contoured Transverse Cutter

value lies between the transverse radius of curvature of the paraboloid at the root and tip of the gore. The cutter radius is chosen to minimize the maximum value of the approximation error to the paraboloid. Calculations show that a cutter radius can be chosen limiting the maximum value of the approximation error to 0.70 mrad for the outer gore and 1.22 mrad for the inner gore. The rms error values associated with the approximation technique will be considerably less; probably of the order of 0.25 and 0.10 mrad for the outer and inner gores, respectively. These approximation errors are of an acceptable magnitude for prototyping since the surface accuracy goal for the reflecting surface is a 1 mrad rms slope error. The latter technique has the potential for the manufacture of good quality prototype gores with a relative low cost machining process. The radial contour of the gores can be controlled by contoured rails or cams to control the cutting head height as a function of radial position, or by numerically controlling the table height of a horizontal mill as a function of cutter position.

The mirrored face sheet can be bonded to the core using either a male contoured metal tool, possibly as a vacuum chuck, to define the contour of the glass mirror during the bonding process, or by vacuum bagging the mirror glass against the machined core, using the contoured surface of the Foamsil® core to define the mirror contour. A better quality mirror will be produced using a master tool, but there are indications that mirrors of adequate precision can be produced by the vacuum bag technique. The latter technique is of particular interest in prototyping, where funding for tooling is limited.

Designs for prototype and production gore blanks are depicted in Figures 3-14 and 3-15. Both blanks are designed to avoid bond joints in

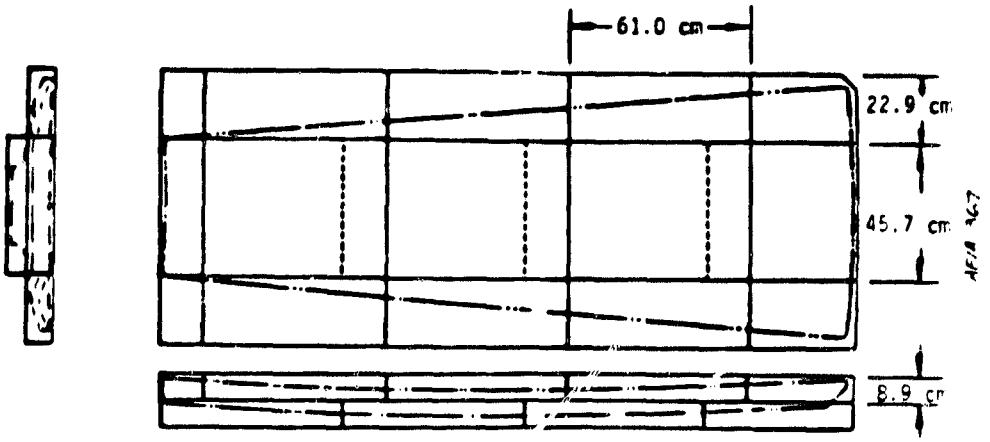

Figure 3-14. Core Blank for a Prototype Outer Gore

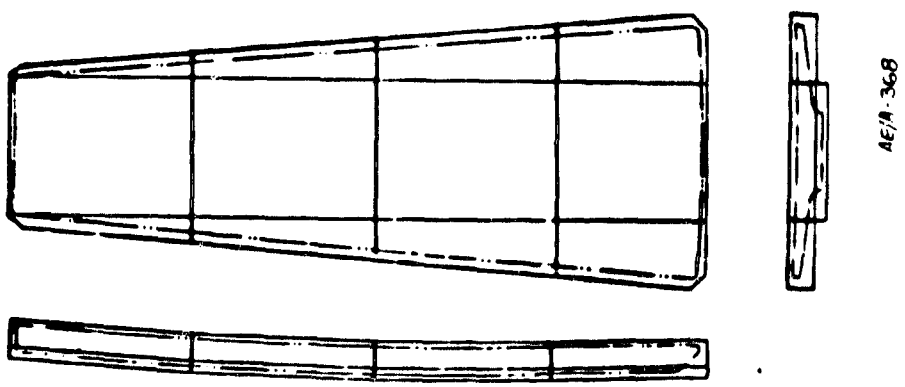

Figure 3-15. Minimal Waste Core Blank for Mass Production

areas of highest stress. The prototype gore is designed to be easy to fabricate and set up for machining with little or no fixturing. The production blank emphasizes maximum use of material and consequently it follows the curved shape of the gore. This blank requires fixturing to miter the block faces and hold them in place for bonding, as well as for machining.

3.5 FINAL GORE DESIGN AND PERFORMANCE SUMMARY

The outer gores consist of a wedge-shaped cellular glass structural core whose thickness varies laterally from a central maximum to the edge. A central spar runs full length along the rear surface of the gore to provide bending stiffness to the tapered face sheet. A full area backsilvered glass face sheet is bonded to the paraboloidal front surface of the gore and a clear glass cap is bonded to the spar, forming a skin-stressed composite structure with a high structural efficiency. The cellular glass face-sheet center thickness is 2.0 in., while the spar thickness is 3.81 cm (1.50 in.) for the outer gore. The gores use a single full-sized face sheet of silvered Corning 7809 glass, 1.0 mm (0.040 in.) thick, flexed to the contour of the paraboloid and bonded in place. A 10-in. wide piece of 1.0-mm (0.040-in.) unsilvered 7809 glass, simply curved to a parabolic shape is bonded to the surface of the cellular glass spar with the same resin system. The glass and Foamsil® form a composite structure in which the mirror and spar cap glass absorb a significant portion of the bending load.

Attachment to the ring truss is accomplished through glass fiber reinforced polyester pads containing threaded metal inserts for attachment of support linkage. The pads are bonded to the gore with an elastomeric adhesive system. After glass and attachment pads are bonded to the gore,

a protective coating is applied to all unmirrored areas of the gore to protect the Foamsil® core and mirror edge seals from the environment.

The outer gores are stress-limited in the cellular glass core when subjected to the governing load condition of a 110-km/hr (68-mph) front-side wind with the concentrator in the worst case aerodynamic orientation to the wind. Figure 3-16 shows the bending moment distribution along with the operating stress levels for the mirror glass, spar cap, and cellular glass core under the design loading conditions.

Gore performance parameters were evaluated at the 50-km/hr (31-mph) wind velocity with a uniform pressure distribution over the gore surface. Uniform pressure coefficients for performance evaluation were stipulated by the contract to be 3.3 for both inner and outer gores. Figure 3-17 presents deflection and slope error values for outer gores under these conditions.

When examining aerodynamic loading profiles generated during preliminary design, it can be seen that under no condition does loading approach the magnitude dictated by uniform pressure at $C_p = 3.3$. It is recommended for future evaluation of gore performance that pressure coefficients of 3.0 and 2.0 be used for the outer and inner gores, respectively. This will allow slightly lower and more realistic slope error values for the outer gore and will allow some weight to be pared from the inner gore (currently deflection limited), which will very likely also become stress-limited.

The performance analysis presented in Section 2.3 was performed at the close of the preliminary design task. The results presented in Table 2-19 of that section were based on an assumed rms manufacturing slope error for the gores of 3.0 mrad. Due to the unproven nature of

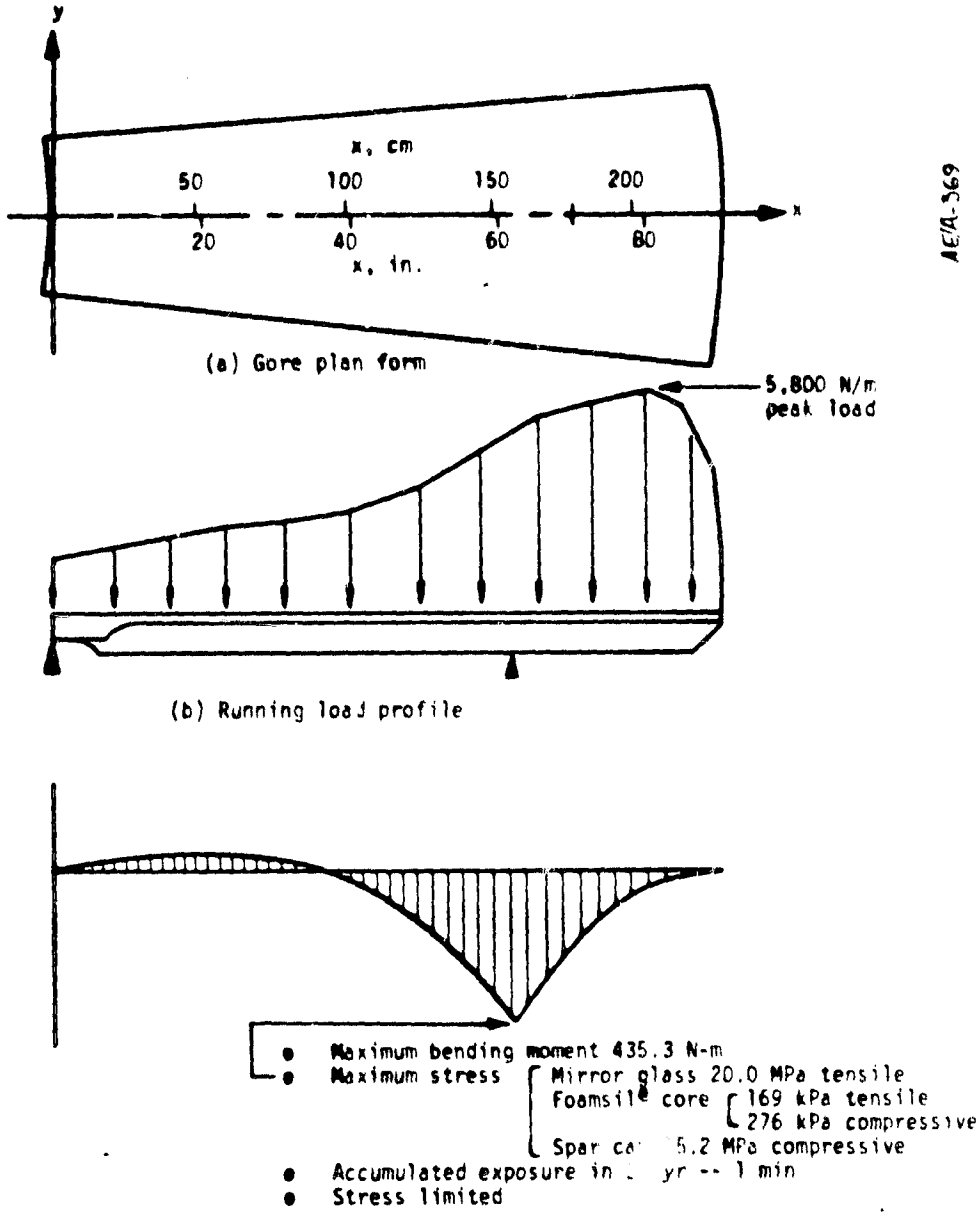

Figure 3-16. Load and Moment Profiles for Outer Gore

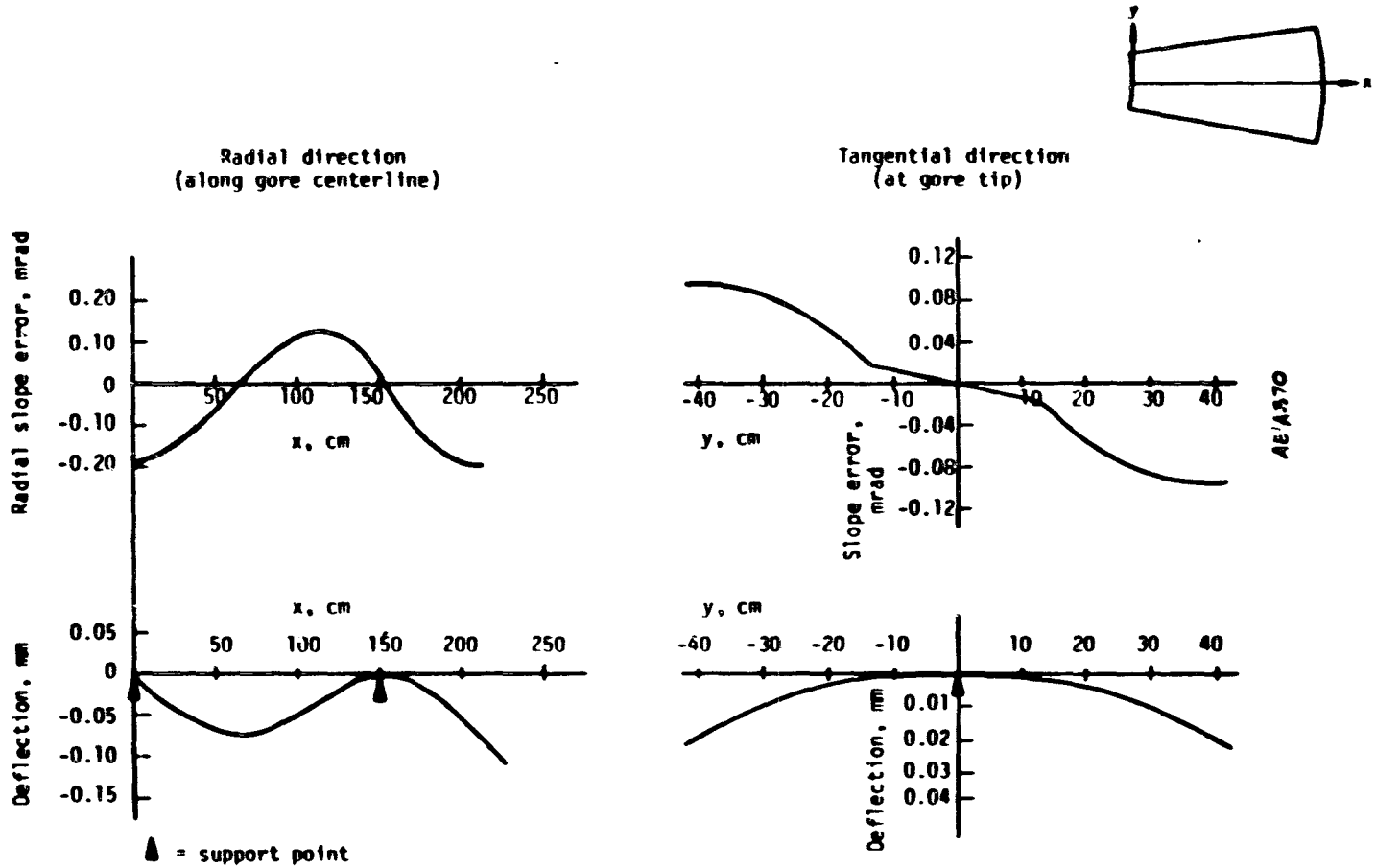

Figure 3-17. Slope Error and Deflection, Outer Gore

using cellular glass as a structural substrate for reflective panels, the 3.0 mrad maximum specified value (Appendix A) was conservatively assumed. This relatively poor surface accuracy led through the optimization trade-offs to a deflection limited structural design with an optimum aperture diameter of 10.9 m.

Concurrent work at JPL in the fabrication of reflective panel elements for the Test Bed Concentrator indicated that manufacturing slope errors of 1.0 mrad or less were achievable with cellular glass substrates. The concentrator performance was therefore reevaluated with a 1.0-mrad gore manufacturing slope error and updated gore deflection slope errors as determined during detailed design. The results are presented in Table 3-2.

The results are presented for an 11.0-m diameter concentrator (the baseline design). Due to the higher accuracy of the gores, the structural stiffness can be relaxed to the point where the structure becomes stress limited. The performance impact of increased gore accuracy far outweighs the effects of reduced structural stiffness. The optical output of the concentrator is increased from 56 kW for the optimized 10.9-m concentrator with the 3.0-mrad gores to 64.5 kW for a stress-limited 11.0-m concentrator with the 1.0-mrad gores. While 2 percent of this increase comes from the diameter change, the remaining 13 percent is a result of the gore and structure changes.

The sensitivity of concentrator performance to gore slope error, wind speed, and pointing error was also determined. As shown in Figure 3-18, for an 11.0-m stress-limited concentrator design, concentrator performance is relatively insensitive to wind speed for gore manufacturing slope errors less than 1.0 mrad. The performance increase from the 50-km/hr design point to a zero wind speed condition is less than

Table 3-2. Final Performance Summary

Design Conditions	
Insolation	$I = 0.845$ kW/m^2
Sunshape error	$\sigma_{ss} = 3.07$ mrad
Wind	$W = 50$ km/hr
Collector rim angle	$\theta = 45^o$
Receiver aperture diameter	$D_r = 22$ cm
Concentrator Parameters	
Concentrator diameter	$D_c = 11.0$ m
Convolved error cone	$\sigma^* = 4.31$ mrad
Specularity	$\sigma_w = 0.25$ mrad
Structural deflection	$\sigma_d = 1.90$ mrad
Gore slope error	$\sigma_s = 1.00$ mrad
Gore deflection	$\sigma_g = 0.132$ mrad
Reflectance	$\rho = 0.94$
Gap loss coefficient	$K_G = 0.919$
Shading loss coefficient	$K_S = 0.998$
Blocking loss coefficient	$K_B = 0.989$
Pointing error	$E_p = 1.7$ mrad
Results	
Optical energy at receiver aperture	$E = 64.5$ kW
r/D	$r/D = 0.0100$
Intercept factor	$\phi = 0.938$

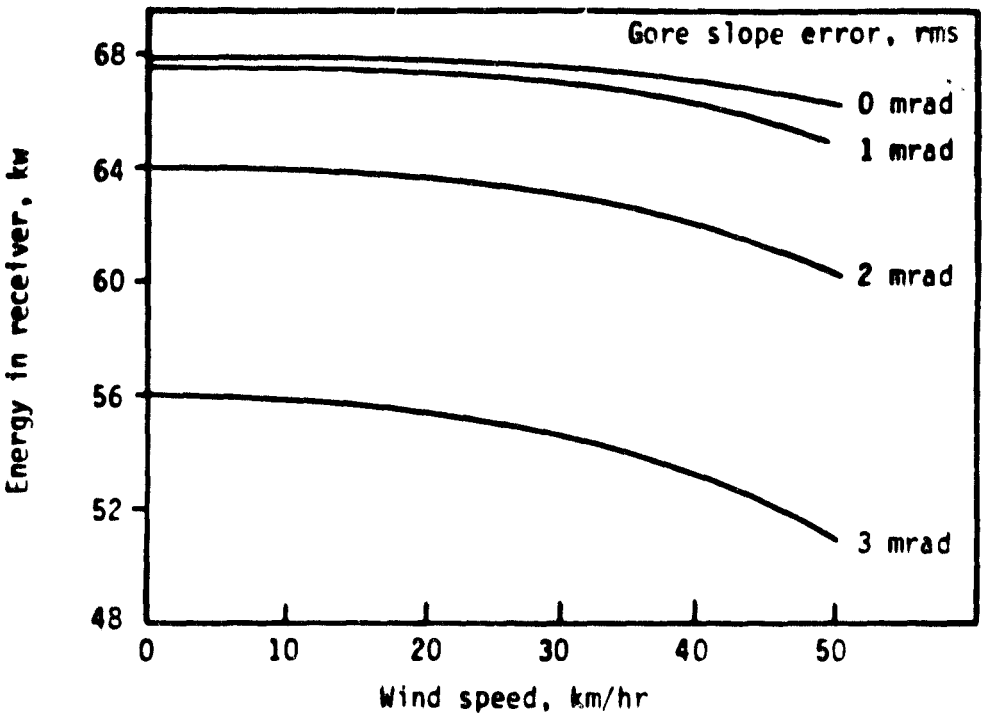

AE/A-371

Figure 3-18. Effects of Wind Speed and Gore Slope Error Upon Collector Performance

5 percent for the 1.0-mrad gore whereas it is roughly 10 percent for a 3.0-mrad gore. Reductions in gore manufacturing slope error below the 1.0-mrad point can also be seen to be of little benefit.

Figure 3-19 presents the performance sensitivity of the concentrator to pointing error. As can be seen from the figure, less than 1 percent of the energy is lost due to pointing errors below the 1.75-mrad specified value. Pointing error becomes a significant factor at values much beyond this point, however.

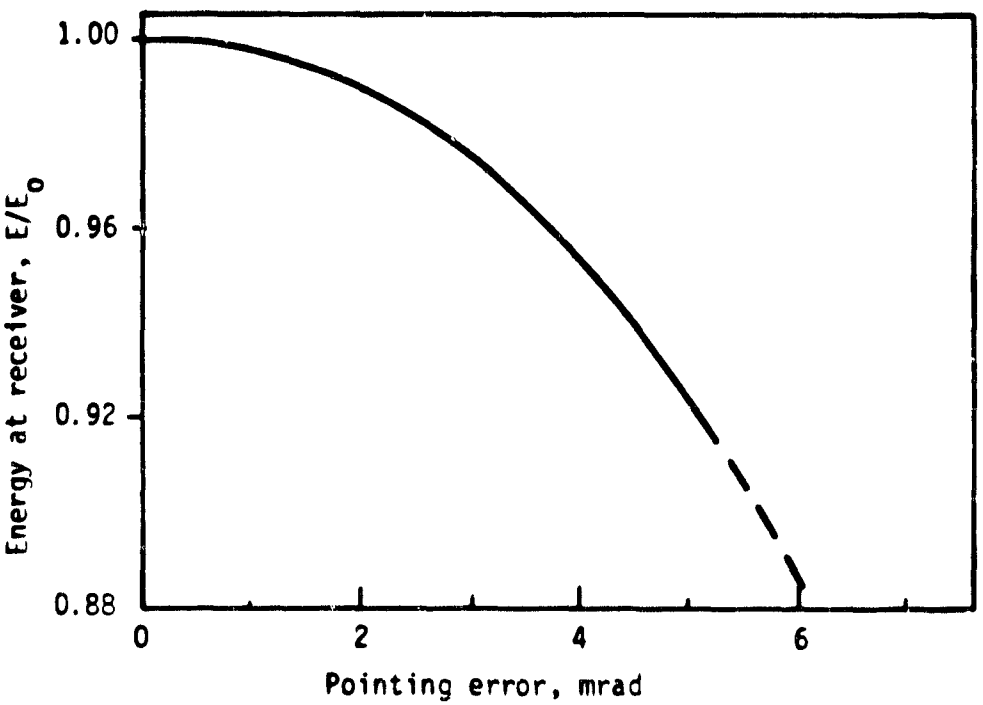

Figure 3-19. Concentrator Sensitivity to Pointing Errors

REFERENCES

1. Giovan, M. and Adams, M., "Evaluation of Cellular Glasses for Solar Mirror Panel Applications," JPL Publication 79-61, June 1979.

2. Moore, D., "A Method for Determining the Thickness of Glass in Solar Collector Panels," JPL Report 80-34.

3. Levy, R. and Kurty, D., "Compilation of Wind Tunnel Coefficients for Parabolic Reflectors," JPL Publication 78-16, April 15, 1978.

4. Author unknown, "Load Distribution on the Surface of Paraboloidal Reflector Antenna," JPL CP-4.

5. "The Cost of Energy from Utility-Owned Solar Electric Systems -- A Required Methodology for ERDA/EPRI Evaluations," ERDA/JPL-1012-76/3.

6. "Grether, D. and Hunt, A., "Description of the LBL Reduced Data Base and Standard Profiles," Lawrence Berkeley Laboratory, August 9, 1977.

7. Biggs, F. and Vittitoe, C., "The Helios Model for the Optical Behavior of Reflecting Solar Concentrators," Sandia Laboratories, March 1979.

8. Pettit, R. and Butler, B., "Laser Ray Trace and Bi-directional Reflectometry Measurements of Various Solar Concentrators," Proceedings of the ERDA Conference on Concentrating Solar Collectors, Georgia Institute of Technology, September 26-28, 1977.

9. Shrenk, G., "The Role of Simulation in the Development of Solar-Thermal Energy Conversion Systems," Proceedings of the ERDA Conference on Concentrating Solar Collectors, Georgia Institute of Technology, September 26-28, 1977.

10. Biggs, F., Vittotoe, C., and Lighthill, R., "HELIOS: A Computer Program for Modeling the Solar Thermal Test Facility," Third Ed., Sandia Laboratories, October 1978.

APPENDIX A

DESIGN REQUIREMENTS, SPECIFICATION AND DEFINITION FOR A POINT FOCUSING ADVANCED SOLAR CONCENTRATOR

EXHIBIT I.

Design Requirements, Specification and Definition for a Point Focusing Advanced Solar Concentrator

1.0 SCOPE

This document covers the design requirements and definitions of terms for a Point Focusing Paraboloidal Concentrator of the Advanced Solar Thermal Technology Project of JPL. The aperture diameter of this Concentrator is about 10 meters and has a focal length to aperture diameter ratio (F/D) of 0.6. The Concentrator, to be combined with a receiver/power conversion package to form a power generation module, has the following general requirements.

(1) Reasonable net thermal power in the receiver per unit module cost.

(2) Thirty year module operational lifetime.

(3) Adaptable for low cost mass production.

(4) Survive wide environmental extremes.

(5) High reliability.

(6) Remotely monitoring with emergency system shutdown capability.

2.0 APPLICABLE DOCUMENTS

The design shall comply with the Industry Standard and Federal Specifications indicated in the technical sections of the specifications and the latest issues of the codes as listed below. In case of conflicting requirements between that contained in the Exhibits and requirements contained in these codes, the Exhibits' requirements shall take precedence.

(1) International Conference of Building Officials - Uniform Building Code - 1976.

(2) American Institute of Steel Construction - Specifications for the Design, Fabrication and Erection of Structural Steel for Building.

(3) The Aluminum Association - Aluminum Construction Manual, Specification for Aluminum Structures.

(4) National Electrical Code - 1978.

(5) American Concrete Institute ACI 310-63 Building Code Requirements for Reinforced Concrete.

(6) American Welding Society Standard Code for Arc and Gas Welding in Building Construction.

(7) Electronic Industries Association RS 195A and RS 222B.

(8) Safety Regulations - California Occupational Safety and Health Administration.

3.0 JPL ADVANCED SOLAR CONCENTRATOR CONCEPT DESCRIPTION

The JPL conceptual design of a point focusing, two axes tracking solar concentrator is shown in Fig. 2 and is described and defined as consisting of:

A. A reflector assembly, composed of the following four components:

1. The concentrator surface, consisting of two groups of independent, optical quality reflective elements forming a physically discontinuous paraboloidal reflective surface with a common focal point. The aperture diameter of the JPL concept is 12 meters and has a focal length to aperture diameter ratio F/D value of 0.6. Each reflective element or gore is designed to be fabricated of thin, backsilvered glass mirror bonded continuously to a contoured substrate of cellular glass with the following specific physical properties:

a) Cellular glass substrate

Flexural-strength (Uniaxial tensile fast fracture strength)	1.03×10^6 Newton/meter^2
Density	240 kg/meter^3
Young's modulus (E)	2.2×10^9 Newton/meter^2
Shear modulus (G)	0.94×10^9 Newton/meter^2
Poisson's Ratio (ν)	0.18

b) Backsilvered glass mirror (with wet chemical silvering process)

Glass type	Fusion glass, Corning 0317
Thickness	0.15 cm
Average total hemispherical reflectance	0.94 ±0.01

These reflective elements are installed on a circular, or polygonal support ring, each with a statically determinant three-point attachment, with sufficient degrees of freedom adjustment capability for fine tuning the composite surface geometry.

2. This circular support ring, with the diameter of 0.6D, is of steel truss construction. The cross section of the circular support ring is an equilateral triangle with a maximum side dimension of 0.096D. The circular support ring forms not only the interface structure for the reflector surface, but also provides interface attachments for the following:

a) Receiver support structure,

b) The elevation drive mechanism and bearings, and

c) The counterweight support structure.

3. A pair of counterweights and their support structure

4. A receiver/power conversion package support structure (the quadripod)

B. A reflector mount capable of articulating the reflector about two axes (azimuth and elevation) for the tracking of the sun, is in the form of a tilted pyramid. It serves as an intermediate structure between the reflector assembly and the pedestal. It is pivoted near its apex, about the azimuth axis at the top of the pedestal. Thrust loads are transmitted at that point to the pedestal through thrust bearings, and through wheels at the two lower corners of the pyramid. The reflector is also pivoted, in elevation, about the two upper corners. Azimuth drive is by means of a cable and drum attached to one of the two wheels and at the base of the pedestal. The elevation drive is accomplished by means of a jack attached between the apex of the intermediate structure and a hard point on the reflector assembly.

C. A pedestal structure in the form of a tripod is constructed of large steel pipes. It provides a fixed axis about which the reflector assembly and the reflector mount are pivoted as a unit, and to react a portion of the thrust load acting on the reflector and its mount.

D. A foundation or pad, on which all of the aforementioned concentrator equipment is installed, provides a stable support for the concentrator.

E. A control system consisting of a group of sun sensors, drive mechanism and control algorithms has the capability of providing the concentrator with accurate sun tracking. It is intended that the specific control system design be tailored for installation at the JPL-PFSTS at Edwards. However, the design would be easily adaptable for mass production and for implementation in a large field of concentrators. Two control system philosophies are presented in Appendix A.

4.0 FUNCTIONAL REQUIREMENTS OF THE ADVANCED CONCENTRATOR

The following are requirements for the advanced solar concentrator design. The concentrator shall, as a minimum, be designed for withstanding the conditions and requirements as stated herein and shall be designed to the listed Codes and Standards as applicable. These functional requirements shall be satisfied based on the mirror glass surface properties and the material properties of the cellular glass as stated in 3.0A above (or as updated by the cellular glass property information supplied by JPL at the commencement of this contract) and the receiver/power conversion package

physical properties as defined in 4.0 A.3 below. Other type of cellular glass may be used for the optimization to reduce the mass of the gores and to meet the prescribed functional requirement. The slow crack growth characteristics of the cellular glass being used for the design shall be considered. Dynamic loading due to the receiver/power conversion package's operation may be assumed small compared to the wind and gravity loadings. Wind pressure distribution over the surface of the paraboloid may be derived from Exhibit II entitled "Load Distributions on the Surface of Paraboloidal Reflector Antenna."

A. General Requirements

1. The concentrator design shall be representative of the Industry's current state-of-the-art for low cost fabrication of equipment of this type and shall be adaptable for fabrication on mass production basis. Steps shall be taken in the design to minimize hazards to personnel and property nearby.

2. The concentrator design shall have an aperture diameter of about 10 meters with a F/D ratio of 0.6. This design shall be derived from JPL's conceptual design as described in Section 3.0.

3. The concentrator design shall have provision for mounting a receiver/power conversion package with its receiver aperture located nominally at the reflector focal plane. The mounting interface configuration is shown in Fig. 3 of Exhibit I.

   The receiver/power conversion package support structure shall be designed to support a 1350 kg package 1.0 meter in diameter and 1.2 meters in length as shown in Fig. 3. The center of mass is located at about 0.6 meters aft of the receiver aperture along the center line of the package. The configuration of the support structure shall be selected with consideration to minimize the shadow on the reflector surface, blockage of the receiver aperture and away from high flux region while keeping the receiver interface deformation small.

4. The solar radiation intercepted by this 10 meter diameter concentrator aperture normal to the solar flux shall be delivered to a 22 cm diameter receiver aperture located at the focal plane with a minimum intercepted solar power value of 56 kW under the following conditions:

   (i) Direct normal insolation level of 845 watts/m^2 (assumed, average cloud free insolation level)

   (ii) Steady state winds of 50 kmph measured 10 meters above ground level with a 20% step function gust factor from any direction.

   (iii) Temperature range of -18°C to 50°C

   (iv) Clean reflector surface

5. The concentrator shall survive without damage in slewing to the stow position from any achievable attitude when subjected to 80 kmph winds measured 10 meters above ground level from any direction, and at temperature range of -18°C to 50°C under the blowing California desert dust and sand conditions.

6. The concentrator shall further survive without any damage which would impair its function in all succeeding operations, after being stowed under the same environment as in 5 above but with a 120 kmph wind from any direction. However, failure of less than 5% of the reflective gores is acceptable with the gores under this 120 kmph wind speed loading condition for a total accumulative time of 360 minutes.

7. The concentrator shall be capable of surviving, with no damage or permanent set, a seismic lateral acceleration of 0.25 g in any direction combined with 1.0 g gravity loading with the concentrator in any position.

8. The concentrator shall be capable of surviving in any position with no damage or permanent set under the following precipitation environment:

   Rain - 6.5 cm for 24 hour period

   Hail - size of 1.0 cm diameter
   - Mohs scale of hardness of 2
   - Wind speed 23 kmph
   - Air temperature 10°C

   Sleet - 1.0 cm thick ice blanket

   Snow - 15 cm thick with specific gravity of 0.125

   Freezing and Thawing - (71 cycles in 1976)

   Humidity - 0 to 100%

9. The concentrator design shall not have any limitation that may have impact on the 30 years life expectancy.

10. The concentrator shall be provided with lightning protection.

11. The concentrator shall have the capability for the installation, removal and servicing of the receiver/power conversion package conveniently and safely.

12. Annual average parasitic power consumption required to operate the concentrator module shall be less than 100 watts. No motor/drive mechanism power consumption such as powered brakes shall be allowed while the concentrator is kept in the stowed configurations.

13. Individual mirrored cellular glass gores shall be easily and safely replaced and adjusted or aligned, but shall not require adjustment after installation.

14. Failure of one component of the concentrator shall not precipitate other failures. However, failure of critical elements should actuate a signal to the remote monitoring station.

15. Reliability shall be such that the concentrator has high availability during the daytime exclusive of down time due to scheduled maintenance, cloudy conditions, high wind over 50 kmph and other external interruptions or conditions.

16. Concentrator design shall be such that loss of power supply to operate the module does not result in damage to the concentrator and the receiver/power conversion package.

B. Specific Requirements for Tracking Mechanism and Control Design

The concentrator shall be capable of two axis automatic tracking of the sun using a sun sensor and shall also be capable of following the sun's position during cloudy conditions and morning sun acquisition. State-of-the-art design with low cost, low maintenance and mass producible component hardware are to be used to meet the requirements.

The specific reauirements and tolerance are:

1. Azimuth (AZ) travel from South shall be $\pm 120^{\circ}$ as shown in Fig. 2.

2. Elevation (EL) travel shall be between -25° to 82° as shown in Fig. 2.

3. The solar tracking error or the offset between the Concentrator's Line of Sight (LOS) and the center of the sun's disc shall not exceed 0.1 degrees for normal operating conditions in steady state winds of 50 kmph.

4. The control system transient response shall be such that the tracking error will return to within 0.1 degree in less than 20 seconds from the onset of a 20% gust condition.

5. The control system shall be able to track automatically to within 1 degree of the sun's expected position during cloudy or overcast conditions using azimuth/elevation positional feedback. The control system shall have an automatic sun reacquisition capability following a condition of sun obstruction or concentrator shutdown. This reacquisition capability will be such that no hazard to personnel will exist and that no short term major damage to the structure will occur.

6. The slew rate for each of the azimuth and elevation axes shall be 400 deg/hr or greater. But, the angular acceleration shall be such that no damage shall be sustained by the concentrator module.

7. The control system with automatic compensation feature for the 1-g deflections of the receiver interface at all elevation positions may be required if it is proven to be cost effective for the receiver/power conversion package mass given in section 4.0A.3.

8. The control system shall have the capability of accepting AZ/EL pointing biases of 0.05 degree increments, or smaller, for alignment purposes.

9. The control system shall have emergency shutdown capability.

10. The control system shall have the capability to position the reflector to the stowed configuration in 80 kmph wind velocity using the slew rate.

11. The control system shall be capable of accepting override commands, and be capable of sending operational data to the remote site. The remote site uses state-of-the-art digital acquisition and command components utilizing a RS232 interface/ 2400 band link and hard wired capability.

C. Specific Requirements for Mirrored Cellular Glass Gore Design

The mirrored cellular glass gore of the paraboloidal reflective surface is one of the major components of the concentrator. Its optical and structural performance to meet certain requirements are of utmost importance for the success of the concentrator module. The following is a listing of the design requirements.

1. Geometric Specifications

   i) The rms slope error of the mirror surface shall be less than or equal to 3 mrad.

2. Optical Specifications

   i) The solar spectrum average total hemispherical reflectance of the mirror surface shall be 0.94 ±0.01.

   ii) A minimum of 99% of the reflected solar energy shall be directed into an aperture of half angle of 18 mrad.

3. Structural Specifications

   i) The mirror glass must be continuously bonded to the cellular glass substrate.

ii) The gore design shall conform to the support boundary conditions described in Fig. 1.

iii) The gore design shall limit the angular rotation at any point on the mirror surface to be less than 4×10^{-4} radians when the gore is supported as specified in Fig. 1 and subjected to uniform pressure of 385 Newton/m^2 over the mirror surface.

4. Weight Specifications

i) The mass of one (1) mirrored cellular glass gore with attachment shall not exceed 55 kg.

5. Environmental Durability Requirements

i) Optical requirements

a) The mirrored glass gore shall survive 24 cycles in the following temperature/humidity environment with less than 10% degradation in optical properties:

1) 4 hours at 50°C maximum temperature

2) 2 hours transient to minimum temperature

3) 4 hours at -12°C minimum temperature

4) 3 hours transient to medium high temperature

5) 3 hours at 25°C medium high temperature

6) 2 hours transient to medium low temperature

7) 4 hours at 5°C medium low temperature

8) 2 hours transient to maximum temperature

9) Relative humidity shall be maintained constant at 75% during cycling

ii) Strength requirements

a) For a period of one (1) week the cellular glass gore must withstand a uniform pressure of 1200 Newton/meter^2 uniformly distributed over the surface when supported by the defined statically determinant points (Fig. 1) and maintained at 50°C and 50% relative humidity.

b) The gore design must survive pressure loading corresponding to 2395 Newton/m^2 uniformly distributed over the whole mirror surface when supported as described in Fig. 1.

c) The gore design must also survive, when supported as described in Fig. 1, a linearly varied pressure loading of 880 Newton/m^2 to 1390 Newton/m^2 (i.e. 1135 ± 255 N/m^2) across the face of the gore in the θ direction but uniformly distributed along the length of the gore.

D. Other Requirements

1. Cable Routing

Provision must be made for routing a minimum of 25 sq. cm of instrumentation and power output cables along each leg of the quadripod from the receiver interface through the intermediate structure to the power processing interface at the pedestal of the concentrator. While these cables are JPL's responsibility, it is desirable to provide protected cableways as an integral part of the support structures.

2. Reflective Element Attachment

The thermal gradients between the reflective element and the support ring structure to which they are mounted are to be minimized.

3. Birds and Wildlife

The concentrator shall be designed to deter detrimental habitation of wildlife. Its reflective surface shall be resistant to degradation by bird drops while being readily cleanable.

E. Soil Properties

The soil properties shall be those of the typical California desert, fine to coarse, silty sand.

F. Electrical Requirements

1. Power Supply

The concentrator shall operate using 110/208 volt 3-phase AC electrical power supplies

2. Power Output Receptacle

Provision must be made for power output cable receptacle at the receiver/concentrator mechanical and electrical interface as shown in Fig. 3. Type of receptacle used in the design shall be compatible with that of the receivers.

5.0 DEFINITION OF TERMS

A. Point Focusing Advanced Solar Concentrator

The Point Focusing Advanced Solar Concentrator is an example of a single reflection point focus design, which concentrates the solar energy upon a receiver's circular aperture located at the reflector focal plane. The concentrator includes the reflector, a two axis elevation-azimuth system driven automatically by a solar tracking sensor and control system, a quadripod structure to support the receiver/power conversion package at the focal point, an intermediate structure, a pedestal and a foundation.

B. Solar Tracker

The Solar Tracker is a system which maintains the beam reflected energy within the receiver aperture. The Solar Tracker is comprised of the sensor(s), a two-axis gimbal drive system, and a controller.

C. Receiver/Power Conversion Package

The package is JPL supplied hardware. It is comprised of two subsystems:

1. The Receiver subsystem is an absorptive cavity surface which converts the concentrated solar energy passing through the cavity aperture into a usable energy form and conducts it via a heat transfer system to the Power Conversion Subsystem.

2. The Power Conversion subsystem includes all the components needed to convert the thermal energy to electrical power and condition the power as required.

D. Solar Tracking Error

The Solar Tracking Error is the angular offset of the centerline of the energy beam from the center of the receiver aperture. It arises from any sensor misalignments, the solar tracker control offsets and hysteresis, and receiver support structural deflections as the Concentrator changes its orientation while tracking the sun.

E. Parasitic Power Consumption

Parasitic Power Consumption is the power required by the control and drive mechanism for the pointing of the concentrator and all power uses other than the generation of electricity (such as navigation safety lights).

F. Concentrator Stowed Position(s)

The stowed position of the concentrator shall be that position in which the concentrator is stowed when not in operation. The position(s) may be chosen to ease the burden of meeting environmental requirements such as wind loading and dust accumulation on the reflector surface.

G. Surface Properties

The surface properties are a measure of the basic reflection optical properties of the reflective surface. The energy striking the surface is reflected with both specular and diffuse components. The surface properties can be specified as a plot of the fraction of the incident energy which is reflected within a cone, with a half angle $\Delta\omega/2$, centered on the pure specular (angle of reflection = angle of incidence) component.

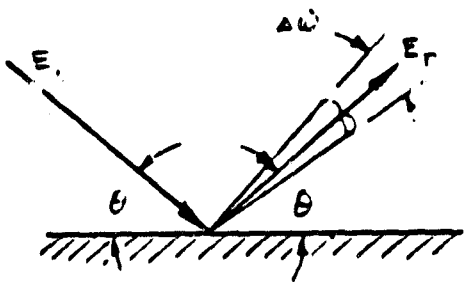

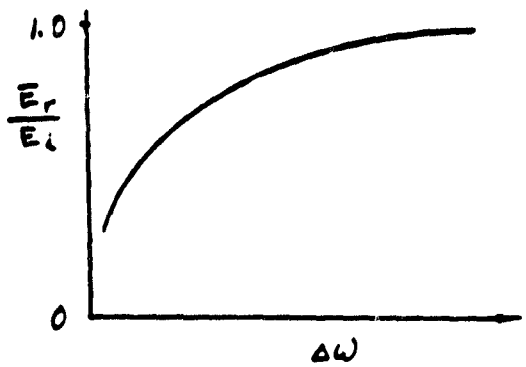

The microroughness inherent with the reflective surface is included in this factor E_r/E_i.

H. Surface Error

The surface error is a composite function which results from the surface slope and location variations due to manufacture, alignment, and structural deflections. The surface error is measured as the average deviation of the reflected energy from the nominal path of the ray (which would pass through the reflector focal point) is reflected from a perfectly specular surface which has no contour or position errors. The path deviations are caused by macroroughness (due to manufacturing methods), subassembly manufacturing errors, installation misalignments and distortions, and structural deflections (due to external forces).

The slope error is a local slope deviation from the slope expected from a theoretical design surface.

I. kmph

kmph is the metric unit for the wind speed measured in kilometer per hour.

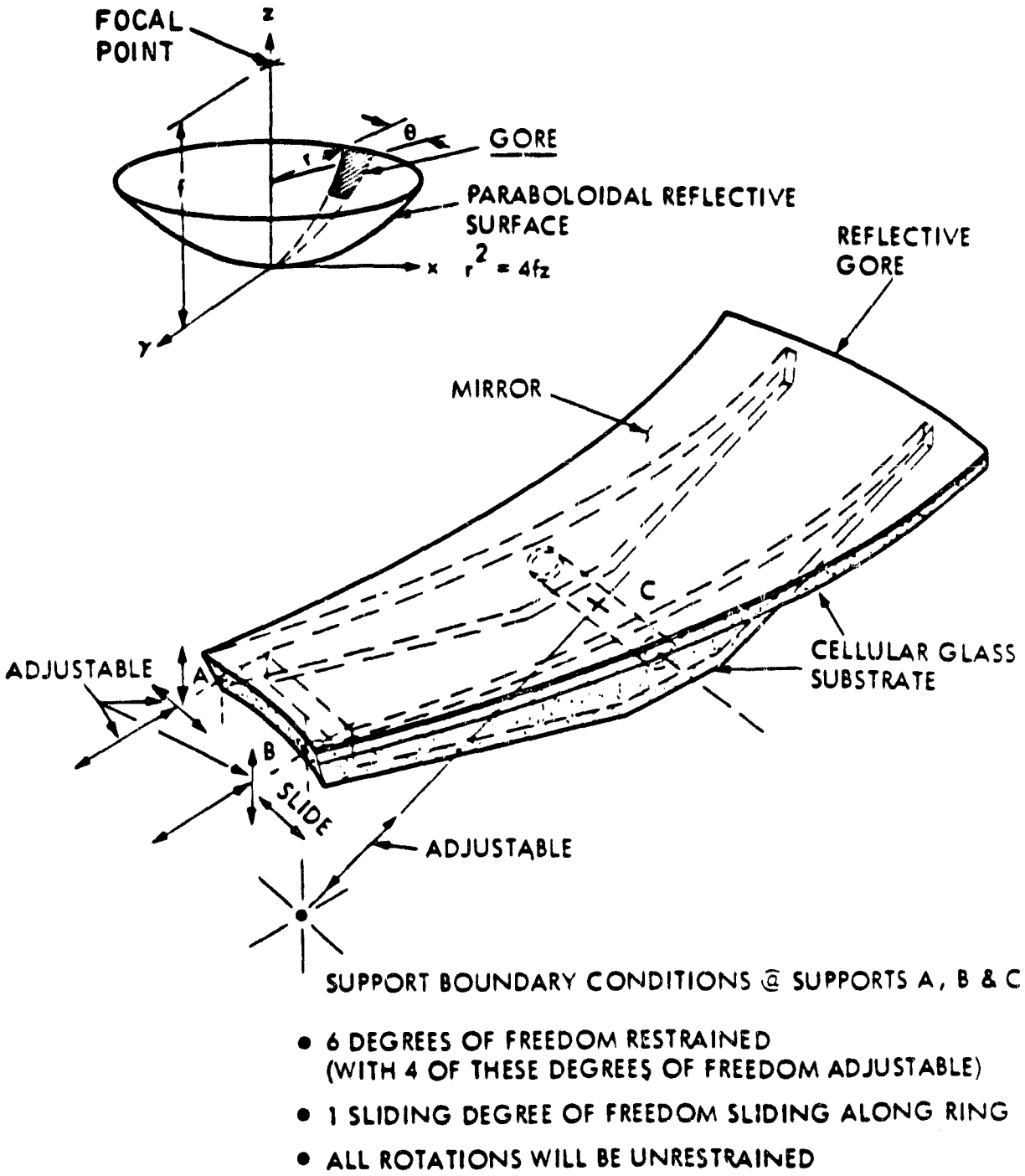

Figure 1. Mirrored Cellular Glass Gore and the Support Boundary Conditions

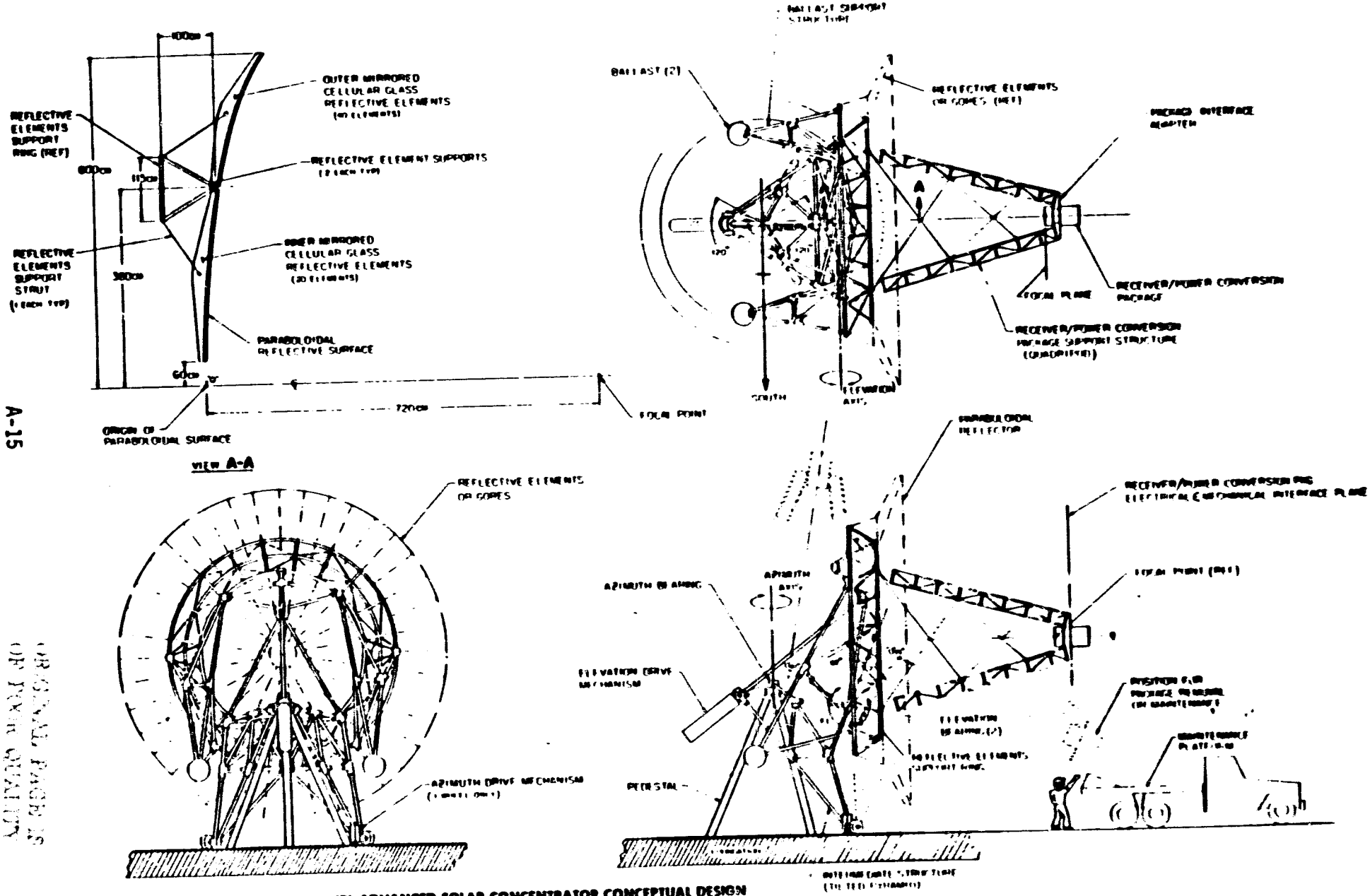

FIG 2. JPL ADVANCED SOLAR CONCENTRATOR CONCEPTUAL DESIGN

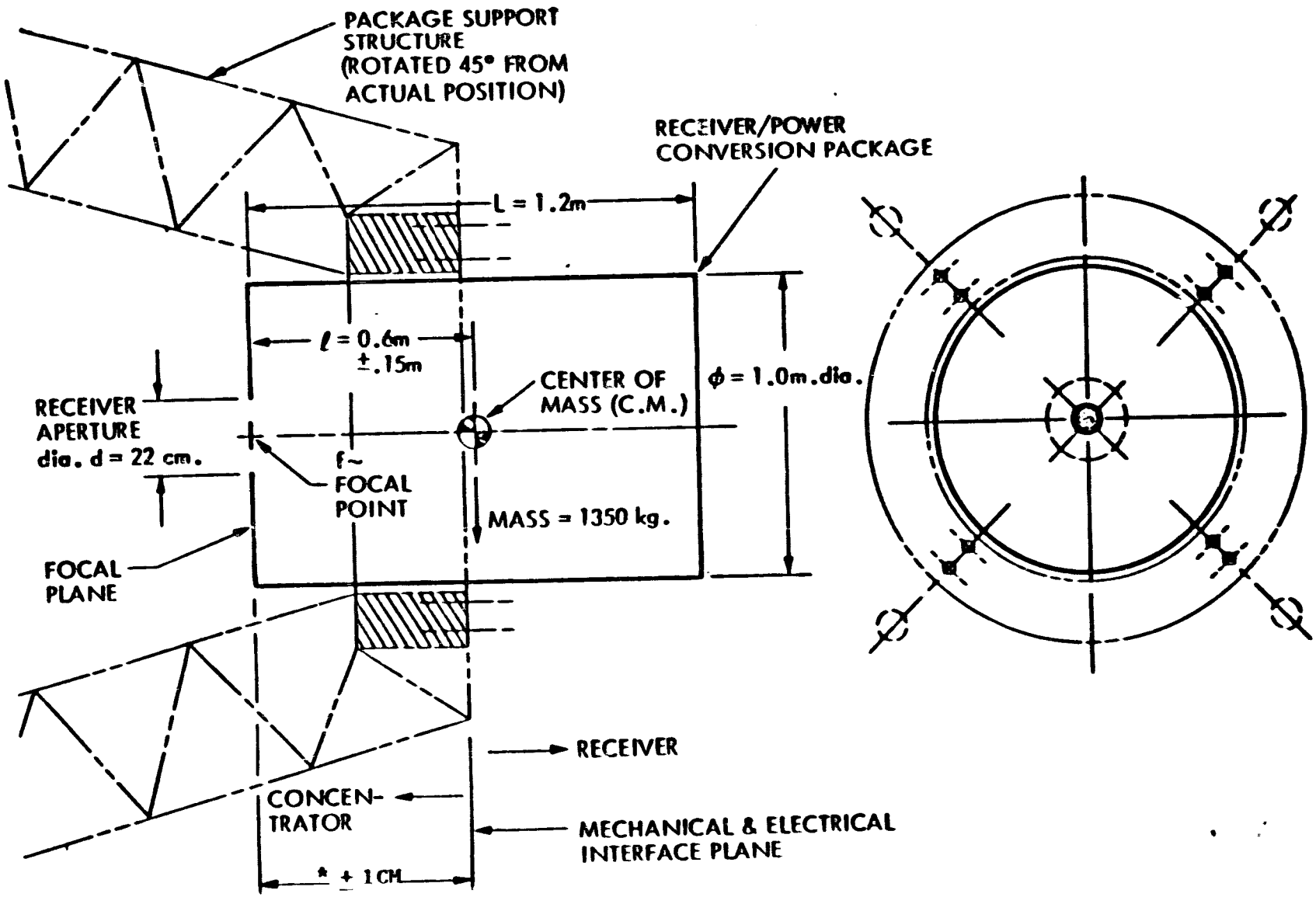

Figure 3. Receiver/Power Conversion Package Physical Properties And Interface Definition with Concentrator

*Adjustment Capability on the Concentrator Side

APPENDIX B

PRELIMINARY DESIGN BASIS AND REQUIREMENTS FOR AN ADVANCED POINT-FOCUSING SOLAR CONCENTRATOR (ACUREX SPECIFICATION NUMBER S-7740-01, REVISION A)

PRELIMINARY DESIGN BASIS AND REQUIREMENTS FOR AN ADVANCED POINT-FOCUSING SOLAR CONCENTRATOR

Specification No. S-7740-01

Revision A

Prepared for

THE JET PROPULSION LABORATORY
SOLAR THERMAL TECHNOLOGY PROJECT

PRELIMINARY

September, 1980

Acurex Corporation

TABLE OF CONTENTS

TABLE OF CONTENTS (Continued)

TABLE OF CONTENTS (Concluded)

1. SCOPE

This specification establishes the design requirements and definitions of terms for an Advanced Point-Focusing Solar Concentrator for the Advanced Solar Thermal Technology project of the Jet Propulsion Laboratory. The concentrator, to be combined with a receiver/power conversion package to form a power generation module, has the following general requirements.

1. Reasonable net thermal power in the receiver per unit module cost
2. Thirty-year module operational lifetime
3. Adaptable for low-cost mass production
4. Survive wide environmental extremes
5. High reliability
6. Remote monitoring with emergency shutdown capability

2. APPLICABLE DOCUMENTS

The following documents apply to the design of the Advanced Concentrator. Unless otherwise specified, any conflicts among the related documents shall be resolved by superceding documents in the following order:

1. This specification number S-7740-01 -- Supersedes JPL's Exhibit I and implements the sense of its requirements
2. Safety Regulations -- California Occupational Safety and Health Administration
3. International Conference of Building Officials -- Uniform Building Code -- 1976
4. National Electrical Code -- 1978
5. National Fire Protection Agency No 78, 1968

6. American Institute of Steel Construction -- Specifications for the Design, Fabrication and Erection of Structural Steel for Building
7. American Concrete Institute ACI 310-63 Building Code Requirements for Reinforced Concrete
8. American Welding Society Standard Code for Arc and Gas Welding in Building Construction
9. Electronic Industries Association RS 195A and RS 222B

3. JPL ADVANCED SOLAR CONCENTRATOR CONCEPT DESCRIPTION

The JPL conceptual design is for a single reflection point-focusing, two-axis tracking solar concentrator with an aperture diameter of approximately 11 meters. The concentrator is defined as consisting of the following five subsystems:

- Reflective Surface
- Support Structures
- Drive Subsystem
- Electrical, Instrumentation and Control Subsystem
- Foundation

Figure 3-1 shows the general configuration of the concentrator assembly. A description of each subsystem follows.

3.1 Reflective Surface

The concentrator surface consists of two concentric rings of independent, optical quality reflective elements which form a physically discontinuous paraboloidal reflective surface with a common focal point. Twenty elements make up the inside ring, and forty comprise the outside ring (Figure 3-1). The aperture diameter is approximately 11 meters with a focal length to aperture diameter ratio (F/D) value of 0.6.

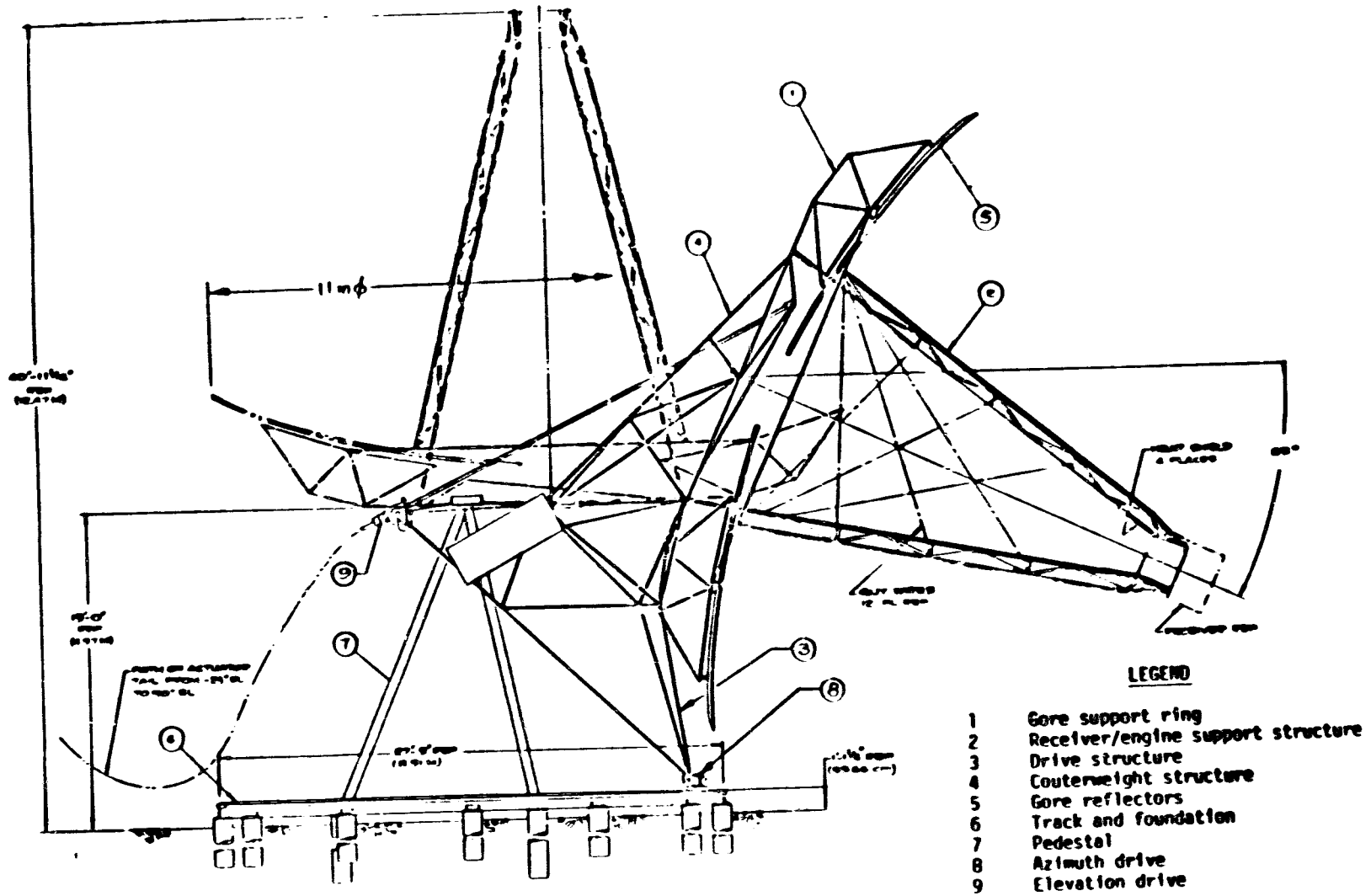

Figure 3-1. JPL Advanced Concentrator description.

Each of the sixty reflective elements are installed on a ring-like gore support structure with statically determinant three-point attachments. These attachments have sufficient degrees of freedom to allow fine tuning of the composite surface geometry and differential/thermal displacements.

Each reflective element, or gore, (Figure 3-2) is fabricated of thin, backsilvered glass mirror bonded continuously to a contoured substrate of cellular glass.

3.2 Support Structure

The support structure subsystem consists of five parts:

- Gore support structure
- Drive support structure
- Counterbalance structure
- Receiver support structure
- Pedestal

These are described below.

3.2.1 Gore Support Structure

The gore support structure is a space frame ring truss made of structural steel. The ring structure provides the structural interface between:

- The reflective gores
- The receiver support structure
- The elevation drive mechanism and bearings
- The counterbalance support structure

3.2.2 Drive Support Structure

The drive support structure serves as an intermediate structure between the reflector assembly and the pedestal. It is pivoted about the

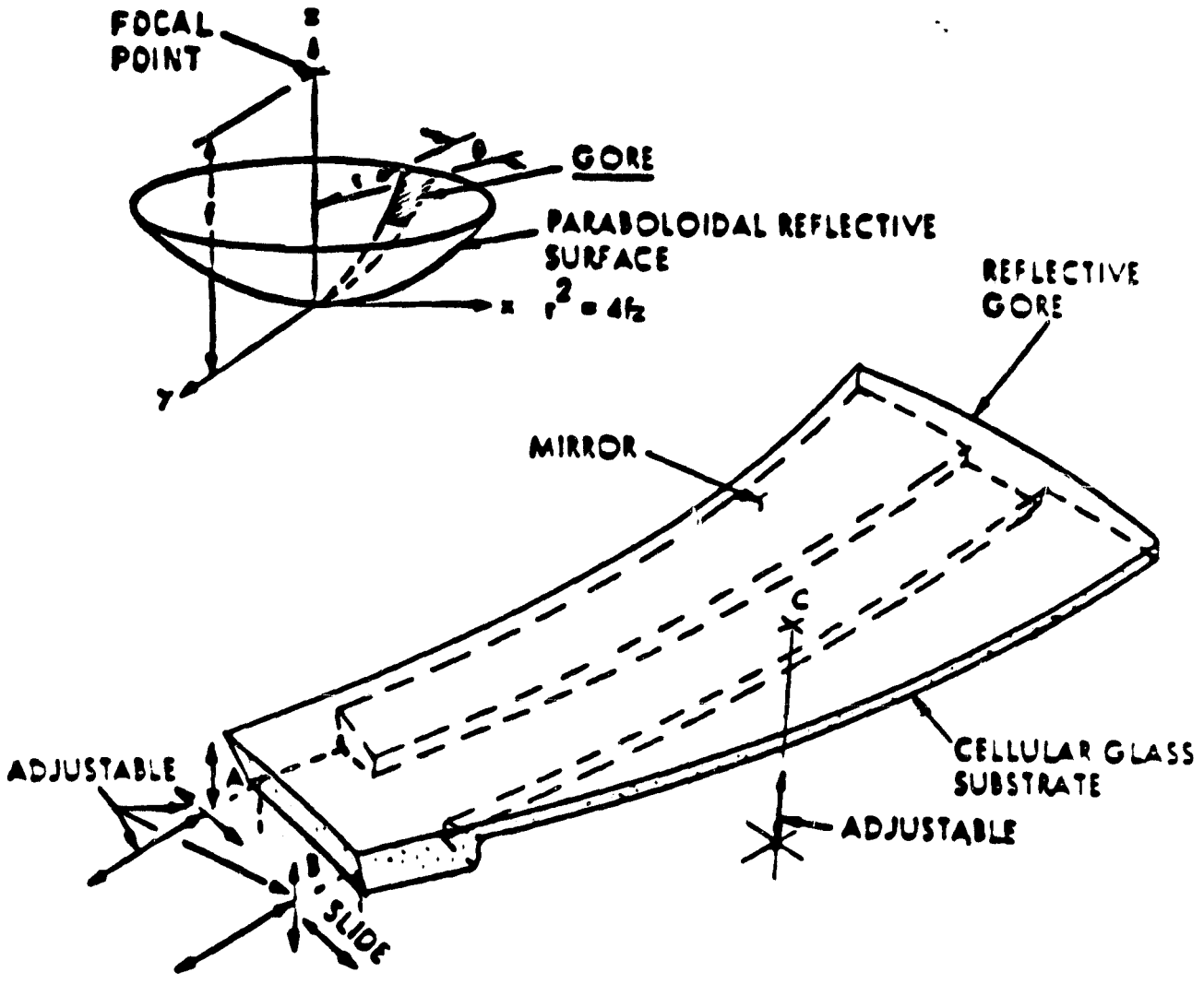

SUPPORT BOUNDARY CONDITIONS @ SUPPORTS A, B & C

- 6 DEGREES OF FREEDOM RESTRAINED (WITH 4 OF THESE DEGREES OF FREEDOM ADJUSTABLE)
- 1 SLIDING DEGREE OF FREEDOM SLIDING ALONG RING
- ALL ROTATIONS WILL BE UNRESTRAINED

Figure 3-2. Mirrored cellular glass gore and the support boundary conditions.

azimuth axis at the top of the pedestal. Thrust loads are transmitted at that point to the pedestal through thrust bearings and through wheels at the two lower corners of the drive support structure. The reflector is also pivoted, in elevation, about the two upper corners of the drive support structure. The elevation drive is mounted to it near the azimuth pivot bearing mount.

3.2.3 Counterbalance Structure

Steel frame counterbalance structures attach to the gore support structure to support counterbalancing components. The counterbalance is sized to approximately balance the receiver/engine/reflector combination to reduce drive loads.

3.2.4 Receiver Support Structure

The receiver support structure is a quadripod formed from four structural steel truss style legs oriented radially and braced with tension elements. The structure is designed to support the JPL receiver/engine package at the focal point of the paraboloidal reflector and is rigidly attached to the gore support structure.

3.2.5 Pedestal

A pedestal structure in the form of a tripod is constructed of structural steel. It provides a fixed axis about which the concentrator assembly is pivoted. It transmits elevation actuator loads and horizontal wind forces to the foundation.

3.3 Drives

The concentrator's tracking motion is divided into rotation about vertical (elevation) and horizontal (azimuth) axes.

3.3.1 Azimuth Drive

Azimuth rotation is provided by a chain stretched around the circumference of the foundation track and a sprocket drive mounted to one of the drive support structure legs. The sprocket winches the concentrator around the foundation track.

3.3.2 Elevation Drive

The elevation rotation is accomplished with a linear actuator mounted between the drive support structure and the gore support structure.

3.4 Electrical, Instrumentation and Control

The electrical system provides power to the tracking system and transmits the output power from the generator to a centralized field power system.

A control system consisting of sun sensors, positional feedback devices, control algorithms, and logic hardware provides input power to the drive subsystem to provide the concentrator with accurate sun tracking. Wind sensors automatically stow the concentrator in high winds, and temperature sensors prevent overheating of the receiver aperture.

3.5 Foundation

The foundation supports the pedestal and the azimuth drive rail. The drive rail is the track on which the drive support structure wheels roll and also serves as a housing for the drive chain.

4. SYSTEM INTERFACE DEFINITION

The Advanced Concentrator shall meet the physical and functional interface requirements defined by the subsystems listed in this section.

4.1 JPL Receiver/Generator (R/G)

4.1.1 Receiver/Generator Configuration

The concentrator shall be designed to support a 1350 Kg (2970 lb) R/G package 1.0 meter (3.28 ft) in diameter and 1.2 meter (3.94 ft) in length as shown in Figure 4-1. The center of mass is located 0.6 ±0.15 meters (1.97 ft) aft of the receiver aperture within 0.15 m (5.90 in) the center line of the R/G package.

4.1.2 Receiver Aperture Diameter

The solar flux produced by the concentrator shall be delivered to a 22 cm (8.66 in) diameter receiver aperture.

4.1.3 Focal Plane Location

at zero wind spped condition the focal plane of the receiver aperture shall be located within ±1 cm (0.39 in.) of the focal distance of the concentrator reflective dish. The center of the receiver aperture shall be concentric with the center line of the concentrator reflective dish within 1 cm radial distance.

4.1.4 Receiver/Generator Mounting

The concentrator design shall have provisions for mounting of the JPL R/G package and adjustment capabilities to locate the focal plane within the tolerances specified in Section 4.1.3. The mounting interface configuration is shown in Figure 4-1.

4.2 Cable Routing and Protection

Protective cableways of 100 cm^2 (15.5 in^2) minimum total cross sectional area, with single conduit size not smaller than 12.5 cm^2, for routing of the instrumentation and power output cables shall be provided from the receiver interface through the intermediate structure to the power processing interface at the pedestal of the concentrator.

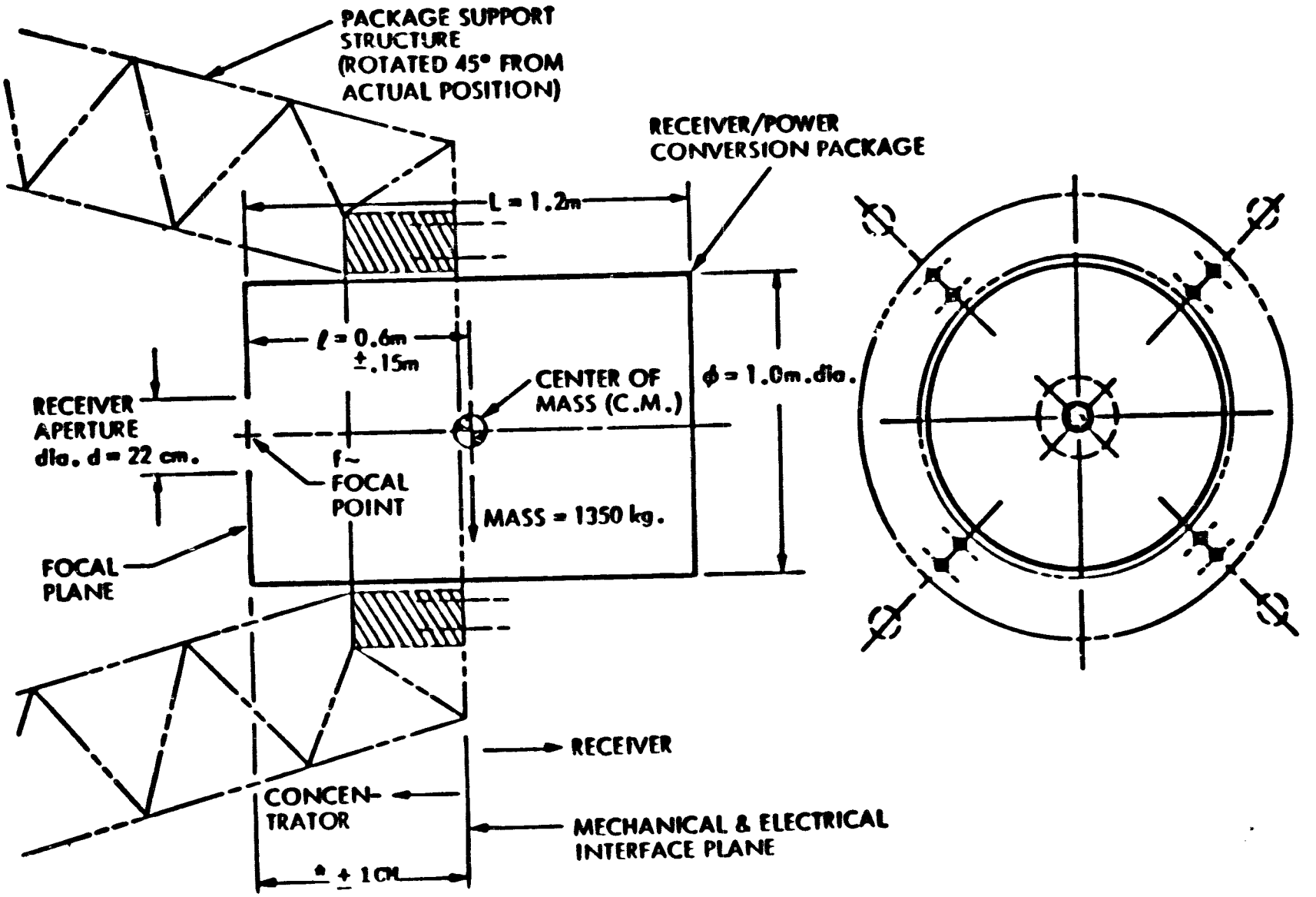

*Adjustment Capability on the Concentrator Side

Figure 4-1. Receiver/power conversion package physical properties and interface definition with concentrator.

Instrumentation cables shall be routed in separate conduits from electrical power cables.

4.3 Control Interfaces

The control inputs and operational data transmission commands shall be compatible with JPL's digital acquisition and command components utilizing an RS 232 interface at a rate of 2400 baud.

5. DESIGN REQUIREMENTS

5.1 Performance Requirements

The solar radiation intercepted by this concentrator shall be delivered to the receiver aperture as specified in Section 4.1.2. A minimum delivered solar power value of 56 kW thermal shall be provided under the following conditions:

1. Direct normal insolation level of 845 Watts/m^2 (assumed, rms width of sunshape distribution of 4.32 mrad)
2. Steady-state winds of 50 kmph (measured at 10 meters above ground level with air density corresponding to standard sea level temperature and pressure)
3. Temperature range of $-18^{o}C$ to $50^{o}C$
4. Clean new reflector surface

5.2 Operational Requirements

The concentrator shall meet the following operational requirements.

5.2.1 Active Tracking

The solar tracking error or the offset between the center of the flux distribution at the focal plane and the center of the receiver aperture shall not exceed 0.1^{o} for normal operating conditions in steady-state winds of 50 kmph.

5.2.2 Synthetic Tracking

The control system shall be able to synthetically track the sun's expected position during cloudy or overcast conditions using azimuth/elevation positional feedback. The synthetic tracking accuracy shall be consistent with the acquisition range of the active tracking components and the response time specified in 5.2.3. The tracking system shall have an automatic sun reacquisition capability following a condition of sun obstruction or concentrator shutdown. This reacquisition capability shall be such that no hazard to personnel and equipment will occur.

5.2.3 Transient Response

The control system transient response shall be such that the tracking error will return to within 0.1^{o} in less than 20 seconds from the onset of a 20 percent step function wind gust with the concentrator in any orientation relative to the wind.

5.2.4 Travel Limits

1. Azimuth (AZ) travel from South shall be $\pm 120^{o}$ minimum
2. Elevation (EL) travel shall be a minimum of -25^{o} to 90^{o}, minimum as shown in Figure 3-1.

5.2.5 Slew Rate

The concentrator shall have an azimuth and elevation slew rate of 400^{o}/hr or greater, but the angular acceleration shall be such that no damage will be sustained by the concentrator.

5.2.6 Stow

In the event of a 50 kmph wind velocity (measured 10 meters above ground level), the concentrator shall assume a zenith pointing stowed configuration using the slew rate defined in Section 5.2.5.

5.2.7 Retire

The concentrator shall automatically assume a "retire" position at the end of the operating day. In the "retire" position, no part of the concentrator nor the surroundings shall be exposed to damaging concentrations of reflected energy when the sun is at any position.

5.2.8 Desteer

A The concentrator shall assume and maintain a desteered position in the event of a receiver overtemperature condition. The desteer position shall locate the off-axis "fireball" in a safe position between the receiver support legs, the guy wires, and the receiver itself.

5.2.9 Override Commands

The concentrator shall be capable of accepting override commands, originated from a central control station. However, these commands shall not override the other automatic safety features.

5.2.10 Emergency Shutdown

The concentrator shall have emergency shutdown capapbilities which will protect/prevent personnel, equipment and/or the concentrator from further damage.

5.3 General Requirements

5.3.1 Physical Characteristics

The point-focusing solar concentrator shall have the following physical characteristics

- Include two shapes of reflective gores made of cellular glass substrate with backsilvered glass mirrors for reflective surfaces
- The reflective gores shall be arranged in two concentric segmented rings

- The reflective parabolic dish shall have an F/D ratio of 0.6
- The reflective gore support structure shall be of a steel truss construction
- Elevation and azimuth drives shall be a combination of devices and mechanisms which give the most cost-effective performance
- The outside diameter of the collector dish aperture shall be about 11 meters

5.3.2 Gore Replacement and Adjustment

Individual mirrored cellular glass gores shall be easily and safely replaced and adjusted or aligned, but shall not require adjustment after installation.

5.3.3 Component Failure

Failure of one component of the concentrator shall not precipitate other failures. Failure of critical elements shall actuate a signal to the remote monitoring station, or take automatic corrective action to prevent further equipment damage.

5.3.4 Power Consumption

Annual average parasitic power consumption required to operate the concentrator module shall be less than 100 Watts based on a 24 hr day. Powered brakes or drive mechanisms requiring power shall not be used to hold the concentrator in a fixed position.

5.3.5 Birds and Wildlife

The concentrator shall be designed to deter detrimental effects from wildlife. Its reflective surface shall be resistant to degradation by bird droppings while being readily cleanable.

5.3.6 Design Life

The concentrator shall be designed to have a normal operating life of 30 years.

5.4 Environmental Requirements

The concentrator shall operate and survive in the following adverse environmental conditions as specified.

5.4.1 Wind

5.4.1.1 Slewing to Stow Position

The concentrator shall survive without damage in slewing to the stow position from any attitude when subjected to an 80 kmph (air density corresponding to Standard Atmospheric Condition) wind from any direction measured at 10 meters above ground level and at a temperature range of $-18^{o}C$ to $50^{o}C$ under the blowing California desert dust and sand conditions.

5.4.1.2 In Stow Position

When in the stowed configuration, the concentrator shall further survive without any damage (except the acceptable failure limits specified in Section 5.4.1.3) which would impair its function in all succeeding operations, a 120 kmph wind from any azimuth direction (all other conditions similar to Section 5.4.1.1).

5.4.1.3 Acceptable Failure Limits

Failure of less than 5 percent of the reflective gores is acceptable when the concentrator is subjected to the conditions of Section 5.4.1.2) for a total accumulative time of 360 minutes.

5.4.2 Temperature

5.4.2.1 Extreme Operating and Storage Temperatures

The concentrator shall meet the performance requirements specified in Sections 5.1 and 5.2 when subjected to the temperature range of -18°C to 50°C and up to 100 percent relative humidity.

5.4.2.2 Freezing and Thawing

The concentrator and its components shall survive and operate after withstanding 71 freeze thaw cycles of between -18°C to 50°C and up to 100 percent humidity.

5.4.3 Precipitation

The concentrator shall be capable of surviving in any position with no damage under the following precipitation environments:

1. Rain -- 6.5 cm within 24-hour period
2. Hail -- size of 1.0 cm diameter
   -- Mohs scale of hardness of 2
   -- Coincident wind speed of 23 kmph
   -- Air temperature 10°C
3. Sleet -- 1.0 cm thick ice blanket
4. Snow -- 15 cm thick with specific gravity of 0.125

5.4.4 Seismic

The concentrator shall be capable of surviving, with no damage, a seismic lateral acceleration of 0.25 g in any direction combined with 1.0 g gravity loading with the concentrator in any position.

5.5 Design and Construction

The fabrication and construction, materials, equipment, and completed system shall comply with the industrial standards and Federal Specifications listed in Section 2. The reflective elements shall be fabricated of

backsilvered glass mirrors bonded continously to a contoured substrate of cellular glass with specific physical properties detailed in Section 6. Supporting structural members and drive components shall be adaptable for fabrication on a mass production basis. The concentrator components design shall be representative of the industry's current state- of-the-art for low-cost fabrication. Steps shall be taken in the design to minimize hazards to nearby personnel and property.

6. COMPONENT AND SUBSYSTEM DESIGN REQUIREMENTS

6.1 Specific Requirements for Mirrored Cellular Glass Gore Design

The following is a listing of design specification and performance requirements pertinent to the preliminary design.

6.1.1 Gore Material Specifications

Each reflective element gore shall be designed to incorporate a backsilvered glass mirror surface, continuously bonded to a contoured substrate of cellular glass with the following physical properties:

1. Cellular glass substrate:
   - -- Type: Corning Foamsil® 75
   - -- Uniaxial tensile fast fracture strength (5 percent failure probability): 0.64×10^6 N/m^2 (93 psi)
   - -- Density: 192 kg/m^3 (12 lbs/ft^3)
   - -- Young's modulus (E): 1.5×10^9 N/m^2 (2.2×10^5 psi)
   - -- Shear modulus (G): 0.64×10^9 N/m^2 (9.8×10^4 psi)
2. Backsilvered glass mirror (wet chemical silvering process)
   - -- Glass type: Corning 7809 fusion glass

6.1.2 Geometric Specifications

The rms slope error of the mirror surface shall be less than or equal to 3 mrad.

6.1.3 Optical Specifications

A The solar spectrum average total hemispherical reflectance of the mirror surface shall be 0.94 $\pm$0.01.

6.1.4 Structural Specifications

1. The mirror glass must be continuously bonded to the cellular glass substrate.
2. The gores shall utilize a three-point kinematic support system with support points located as shown in Figure 3-2.
3. The gore design shall limit the angular rotation at any point on the mirror surface to be less than 4×10^{-4} radians, when the gore is supported as specified in paragraph 2 and subjected to a uniform pressure of 385 N/m^2 over the mirror surface.

6.1.5 Environmental Durability Requirements

6.1.5.1 Optical Requirements

The mirrored glass gore shall survive 24 cycles of the following temperature/humidity environments with less than 10 percent degradation in specular reflectance within a half angle of 18 mrad..

1. Four hours at 50°C maximum temperature
2. Two hours transient to -18°C minimum temperature
3. Four hours at -18°C minimum temperature
4. Three hours transient to 25°C medium high temperature
5. Three hours at 25°C medium high temperature
6. Two hours at 5°C medium low temperature
7. Four hours at 5°C medium low temperature

8. Two hours transient to 50°C maximum temperature

9. Relative humidity shall be maintained constant at 75 percent during cycling

6.1.5.2 Strength Requirements

The gore when supported on its three statically determinant support points shall withstand the wind loads imposed under the following conditions with a 5 percent probability of failure for accumulated exposure times consistent with a 30 year operating life:

- Relative humidity of 40 percent
- 50 km/hr winds -- operating
- 60 km/hr wind gusts -- operating
- 80 km/hr winds -- driving to stow
- 110 km/hr winds -- a single "short" exposure
- 120 km/hr winds -- stowed

A

6.2 Structure and Foundation Design Requirements

6.2.1 Design and Construction

Supporting structural members and foundations shall be adaptable for mass production techniques. These components shall be representative of the industry's current state-of-the-art for low-cost fabrication.

6.2.2 Design Safety Factors

6.2.2.1 Structures

The concentrator structures shall be designed to the following safety criteria:

1. Members for which instability is not a design constraint --
   - Factor of safety of 2.0 based on minimum yield strength of material when operational loads are applied

- Minimum factor of safety of 1.5 on yield strength and 2.0 on the ultimate strength of material when worst-case survival loads are applied

2. Members for which instability is the primary design constraint -- stability factor of 3.0 on the critical load calculated by the equation:

$$P_{cr} = \frac{\pi^2 E I}{L^2}$$

where

E = Young's modulus

I = Area moment of inertia

L = Effective length

6.2.2.2 Foundations

The foundation shall be designed to the safety requirements specified in the latest edition of the Uniform Building Code.

6.2.3 Foundation Soil Properties

The foundation shall be designed for, fine to coarse, silty sand with a minimum soil bearing strength of 71.8 kPa (1500 psf) and minimum lateral bearing strength of 7.2 kPa (150 psf) per foot of depth below natural grade. (Type 4 soil in UBC Table 29-B.)

6.2.4 Frost Penetration

The maximum frost penetration shall be 0.91 meters (36 inches).

6.3 Drive System Design

6.3.1 Design and Construction

Drive system components shall be low maintenance and mass producible. These components shall be representative of the industry's current state-of-the-art for low-cost fabrication.

6.3.2 Design Safety Factors

The drive system components shall be designed to meet the safety requirements defined in 6.2.2.1 based on an applied dynamic load factor of 1.25 times the static loads.

6.3.3 Operational Requirements

The drive system shall be designed to support the operation of the concentrators specified in Section 5.2.

6.3.4 Compatibility Requirements

The drive system operational philosophy shall be compatible with the tracker control logic, wind sensing and overtemperature sensing command signals.

6.4 Instrumentation and Control

6.4.1 Tracker Control

The tracker control system shall provide two-axis automatic tracking of the sun and shall control the concentrator to meet the operational requirements specified in Sections 5.2.1 through 5.2.4, and 5.2.7.

6.4.2 Wind Sensing and Control

The control system shall accept a high wind velocity signal to stow the concentrator when wind velocity approaches the limit specified in Section 5.2.5.

6.4.3 Overtemperature Protection

The control system shall accept an overtemperature signal to desteer or stow the concentrator in the event the receiver/receiver aperture is in danger of being overheated.

6.4.4 Manual Override Command

The control system shall be capable of accepting override commands from a remote control station.

6.4.5 Pointing Bias

The control system shall have the capability of accepting AZ/EL pointing biases in 0.05^{o} increments, or smaller, for 1.0^{o} range for alignment purposes.

6.4.6 Emergency Overriding Commands

The overriding command hierarchy shall be as follows:

1. Manual Maintenance Control
2. Emergency Sensing Control
3. Desteer command
4. Stow command
5. Retire command
6. Manual ON/OFF
7. Tracking command

6.5 Electrical Requirements

6.5.1 Power Supply

The concentrator shall operate using 110 sinlge phase and/or 208 volt, 3-phase AC electrical power supplies.

6.5.2 Power Output Receptacle

Provision shall be made for a power output cable receptacle at the receiver/concentrator mechanical and electrical interface as shown in Figure 4-1. Type of receptacle used in the design shall be compatible with that of the receivers.

6.5.3 Lightning Protection

Lightning protector shall be provided based on the requirements of NFPA No. 78, 1965. A lightning stroke with a peak current of 35 kA dissipating 88 coulombs over a total time of 1/2 second will be protected against.

7. REFERENCES

The following references have been identified as the best sources of data available for determining design loads on the concentrator in accordance with JPL recommendations.

1. Stearns, J. W., et al., Solar Stirling System Development. JPL Report 79-1009, presented at the AIAA Terrestrial Energy System Conference, Orlando, Florida, June 4-6, 1979.

2. Levy, R. and McGinness, H., Wind Power Prediction Models. JPL Technical Memorandum 33-802. November 15, 1976.

3. Levy, R. and Kurtz, D., Compilation of Wind Tunnel Coefficients for Parabolic Reflectors. JPL Publication. April 15, 1978.

4. "Load Distribution on the Surface of a Paraboloidal Reflector Antenna" Exhibit II, Advanced Concentrator RFP.

8. DEFINITION OF TERMS

1. JPL

   Jet Propulsion Laboratory

2. Receiver/Engine Package

   The package is JPL supplied hardware. It is comprised of two subsystems:

   a. The Receiver subsystem is an absorptive cavity surface which converts the concentrated solar energy passing through the cavity aperture into a usable energy form and conducts it via a heat transfer system to the Power Conversion Subsystem

b. The Power Conversion subsystem inclues all the components needed to convert the thermal energy to electrical power and condition the power as required.

3. Solar Tracking Error

The Solar Tracking Error is the angular offset of the centerline of the energy beam from the center of the receiver aperture. It arises from any sensor misalignments, the solar tracker control offsets and hysteresis, and receiver support structural deflections as the Concentrator changes its orientation while tracking the sun.

4. Parasitic Power Consumption

Parasitic Power Consumption is the power required by the control and drive mechanism for the pointing of the concentrator and all power uses other than the generation of electricity.

5. Concentrator Stowed Position

The stowed position of the concentrator is a zenith pointing wind drag position.

6. Concentrator Retired Position

The retired position of the concentrator is when the concentrator faces South at -25^{0} elevation. This is the position the concentrator assumes after dusk and during maintenance.

7. Surface Error

The surface error is a composite function which results from the surface slope and location variations due to manufacture, alignment, and structural deflections. The surface error is

measured as the average deviation of the reflected energy from the nominal path of the ray (which would pass through the reflector focal point) is reflected from a perfectly specular surface which has no contour or position errors. The path deviations are caused by macroroughness (due to manufacturing methods), subassembly manufacturing errors, installation misalignments and distortions, and structural deflections (due to external forces and gravity).

The slope error is a local slope deviation from the slope expected from a theoretical design surface.

10. kmph

    kmph is the metric unit for the wind speed measured in kilometer per hour.

11. Gust Factor

    Gust factor is a percentage step increase in the wind velocity with the wind direction being unchanged.

APPENDIX C

PRELIMINARY HAZARDS ANALYSIS (PHA) FOR THE ADVANCED POINT-FOCUSING SOLAR CONCENTRATOR

ACUREX Corporation

HAZARD ANALYSIS

☐ SYSTEM ☐ FAILURE MODE & EFFECT ☒ PRELIMINARY ☐ OPERATIONAL

PROGRAM Advanced Point-Focusing Solar Concentrator

PREPARED BY T.J. Liddy

DATE November 13, 1979 REVISION _____ SHEET 1 OF 8

DEFINITIONS

Probability of Failure (P)

P is the qualitative rank ordering of the expected frequency of individual component failure. Selection of P is based on the Frequency of Failure (F).

F = 1 — RELIABILITY (R)

P	Frequency of Failure (F)	
	Category	Range
6	Frequent	1 to 10^{-1}
5	Probable	10^{-1} to 10^{-3}
4	Occasional	10^{-3} to 10^{-5}
3	Remote	10^{-5} to 10^{-7}
2	Improbable	10^{-7} to 10^{-9}
1	Impossible	10^{-9} to 0

Hazard Severity (S)

S is the weighting factor for the severity of a hazard resulting from an individual component failure.

S	Hazard	
	Category	Severity
4	I — Catastrophic	May cause death or system loss
3	II — Critical	May cause severe injury, severe occupational illness, or major system damage
2	III — Marginal	May cause minor injury, minor occupational illness, or minor system damage
1	IV — Negligible	Will not result in injury, occupational illness or system damage

Hazard Priority (H_p)

H_p shows the criticality of the hazard and establishes the priority for corrective action.

$$H_p = (P \times S)$$

H_p	Corrective Action
1 to 4	Not required
5 to 8	Recommended but not required
9 to 15	Required to operate without restrictions
16 to 24	Required before operation

Form AG-072 A 9 79

ACUREX Corporation

PROGRAM: Advanced Point-Focusing Solar Concentrator

SHEET 1 OF 1

SUBSYSTEM: Foundation/Structure

REV.

PRELIMINARY HAZARD ANALYSIS

Item No.	Hazardous Component or Condition	Description of Potential Hazard	PROBABILITY/SEVERITY: Probability (P)	Severity (S)	Priority (PxS)	Recommended Action
1	Structure to foundation interface	Dynamic loading from wind or earthquake may cause positive or negative thrust loads at the attachment points of the pedestal structure to the foundation and/or the track to the foundation. Failure of one of these attachment points could result in the concentrator tipping over.	3	4	12	a - Make sure dynamic loading is considered in foundation design. b - Consider fatigue failure carefully. c - Protect interface points from corrosion.
2	Thermal expansion	Damage to foundation from temperature extremes	3	2	6	a - Design for no damage from -40°C to +60°C (-40°F to +140°F) at 100% relative humidity. b - Design for maximum frost penetration of 0.91 meters (36 inches).
3	Inadequate soil conditions	Foundation not compatible with soil properties.	2	3	6	a - Verify soil properties and foundation design are compatible.
4	Structure collapse	Collapse of the structure or buckling of any structural element could occur if dynamic loads are not carefully considered.	2	4	8	a - Be sure to consider max. wind loads and earthquake loads in the design. b - Use redundant structure at critical points. c - Perform stress analyses with various highly stressed members absent to verify structural integrity. d - Design to the following safety criteria: (1) F.S. of 2.0 based on minimum yield, for operational loads. (2) F.S. of 1.5 based on minimum yield and/or 2.0 on ultimate strength, for worst-case loads.
5	Structure tipping over with high wind gusts.	A high wind gust occuring before the collector can reach stow position tipping over the structure.	3	4	12	a - Consider a device to prevent the wheels from lifting off the track, thereby using the track to help prevent tipover. b - Program the computer to use the azimuth drive, as well as the elevation drive to position the collector for least wind resistance.
6	Vibration	Mechanical failure due to vibration	3	4	12	a - Design all mechanical and structural connections so that no fixed part will come loose due to vibration and/or shock.
7	High winds in maintenance position	Structural failure	4	4	16	a - Provide an audible alarm at concentrator and at the control room to signal high wind speeds when collector is in the maintenance mode.

ACUREX Corporation

PROGRAM: Advanced Point-Focusing Solar Concentrator SHEET 1 OF 1

SUBSYSTEM: Drive REV.

PRELIMINARY HAZARD ANALYSIS

Item No.	Hazardous Component or Condition	Description of Potential Hazard	PROBABILITY/ SEVERITY			Recommended Action
			Probability (P)	Severity (S)	Priority (PxS)	
1	Loss of Elevation Drive	Loss of the ability to change the elevation of the collector due to electrical or mechanical failure could result in the inability to position the collector in the STOW position, or to perform the DESTEER function, either of which could result in structural failure. Mechanical failure could also result in the collector banging to the STOW or RETIRE position with resultant structural and/or reflective surface damage.	4	3	12	a - Program the microprocessor to use the azimuth drive to perform DESTEER if elevation drive does not operate. b - If STOW command is not executed, program the computer to use the azimuth drive to position the collector so the parabolic dish is positioned for least wind resistance. c - Install damping device to limit acceleration in elevation direction to a safe value. d - Design drive hardware to withstand max. loading for expected life span without failure. e - Provide alarms to signal abnormal conditions.
2	Loss of azimuth Drive	Electrical failure will result in the inability to move the collector in the azimuth direction. Mechanical failure in the motor, or reduction gears could also result in the inability to move the collector, or could result in the inability to control movement caused by wind forces, depending on the failure mode. Such inability could result in structural failure.	4	3	12	a - Program the computer to position the collector to the STOW position if azimuth error is out of spec. b - Provide a means of disengaging the chain sprocket and manually positioning the collector in azimuth direction. c - Provide a braking system to prevent possible weathervaneing. d - Provide appropriate alarms to indicate abnormal condition.
3	Azimuth drive chain	A chain and sprocket arrangement can result in numerous "pinch points" where personnel can be injured by contact with moving parts. Chain breakage will also result in the loss of azimuth drive as described in the previous item.	3	3	9	a - Provide suitable guards to prevent accidental contact with chain and sprocket. b - Choose chain which will withstand maximum tensile load possible with selected azimuth drive motor.
4	Overload of drive Motors	Inability to position collectors in elevation or azimuth. Overload can be caused by mechanical binding or obstruction of moving components by a foreign object. Potential hazards are the same as for items 1 and 2.	3	3	9	a - Choose motors with adequate power to drive the concentrator to STOW with an 80kmph (50mph) wind. b - Equip motors with self-resetting thermal overload devices to prevent motor damage in overload condition. c - Provide a device (scraper/wiper) to clear foreign objects from track. d - Define perimeter area where no equipment or vehicle may be located. e - Provide for adequate lubrication of moving parts. f - Recommend periodic inspection and maintenance requirements. g - Provide and alarm to indicate when the thermal overload trips.

ACUREX Corporation

PROGRAM: Advanced Point-Focusing Solar Concentrator

SHEET 1 OF 1

SUBSYSTEM: Electrical

REV.

PRELIMINARY HAZARD ANALYSIS

Item No.	Hazardous Component or Condition	Description of Potential Hazard	PROBABILITY/ SEVERITY: Probability (P)	Severity (S)	Priority (PxS)	Recommended Action
1	High Voltage	Personnel exposure to energized 110V. and/or 208V. equipment.	3	4	12	a - Design all electrical equipment to the National Electric Code. b - Use cabling with insulation and jacketing compatible with environmental exposures expected. c - Make sure all live electrical circuits are protected from inadvertent contact by operating or maintenance personnel. d - Make sure any power connectors have the receptacle (female) pins "hot" and the plug (male) pins "cold" when not connected. e - Design to ensure all external parts are at ground potential. f - Equip any convenience outlets with ground fault detectors.
2	Circuit Overload	Overheating of cables causing fire or equipment damage	2	4	8	a - Be sure the conductor size chosen will provide the required current-carrying capacity at all expected operating temperatures. b - Provide circuit breakers, or other overload protection, to all power circuits. c - Provide protection from lightning.
3	Loss of power	Loss of commercial electric power causing the inability to position the collector to a safe attitude.	3	4	12	a - Provide emergency backup power for the computer and drive motors. The emergency source must be selfstarting with an automatic switchover at loss of commercial power. b - Provide an alarm to indicate when emergency power is being used. c - Make sure emergency power source has adequate voltage, current, and phase control to prevent equipment damage.
4	Vibration	Power connections coming loose causing short circuits.	3	4	12	a - Design equipment so that no fixed part will become loose under all expected conditions.
5a	Output power	Damage to cables during reflector positioning.	2	3	6	a - Provide protective cableways for output power cables, separate from instrumentation cables. b - Consider movement of reflector in designing cable routing. c - Make sure twisting of cables cannot occur.
5b	Output power	Incompatibility with power grid	2	3	6	a - Design electrical interface to maintain proper voltage and phasing.

ACUREX Corporation

PROGRAM: Advanced Point-Focusing Solar Concentrator

SHEET 1 OF 1

SUBSYSTEM: Reflective Gore

REV.

PRELIMINARY HAZARD ANALYSIS

Item No.	Hazardous Component or Condition	Description of Potential Hazard	PROBABILITY/ SEVERITY			Recommended Action
			Probability (P)	Severity (S)	Priority (PxS)	
1	Reflective Element fracture	Injury to maintenance personnel	3	3	9	a - Design gore attachment so that individual elements can be removed and replaced safely under field conditions. b - Design gores to withstand the most severe environmental conditions expected throughout their lifetime. c - Design gores without sharp edges if possible. d - Consider static and dynamic fatigue in gore design.

Form AG-372 F 8/78

ACUREX Corporation

PROGRAM: Advanced Point-Focusing Solar Concentrator SHEET 1 OF 2

PRELIMINARY HAZARD ANALYSIS

SUBSYSTEM: Instrumentation and Control REV.

Item No.	Hazardous Component or Condition	Description of Potential Hazard	PROBABILITY/ SEVERITY			Recommended Action
			Probability (P)	Severity (S)	Priority (PxS)	
1	Shaft encoder	Loss of, or wrong, position code resulting in collector being positioned such that overtemperature or wind forces are not corrected for.	4	4	16	a - Provide redundant encoders b - Program the computer to compare the signal from the redundant encoders to detect any discrepancy, to decide which output is correct, and to initiate an alarm indicating the malfunction.
2	Loss of Microprocessor	No control over concentrator movement	4	4	16	a - Provide redundant microprocessor b - Design control loop failsafe, such that loss of control signal causes the reflector to drive to the stow position.
3	Tracking error	Concentrator not properly aligned with sun	2	2	4	a - Program the computer to compare actual concentrator position with expected position based on time-of-day and to signal abnormal conditions.
4	Loss of datalink from remote control station	Local malfunctions not communicated to control Room.	3	2	6	a - Provide alarms at remote control room to signal operator of any such signal loss. b - Be sure local control of critical functions is maintained. c - Design control loops to position the reflector to "stow" should the data link be lost.
5	Loss of wind direction or velocity signals	Structural damage to collectors	4	4	16	a - Design for redundant sensors. b - Program computer to place collector in stow if direction or velocity signal is lost.
6	Signal compatibility	Incompatible signals between sensors and control computer.	2	4	8	a - Verify compatibility of signals when specifying components.
7	Maintenance Mode	Hazardous conditions while in maintenence mode not being detected.	4	4	16	a - Provide local and remote alarm for generator overtemperature, high winds, or any other hazardous condition that would normally cause the concentrator to desteer or stow. b - Provide instructions to maintenance personnel on actions to take if such alarms occur. c - Design hardware so that it is possible to place the concentrator in a safe position in the maintenance mode.

ACUREX Corporation

PROGRAM: Advanced Point-Focusing Solar Concentrator

SHEET 2 OF 2

SUBSYSTEM: Instrumentation and Control

REV.

PRELIMINARY HAZARD ANALYSIS

Item No.	Hazardous Component or Condition	Description of Potential Hazard	PROBABILITY/ SEVERITY			Recommended Action
			Probability (P)	Severity (S)	Priority (PxS)	
8	Concentrated sunlight	Concentrated sunlight being directed at normally occupied areas, or focused on the collector's structure.	4	3	12	a - Program computer to prevent positioning the concentrator in an attitude that would direct sunlight toward any area occupied by personnel, or focus the reflected beam on any structural element of the concentrator. b - Consider nearby roads in suggestion (a) to avoid temporary blinding of drivers.
9	Override Commands	Commands from remote control station by-passing safety devices.	2	4	8	a - Design control logic with the following priority of commands: 1 - Maintenance Mode. 2 - Emergency Control. 3 - Desteer command. 4 - Stow command. 5 - Retire command. 6 - Manual control. 7 - Tracking command. b - Provide local and remote audible alarm for all safety devices to indicate an alarm situation without automatic correction.

ACUREX Corporation

PROGRAM: Advanced Point-Focusing Solar Concentrator

SHEET 1 OF 1

SUBSYSTEM: Interface with Receiver

REV.

PRELIMINARY HAZARD ANALYSIS

Item No.	Hazardous Component or Condition	Description of Potential Hazard	PROBABILITY/ SEVERITY			Recommended Action
			Probability (P)	Severity (S)	Priority (PxS)	
1	Electrical Interface	Incompatibility of connectors	3	2	6	a - Coordinate hardware selection with receiver supplier.
2	Misalignment of receiver	Inability to fine align receiver at concentrators focal point	3	2	6	a - Provide mechanical adjustment, along and normal to the collectors focal axis, for the receiver.

APPENDIX D

JPL ADVANCED CONCENTRATOR PRELIMINARY DESIGN DRAWING PAC E

DRL 012

DRD SE001

Drawing Number	Revision	Title	Number of Sheets
7740-001	A	Assembly	3
7740-002	A	Gore Support Ring	4
7740-003	B	Receiver/Engine Support Structure	2
7740-004	A	Drive Structure	2
7740-005	A	Counterweight Structure	1
7740-006	A	Foundation and Pedestal Subassembly	2

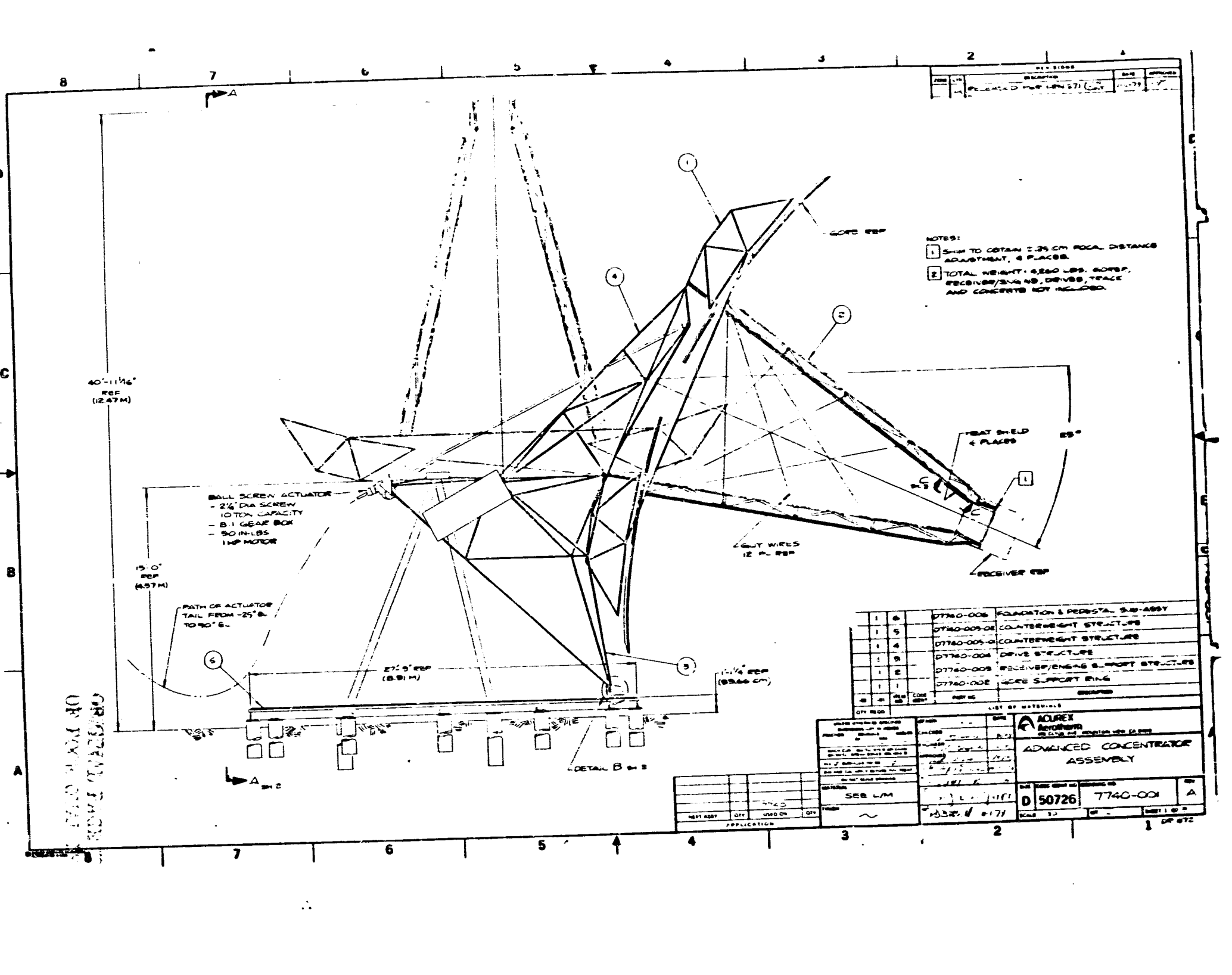
NOTES:
1. SHIM TO OBTAIN ± .25 cm FOCAL DISTANCE ADJUSTMENT, 4 PLACES.
2. TOTAL WEIGHT: 4,260 LBS. DOES NOT INCLUDE RECEIVER/ENGINE ASSEMBLY, DRIVES, TRACK AND CONCRETE.
CORE REF
HEAT SHIELD 4 PLACES
RECEIVER REF
BALL SCREW ACTUATOR
- 2¼" DIA SCREW
10 TON CAPACITY
- 8:1 GEAR BOX
- 50 IN-LBS
1 HP MOTOR
PATH OF ACTUATOR TAIL FROM -25° E. TO 90° E.
DETAIL B
SEE L/M
ACUREX Aerotherm
ADVANCED CONCENTRATOR ASSEMBLY
D 50726
7740-001

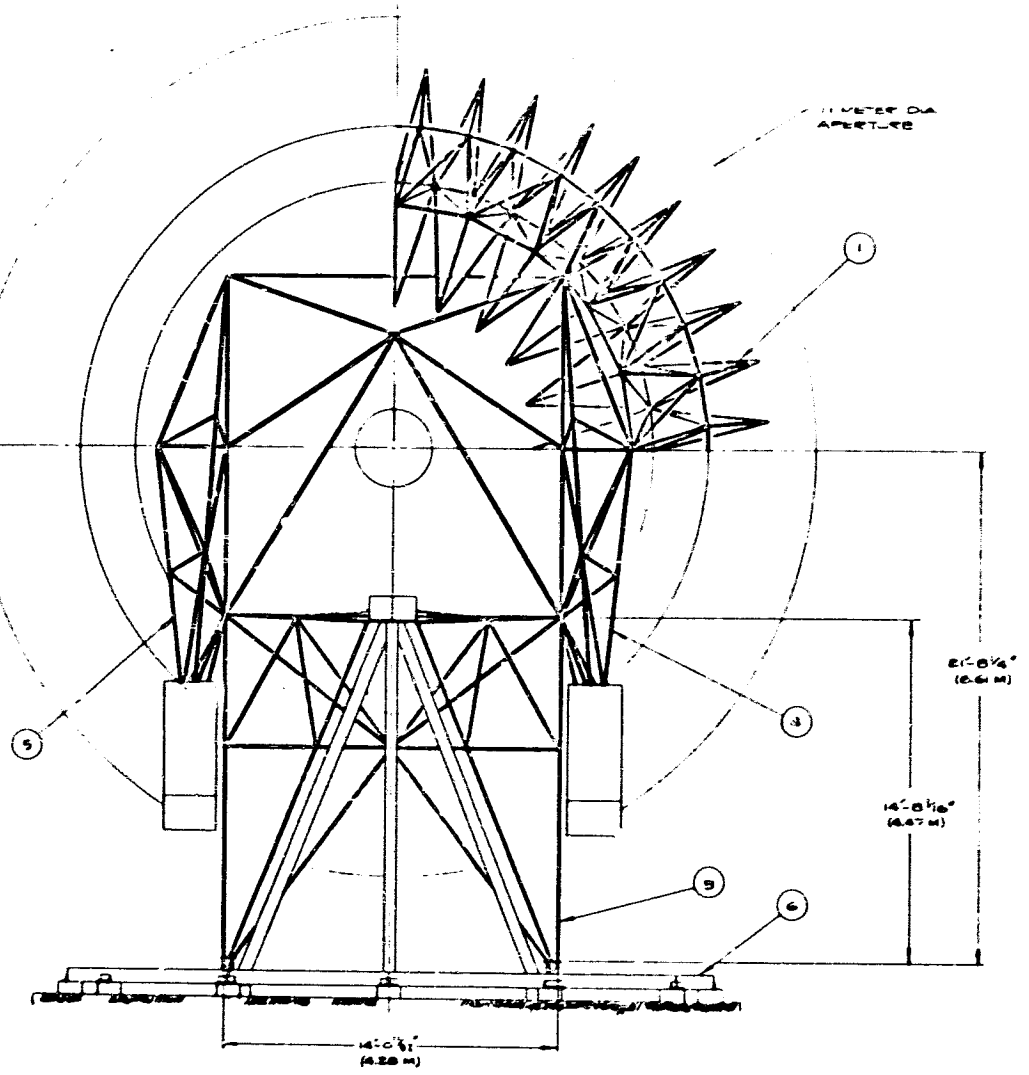

VIEW A-A
CORE SUPPORT RING
SHOWN IN VERTICAL POSITION
ACTUATOR NOT SHOWN
FOR CLARITY

		ADVANCED CONCENTRATOR ASSEMBLY	
		D 50726	7740-001 A

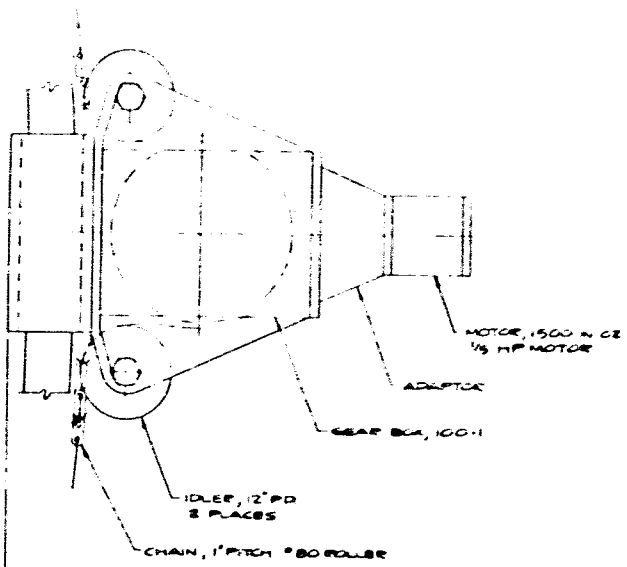

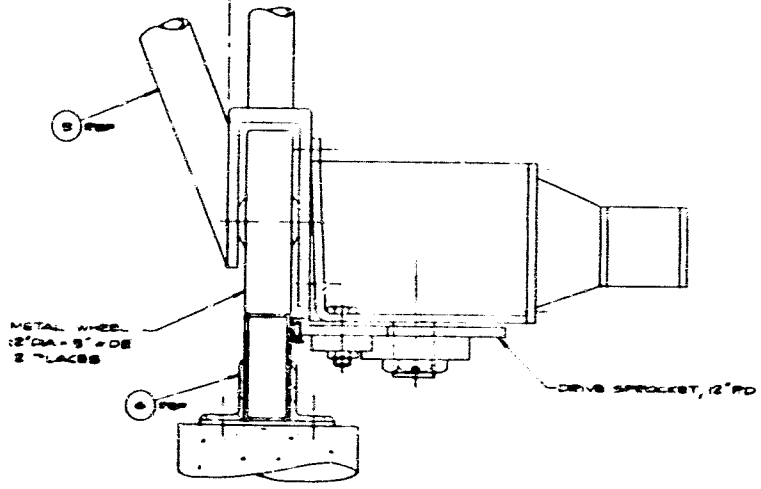

DETAIL B
AS MULTIPLIED
SCALE: NONE

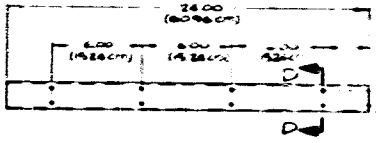

VIEW C-C

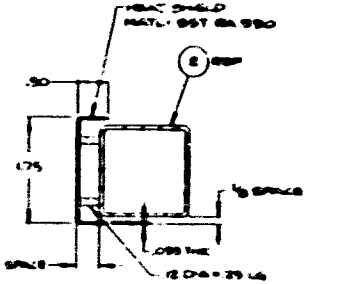

SECTION D-D
SCALE: 1/1

ACUREX AEROTHERM			
ADVANCED CONCENTRATOR ASSEMBLY			
D	50726	7740-C01	A

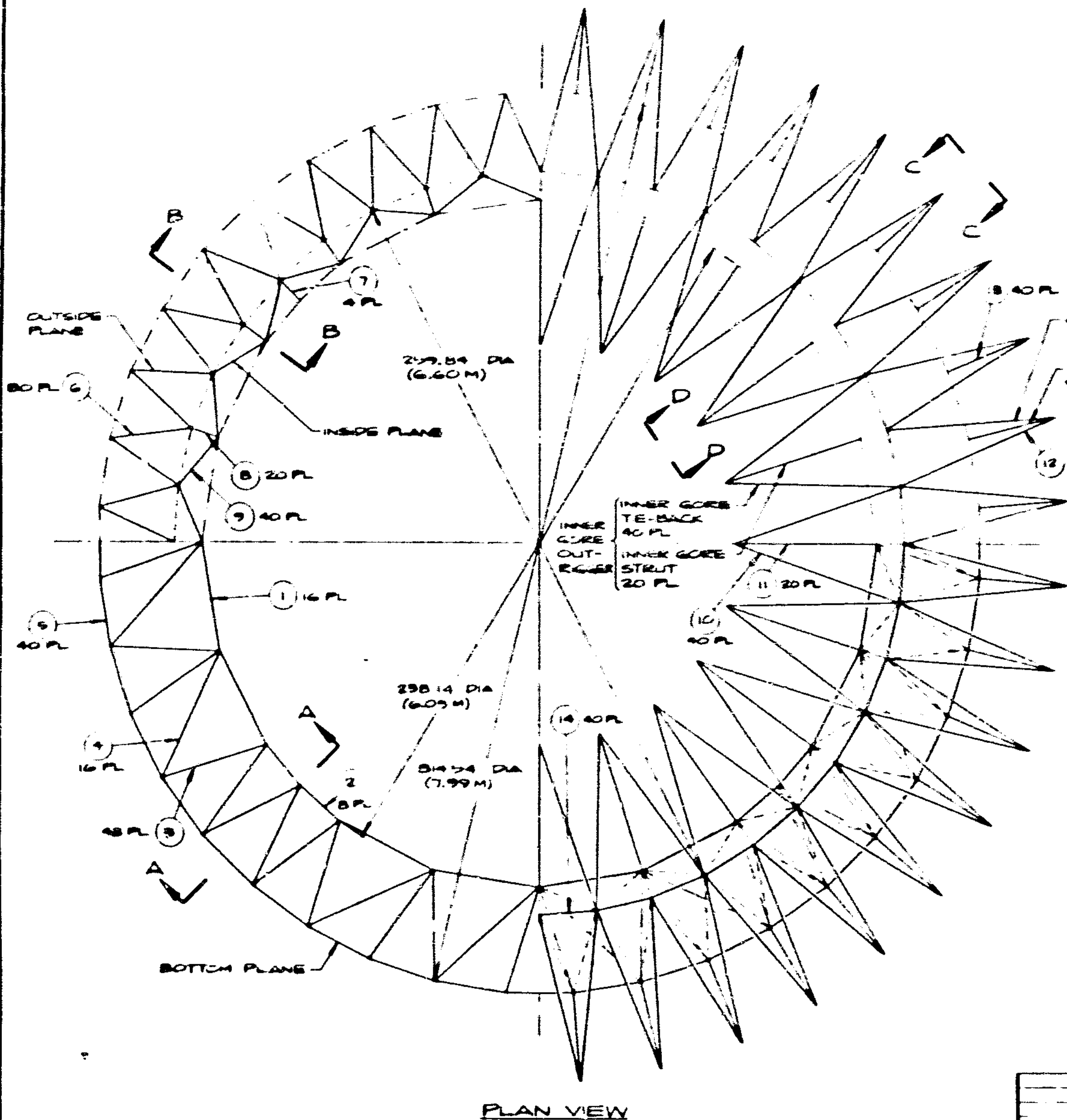

PLAN VIEW

NOTES:
1. ALL LENGTHS SHOWN ARE ℄ TO ℄.

QTY REQD	ITEM NO	CODE IDENT	SIZE	DESCRIPTION
2	17		[illegible]	STRUT-88.79(2.25M)LG ASTM A36
2	16		[illegible] OD	STRUT-168.41(4.[illegible]M)LG
4	15		[illegible] OD	STRUT-168.99(4.2[illegible]M)LG
40	14		[illegible]	STRUT-20.99(51.79CM)LG
40	13		[illegible] OD	STRUT-56.08(1.42M)LG
80	12		[illegible] OD	STRUT-62.78(1.59M)LG
20	11		[illegible] OD	STRUT-56.06(1.4[illegible]M)LG
40	10		[illegible] OD	STRUT-63.2[illegible](1.[illegible]M)LG
40	9		[illegible] OD	STRUT-48.94(1.12M)LG
20	8		[illegible] OD	STRUT-39.37(1M)LG
4	7		[illegible] OD	STRUT-39.37(1M)LG
80	6		[illegible] OD	STRUT-40.94(1.03M)LG
40	5		[illegible]	STRUT-24.69(62.71CM)LG
16	4		[illegible]	STRUT-50.84(1.29M)LG
48	3		[illegible]	STRUT-40.81(1.04M)LG
8	2		[illegible]	STRUT-18.68(47.5CM)LG
16	1		[illegible]	STRUT-37.25(94.62CM)LG ASTM A36

LIST OF MATERIALS

MATERIAL: SEE L/M

FINISH: [illegible]

ACUREX Aerotherm

GORE SUPPORT RING-
ADVANCED CONCENTRATOR

SIZE D | CODE IDENT NO 50726 | DRAWING NO 7740-002 | REV A

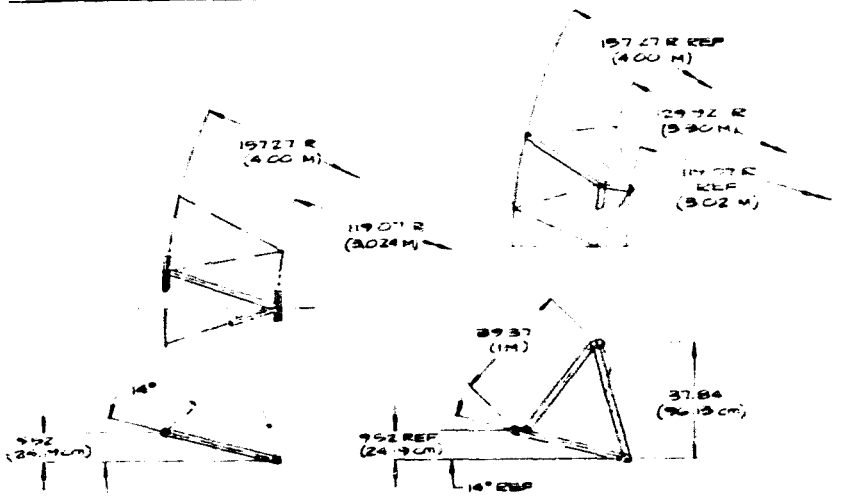

SECTION A-A
ROTATED 45° CW
ALL DIMS ARE
TYPICAL

SECTION B-B
ROTATED 30° CW
ALL DIMS ARE
TYPICAL

VIEW C-C
ROTATED 30.50 CW
ALL DIMENSIONS
ARE TYPICAL

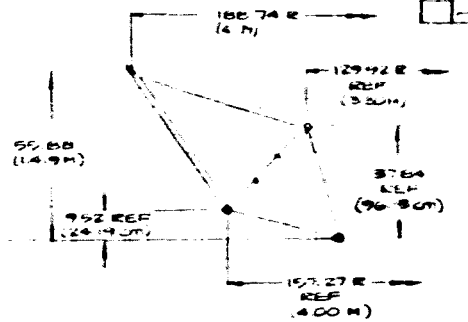

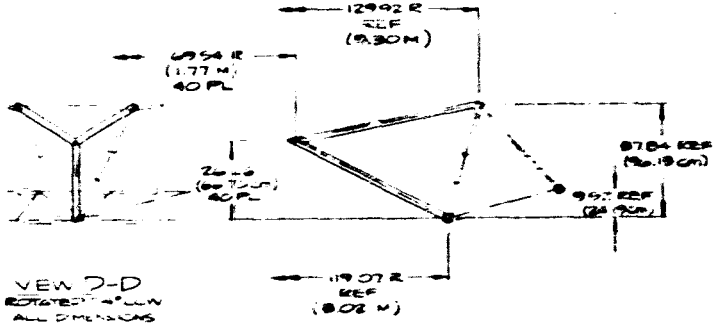

VIEW D-D
ROTATED 45° CW
ALL DIMENSIONS
ARE TYPICAL

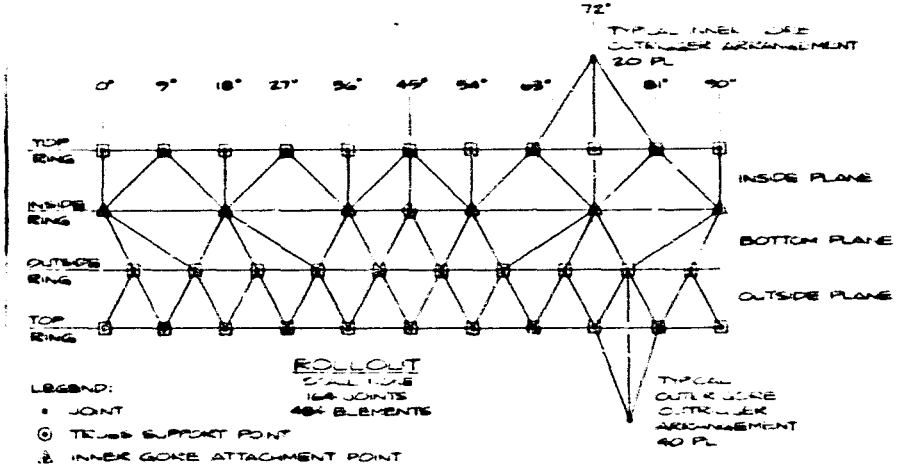

LEGEND:
- • JOINT
- ⊙ TENSION SUPPORT POINT
- ⓐ INNER GORE ATTACHMENT POINT
- ⓑ OUTER GORE ATTACHMENT POINT
- ⓒ INNER & OUTER GORE ATTACHMENT POINTS (TOP RING ONLY)

ACUREX Aerotherm

GORE SUPPORT RING - ADVANCED CONCENTRATOR

D 50726 7740-002 A

7740-002

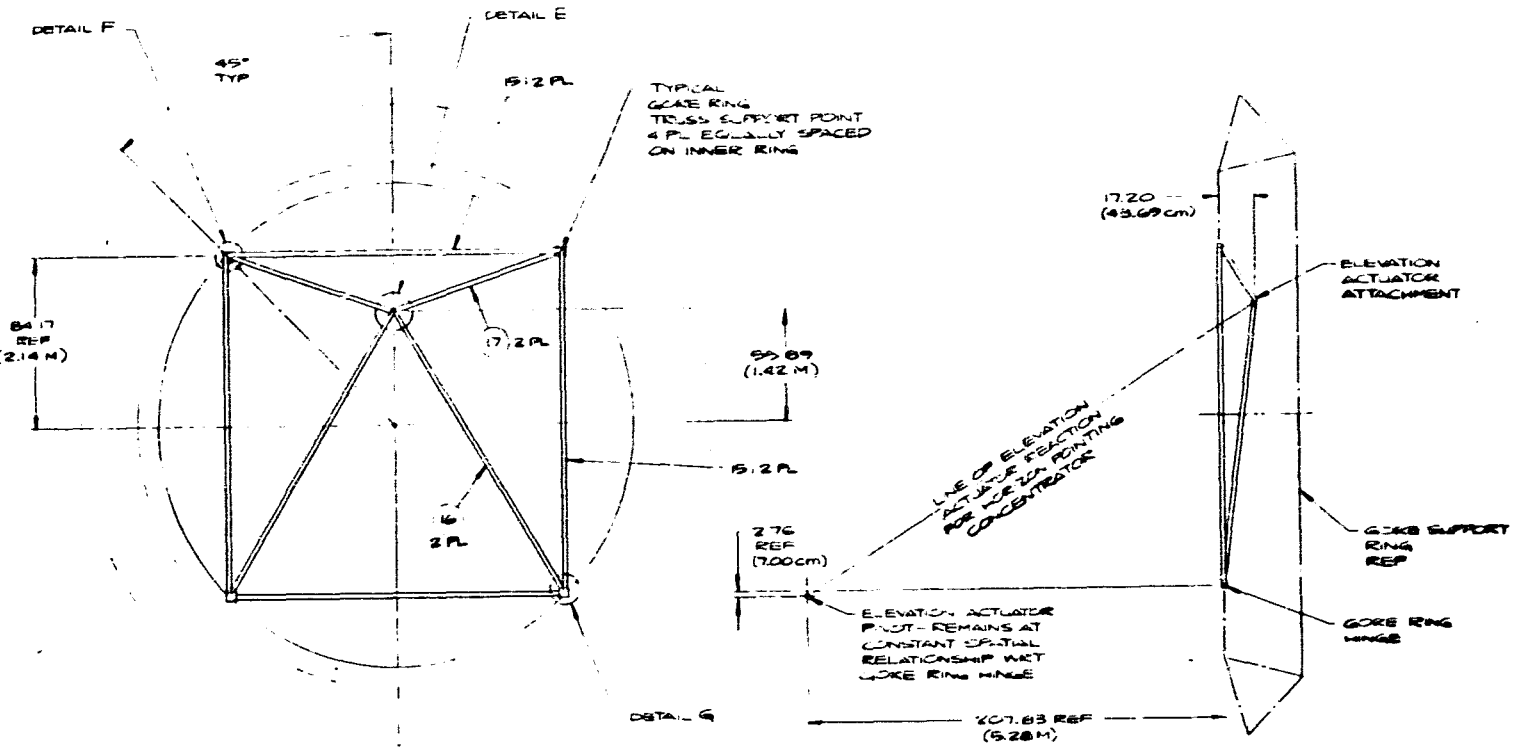

BOTTOM VIEW

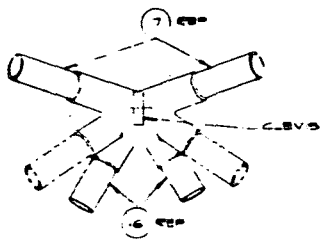

DETAIL E
SCALE: NONE

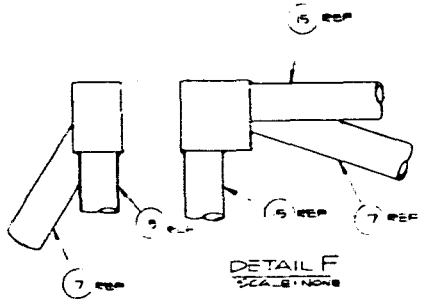

DETAIL F
SCALE: NONE

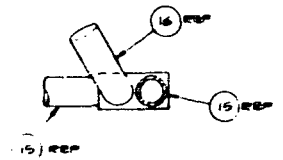

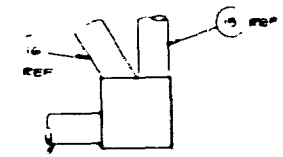

DETAIL G
SCALE: NONE

ACUREX Aerotherm			
GORE SUPPORT RING ATVANCED CONCENTRATOR			
D	50726	7740-002	A

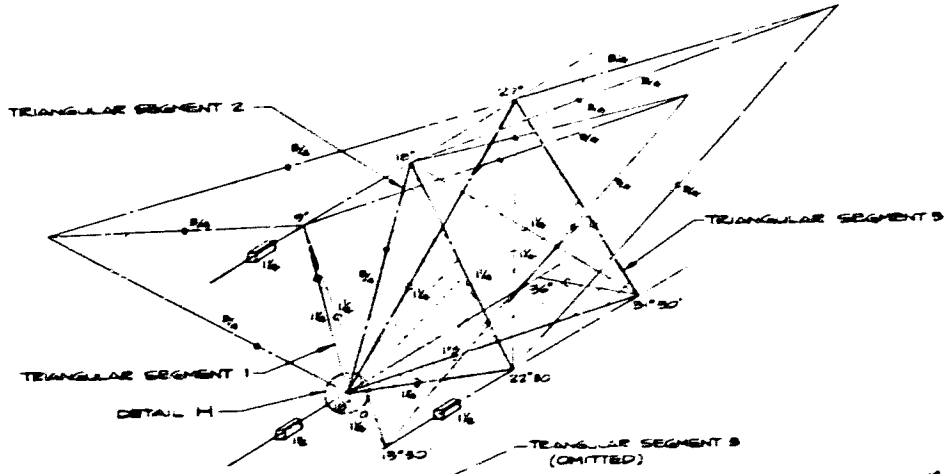

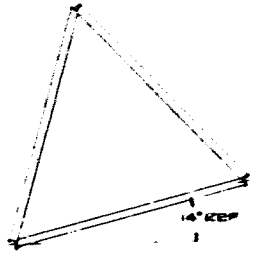

TYPICAL TRIANGULAR SEGMENT FABRICATION

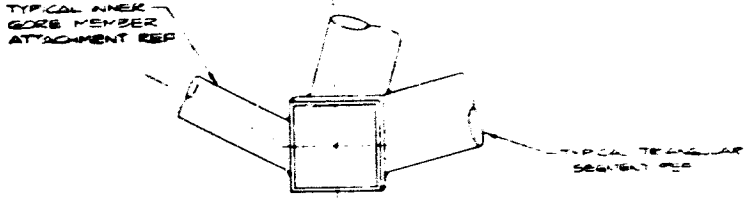

DETAIL H
TYPICAL
CONSTRUCTION

ITEM NO	QTY	PART NO	DESCRIPTION
			LIST OF MATERIALS

ACUREX Aerotherm

GORE SUPPORT RING-
ADVANCED CONCENTRATOR

SIZE	DRAWING NO	REV
D	50726	7740-002

7740-002

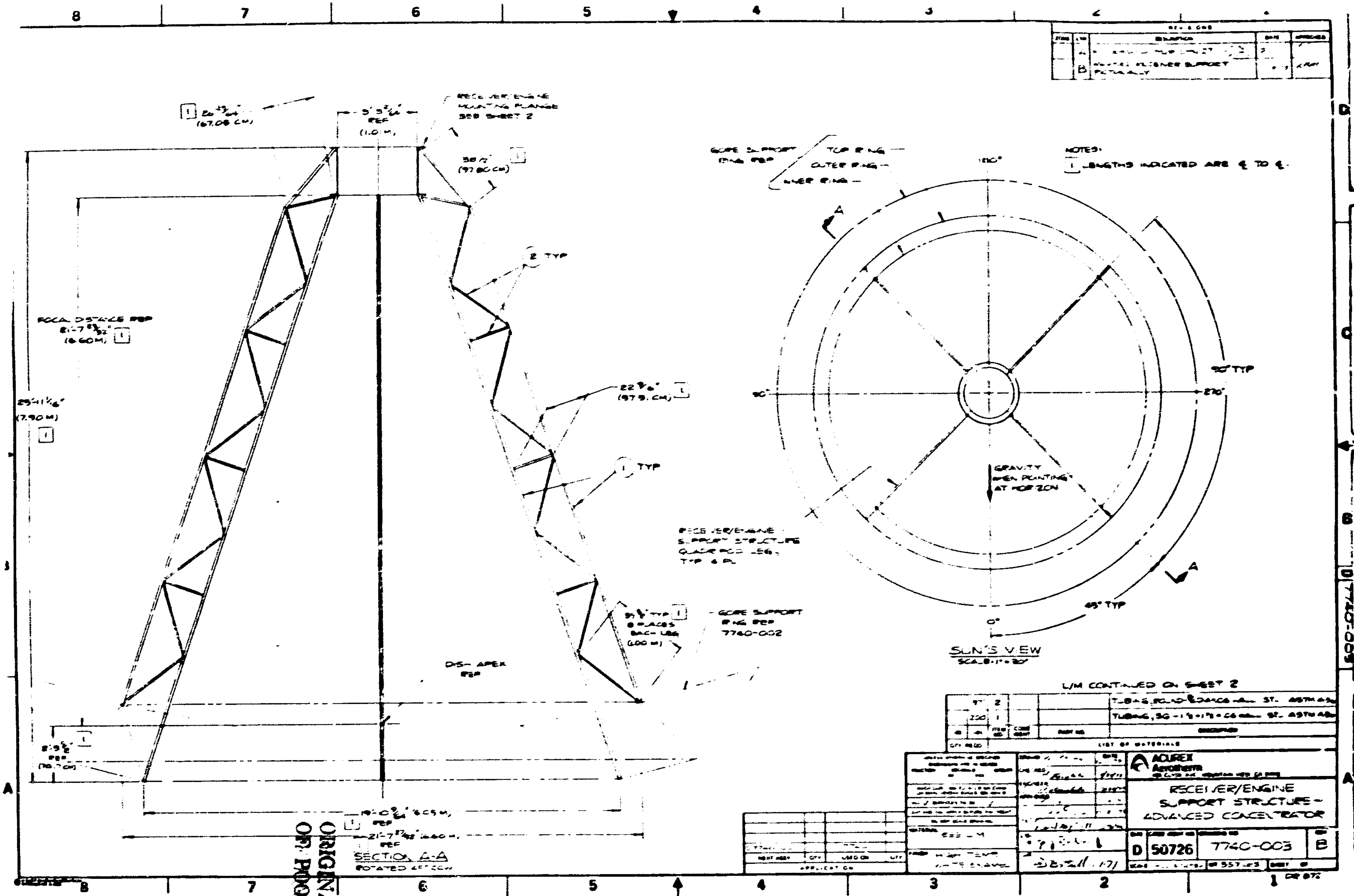

ORIGINAL PAGE IS OF POOR QUALITY

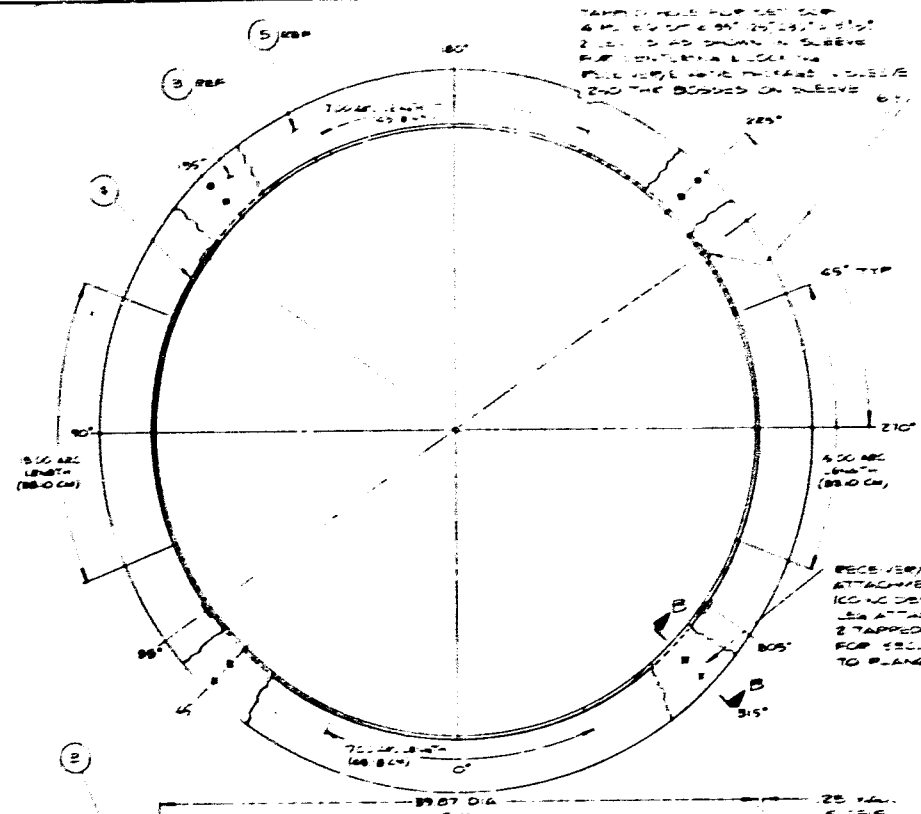

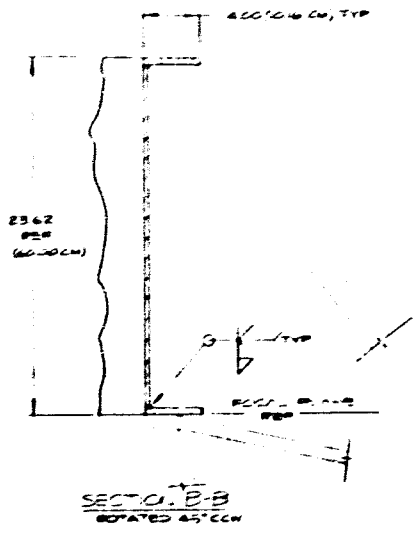

SECTION B-B
ROTATED 45° CCW

RECEIVER/ENGINE ATTACHMENT LOCATION 4 PL ICONIC DESIGN W/GUSSETED ATTACHMENT PLATES, 2 TAPPED HOLES PER LOCATION FOR FASTENING RECEIVER/ENGINE TO FLANGE.

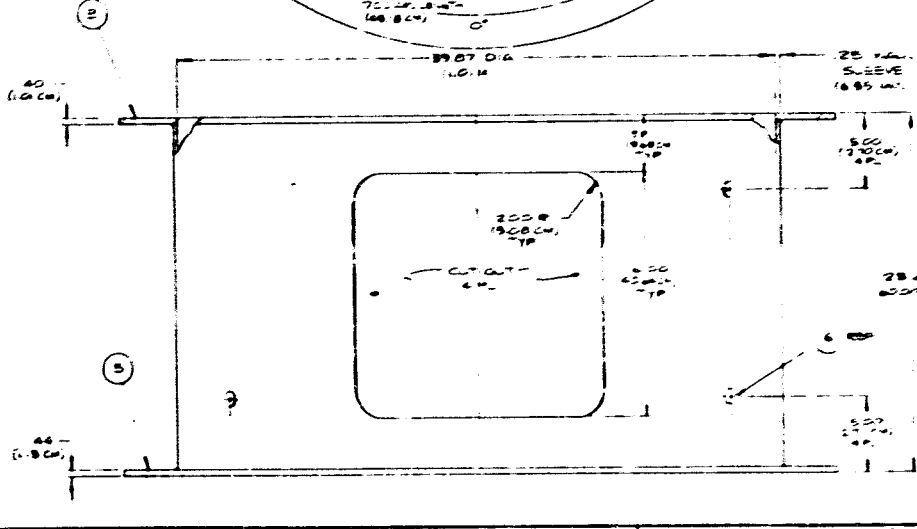

6			
5			
4			
3			

PLATE - I.C. DIA = 39.87 THK 6T. ASTM A36
FLANGE - 48.75 DIA x .40 THK 6T. ASTM A36
PLATE - 26.00 x 27.00 x .25 THK 6T. ASTM A36
FLANGE - 48.75 DIA x .44 THK 6T. ASTM A36

LIST OF MATERIALS

ACUREX
Aerothermal

RECEIVER/ENGINE SUPPORT STRUCTURE - AT ANGLE CONCENTRATOR

D 50726 | 7740-003 | B

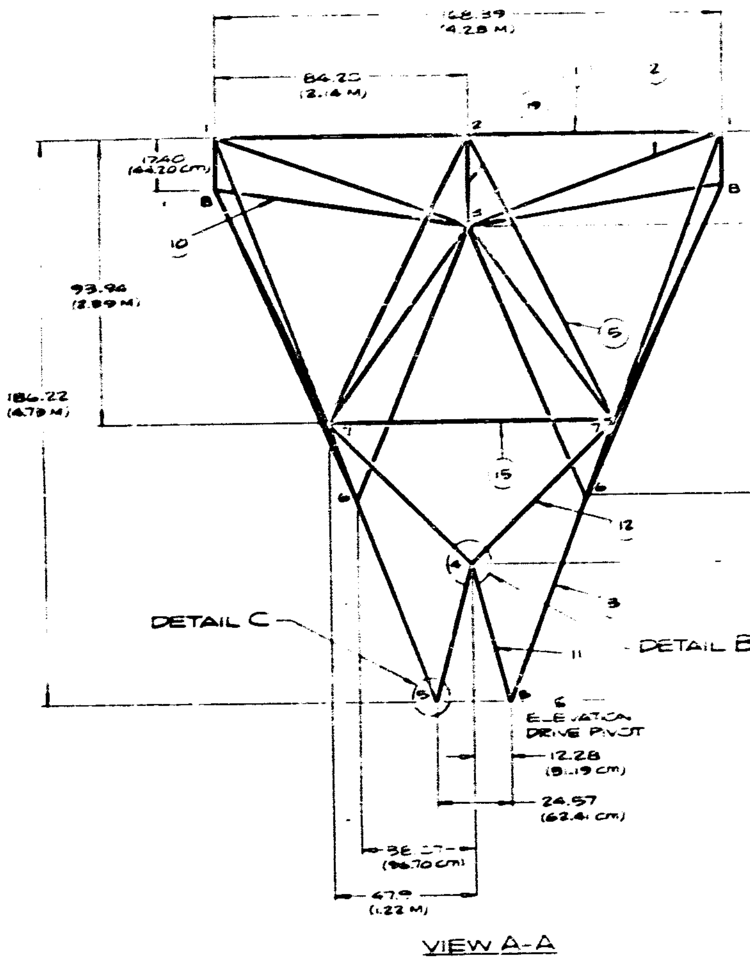

VIEW A-A

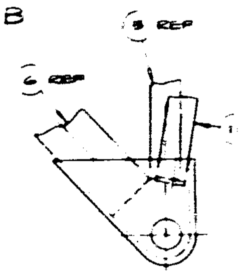

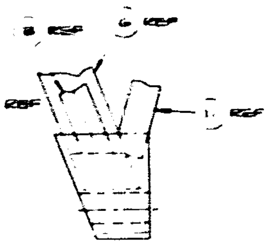

DETAIL C
2 PL
SCALE 1/4

NOTES:
1. ALL LENGTHS SHOWN ARE ℄ TO ℄.

JOINT REF	QTY REQD		ITEM NO	CODE IDENT	SIZE	DESCRIPTION	MATERIAL
		1	23			UPPER BEARING RETAINER	
		1	22			LOWER BEARING RETAINER	
		2	21			BEARING, TURNTABLE - 8600 LB RADIAL 37900 LB THRUST	
		1	20			PIVOT BRACKET	
2-9		1	19		1×1×1/8 WALL	STRUT - 71.98 LG (1.83 M)	ASTM A36
[illegible]			18		1×1×1/8 WALL	STRUT - 168.99 LG (4.29 M)	ASTM A36
E-?		2	17		3×3×3/16 WALL	STRUT - 112.59 LG (2.86 M)	
7-E		2	16		2×2×1/8 WALL	STRUT - 105.89 LG (2.69 M)	
7-7		1	15		1½×1½×1/8 WALL	STRUT - 95.89 LG (2.43 M)	
?-E		2	14		2½×2½×1/8 WALL	STRUT - 111.95 LG (2.84 M)	
?-7		2	13		[illegible] WALL	STRUT - 69.14 LG ([illegible] M)	
4-7		2	12		2×2×1/8 WALL	STRUT - 66.73 LG (1.69 M)	
4-5		2	11		2×2×1/8 WALL	STRUT - 48.22 LG (1.22 M)	
5-6		2	10		[illegible] WALL	STRUT - 89.5 LG (2.6 M)	
3-7		2	9		2½×2½×1/8 WALL	STRUT - 10?.91 LG (2.99 M)	
3-6		2	8		[illegible] WALL	STRUT - 97.00 LG (2.46 M)	
3-9		2	7		2½×2½×1/8 WALL	STRUT - 142.69 LG (3.62 M)	
5-9		2	6		3½×3½×1/8 WALL	STRUT - 264.9 LG (6.71 M)	
2-7		2	5		2×2×1/8 WALL	STRUT - 105.40 LG (2.68 M)	
1-8		2	4		3×3×3/16 WALL	STRUT - 67.2 LG (1.70 M)	
1-5		2	3		2×2×1/8 WALL	STRUT - 199.68 LG (5.07 M)	
1-3		2	2		2½×2½×1/8 WALL	STRUT - 110.69 LG (2.81 M)	
1-1		1	1		2×2×1/8 WALL	STRUT - 168.90 LG (4.29 M)	ASTM A36

LIST OF MATERIALS

ACUREX Aerotherm

DRIVE STRUCTURE - ADVANCED CONCENTRATOR

SIZE	CODE IDENT NO	DRAWING NO	REV
D	50726	7740-004	A

FINISH: WHITE ENAMEL

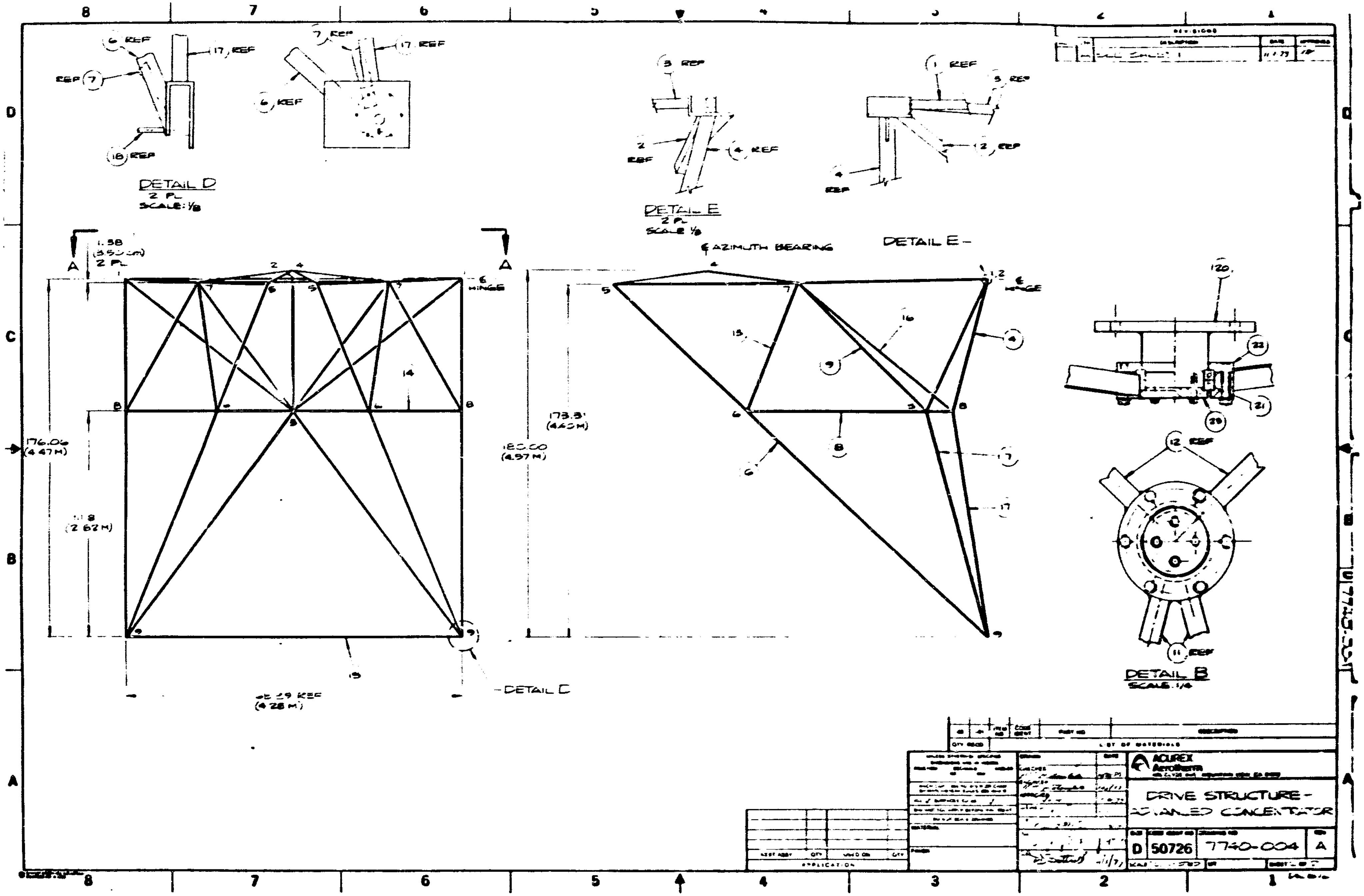
DETAIL D
2 PL
SCALE: 1/8
DETAIL E
2 PL
SCALE 1/8
DETAIL E -
℄ AZIMUTH BEARING
℄ HINGE
1.58
2 PL
176.06
(4.47 M)
(2.62 M)
180.00
(4.57 M)
173.3'
(4.40 M)
(4.28 M)
DETAIL C
DETAIL B
SCALE 1/4
REF
ACUREX
Aerotherm
DRIVE STRUCTURE -
D
50726
7740-004
A
LIST OF MATERIALS
APPLICATION

ZONE	LTR	DESCRIPTION	DATE	APPROVED
	A	RELEASED PER ECN 27	2-2-79	

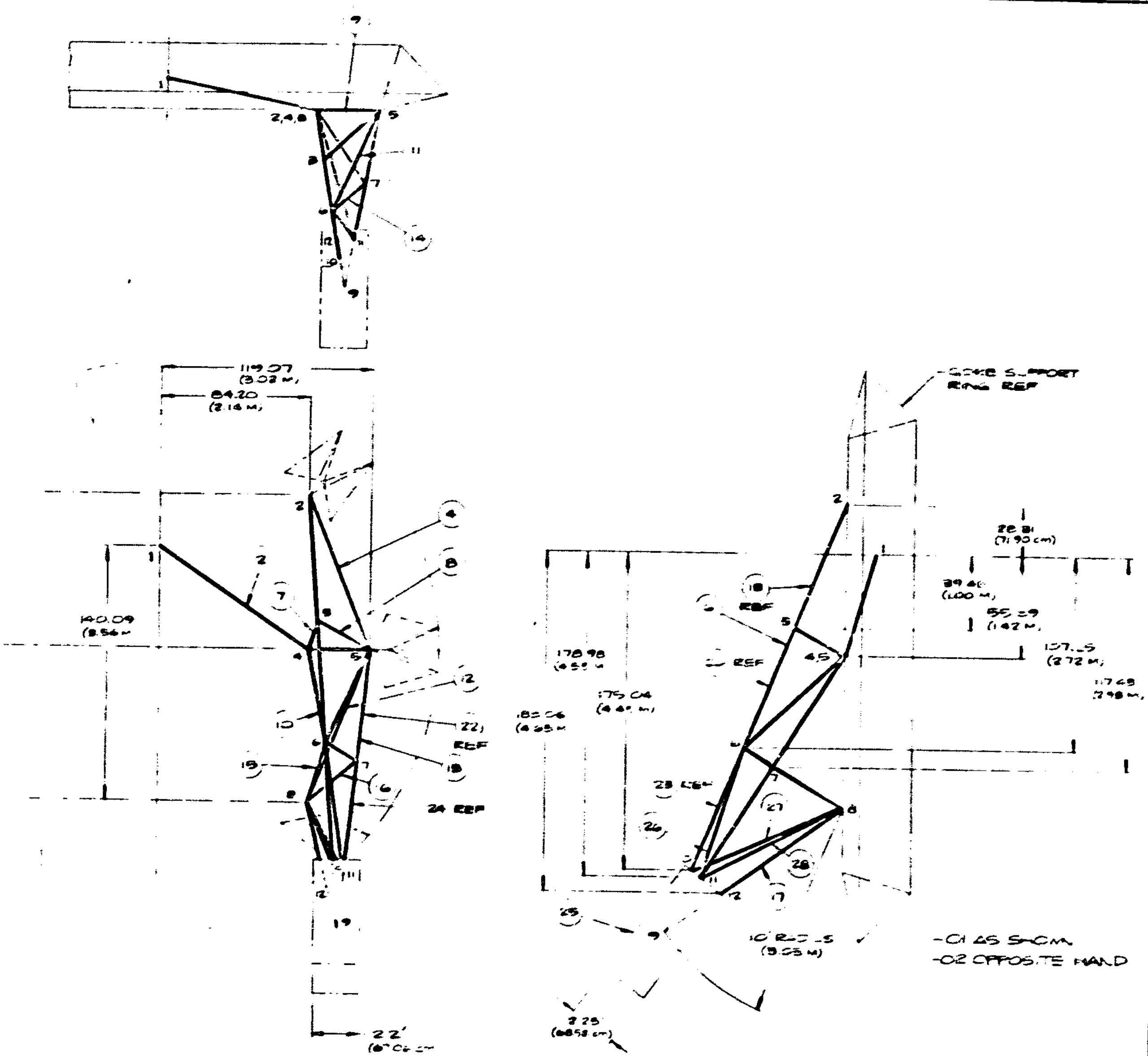

NOTES:
1. LEFT AND RIGHT HAND STRUCTURES WEIGH 340 LBS EACH. COMBINED WEIGHT IS 680 LBS
2. ALL LENGTHS SHOWN ARE ℄ TO ℄.

CONT REF	-01 QTY REQD	-02 QTY REQD	ITEM NO	CODE IDENT	STOCK SIZE	DESCRIPTION	MATERIAL
8-11	1	1	28		1.00 x 1/8 WALL	STRUT-[illegible] LG (2.90 M)	ASTM A36
8-10	1	1	27		1.00 x 1/8 WALL	STRUT-[illegible] LG (2.34 M)	ASTM A36
6-11	1	1	26		1.00 x 1/8 WALL	STRUT-76.07 LG (1.93 M)	ASTM A36
	1	1	25			5000 LB COUNTERWEIGHT [illegible]	CONCRETE
7-9	REF	REF	24		PART OF ITEM 9	STRUT-109.21 LG (2.77 M)	ASTM A36
6-9	REF	REF	23		PART OF ITEM 6	STRUT-110.27 LG (2.80 M)	ASTM A36
9-7	REF	REF	22		PART OF ITEM 9	STRUT-73.49 LG (1.87 M)	ASTM A36
8-6	REF	REF	20		PART OF ITEM 6	STRUT-73.54 LG (1.87 M)	ASTM A36
2-5	REF	REF	18		PART OF ITEM 6	STRUT-73.54 LG (1.87 M)	ASTM A36
8-9	1	1	17		2 x 2 1/2 x 1/8 WALL	STRUT-[illegible] LG (3.08 M)	
7-8	1	1	16		1.00 x 1/8 WALL	STRUT-[illegible] LG (1.96 M)	
6-8	1	1	15		1.00 x 1/8 WALL	STRUT-65.82 LG (1.67 M)	
6-7	1	1	14		1.00 x 1/8 WALL	STRUT-26.47 LG (67.23 CM)	
5-9	1	1	13		2 x 2 1/2 x 1/8 WALL	STRUT-[illegible] LG (4.64 M)	
5-8	1	1	12		2 x 2 x 1/8 WALL	STRUT-[illegible] LG (2.92 M)	
5-6	1	1	11		1.00 x 1/8 WALL	STRUT-80.10 LG (2.03 M)	
4-6	1	1	10		1.00 x 1/8 WALL	STRUT-76.77 LG (1.95 M)	
4-5	1	1	9		1.00 x 1/8 WALL	STRUT-34.88 LG (88.60 CM)	
8-5	1	1	8		1.00 x 1/8 WALL	STRUT-42.21 LG (1.07 M)	
5-4	1	1	7		1.00 x 1/8 WALL	STRUT-32.91 LG (83.59 CM)	
2-9	1	1	6		2 x 2 x 1/8 WALL	STRUT-[illegible] LG (6.96 M)	ASTM A36
2-5	1	1	4		2 x 2 x 1/8 WALL	STRUT-[illegible] LG (2.96 M)	ASTM A36
1-4	1	1	2		[illegible] x 1/8 WALL	STRUT-[illegible] LG (2.40 M)	ASTM A36

LIST OF MATERIALS

NEXT ASSY	QTY	USED ON	QTY
	APPLICATION		

FINISH: SEE D/M
WHITE ENAMEL

ACUREX Aerotherm

COUNTERWEIGHT STRUCTURE
ADVANCED CONCENTRATOR

SIZE D | CODE IDENT NO 50726 | DWG NO 7740-005 | REV A

SHEET 1 OF 1

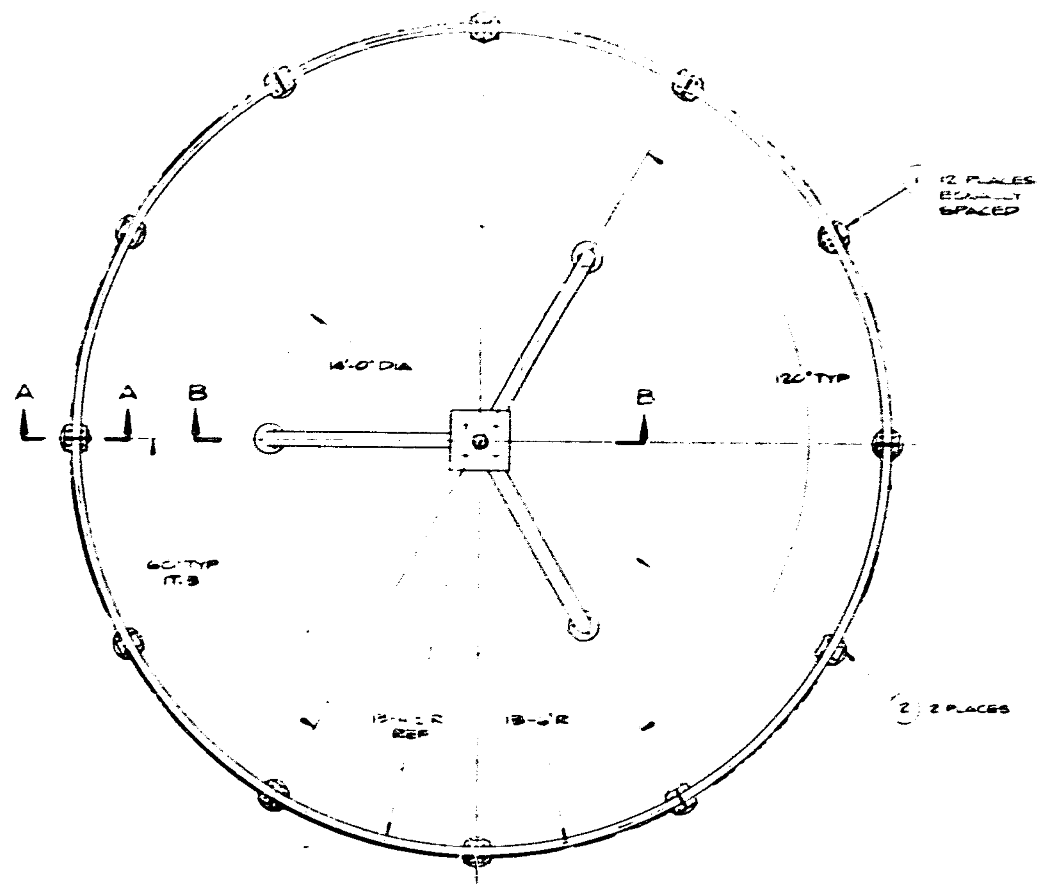

PLAN VIEW

NOTES

1. GALVANIZE ALL STEEL PARTS PER ASTM A 123

QTY REQD	ITEM NO			DESCRIPTION
3	19			GUSSET - 5/16 THK PL
12	18			ANGLE - ∠4×3×5/16 LC STEEL
9	17			ANCHOR BOLT - 3/4-10UNC
48	16			ANCHOR BOLT - 1"-8UNC
3	15			PLATE, FOOT - 1/2 THK PL
9	14			NUT, HEX - 3/4-10UNC
9	13			WASHER, FLAT - .812 NOM
1	12			PLATE, TOP - 24.00 × 24.00 OF 1/2 THK PL
3	11			LEG - 6.00 × .25 WALL TUBING
3	10			PEDESTAL FOUNDATION PER -
12	9			PLATE - 9.00 × 9.00 OF 1/2 THK PL
48	8			NUT, HEX 1"-8UNC
48	7			WASHER, FLAT 1.062 NOM
12	5			CHAIN GUARD - 1/8 THK EXTRUDED RUBBER
6	4			CHAIN GUARD CHANNEL 1/8 THK PL
6	3			TRACK - 7"×8×3" STRUCTURAL
24	2			ANGLE - ∠4×3×5/16 LC STEEL
12	1			FOUNDATION, PIER, REINFORCED CONCRETE 2.00 DIA

LIST OF MATERIALS

ACUREX Aerotherm

FOUNDATION, PEDESTAL SUB-ASSEMBLY - SOLAR CONCENTRATOR

D 50726 770-006 A

ORIGINAL PAGE IS OF POOR QUALITY

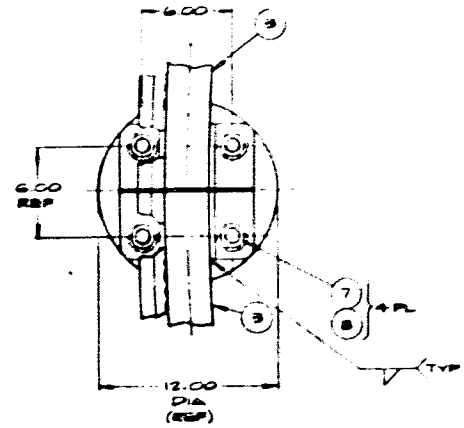

SECTION A-A

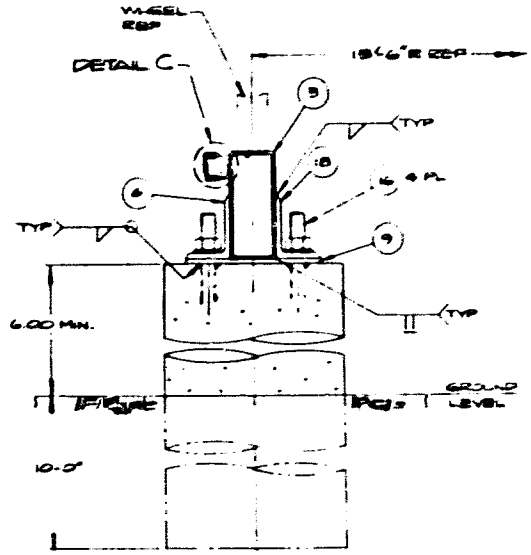

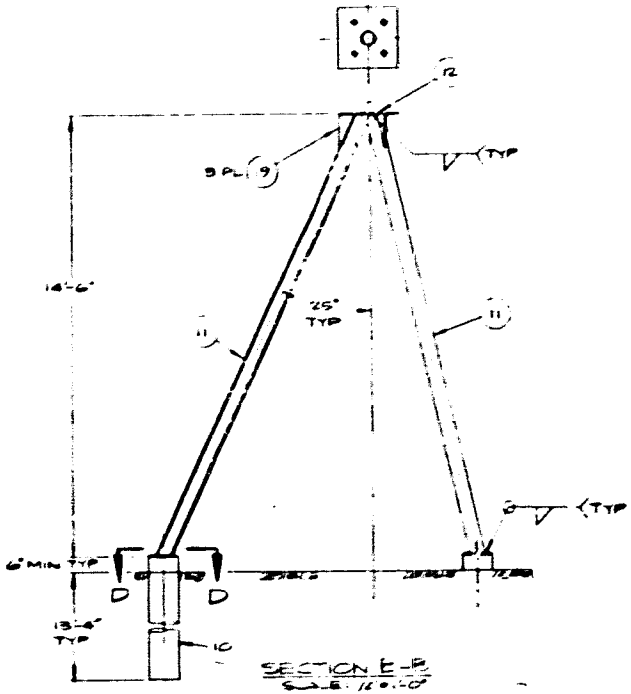

SECTION E-E
SCALE: 1/2"=1'-0"

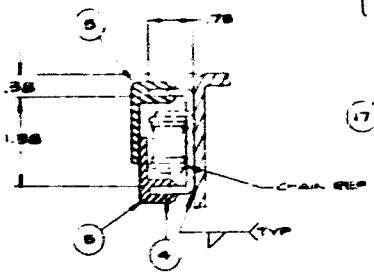

DETAIL C
SCALE: 1/1

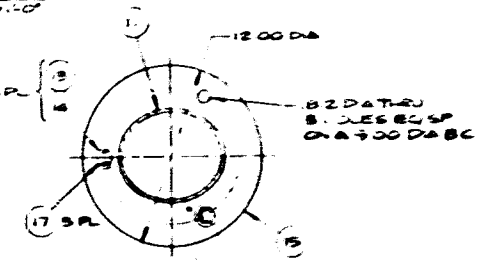

SECTION D-D
TYP OF 8 PL
SCALE: 1/4

ACUREX Aerotherm	
FOUNDATION & PEDESTAL SUB-ASSEMBLY - ADVANCED CONCENTRATOR	
D 50726	77-20-006 A

APPENDIX E

JPL ADVANCED CONCENTRATOR OUTER GORE DETAILED DRAWING PACKAGE

DRL 013

DRD SE001

Drawing Number	Revision	Title	Number of Sheets
7740-010	A	Outer Gore Assembly	1
7740-011	A	Core Blank	1
7740-012	A	End Support Pad	1
7740-013	A	Main Support Pad	1
7740-014	A	Insert	1

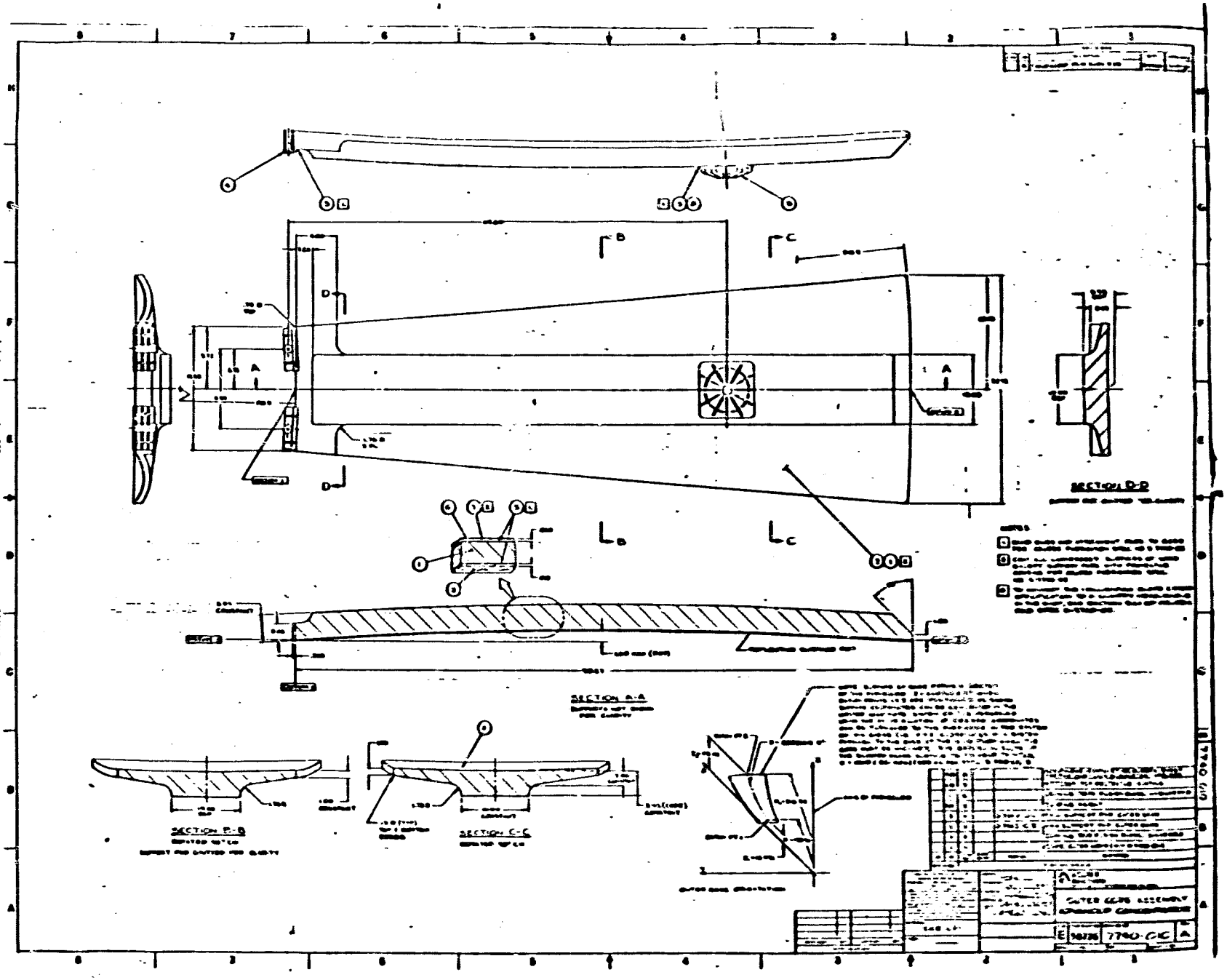

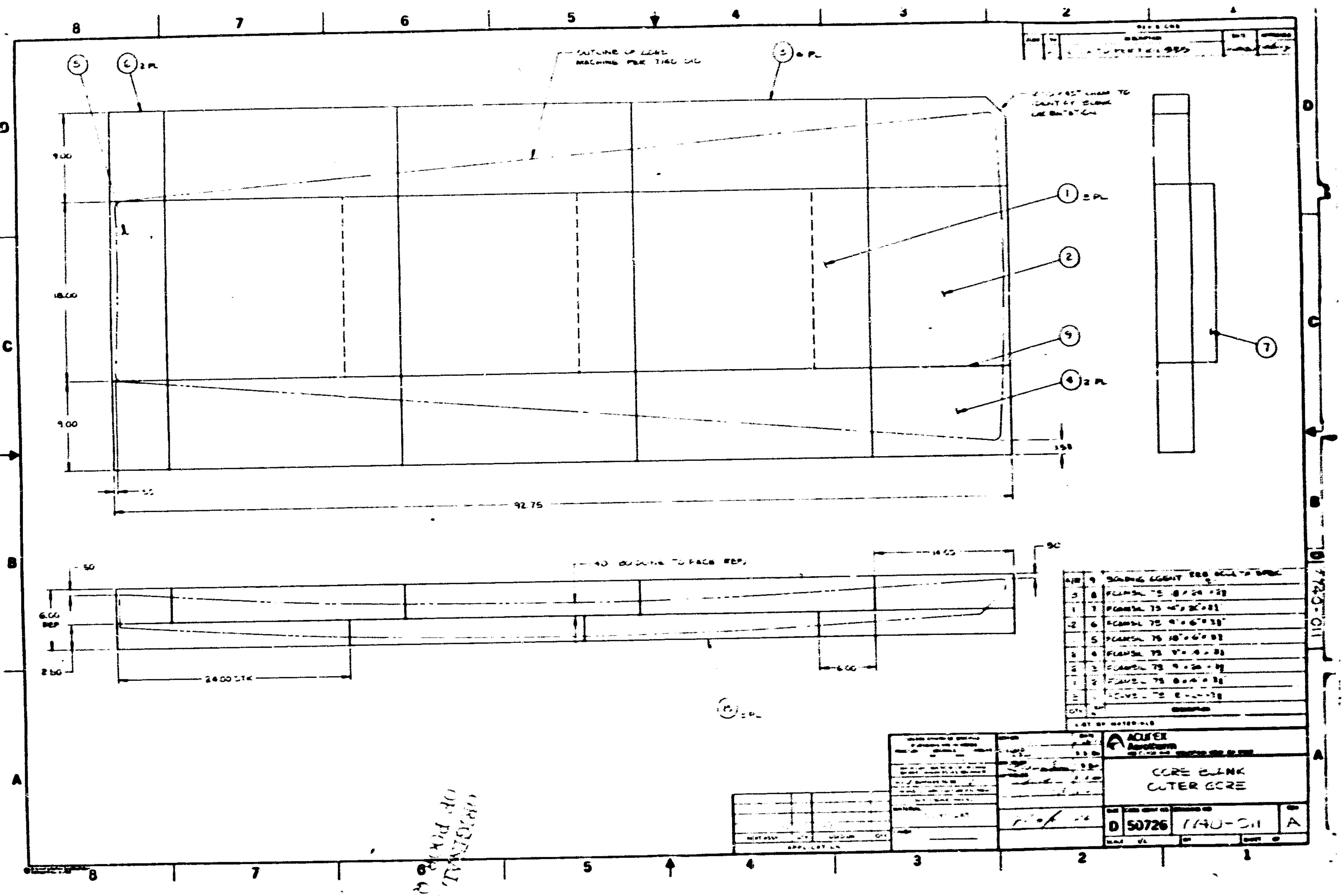

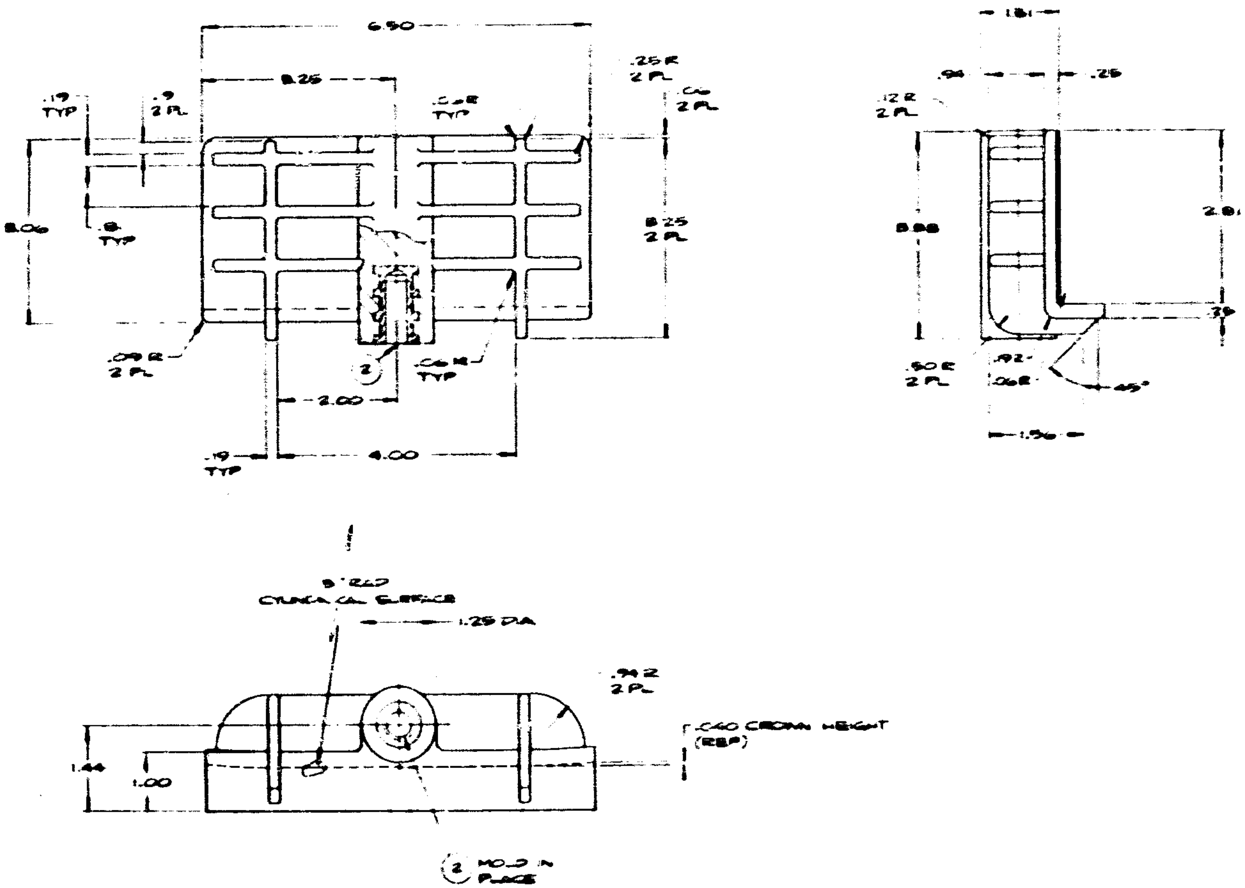

NOTES

1. MATERIAL: GRAPHITE/GLASS FILLED POLYESTER MOLDING COMPOUND, HAVEG/MOLD HEA 129 OR EQUIV.
2. 1-3° DRAFT ANGLES PERMISSIBLE

2	8740-04	INSERT	
		END SUPPORT PAD -	1

LIST OF MATERIALS

ACUREX Aerotherm

END SUPPORT PAD
OUTER GAGE

D 50726 7740-012 A

AS MOLDED

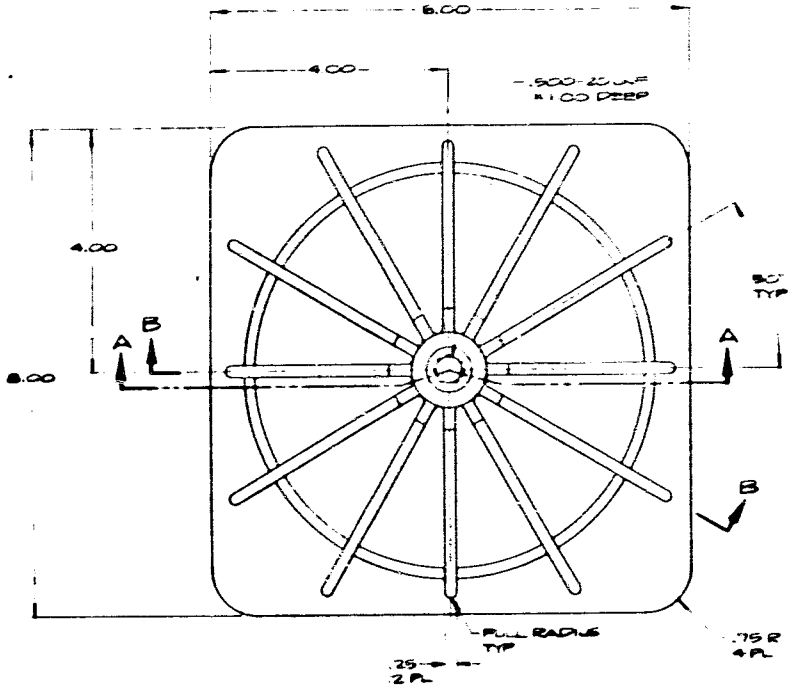

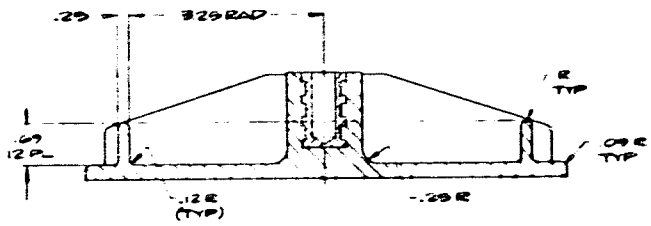

SECTION A-A

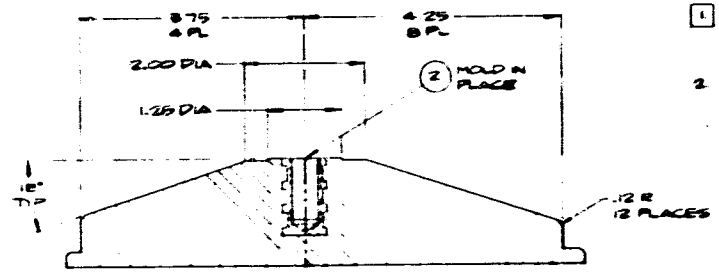

SECTION B-B

NOTES:

1. MATERIAL: GRAPHITE/GLASS FILLED POLYESTER MOLDING COMPOUND HAVHOLD MDA #29 OR EQUIV
2. 1°-2° DRAFT PERMISSIBLE ON ALL VERTICAL SURFACES.

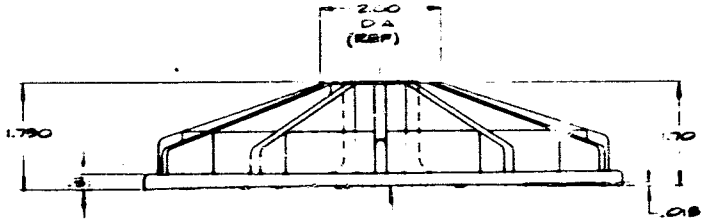

BOTTOM SURFACE CYLINDRICAL
600" RADIUS OF CURVATURE (REF)

7740-013 INSERT
MAIN SUPPORT PAD

ACUREX
Appliances

MAIN SUPPORT PAD
OUTER GORE

D | 50726 | 7740-013 | A

B 7740-014

ZONE	LTR	REVISIONS DESCRIPTION	DATE	APPROVED
	A	RELEASED PER ERN 335	3/21/80	

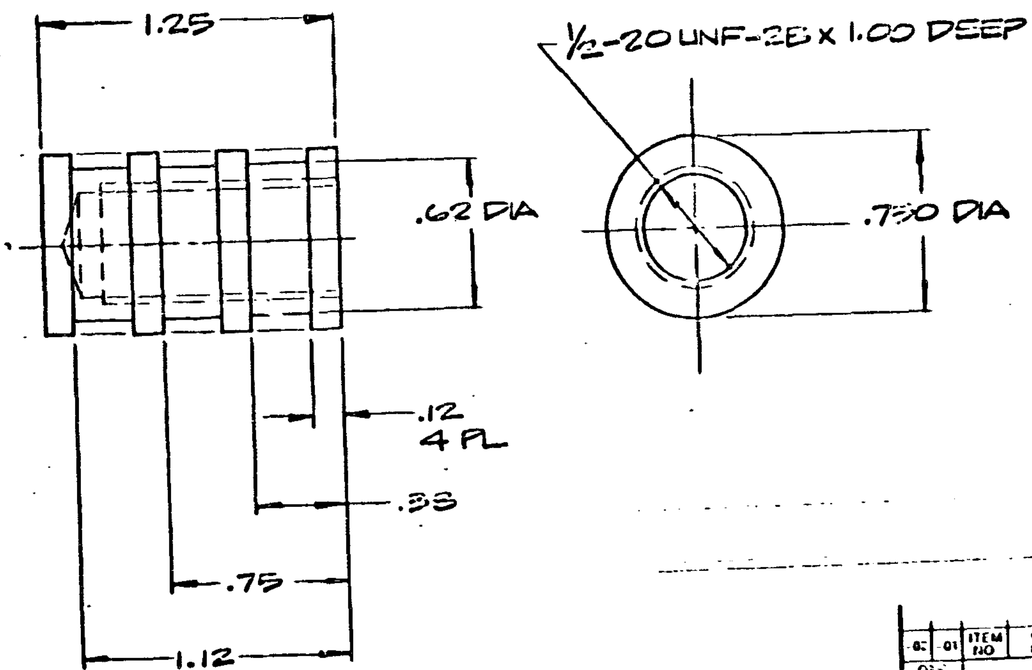

LIST OF MATERIALS

QTY REQD -02	-01	ITEM NO	CODE IDENT	PART NO	DESCRIPTION

NEXT ASSY	QTY	USED ON
D7740-013	1	7740
D7740-012	1	7740

APPLICATION

UNLESS OTHERWISE SPECIFIED DIMENSIONS ARE IN INCHES

MATERIAL 304 SST

FINISH ———

ACUREX Aerotherm
485 CLYDE AVE MOUNTAIN VIEW CA 94042

INSERT

SIZE	CODE IDENT NO	DRAWING NO	REV.
B	50725	7740-014	A

SCALE 2/1 SHEET 1 OF 1

APPENDIX F

PROTOTYPE FABRICATION SPECIFICATION FOR A REFLECTIVE ELEMENT (GORE) OF AN ADVANCED POINT-FOCUSING SOLAR CONCENTRATOR (ACUREX SPECIFICATION NUMBER S-7740-02)

REVISION STATUS SHEET

Rev. No.	Date	Description	Approved by

Sign off status:

Written by Winston Love
Date 3-4-80

Approved by David M. Bell
Date 3-4-80

Aproved by Roger J. Benlamin
Date 3-4-80

JPL Approval

Approved by _____
Date _____

Approved by _____
Date _____

TABLE OF CONTENTS

TABLE OF CONTENTS (Concluded)

LIST OF TABLES

1. SCOPE

This specification summarizes the design performance goals and establishes the requirements for fabrication and acceptance testing of prototype cellular glass reflective panel outer gore assemblies for a point-focusing solar concentrator. This specification provides a framework in which all fabrication drawings, methods, material specifications, manufacturing procedures, and verification techniques are referenced. Information currently unavailable has been identified as TBDs in this specification. Such information must be determined and provided prior to the prototype fabrication phase.

2. APPLICABLE DOCUMENTS

2.1 Government Documents

Unless otherwise specified, the following documents form a part of this specification to the extent specified herein.

- Military specification MIL-P-116 -- Methods of Preservation
- Military standard MIL-STD-794 -- Procedures for Packaging and Packing of Parts and Equipment

2.2 Nongovernment Documents

2.2.1 Specifications

The reference specifications listed in Table 2-1 form a part of this specification to the extent specified herein.

2.2.2 Manufacturing and Test Procedures

The documents listed in Table 2-2 provide the procedures to be followed for fabrication and testing of the gore assembly and its components.

2.3 List of Acurex Drawings

The drawings listed in Table 2-3 describe and define the physical dimensions and requirements of the reflective element.

TABLE 2-1. REFERENCE SPECIFICATIONS LIST

Ref. Spec. No.	Spec. Identification	Description
S-1	Acurex Spec. S-7740-01	Preliminary Design Basis and Requirements for an Advanced Point-Focusing Solar Concentrator
S-2	TBD	Pittsburg Corning Foamsil® 75 Cellular Glass Spec
S-3	TBD	Corning 7809 Fusion Sheet Glass Spec
S-4	TBD	Sheet Molding Compound (SMC) Spec
S-5	TBD	Adhesive Spec for Cellular Glass Blocks
S-6	TBD	Adhesive Spec for Glass Bonding
S-7	TBD	Adhesive Spec for Support Pad Bonding
S-8	TBD	Edge Sealing Compound Specification
S-9	TBD	Pittsburg Corning Pitcoat® 404 Specification

TABLE 2-2. REFERENCE PROCEDURES LIST

Ref. Procedure No.	Spec. Identification	Description
P-1	TBD	Core Blank Bonding Procedure
P-2	TBD	Core Blank Machining Procedure
P-3	TBD	Sheet Glass to Core Bonding Procedure
P-4	TBD	Pad to Glass and Cellular Glass Bonding Procedure
P-5	TBD	Edge Sealing Procedure
P-6	TBD	Protective Coating Application Procedure
P-7	TBD	Cellular Glass Material Verification Procedure
P-8	TBD	Sample Core Bonding and Machining Qualification Test Procedure
P-9	TBD	Sample Gore Assembly Bonding Qualification Test Procedure

TABLE 2-3. DRAWING LIST

Description	Drawing No.
Outer Gore Assembly	7740-010, Rev. A
Core Blank, Outer Gore	7740-011, Rev. A
End Support Pad, Outer Gore	7740-012, Rev. A
Main Support Pad, Outer Gore	7740-013, Rev. A

3. FURNISHED MATERIALS

The following items and material shall be furnished to the fabricator:

- Foamsil® 75 Cellular Glass Blocks (drawing 7740-011 Ref.)
- Corning 7809 Fusion Glass Sheets (mirror face), cut to size and silvered
- Corning 7809 Fusion Glass Sheets (spar cap), cut to size
- End Support Pads (Drawing 7740-012 Ref.)
- Main Support Pads (Drawing 7740-013 Ref.)

4. ITEM DEFINITION

4.1 General Description

The reflective surface of the concentrator consists of two concentric rings of independent, optical quality reflective elements, or gores, which form a physically discontinuous paraboloidal surface with a common focal point. Two types of reflective elements, designated as inner and outer gores, are used to makeup the reflective surface. Each gore is a sandwich construction of two glass sheets bonded to a cellular glass core. The gores are installed on a ring-like gore support structure with statically determinant three-point attachments. These attachments have sufficient

degrees of freedom to allow fine tuning of the composite surface geometry and to accommodate differential thermal expansion between the gores and the structure. For a more detailed description of the concentrator system see Reference Specification S-1.

Only the outer gore assembly is covered by this specification.

4.2 Major Components

The following major components makeup the gore assembly.

4.2.1 Cellular Glass Core (Reference 7740-011)

The core is formed by bonding together a series of cellular glass blocks to makeup the core blank, and then machining all surfaces of the blank to form the finished shape.

4.2.2 Glass Sheets (Reference 7740-010)

Precut glass sheets are bonded to the top and bottom of the finished core. The upper full surface, silvered sheet forms both the reflective surface and top structural skin. The lower, unsilvered sheet is a 10-inch wide longitudinal spar which forms a structural cap.

4.2.3 Support Pads (Reference 7740-012, -013)

One main and two end support pads distribute reaction loads into the cellular glass core and serve as attachment points to the concentrator structure.

4.3 Material Description

4.3.1 Cellular Glass

The cellular glass core is made with Pittsburg Corning Foamsil® 75. This material is easily machineable and has a coefficient of expansion closely matched to that of the sheet glass. See Reference Specification S-2 for details.

4.3.2 Sheet Glass

Both top and bottom sheet glass skins are 0.040 inch thick Corning 7809 aluminoborosilicate fusion glass. Its relatively high strength and flexibility allow it to conform to the top machined contour of the cellular glass core, yet carry much of the structural load of the assembly. See Reference Specification S-3 for details.

4.3.3 Support Pads

The support pads are compression moldings of sheet molding compound (SMC) with a threaded insert in each to attach to a support link. This material has a tensile strength of 12,000 psi (approximate) and a coefficient of expansion close to that of the glass sheets. See Reference Specification S-4 for details.

5. DESIGN GOALS

5.1 Performance Goals

The gore assembly performance is defined in terms of slope error and structural deflection. The following paragraphs describe the design targets for the outer gore assembly. These performance goals are the result of design requirements set forth in Reference Specification S-1.

5.1.1 Slope Error

The overall rms slope error of the top surface of the gore assembly shall be no more than 1.0 mrad. The local maximum slope error anywhere on the top surface of the gore assembly will not exceed TBD mrad. These characteristics will be verified by Acurex with methods specified in paragraph 7.2.1.

5.1.2 Structural Deflection

The deflection of the gore assembly will not exceed TBD inches at the four corners when uniformally loaded with TBD lb/in^2 while supported horizontally at the three support pads.

5.1.3 Conditions in Which Performance is Measured

5.1.3.1 Ambient Temperature

Test sample and ambient temperatures will be 68 $\pm 5^{o}F$ during all performance tests.

5.1.3.2 Specimen Temperature

The specimen temperature will be kept uniformly within 68 $\pm 5^{o}F$ during all performance tests.

5.1.3.3 Humidity

Ambient relative humidity of the test area will be 40 ± 20 percent during all performance tests.

5.1.3.4 Weight

The gore assembly weight will not exceed 65 pounds.

6. REQUIREMENTS

The following section describes the prototype gore fabrication requirements which must be met by the fabricator to ensure prototype acceptance.

6.1 Physical Characteristics

6.1.1 Physical Size

Sizes, dimensions, and configurations of the gore assembly shall be as specified in Acurex drawing 7740-010.

6.1.2 Surface Finishes

The finish on all cellular glass surfaces prior to coating or sheet glass assembly shall be smooth and free from cracks, chips, or irregularities. Calking of chipped or cracked surfaces is not acceptable.

6.2 Design and Construction

6.2.1 Fabrication Documents

The core blank and gore assembly shall be fabricated per this specification and the drawings listed in paragraph 2.3.

6.2.2 Standards of Manufacturing

6.2.2.1 Core Blank (Drawing 7740-011)

6.2.2.1.1 Material Specification

A. Cellular Glass -- The cellular glass used for the fabrication of the core blanks shall satisfy all the physical and mechanical characteristics of Reference Specification S-2.

B. Adhesive -- The adhesive used to bond the individual celluloid glass blocks together to form the core blank shall conform to the properties of Reference Specification S-5.

6.2.2.1.2 Bonding Procedure Requirements

A. Procedures -- The core blank shall be bonded together using procedures specified in Reference Procedure P-1.

B. Bonding Fixtures -- Fabricator shall design, fabricate, and procure all fixtures and tooling required for bonding together the core blank.

6.2.2.1.3 Machining Procedures

A. Procedures -- The core blank shall be machined using procedures recommended in Reference Procedure P-2.

B. Machining Fixtures and Tooling -- The fabricator shall design, fabricate, and procure all fixtures and tooling required for machining the core blank.

C. Top Surface Contour as per Drawing 7740-010 -- Acurex will supply the dimensions and/or surface coordinates in the coordinate system most useful to the fabricator.

6.2.2.2 Gore Assembly (Reference Drawing 7740-010)

6.2.2.2.1 Material Specification

A. Sheet Glass -- The sheet glass used for fabrication of the gore assembly shall satisfy all the physical and mechanical properties specified in Reference Specification S-3.

B. Adhesives -- Adhesives for bonding sheet glass to machined core blanks shall conform to properties specified in Reference Specification S-6. Adhesive for bonding the rubber sheet between the SMC support pads and the sheet glass shall conform to properties specified in Reference Specification S-7.

C. Support Pads -- Support pad materials shall satisfy all the physical and mechanical properties specified in Reference Specification S-4.

6.2.2.2.2 Bonding Procedures

A. Procedures -- The sheet glass shall be bonded to the cellular glass core using procedures recommended in Reference Procedure P-3. The support pads shall be bonded to the assembly prior to the application of protective coatings using procedures recommended in Reference Procedure P-4.

B. Bonding Fixtures -- Contractor shall design, fabricate, and procure all fixtures and tooling required for bonding the sheet glass and support pads to the machined cellular glass core.

6.2.2.3 Protective Systems

6.2.2.3.1 Material Specifications

A. Mirror Edge Sealing -- Edge sealing material shall conform to material properties specified in Reference Specification S-8.

B. Protective Coating -- All surfaces specified in drawing 7740-011 shall be coated with Pitcoat® 404. This coating material shall conform to all requirements specified in Reference Specification S-9.

6.2.2.3.2 Procedures

A. Edge Sealing Procedure -- After bonding glass sheets to the cellular glass core, all edges on the silvered top glass sheet shall be completely sealed with a TBD inch wide bead. This bead shall be applied in accordance with the procedures specified in Reference Procedure P-5.

B. Protective Coating Application Procedure -- After final gore assembly and glass edge sealing, all surfaces except the top reflective surface and support pads shall be given a protective coating. The coating shall be applied in accordance with Reference Procedure P-6. The coating shall completely cover all specified surfaces as indicated in drawing 7740-010, leaving no gaps, voids, or exposed cellular glass pores.

6.3 Process Verification

All fabrication and testing specified in Section 6.3 shall be satisfactorily completed before beginning fabrication of the prototype gore assemblies described in the previous paragraphs.

6.3.1 Cellular Glass Material Verification

Three cellular glass samples taken from the batch delivered for the gore assembly shall be tested for deflection and breaking strength to verify conformance to mechanical properties specified in Reference Specification S-2. Test procedures shall be in accordance with Reference Procedure P-7.

6.3.2 Cellular Glass Blocks Bonding Qualification

Upon satisfactory completion of tests specified in paragraph 6.3.1, the fabricator shall bond and machine four laminated cellular glass bonding samples using bonding and machining procedures specified in the bonding and machining procedure requirements of this document. Two of the cores shall be tested for structural stiffness and bond strength for conformance to requirements specified in Reference Procedure P-8. Satisfactory completion of test shall constitute acceptance of fabrication bonding and machining capabilities. The size and configuration of the sample and the structural and bonding strength testing procedures are specified in Reference Procedure P-8.

6.3.3 Sheet Glass Bonding Qualification

Upon satisfactory completion of the tests specified in paragraph 6.3.2, the fabricator shall bond a silvered and unsilvered glass sheet to each of the remaining two samples. These two sandwiched assemblies shall be tested for structural stiffness and bond strength for conformance to requirements specified in Reference Procedure P-9.

Satisfactory completion of tests shall constitute acceptance of fabricator's bonding facilities and capabilities. The size and configurations of the test samples and the qualification test procedures are specified in Reference Procedure P-9.

7. QUALITY ASSURANCE PROVISIONS

7.1 General

7.1.1 Responsibility for Tests

Acurex will perform testing on the gore assembly to determine whether the design goals described in Section 5 have been achieved. Methods of verification are specified in paragraph 7.2.1. The fabricator shall formally demonstrate that all requirements set forth in Section 6 have been met. The various methods of verification to be used are specified in paragraph 7.2.2. Except as otherwise specified, the fabricator may use his own facilities, JPL-owned, or Acurex-owned facilities, or any other commercial laboratory acceptable to Acurex. Acurex reserves the right to perform or witness any of the tests or inspections when such action is deemed necessary to assure that the reflective elements are built to the specification.

7.1.2 Special Test Equipment

7.1.2.1 Load/Deflection Test Fixture

Acurex/JPL will supply a load/deflection test fixture to support gore elements for verification of structural integrity.

7.2 QUALITY CONFORMANCE VERIFICATION

7.2.1 Design Goals Verification

7.2.1.1 Slope Error

The overall or rms slope error of the gore assembly as specified in paragraph 5.1.1 will be measured by Acurex.

7.2.1.2 Structural Deflection

Structural stiffness of the gore assembly as specified in paragraph 5.1.2 will be verified by Acurex using the Load/Deflection Test Fixture described previously.

7.2.1.3 Conditions in Which Performance is Measured

Prior to commencement of tests to verify slope error and structural deflection, the environmental and specimen conditions in paragraph 5.1.3 shall be verified by tests.

7.2.1.4 Weight

Acurex will perform tests to verify that the gore assemblies do not exceed the maximum weight requirements specified in paragraph 5.1.4.

7.2.2 Requirements Verifications

Each requirement specified in Section 6 shall be verified by one or a combination of any four methods specified in Table 7-1. These four methods are:

- Examination
- Inspection
- Demonstration tests
- Vendor certifications

(See Section 9.)

7.2.3 Acceptance Criteria

Proof of satisfactory completion of above methods of verification shall constitute acceptance to compliance of this specification.

TABLE 7-1. VERIFICATION OF REQUIREMENTS

Section 6 Requirements Paragraph No.	Requirements Titles	Verification Methods				Remarks
		Examination	Inspection	Demonstration Test	Vendor Certification	
6.0	Requirements					Sect. heading
6.1	Physical characteristics					Para. heading
6.1.1	Physical size	X	X			
6.1.2	Surface finishes	X				
6.2	Design and construction					Para. heading
6.2.1	Fabrication documents					N/A
6.2.2	Standards of manufacturing					Para. heading
6.2.2.1.1	Material specifications					Para. heading
A.	Core blank			X	X	
B.	Adhesives			X	X	
6.2.2.1.2	Bonding procedure requirements					Para. heading
A.	Procedures			X		
B.	Bonding fixtures			X		Negotiable
6.2.2.1.3	Machining procedures					
A.	Procedures			X		
B.	Fixtures and toolings			X		
C.	Top surface contour					N/A
6.2.2.2	Gore assembly					Para. heading
6.2.2.2.1	Material specification					Para. heading
A.	Sheet glass			X	X	
B.	Adhesives			X	X	
C.	Support pads			X	X	

TABLE 7-1. Concluded

Section 6 Requirements Paragraph No.	Requirements Titles	Verification Methods				Remarks
		Examination	Inspection	Demonstration Test	Vendor Certification	
6.2.2.2.2	Bonding procedures					
A.	Procedures			X		
B.	Bonding fixture			X		
6.2.2.3	Protective System					Para. heading
6.2.2.3.1	Material Specification					Para. heading
A.	Mirror Edge Sealing			X	X	
B.	Protective Coating			X	X	
6.2.2.3.2	Procedures					Para. heading
A.	Edge Sealing Procedure			X		Vendors certs.
B.	Protective Coating Application Procedure			X		
6.3.	Process verification (Preprototype)					Para. heading
6.3.1	Cellular Material Verification			X	X	W/test fixture
6.3.2	Cellular Glass Blocks Bonding Qualification			X		
6.3.3	Sheet Glass Bonding Qualification			X		

8. PREPARATION FOR DELIVERY

The gore assembly shall be prepared for delivery using Method III of MIL-D-116 or Level C of MIL-STD-794 as guidelines.

8.1 Handling

The gore assembly and all of the subcomponents shall be handled with care to prevent damage and breakage. If necessary, special handling fixtures shall be provided by the fabricator.

8.2 Packaging

The gore assembly shall be packaged properly to protect it from damage caused by weather, storage, or shipping.

8.3 Shipping

The gore assembly shall be packed properly to survive the normal handling and shipping shock loads.

9. DEFINITIONS

The terms used in this specification are defined as follows:

Core	The finished machined cellular glass structure onto which glass sheets are bonded to form a gore.
Core Blank	The roughly formed block of cellular glass structure formed by bonding several smaller cellular glass blocks.
Demonstration tests	Tests which are conducted to demonatrate that pilot production models meet the design specification requirements. Demonstration tests include inspection and examination when applicable.
Examination	Verification is inherently evident upon examination; i.e., gore assembly has all three pads attached; no cracks on mirror surfaces; sharp edges are removed.
Gore Assembly	The parabolic reflective element of sandwich construction of two glass sheets bonded to a cellular glass core.
Inspection	An operation where measurements are made: i.e., one would measure a part dimension and compare it to the drawing; one would not inspect a document.
Shall	Expresses a provision of the specification that is binding on the contractor.
Vendor Certification	Formal documents from the vendor attesting that material delivered meets all requirements specified in his contract.

Will	Expresses a declaration of purpose on the part of the Government, or, if the context so indicates, merely describes what is expected to occur.
mrad	Milliradians (0.001 rad)
N/A	Not applicable
rms	Root mean square

APPENDIX G

CELLULAR GLASS GORE TEST PLAN

DRL 017
DRD TE001

Acurex Project 7740

AN ADVANCED SOLAR CONCENTRATOR DESIGN
CELLULAR GLASS GORE TEST PLAN

DRL 017
DRD TE001

Acurex Corporation
Alternate Energy Division
485 Clyde Avenue
Mountain View, California 94042

Prepared for

California Institute of Technology
Jet Propulsion Laboratory
4800 Oak Grove Drive
Pasadena, California 91103

TABLE OF CONTENTS

CELLULAR GLASS GORE TEST PLAN

1. INTRODUCTION

This test plan covers the optical, structural, and environmental evaluation of the Advanced Solar Concentrator outer gore. The outer gore is a cellular glass/sheet glass reflective panel with a backsilvered glass reflective surface. It is one of two reflective panel shapes which are used to form the paraboloidal reflecting surface of the Advanced Solar Concentrator point focusing dish. The gore consists of a contoured cellular glass core with a paraboloidal front surface and spar-stiffened rear surface, a large full surface facet of flexed glass mirror bonded to the paraboloidal front surface, and a full-length structural glass cap bonded to the spar on the rear surface. The cellular glass core is protected from environmental degradation by a coating of butyl rubber, which is applied to all unmirrored surfaces of the gore. Butyl rubber is also used to form an edge seal around the mirrored face of the gore to prevent moisture from attacking the reflective silver coating. An overcoating of white silicone/alkyd paint shields the butyl rubber coating from ultraviolet radiation and provides the exterior finish of the panel. Three mounting pads, bonded to the gore prior to coating, provide for structural attachment of the gore to the dish structure.

2. TEST OBJECTIVES

The purpose of this test program is to verify the ability of the gore to meet its major performance goals. These are: (1) survival in a severe external environment for a useful life of 30 years, (2) survival under the specified wind conditions with less than a 5 percent failure rate, and (3) to provide a precise optical reflecting surface under no-load and 30 mph windload conditions. These performance objectives will be verified by a series of optical, structural and environmental tests.

This test plan is based on the "mass production" gore design developed during the Detailed Design task of the Acurex/JPL Advanced Solar Concentrator Project (Contract No. 955477). It should be noted that initial prototype gores, fabricated from standard materials, cannot be expected to meet the production design goals.

3. PRODUCTION DESIGN GOALS

The Advanced Solar Concentrator gores are designed to meet the following requirements:

- Optical
  - The rms slope error of the mirror surface shall be less than or equal to 1 mrad
  - The solar spectrum average total hemispherical reflectance of the mirror surface shall be 0.94 $\pm$0.01
  - The mirrored glass gore shall survive the specified number of freeze/thaw cycles (see environmental requirements) with less than 10 percent degradation in specular reflectance within a half-angle of 18 mrad

- Structural
  - -- The gore when supported on its three statically determinant support points shall withstand the wind loads imposed under the following conditions with a 5 percent probability of failure for accumulated exposure times consistent with a 30 year operating life:
    - Relative humidity of 40 percent
    - 50 km/hr winds -- operating
    - 60 km/hr wind gusts -- operating
    - 80 km/hr winds -- driving to stow
    - 110 km/hr winds -- a single "short" exposure
    - 120 km/hr winds -- stowed
  - -- The maximum angular rotation at any point on the mirror surface shall be less than 4×10^{-4} radians, when the gore is kinematically supported and subjected to a uniform pressure of 385 N/m^2 over the mirror surface
  - -- The gore shall be capable of surviving, with no damage, a seismic lateral acceleration of 0.25 g in any direction combined with 1.0 g gravity loading with the concentrator in any position.
- Environmental
  - -- The gore shall be capable of surviving in any position with no damage under the following precipitation environments:
    1. Rain -- 6.5 cm within a 24-hour period
    2. Hail -- size of 1.0 cm diameter
       -- Mohs scale of hardness of 2

— Coincident wind speed of 23 kmph

— Air temperature 10°C

3. Sleet — 1.0 cm thick ice blanket

4. Snow -- 15 cm thick with specific gravity of 0.125

— The gore shall be capable of withstanding 24 of the following freeze/thaw cycles

- Four hours at 50°C maximum temperature
- Two hour transient to -18°C minimum temperature
- Four hours at -18°C minimum temperature
- Three hour transient to 25°C medium-high temperature
- Three hours at 25°C medium-high temperature
- Two hour transient to 5°C medium-low temperature
- Four hours at 5°C medium-low temperature
- Two hour transient to 50°C maximum temperature

A minimum dew point of 10°C shall be maintained throughout the cycle

4. OPTICAL TESTS

Optical tests will be performed to determine the rms slope error of the finished gore, the solar spectrum averaged total hemispherical reflectance of the mirror surface, and the reflectance degradation due to temperature and humidity environmental cycling.

4.1 Slope Error

The optical precision of the gore (slope error) must be characterized in the absence of external loads. This can be accomplished by either a comprehensive ray trace of the mirror surface with a computer-coupled laser ray trace facility (similar to those at Sandia Laboratories in Albuquerque), or by the evaluation of an image formed by

the entire panel. Since no ray trace facility with the capability of handling a reflective panel with a focal length of 6.6 m is available (Sandia is currently limited to 4.2 m), the image evaluation approach is recommended. This technique has been successfully utilized by JPL to evaluate the spherical optics of the Test Bed Concentrator panels. For a spherical reflective surface, illumination is accomplished by a source of light which approximates a point source at the panel center of curvature. The image is reformed at the center of curvature and analyzed photometrically with the assistance of a system of apertures and occulting disks which allow the intercepted energy fraction to be determined as a function of radius from the image center. From the image energy distribution, slope error can be determined for the panel. A very nice technique for visualizing panel surface topology involves photographing the illuminated panel through the test aperture. The resulting photograph reveals portions of the mirror surface whose energy passes through the test aperture in the image plane as brightly illuminated, while noncontributing areas are rendered dark. A quantitive assessment of the slope error associated with a dark area can be made by increasing the aperture size until the energy of that region passes through, and computing the slope error associated with that aperture radius.

The test setup described above, with a point source at the center of curvature, works only for spherical optics. If a paraboloid is illuminated in this manner, a planar image will not be formed, because the resulting optical system will suffer from spherical aberration. In optically fast paraboloids, such as the Advanced Solar Concentrator, spherical aberration is severe. However, an image free of spherical aberration can be formed by using a full (panel) aperture collimated light

source to illuminate the panel. This collimated source can be the sun (or the moon), provided a tracking system can be provided to follow the sun (or the moon) with the panel and test system, or a large artificially collimated light source such as JPL's space simulator.

An alternative is to use a light source at the center of curvature, coupled with a lens to introduce a quantity of negative spherical aberration into the illuminating beam that will precisely cancel the spherical aberration introduced by the panel. The resulting image will appear as if the panel were illuminated by a collimated source. This technique has been used to test astronomical telescope mirrors whose precision exceeds the panel requirements by orders of magnitude. All that is usually required is a reasonably monochromatic light source and a small plano-convex lens of the right focal length spaced a short distance from the pinhole source of illumination.

The combination of lens focal length and spacing from the pinhole are used to produce the compensating aberration required for a null test. This allows lenses in the range of 5 to 20 percent of the mirror focal length to be used. Although a quick estimate of the lens focal length for gore tests indicates lenses between 12-in. and 52-in. focal lengths would suffice, the lends diameter required for an F/0.6 paraboloid will be in excess of 12 in. This would be a costly lens and may preclude this test method.

The ultimate choice of the panel illumination approach will be determined by hardware availability and cost. With JPL's ready access to the "precursor" tracking unit, it would appear that optical evaluation of the image formed by reflected light from the moon might well prove least

expensive. A series of photographs taken with various occulting disks will allow a rapid estimation of rms slope error.

4.2 Reflectance

While the hemispherical reflectance of a mirror surface should be independent of the surface curvature, the effects of temperature and humidity environmental cycling on reflectance may be dependent upon the silver/glass stress level. Reflectance tests must therefore be performed on samples with mirror curvature stresses equal to those of the finished gore.

Three reflectance measurements are required:

- Flat mirror sample (solar averaged hemispherical and 18 mrad half-angle)
- Equivalent curvature stressed mirror glass/cellular glass sample before temperature and humidity cycling (solar averaged hemisphierical and 18 mrad half-angle)
- Equivalent curvature stressed mirror glass/cellular glass sample after temperature and humidity cycling (solar averaged hemispherical and 18 mrad half-angle)

The flat mirror sample will serve as a control to separate any unforseen effects due to curvature or bonding from the data. The equivalent curvature stress samples can be either full finished gores or subscale panels sized to duplicate the mirror stresses. Any subscale panels must be fabricated from a minimum of two cellular glass block segments bonded together with the selected adhesive system with all nonreflective surfaces protected with the specified conformal coating. This will ensure a realistic test of the temperature and humidity sensitivity of the design.

Reflectance measurements can be made on the control sample with a standard bidirectional reflectometer. Reflectance measurements on the test panel will be made with a portable version of a bidirectional reflectometer, such as the one used by Sandia Laboratories for evaluation of collector reflectance in the field. Measurements will be taken prior to environmental exposure, after 5, 10 and 24 cycles of temperature and humidity. Measurements will be compared to determine if any degradation in reflectance has occurred.

5. STRUCTURAL TESTS

Structural tests will be performed to verify the gore's ability to withstand the wind, gravity and seismic loads and to demonstrate that the gore meets or exceeds the specified stiffness criteria. The lack of structural design experience and the limited statistical design data for both cellular and sheet glass, create a higher degree of uncertainty as to the long-term load bearing capability of the gore design than would exist with conventional materials.

Due to the static fatigue susceptibility of cellular and sheet glass, the design of the gore is based on an allowable failure rate as a function of load duration. Valid test results can therefore only be obtained with a large statistical sample of failed panels. Due to the relatively high cost of each gore at the prototype or first article production level, a statistically significant sample of full gores may be prohibitively expensive. An alternative to full-scale structural testing of completed gores is the testing of relatively low cost samples representative of critically loaded gore segments.

The design is based on a 5 percent allowable failure rate for the specified load conditions at an accumulated exposure time equivalent to a

30 yr operating period. When subjected to the governing load condition for the appropriate duration, 5 percent of the gores tested would therefore be expected to fail. Even those panels which do not fail under test will no longer be useful since they will already have accumulated an exposure to the governing design load equal to that of a 30 year operating period.

The gore design has been shown analytically to be stress limited in the cellular glass core under worst-case loading conditions corresponding to the 110 km/hr single "short" exposure condition. The duration of this one-time load was taken to be 1 minute. The gore is also very near to being stress limited in the core under the 80 km/hr drive to stow condition with a 30 year accumulated exposure of 8 hours. Due to the difficulty of testing the short duration load and the relatively arbitrary nature of that requirement (see Section 2.2.1 of Acurex Final Report FR-80-16/AE) it is recommended that all tests be performed to verify the design's adequacy to meet the 80 km/hr, 8 hour load condition.

Three aspects of the design are of primary concern. These are: (1) the actual allowable stress for the cellular glass core with a 5 percent failure probability after an 8 hour accumulated load, (2) the actual allowable stress for the sheet glass mirror with a 5 percent probability of failure after a 30 year steady state stress, and (3) the actual stress distribution under load between the sheet glass skins and the cellular glass core.

The structural adequacy of the gore design can most cost-effectively be demonstrated by addressing these design concerns separately. If the most highly stressed core section can be shown to statistically meet or exceed the life expectancy under the governing load condition and the

mirror glass can be shown to meet its 30 year target under steady state curvature stress conditions, the confidence level in the gore design can be significantly improved.

5.1 Core Stress

The most highly stressed core section is located directly over the main support pad under front-side wind load conditions. It is centered within the spar section near the mirror face. Both the load sharing between sheet and cellular glass and the allowable stress limit can be verified by testing a simple sheet glass and cellular glass bar sample as described below. While actual stresses will not be determined, the adequacy of the design can be verified.

The test samples will be flat beams 10-in. wide by 3-1/2-in. thick by 48-in. long with sheet glass strips bonded to the top and bottom faces. This sample configuration will provide a comparable volume of cellular glass subjected to a similar stress profile (both important factors impacting allowable stress values). The flat beam configuration does not fully reflect the curved beam stress effects nor does it produce the steady state sheet glass stresses seen in the full-scale gore. These limitations are slight due to the shallow radial curvature of the full-scale gore and the fact that sheet glass curvature stresses impart relatively small additional loads on the cellular glass core.

These relatively low cost test samples can be fabricated in sufficient quantity to allow statistically meaningful tests to be performed.

For the tests, the samples will be attached to a support frame using attachment linkage similar to that used in mounting the gore to the concentrator truss structure. A full size main attachment pad will be

bonded to the rear glass sheet to duplicate local stress profiles and a simple angle attachment will be bonded to the "root" of the test sample. The wind load will be simulated by distributing sandbags over the front glass surface. All samples will be loaded for the required 8 hour duration and visually evaluated to determine if any core failures have occurred. A minimum of 60 samples should be tested.

5.2 Mirror Glass Stress

The adequacy of the design with respect to the steady state mirror glass curvature stress must also be evaluated statistically. Only limited data exists relating sheet glass stress and load duration to failure probability. The design target of a 5 percent failure probability after 30 years of service is very difficult to verify. The recommended approach is to run a series of stress versus time-to-failure tests with representative sheet glass samples to obtain an adequate statistical data base. Test samples must not only have the proper thickness, but also reflect a comparable stressed surface area. A four point bend test with samples sized to conservatively reflect worst-case stress areas will provide a simple, low cost means of developing a stress and time-to-failure data base for the 5 percent failure criteria. Since only reasonably short-term tests can be performed, the 30 year allowable stress values must be based on a great deal of extrapolation. The accuracy of that extrapolation is strongly dependent upon the accuracy of the short-term data. A rather large statistical sample will therefore be required.

5.3 Seismic Loading

The seismic load resistance will be verified with full-scale gore samples. Due to the dynamic nature of the seismic loading, the static fatigue characteristics of the sheet and cellular glass materials can be

ignored. A relatively small statistical sample can be used to verify the seismic load resistance of the gore. A minimum of three full-scale gores are recommended for test to minimize data scatter effects. A shaker table with a sinusoidal forcing function with a frequency between 1 and 5 hz and a maximum acceleration of 0.25 g can be used. A series of tests should be run with each gore kinematically supported. Accelerations in the plane of the support pads and perpendicular to that plane should be tested.

5.4 Gore Stiffness

The stiffness of the gore will be tested to ensure compliance with the maximum angular rotation criteria. For the test, full-scale gores will be attached to a support frame using the type of attachment linkage used in mounting the gore to the concentrator truss. The wind pressure load will be simulated by distributing sandbags over the mirrored face of the panel. Key locations on the mirror face will be strain gaged to measure bending induced strain levels for comparison with design predictions. Slope changes at the panel tip will be estimated by measuring the axial displacement of a reflected laser beam on a target scale. Gore tip deflection will be measured with a dial indicator as a backup to the slope data. Slope, strain, and deflection data can be used to verify the stiffness of the gore.

5.5 Attachment Pads

Finally, to verify the attachment pad's ability to withstand the worst-case rear-side wind loads, simple shear and tensile tests will be performed. Two test specimen types will be used. The main support pad test samples will consist of two main support pads bonded to opposite sides of a sheet-glass-faced block of cellular glass. A worst-case tensile loading of the pads will be maintained for a duration of 8 hours

to verify the creep resistance of the adhesive system. The root support pad test samples will consist of four root pads bonded directly to a block of cellular glass. The pads will be attached to four parallel edges of the block and oriented to form two adjacent tensile test sets. Spreader bars will be used with a tensile test unit to apply and maintain the worst-case load for a minimum duration of 8 hours.

6. ENVIRONMENTAL TESTS

The primary environmental requirements for the gore are the ability to withstand the widely varying temperature extremes and the ability to withstand hail impact. Snow and sleet loads prove to be far below the governing wind loads and therefore do not require separate testing.

6.1 Temperature Extremes

Full-scale gores will be placed in an environmental chamber and exposed to repeated freeze/thaw cycles to test the ability of the protective coating to protect the silver reflective coating and the cellular glass core from environmentally induced degradation. The humidity level will be sufficient to ensure surface condensation during cooldown cycles.

6.2 Ultraviolet Degradation

In addition, conformal coated cellular glass samples will be exposed to ultraviolet radiation to test the ability of the silicone alkyd paint to protect the vital butyl rubber undercoat from degradation. Several samples will be exposed to ultraviolet radiation for extended periods of time and sectioned to examine the butylite undercoat for degradation. Samples will have a silvered glass face sheet with the same edge seal configuration as the gores, to evaluate the effects which might be specifically associated with the mirror edge seals.

6.3 Hail Impact

Subscale test panels duplicating the stressed mirror surface of the gore will be subjected to simulated hail impact. Ice balls will be launched at a velocity corresponding to a combination of the hailstone terminal velocity and the specified wind velocity.

7. TEST CONDITIONS

The tests to be performed and the test conditions are summarized in Table 1 and 2, respectively.

Table 1. Cellular Glass Gore Test Matrix

Sample[a] Type	Number of Samples	Test Sequence[b]
1 or 2	2	R/FT/R
5	2	R
1	3	SE/SD/SL/FT/SE[c]
3	60	CS
4	200	GS
2	6	HI
2	3	UV
6	2	PT
7	2	PT

[a]Sample type
1. Full finished gore
2. Subscale equivalent mirror curvature stress panel, no back glass sheet, conformal coated
3. Subscale flat beam, front and back glass sheets, no conformal coating
4. Glass sheet four point bend samples
5. Flat mirror glass sample
6. Pad pull tests sample (main pad)
7. Pad pull test sample (root pads)

[b]Test type
R Mirror glass reflectance
SE Slope error
FT Freeze/thaw cycle
SD Structural deflection
CS Core Stress
GS Glass stress
SL Seismic loading
HI Hail impact
UV UV degradation
PT Pull test

[c]Optional test

Table 2. Cellular Glass Gore Test Conditions

Test Type	Conditions
Freeze/thaw (FT)	Twenty-four temperature cycles from 50° to -18°C with dew point maintained above 10°C. Each cycle consists of the following conditions: 4 hour hold at 50°C 2 hour transient to -18°C 4 hour hold at -18°C 3 hour transient to 25°C 3 hour hold at 25°C 2 hour transient to 5°C 4 hour hold at 5°C 2 hour transient to 50°C Gore positioned horizontally, mirror side up for this test. Reflectance tests and visual damage inspection shall be performed after 5, 10, and 24 cycles.
Structural deflection (SD)	Gore mounted horizontally, supported by standard attachment hardware. Gore loaded by sandbags on mirror face to a pressure of 385 N/m^2. Slope error measured by the motion of a laser beam reflected from the mirror surface at the point of maximum rotation
Slope error (SE)	Gore in thermal equilibrium with environment at ambient temperature. Gore supported with standard attachment hardware at its three mount points. Test can be conducted with gore in either the horizontal or vertical position.
Core stress (CS)	Test samples loaded with sandbags to simulate the bending stress distribution experienced by the most severely loaded gore during drive-to-stow in a 80 km/hr wind. Samples supported by standard linkage using attachment points provided on the sample. Each sample loaded for 8 hours and any core fractures noted. All tests conducted at ambient temperature.
Seismic loads (SL)	Gore mounted to the table of a vibration test machine using standard mounting hardware. Gore shall be subjected to 0.25 g acceleration over a frequency range of 1 to 5 hz in the longitudinal and lateral directions. All tests conducted at ambient temperature.

Table 2. Concluded

Test Type	Conditions
Glass stress (GS)	Standard four point bend test samples of mirror glass shall be subjected to three bending loads and left under load until 5 percent of each group fails. Three bending stress levels will be selected such that 5 percent failures are anticipated in 10^3, 10^4, and 10^5 minutes (16 hours, 7 days, 2 months) respectively. Sixty samples shall be tested at each stress level. All tests conducted at ambient temperature.
Ultraviolet radiation (UV)	Samples shall be subjected to accelerated exposure to ultraviolet radiation. Test duration and radiation intensity shall be chosen to provide a simulation of a lifetime exposure to UV degradation at a radiation intensity which does not degrade the paint in a manner not typical to a 30 year exposure at an intensity level of one sun.
Attachment pad pull test (PT)	Sample shall be subjected to tensile loads simulating back-side wind loading at 80 km/hr. The load shall be held for 8 hours to test the bonding agent for creep. After an 8 hour hold at this load level, the load will be increased to failure. All tests conducted at ambient temperature.
Reflectance test (R)	Spectral reflectance measurements shall be taken on a flat control sample of mirror glass with a bidirectional reflectometer. A portable version of this instrument shall be used to take spectral reflectance measurements at 10 locations on the curved mirror surface of the test panel.
Hail impact (HI)	Samples shall be subjected to a series of impacts made by a 1.0-cm diameter ice ball traveling at speeds up to 20 m/sec. A series of six impacts at a given speed without fracture of the mirror glass will constitute proof of hail resistance. Tests shall be conducted with samples at ambient and -20°C.